DESIGN, CONSTRUCTION AND MONITORING OF ECO-FRIENDLY REVETMENTS FOR COASTAL PROTECTION

SHERVIN MOTAMEDI

FACULTY OF ENGINEERING
UNIVERSITY OF MALAYA
KUALA LUMPUR

2016

DESIGN, CONSTRUCTION AND MONITORING OF ECO-FRIENDLY REVETMENTS FOR COASTAL PROTECTION

SHERVIN MOTAMEDI

THESIS SUBMITTED IN FULFILMENT OF THE REQUIREMENTS FOR THE DEGREE OF DOCTOR OF PHILOSOPHY

FACULTY OF ENGINEERING
UNIVERSITY OF MALAYA
KUALA LUMPUR

UNIVERSITY OF MALAYA

UNIVERSITI MALAYA

ORIGINAL LITERARY WORK DECLARATION

Name of Candidate: Shervin Motamedi

Registration/Matrix No.: KHA120100

Name of Degree: Doctor of Philosophy

Title of Thesis: DESIGN, CONSTRUCTION AND MONITORING OF ECO-FRIENDLY REVETMENTS FOR COASTAL PROTECTION

Field of Study: Geotechnical Engineering

I do solemnly and sincerely declare that:

(1) I am the sole author/writer of this Work;
(2) This work is original;
(3) Any use of any work in which copyright exists was done by way of fair dealing and for permitted purposes and any excerpt or extract from, or reference to or reproduction of any copyright work has been disclosed expressly and sufficiently and the title of the Work and its authorship have been acknowledged in this Work;
(4) I do not have any actual knowledge nor do I ought reasonably to know that the making of this work constitutes an infringement of any copyright work;
(5) I hereby assign all and every rights in the copyright to this Work to the University of Malaya ("UM"), who henceforth shall be owner of the copyright in this Work and that any reproduction or use in any form or by any means whatsoever is prohibited without the written consent of UM having been first had and obtained;
(6) I am fully aware that if in the course of making this Work I have infringed any copyright whether intentionally or otherwise, I may be subject to legal action or any other action as may be determined by UM.

Candidate's Signature Date

Subscribed and solemnly declared before,

Witness's Signature Date

Name:
Designation:

ABSTRACT

Cutting of mangroves along the Malaysian coastlines has exposed these areas to tidal inundation and wave action. These areas have experienced severe erosion. Dikes have been constructed across the eroding coastlines to preserve these low-lying lands from flooding. Although these structures are often successful as rectification measures, they have negative impacts on the environment. It is essential to develop novel coastal protection methods that better integrate with the natural environment.

The primary objective of this study was to propose innovative eco-friendly revetments for coastal protection. Based on the empirical methods, this study introduces the *Double-layer* and *LEco* revetments. Laboratory experiments and numerical models were used to verify the performance of the developed structures. A pilot project was carried out in a representative eroding site at the muddy coast of the Carey Island, Malaysia. This study introduced an integrated coastal rehabilitation program. A series of mangrove plantation works were established to rehabilitate the area towards a long-term trajectory restoration. Further, two indigenous species of coastal flora were planted on the revetments to include more green elements in the systems.

A series of experiments evaluated the efficiency of the developed revetments. The innovative and sustainable *LEco* armoring unit ($K_D = 20$) had a negligible displacement ($< 7.8 \pm 0.1$ *mm*), when used on the *LEco* revetment of $\theta = 53°$. Numerical study under various loading conditions was carried out for the developed revetments. Performance of the systems was evaluated to be safe based on the factors of safety against the high exit gradient (> 3), uplift pressure (> 1.5), and sliding (> 1.3).

The study site was monitored for changes in topography and physical changes. Construction of the revetments was successful for establishing a state of equilibrium for the sediment deposition. This finding is important because the increase in sediment burial

depth has a negative impact on mangrove rehabilitation works. Characterization of the near-surface soil stratum indicated that the site has a high buffer of silt and clay content (60-70%).

This study carried out a series of mangrove rehabilitation works at two zones within the study site. Zone A was protected behind a detached breakwater and zone B was beyond the shelter of the structure. Measurements showed that six months after the beginning of the replanting works, the average mortality rate of the replanted mangroves for zone A (5.1 ± 0.1 %) and B (45.8 ± 0.1 %) decreased to 0.8 ± 0.1 % and 12.3 ± 0.1 %, respectively. Plantation of the coastal flora species exhibited a negligible mortality rate, when planted on the deck of the revetments. These findings suggest that the rehabilitation works were successful.

In conclusion, the proposed integrated coastal rehabilitation program was efficient in providing a calm area to shelter the replanted mangroves. The revetments facilitated the growth of coastal vegetation by establishing an equilibrium state. The site is representative of the majority of areas along the coastlines of the West Malaysian Peninsular. Therefore, the findings can be a gear towards mitigating coastal erosion and mangrove degradation problems at similar sites.

ABSTRAK

Sejak beberapa dekad yang lalu, jelas menunjukkan bahawa dengan memusnahkan hutan bakau di sepanjang pantai Malaysia telah mengakibatkan kawasan-kawasan ini terdedah kepada ribut, banjir pasang surut dan hakisan ombak. Oleh itu, kawasan-kawasan ini telah mengalami hakisan yang teruk. Dalam usaha untuk memelihara kawasan yang berkedudukan rendah dari banjir dan juga pengunaan tanah untuk penanaman, daik telah dibina di seluruh pantai yang terhakis. Walaupun struktur ini berjaya sebagai langkah-langkah pembaikan, ia juga menyebabkan kesan negatif kepada alam sekitar. Oleh itu, adalah penting untuk membangunkan kaedah yang mesra alam untuk perlindungan pantai yang lebih baik.

Objektif utama kajian ini adalah untuk mencadangkan sistem lapisan perlindungan mesra alam yang inovatif untuk perlindungan pantai. Berdasarkan kaedah empirikal, *dwi-lapisan* dan lapisan perlindungan *LEco* telah diperkenalkan untuk kajian ini dengan menggunakan eksperimen makmal dan model berangka telah menunjukan hasil yang positif dan ini telah diteruskan dengan projek perintis yang telah dijalankan di tapak pantai yang terhakis iaitu di pantai berlumpur di Pulau Carey, Malaysia. Kajian ini memperkenalkan program pemulihan pantai bersepadu. Dalam hal ini, satu siri kerja-kerja penanaman semula bakau telah dijalankan untuk memulihkan semula kawasan itu ke arah jangka masa panjang. Selain itu, untuk memasukkan unsur-unsur yang lebih hijau dalam sistem, dua spesies asli flora pantai telah ditanam di atas dek dan permukaan lapisan perlindungan.

Satu siri eksperimen tertakluk kepada pelbagai konfigurasi makmal telah dijalankan untuk menilai keberkesanan lapisan perlindungan. *LEco* unit armoring ($K_D = 20$) mempunyai anjakan kecil ($< 7.8 \pm 0.1$ *mm*) apabila digunakan pada lapis lindung *LEco* di $\theta = 53°$. Di samping itu, kajian di bawah pelbagai keadaan bebanan telah dijalankan bagi

LEco dan lapisan perlindungan *dwi-lapisan* yang diperkenalkan. Prestasi sistem ini telah diuji berdasarkan faktor-faktor keselamatan terhadap kecerunan (>3), tekanan (>1.5), dan gelongsor (>1.3). Susun atur awal telah dipinda untuk memasukkan keadaan tempatan dan kemudian aktiviti pembinaan bagi projek perintis telah dilaksanakan.

Tapak kajian telah dipantau dari segi topografi dan pembahan fizikal. Pembinaan lapisan perlindungan berjaya untuk mewujudkan keadaan keseimbangan untuk pemendapan sedimen. Penemuan ini adalah penting kerana peningkatan dalam kedalaman pemendapan sedimen mempunyai kesan negatif kepada kejayaan kerja-kerja pemulihan bakau. Di samping itu, pencirian stratum tanah berhampiran permukaan menunjukkan bahawa kawasan ini mempunyai penampan yang tinggi kelodak dan kandungan tanah liat (60-70%).

Satu siri kerja-kerja pemulihan menggunakan spesies bakau asli telah dijalankan di dua zon dalam kawasan kajian. Zon A telah dilindungi di belakang pemecah ombak yang terpisah dan zon B adalah di luar perlindungan struktur. Selepas enam bulan pertama pemantauan, kadar kematian purata bakau ditanam semula untuk zon A (5.1 ± 0.1 %) dan B (45.8 ± 0.1 %) menurun kepada 0.8 ± 0.1 % dan 12.3 ± 0.1 %. Di samping itu, spesies flora pantai yang ditanam di atas lapisan perlindungan juga menunjukkan kadar kematian yang rendah. Penemuan ini menunjukkan bahawa kerja-kerja pemulihan pantai menggunakan kaedah ini menghasilkan kejayaan yang diharapkan.

Kesimpulannya, program pemulihan yang dicadangkan telah berjaya menyediakan kawasan yang sesuai untuk tempat perlindungan bakau. Di samping itu, lapisan perlindungan ini juga dapat menggalakkan pertumbuhan tumbuh-tumbuhan pantai. Tapak kajian adalah wakil majoriti kawasan di sepanjang pantai barat Semenanjung Malayisa. Oleh itu, hasil kajian ini akan menjadi persiapan ke arah mengurangkan hakisan dan kemusnahan bakau masalah pantai di Malaysia.

ACKNOWLEDGEMENTS

This thesis could not have been completed without the kind support and sincere advices of *Dato'. Prof. Ir. Dr. Roslan Bin Hashim*. Words are in short to describe the efforts been made by this humble man for this work. I must express my gratitude for his supervision and moral lessons throughout the preparation of the work.

Moreover, I shall thank *Professor. Associate. Dr. KI-IL Song* for his patience to read and review my research activities. His advices shaped my academic mindset and his guidelines will be like a torch to light up my future career path.

I should also be grateful of helps and supports of my lovely parents and kind grandmother, *Azam*, *Dr. Samsudin Bin Haji Taeb*, *Dr. Mansoor Baghersad*, and *Mr. Mohd. Termizi Bin Mohd. Kassim*.

Finally, I acknowledge the support and funding received to accomplish this research:

1. Funding from *HIR-MOHE Engineering grant* no. "UM.C/HIR/MOHE/ENG/34" and awarding the *GRAS scholarship (2012-2015)* to pursue this degree.

2. Support received from *Institute of Ocean and Earth Sciences (IOES)*, University of Malaya through providing research/transportation facilities.

3. Transportation facilities and funding for research from *UPUM Sdn. Bhd.* (Consultancy Unit University of Malaya).

Shervin Motamedi *Spring 2016*

TABLE OF CONTENTS

LIST OF FIGURES

LIST OF TABLES

LIST OF SYMBOLS AND ABBREVIATIONS

α	:	Angle of revetment slope
γ_s	:	Bulk Density of soil
γ_S	:	Unit weight of armoring block
δ_s	:	Design storm surge
δ_t	:	Spring tidal range
δ_w	:	Wave setup
δ_z	:	Design storm surge
Δ	:	Relative buoyant density
ε_m	:	Surf similarity parameter
εmc	:	Coefficient of transition
θ	:	Slope angle
ν	:	Velocity of flow
ρ_a	:	Unit density of armoring units
ρ_c	:	Unit density of concrete
ρ_w	:	Density of seawater
ϕ	:	Angle of internal friction
Φ	:	Packing density
A_e	:	Mean cross-section eroded/eroding area
BH	:	Borehole
BS	:	British Standards
CI	:	Carey Island
d_b	:	Water depth at wave breaking point
d_s	:	Water depth at the toe of the structure
C	:	Cohesion
CRL	:	Maximum controllable level
CS	:	Cockle shell
$D\%$	:	Relative damage
D_{b85}	:	Grain size of the base layer
D_{f15}	:	Grain size of the filter layer
D_n	:	Nominal diameter
D_{N50}	:	Medium equivalent cubical length
DL	:	Double-Layer
F	:	Free board width
F_r	:	Froude number
FOS	:	Factor of Safety
g	:	Gravitational acceleration
GMSL	:	Global Mean Seal Level
h_e	:	Height of protection
H_0	:	Wave height at deep water
H_b	:	Breaker height
H_d	:	Design wave height
H_{mo}	:	Energy-based height of the zeroth moment
H_s	:	Significant wave height
H	:	Design wave height
HACD	:	Height above chart datum
HE	:	High elevation
I_c	:	Critical gradient
I_e	:	Predicted or measured exit gradient
K	:	Hydraulic conductivity

K_D : Coefficient of stability
K_{rr} : Stability coefficient for angular or graded riprap
L_0 : Wave length at deep water
LE : Low elevation
M_{50} : Medium mass of armoring unit
MC : Mohr-Coloumb
MHW : Average of high tide
MLLW : Mean lower low water
MLW : Average of low tides
MTL : Average of high and low tide
MN : Range of tide
MP : Morgenstern-Price
MSL : Mean sea level
N : Number of waves
N_L : Geometric linear scale factor
N_{od} : Relative damage parameter
N_s : Stability number
OMC : Optimum moisture content
P : Coefficient of permeability
PFA : Pulverized fuel ash
r_{min} : Minimum layer thickness
R_{max} : Maximum run-up
RMSE : Root mean square error
RTC : Relative topographic change
RTT : Relative topographic change over total topographic change
RTT_i : Relative topographic change over initial topographic change
S : Dimensionless damage parameter
S_r : Specific gravity of the unit
SPT : Standard penetration test
SWL : Still water level
T_m : Mean wave period
T_p : Spectral peak period
$T_s e$: Thickness of the secondary cover layer
TBM : Temporary benchmark
TTC : Total topographic change
UCS : Unconfined compressive strength
UCT : Unconfined compressive test
W : Mass of armoring unit
W_{min} : Minimum weight of the armoring unit
W_L : LEco unit mass
W_S : Minimum weight of the secondary cover layer

LIST OF APPENDICES

CHAPTER 1: INTRODUCTION

1.1 Introduction to coastal protection

Coastal areas are rapidly developing owing to their delightfulness for recreation activities and scarcity of land. Over the last decades, the world population that resided in the coastal areas has been multiplied. This trend is anticipated to be persistent in the forthcoming years (Small & Nicholls, 2003). These have led to an ongoing pressure exerted on the authorities to legitimize the efforts to protect the coastal areas (Piwowarczyk, Kronenberg, & Dereniowska, 2013).

The current state of coastal community presents unfavorable impact of anthropogenic activities on the environment (Sheaves et al., 2014). For instance, in many coastal areas, the consequences of climate change particularly in the view of sea level rise have already been experienced (Anderson, Wallace, Simms, Rodriguez, & Milliken, 2014). The rising sea-level is accompanied by more frequent storm events, coastal flooding and erosion, and gradual submersion of low lands (Church & White, 2011). Even under the most optimistic mitigation scenarios, these impacts are likely to be considerable and will continue increasing over the next decades.

The decline in the extent and livelihood of coral reefs (Graham, Nash, & Kool, 2011), salt marshes (Coverdale, Bertness, & Altieri, 2013), seagrasses (Short et al., 2011, 2014) and mangrove forests (Krauss et al., 2008) are examples of negative effects of climate change on the flora aqua-species. The coastal flora species play a key role in the protection of coastal areas. For instance, their ability for attenuating waves and reducing the flood risks are of high importance for protecting the coastal areas (Kathiresan & Rajendran, 2005).

The global trend in the decline of these species has resulted in loss of all the supportive, regulating and cultural services that they offer to coastal communities (Balmford et al., 2011; Cardinale et al., 2012). In addition, rapid acceleration in the sea-level rise and escalation in storminess conditions necessitate the incorporation of innovative techniques to the conventional coastal protection measures. Integration of natural elements into the coastal protection structures are considered as an attractive and cost-optimized method to protect the coastal areas (Feagin et al., 2010).

Up to the present, coastal protection efforts in the developed coastal zones mainly reckoned on '*hard*' structures. Even though these systems are efficient to counter the coastal hazards, they can be costly, both to construct and to retain (van Rijn, 2011). These structures are not designed to exist forever and therefore are vulnerable to failure. Many incidents were documented for these structures aggravating problems in relation to deterioration of coastal assets and erosion of the neighboring areas (e.g., Mase et al., 2013). There is an increase in the number of strategies that acknowledge the role of ecosystem in coastal protection, management and planning (Olsen, 2003). These approaches are usually known as '*soft*' coastal protection measures (Borsje et al., 2011).

A magnificent example for adaptation of ecosystem in the coastal protection is the role of coastal wetlands. On the whole, wetlands decrease the wave energy, reduce erosion and increase the sedimentation at the coasts (Barbier, 2012). Mangrove forests and salt marshes are two common vegetation covers at the coastal wetlands (McKee, Rogers, & Saintilan, 2012).

Mangroves decelerate the storm surges when a wide mangrove belt exists. For example, studies of Othman (1994), White et al. (2014), Lee et al. (2014), and Giri et al. (2014) proved that at least several kilometers of mangrove tracts may be necessary to observe alleviating impacts on the storm surges. Unfortunately, a large body of literature on the effect of mangroves for coastal protection lacks experimental control and data verification which commonly leads to exaggeration of their role in the coastal protection (e.g., Xu, Zhang, Shen, & Li, 2010).

1.2 Problem statement

The coastal areas are inhabitant to numerous terrestrial and aquatic species which have influenced the well-being of mankind (Lotze et al., 2006). In many coastal areas the impacts of climate change have been experienced to a significant extent (Parmesan & Yohe, 2003). The impacts, such as the coastal erosion and flooding (Kirshen et al., 2008), have put the integrity of coastal environments at risk.

Coastal erosion is a natural process that takes place across the length of coastlines (Leatherman, Zhang, & Douglas, 2000). It occurs due to the hydrodynamic interactions of waves and currents as they approach the land mass. These are accompanied by loss of sediment buffer in some places and accretion in some others (Stive, 2004).

In the last two decades, there has been a catastrophic change in the patterns of coastal erosion around the world (Erlandson, 2008). In addition, erosion dramatically affects the coastal ecology and its habitats (FitzGerald, Fenster, Argow, & Buynevich, 2008). The decline of coastal habitats due to erosional forces is the main cause of reduced ecological services that they offer to coastal communities (Feagin et al., 2010). This has led to destruction of beaches both in dimension and living capacity for aquatic species.

Malaysia with a total coastline of 4,810 km is the home to nearly 70% of its' population (Ghazali, 2006). Malaysian waters are within the geographical boundaries of the *Coral Triangle*. This area is believed to be the global center of marine diversity, also known as the "*Amazon of the seas*" (Montagne, Naim, Tourrand, Pierson, & Menier, 2013). The biodiversity of the *Coral Triangle* is under direct intimidating remark due to climate change related problems, rapid coastal development and expansion of population (McLeod et al., 2010; Unsworth & Cullen, 2010). Studies around the world (e.g., Bellwood, Hughes, Folke, & Nystrom, 2004; Hoegh-Guldberg et al., 2007) have proved that in the last four decades these factors have resulted a high rate (30-40%) in disappearance of coral reefs and mangroves within the *Coral Triangle*; a rate that is yet persistent and increasing.

Mangrove forests are mainly located at latitudes between 25°N and 25°S at the verge of land and sea in tropical and subtropical regions (Alongi, 2008). Despite all the efforts to rehabilitate the degraded mangroves (e.g., Field, 1999a, 1999b; Primavera & Esteban, 2008), they have been under persistent decay over the past few decades with the rate of 1% per annum (Polidoro et al., 2010). A study of Giri et al. (2011) on distribution of mangrove forests around the globe substantiated that total mangroves in 2010 was 12.3% lower than the amount earlier reported by FAO in 2007 (about 150,000 km^2 total surface area of the earth). Coastal erosion is one of the most influential factors that have affected the integrity of mangroves (Sakho et al., 2011).

1.3 Need for research

The west coast of Peninsular Malaysia is adjacent to the narrower channel of the Malacca Straits. This area has been natural habitat of mangrove forests for many centuries. Over the few last decades, the mangroves have been retreated due to dramatic coastal erosion in this area.

Since 1950, a large extents of inter-tidal wetland regions have been converted to agricultural farms to harvest palm oil (Motamedi, Hashim, Zakaria, Song, & Sofawi, 2014). From early 1950s to the late 1980s, the Department of Irrigation and Drainage (DID) built long stretches of *earthen dikes* along the west coast to protect the palm tree plantations against the erosional forces induced by waves and tidal inundation (Kamali & Hashim, 2011). As a common practice, during the construction works, 200 meters of mangrove belt were left between coastlines and farms to provide an additional protection (Othman, 1994). It is obvious that at that time, the merits of mangroves in the coastal communities were not recognized (Snedaker, 1984).

Recent studies on the rehabilitation of mangroves unfolded that the dikes behind the mangroves catch the water particles (Bosire et al., 2008), hence a pond is formed between the dikes and mangroves. It is evident that many species of mangroves are vulnerable to inundation (Allen, 1998). In addition, the retreat of coastlines caused by the frequent storm conditions and sea level rise has resulted in scouring of the soil beneath the mangroves' root system (Brander et al., 2012). Therefore, a massive loss of mangroves has occurred at the west Peninsular Malaysia.

Rigid one-dimensional coastal protection measures solely rely on incorporation of man-made structures to shelter the coastal environment. Although they are successful to counter the problems to some extent, if not implemented correctly, these techniques may cause long-term imbalances to the natural processes (Firth et al., 2014). Integration of *hard engineering* and *soft engineering* as described in the earlier definitions of ecological engineering (Odum & Odum, 2003) is a better alternative to alleviate the impacts caused by aritificialization in the coastal ecosystems.

A potential area of research in relation to the integrated coastal protection methods would be development of innovative eco-friendly revetment structures. Revetments are constructed along the coastlines to protect natural slopes against erosion and flooding. The need for design of novel revetment systems should be addressed by researchers to develop structures that have more ecological functions, erosion and flood control features and aesthetic values. This is believed to be the main stream in future research works to address the shortcomings of the conventional revetment systems (Borsje et al., 2011).

1.4 Research objectives

The main objectives of this research were as follows:

1. To develop eco-friendly armoring unit for coastal revetments

2. To appraise the hydraulic stability of the developed armoring unit through physical modeling

3. To develop eco-friendly cement-based mixtures for fabrication of the proposed armoring unit

4. To design, construct and evaluate the performance of the developed revetments

5. To evaluate the performance of the developed revetments for coastal rehabilitation program

1.5 Research methodology

The research objectives were established by a thorough review of the literature in relation to the ecological engineering, sea level rise, coastal protection, design and construction of revetments, and rehabilitation of tropical coasts. Figure 1.1 illustrates the flow of research activities in this study.

The initial layouts of the proposed innovative eco-friendly revetments were developed on the basis of empirical design approaches. Further, based on physical modeling, these layouts were tested in a two-dimensional flume channel for various wave set-up. In addition, numerical modelings were conducted to predict geotechnical response of the proposed revetment systems under various loading conditions. Finally, a pilot project was carried out to evaluate the effectiveness of developed systems for coastal rehabilitation purposes.

A pilot project was carried out to establish a coastal rehabilitation work at the west coast of Peninsular Malaysia. The site located at the Carey Island has undergone severe erosion over the last few decades. Moreover, a massive degradation of mangrove forests at the inter-tidal wetland adjacent to the strait of Malacca is evident. These problems made it necessary to implement an integrated coastal rehabilitation program. The program aimed to augment the hard engineering (revetment and breakwater) and soft engineering (mangrove re-plantation and vegetation plantation) towards rehabilitating the coastal environment.

In this view, six units of the proposed revetments were designed and constructed to evaluate the performance of the developed rehabilitation program. In addition, the impacts of an existing breakwater (Kamali & Hashim, 2011) at the study site was evaluated on the basis of geo-environmental changes after installation of the proposed revetments. Finally, series of monitoring activities were carried out to evaluate the response of surrounding environment to implementation of the program. The monitoring activities were carried out for a period of 12 months after construction of the revetments in terms of topography, sedimentology, biotic and abiotic features of the representative site.

1.6 Scope of the research

This main purpose of the study was to evaluate the effectiveness of the proposed revetments for coastal rehabilitation works. For this purpose, within a pilot project, two eco-friendly revetments were designed, constructed and monitored. The effectiveness of the proposed revetments with regards to rehabilitation of the coastal environment at the west coast of Malaysia was evaluated.

To provide eco-friendly materials for fabrication of the proposed armoring unit (*LEco*), two types of cement-based composite materials were developed. Prior to construction of the LEco revetment at the site, the hydraulic stability of the units were tested through experiments at laboratory scales.

To restore the environmental site condition to its trajectory level, a series of mangrove rehabilitation works was conducted at the site. The replanted mangroves were monitored for their survival rate after construction of the revetments.

1.7 Novelty and contributions

Historically, protection of coastal areas from inundation and erosion has been approached through one-dimensional engineering perspectives. In lieu of these strategies, the use of integrated approaches provides a better platform for rehabilitation purposes at the degraded environments. This is due to the negative impacts of hard structures on the coastal ecology and the surrounding environment on larger scales. More recently, the general notion of 'working with natural processes' forms the core of the adapted rehabilitation methods dealing with eventual trajectory restoration of affected biotic and abiotic features at coastal areas. This perspective is geared towards enabling coastline to oscillate freely in response to natural processes.

By adapting this concept, an innovative coastal rehabilitation program was carried out to provide a cost-effective and environmentally-friendly solution for the coastal erosion and mangrove deforestation problems along the west coast of Peninsular Malaysia. The refuges created by the installation of inventive hard structures at the representative site has promoted the process of repairing the degraded ecosystem on the tropical coasts through facilitating natural colonization by volunteer mangroves. The proposed approach can enhance the socio-economic and ecological aspects of the coastal areas underpinning the erosion mitigation plans.

1.8 Outline of the thesis

This thesis is composed of five chapters. Chapter 1 provides background information on coastal protection, statement of problem, objectives of the study, summary of research methodology and the scope of the research works. Chapter 2 presents a broad range of literature. The scope of the literature entails topics such as ecological engineering, causes and effects of sea level rise, methods of coastal protection, previous studies on various topics related to design and construction of revetments, accompanied by theoretical and practical matters related to rehabilitation of mangroves. Chapter 3 provides a thorough explanation of the methodologies employed in this study. First, desktop study for designing of the proposed revetments are delivered. For verification of the preliminary design, the details of physical and numerical modeling set up are discussed. The experimental part of this study enables enhancement of the preliminary design towards implementation of a pilot project for the integrated coastal rehabilitation program at the Carey Island, Malaysia. Chapter 4 presents the results and discussion related to the experiments and pilot project. Finally, Chapter 5 provides the conclusions and recommendations for future research works.

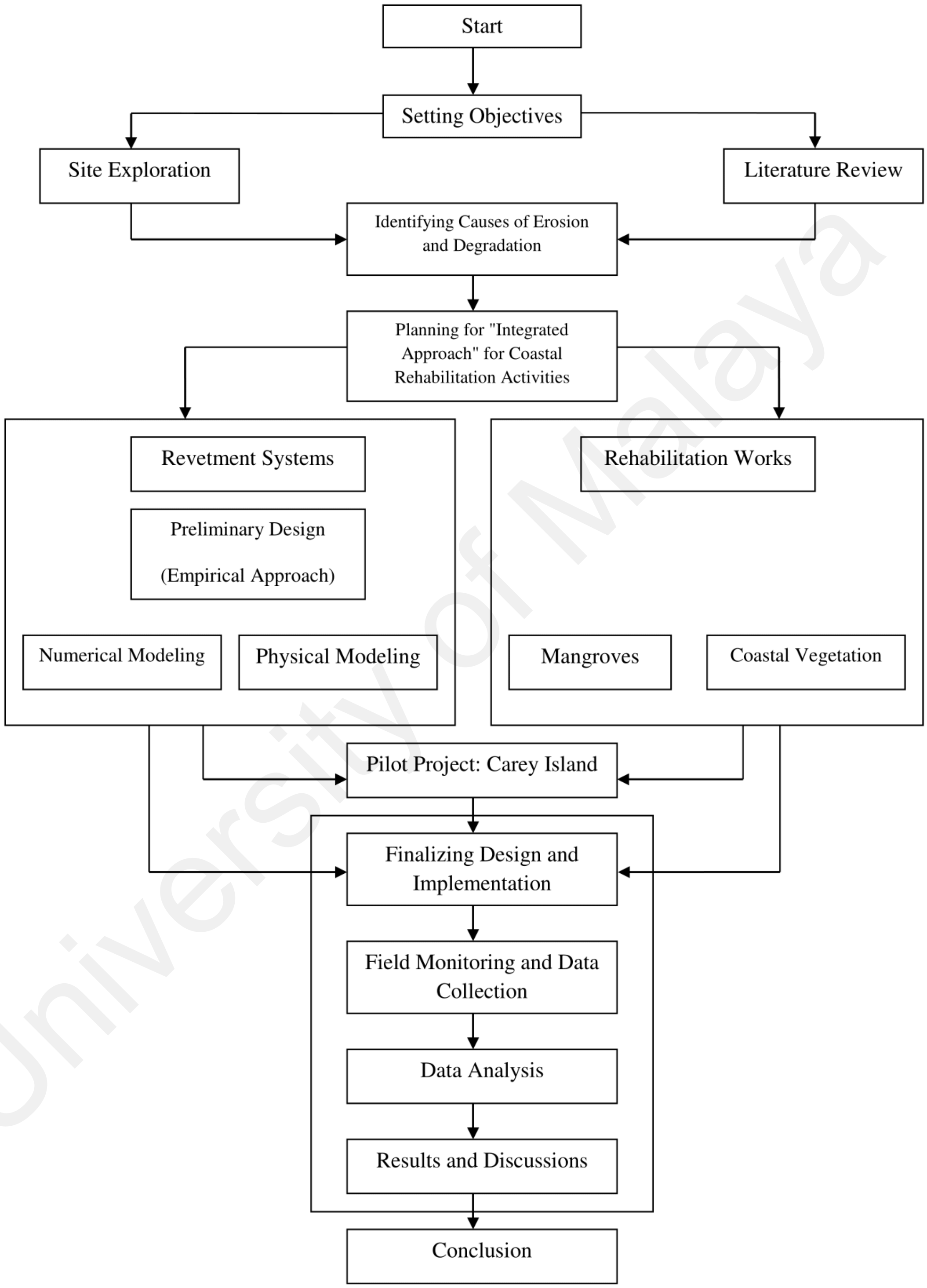

Figure 1.1: Flowchart of the research.

CHAPTER 2: LITERATURE REVIEW

2.1 Introduction

The rapid advancement in technology and industry brings forth the high demand for energy. The easiest way to satisfy this need is to utilize more fossil fuel resources. This has resulted in a tremendous increase in the amount of greenhouse gases at the atmosphere. Over the last century, the climate has uncontrollably changed. The key consequences of such changes in the climate are the sea level rise, unexpected storm events and melting of ice sheets.

The Global Mean Sea Level (GMSL) has increased non-linearly over the last century. This has resulted in the damage of coastal properties, loss of lives and ecological shifts. Such consequences must be prevented in future and the focus of efforts in restoration and rehabilitation projects at the coastal areas must set on techniques to reconcile the nature and human knowledge for the benefit of both. For instance, mangroves are the species that exist in the inter-tidal marshes at the tropical and sub-tropical areas. Due to a direct impact of the sea level rise, these species have been tremendously deteriorated in the last 30 years. There is an urgent need for mitigation measures to reduce the rate of their dissipation and restore those that have been lost.

In this chapter, Section 2.2 will discuss the concept of ecological engineering. A comprehensive review is delivered in Section 2.3 on causes and effects of the sea level rise. Various approaches of coastal protection are distinguished in Section 2.4. Emphasis in this section is on rather a conceptual understanding of hard and soft engineering methods to counter the coastal hazards. Revetments as a common type of coastal defense structure are reviewed in Section 2.5. The key matters related to the integrity and safeties of these systems are discussed as well. Finally, the importance of mangroves and some examples of successful mangrove rehabilitation projects are delivered in Section 2.6.

2.2 Fundamental elements of Ecological engineering

The term *ecological engineering* was first introduced by Howard T. Odum in early 60's (Odum, 1962). Since then, many research works have been have attempted to enhance the concept (e.g., Mitsch, 2012).

The initiations in the field were first established by the works of traditional engineers and applied ecologists as well as the engineers with basic training in ecology and frontiersmen in the field. In spite of all the efforts, the lack of integrity between the theory and practice has always been considered as a setback (Mitsch, 2012). The supporters of the ecological engineering agree that there is a doubt in the availability of quantitative basis in this discipline (Costanza, 2012; Stokes et al., 2012). Some critics (e.g., Seddon, 2010) believe that the deep rooted science of environmental engineering is self-sufficient for remarking environmental challenges. At present, there is a general debate on the recognition of ecological engineering discipline as an emerging science.

A conventional description of ecological engineering is "*a combination of design methodologies to deal with ecological systems*" (Heinimann, 2010). A more recent design agreement on the definition of the discipline is "*the design of sustainable systems, consistent with self-design and other ecological principles, which integrate human society with the natural environment for the merits of both*" (Mitsch, 2012).

In spite of all the efforts, currently, the ecosystem is downgrading, putting the survival of mankind at risk. From there, the new discipline of ecological engineering was established aiming to protect the ecosystem and humankind. The basic engineering methodologies coupled with the fundamental applied sciences has formed the base of ecological engineering discipline.

2.3 Sea level rise and changes at coastal areas

The future projected rates of sea level rise do not fit into the current coastal management scenarios (Pethick, 2001). These high rates have already drawn the attention of the countries with wide coastline stretches (Alexander, Ryan, & Measham, 2012). Of particular interests are the nations that live at small islands and low-lying regions. These areas are highly defenseless against the erosional forces and flooding events if the sea level rise continues. Probable as it may sound, a huge portion of the world population residing at the coastal areas will likely be forced to accept migration to other countries. Thus, the sea level rise as major consequence of climate change has been emphasized in recent coastal management scenarios.

The sea level differs in space and time ascribable to coastal processes, i.e., waves and tide. The Mean Sea Level (MSL) at a specific point is put into words as the average of sea horizontal surface elevation over a time span (Chambers, Merrifield, & Nerem, 2012). This period must be sufficient to the extent that the fluctuations due to waves and tide are significantly negligible. The MSL varies spatially throughout the world. If the mean sea level is divided by total area of global ocean, it returns the Global Mean Sea Level (GMSL).

The causes of rise in the sea level are not only those linked to the climate change. It is widely known that the MSL has had fluctuation up to 120 meters for the past several hundred years in the Holocene as a result of changes in glacial and inter-glacial periods (Rashid, 2014). The more recent sea level rise due to climate change is unique in the sense that the drastic jump in the sea level has never occurred in such a huge scale (Siddall, Stocker, & Clark, 2010).

The most up to date data on impacts of climate change on the sea level has been published by the *Intergovernmental Panel on Climate Change* (IPCC). Since its foundation in 1988, the IPCC has produced five comprehensive evaluation report on the future sea level rise by 2100 (IPCC, 1990, 1996, 2001, 2007, 2013). From the first to the last report, the expected sea level change has been reported differently. The most important reason for the difference among the projected MSL values is that the IPCC has applied non-identical scenarios to the climate models. Therefore, it is believed that these values may only be valid for the lowest-bounds of actual sea level in the future (Jacob, Wahr, Pfeffer, & Swenson, 2012).

Subsequent to the publication of the fourth IPCC assessment report, many more definitive and precise statistics on the sea level rise was provided (e.g., Cazenave & Llovel, 2010; Kemp et al., 2011) by enhancement in analysis of data collected via tide gauge and satellite altimeter.

At the moment, the data collected via 1,900 tide gauges in around 200 countries are being transferred to the *Permanent Service for Mean Sea Level* (PSML) (Church & White, 2011) at Bidston Observatory, Proudman Oceanographic Laboratory, U.K. In spite of the fact that the number of gauges is considerable, these are unevenly distributed in the northern hemisphere. To reach long-term and reliable variance in the GMSL, it should be ensured that the land movement measurements at the observing points are subtracted from the uncorrected tide gauge data (Houston & Dean, 2011).

The satellite altimetry has turned into the most common and precise technique to measure the sea level (Grinsted, Moore, & Jevrejeva, 2010). The satellite observations were initiated via the *Topex/Poseidon* (T/P) (1992) and continued further through *Jason-1 and 2*. The errors were gradually improved through modification of the system design and data processing methods. Compared with the tide gauges, the satellite altimeter has two advantages; first, the absence of land movement noise in the data and second, the ease of access to a vast horizon as well as recurrent revisit patterns (Oreiro, D'Onofrio, Grismeyer, Fiore, & Saraceno, 2014).

Numerous authors (e.g., Wunsch, Ponte, & Heimbach, 2007) have outlined the contemporary rise of the GMSL. Figure 2.1 depicts a tour d'horizon of the upward trend for GMSL in the period of 1860-2009. From this Figure, it can be observed that the GMSL increment rate was not significant before 1930. In addition, the graph shows an accelerating pace ever after that point. Church and White (2011) reported that the GMSL rise for the period of 1880 until 2009 was 0.21 m, a rate that is two times higher than 0.4 mm per annum (1993-2009) and to 0.2 mm per year (1900-2009).

Figure 2.2 shows the rise of GMSL for the period from 1993 to 2008 that was derived via satellite altimetry. An abrupt rise of GMSL has been recorded between 1997 and 1999, followed by a decline in 2008. These irregular fluctuations are related to hurricane events and oscillations at various parts of the world (Cazenave & Llovel, 2010). It is worthy to stress that the data obtained via altimetry since 1993 lies at the upper limits of the GMSL future projections reported in the third and fourth IPCC assessments.

2.3.1 Climate-related drivers at coastal areas

The climate change influenced the coastal physical processes (Nicholls et al., 2011). In short-term scenarios, climate change-related impacts such as severe erosion, inundation and extreme flooding events are the consequences of unforeseen wave over-topping, rainfall runoff and storm-induced surges (Kelly & Adger, 2000). In the long-term impact scenarios (Rosenzweig et al., 2008), climate change-related drivers such as massive wind and wave energy are responsible for the accelerated changes in the sediment budget at the coastal areas, thereby severe erosion and accretion events have been experienced. The climate-related drivers at the coasts are explained in the following section.

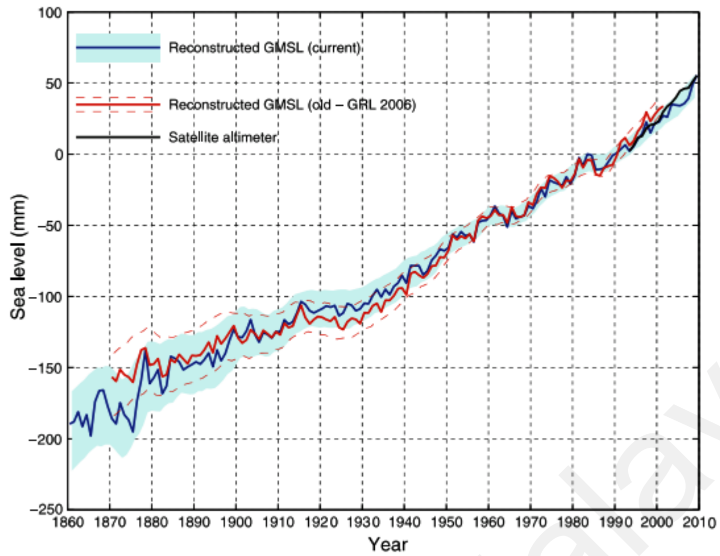

Figure 2.1: The global average sea level between 1860 and 2009 (blue). The shading indicates the one standard deviation uncertainty estimates. The red solid lines are the estimates of Church and White (2011) from 1870 to 2001, and dashed red lines illustrate the one standard deviation errors. The black line represents the satellite altimeter data from 1993 [from Miumura (2013)].

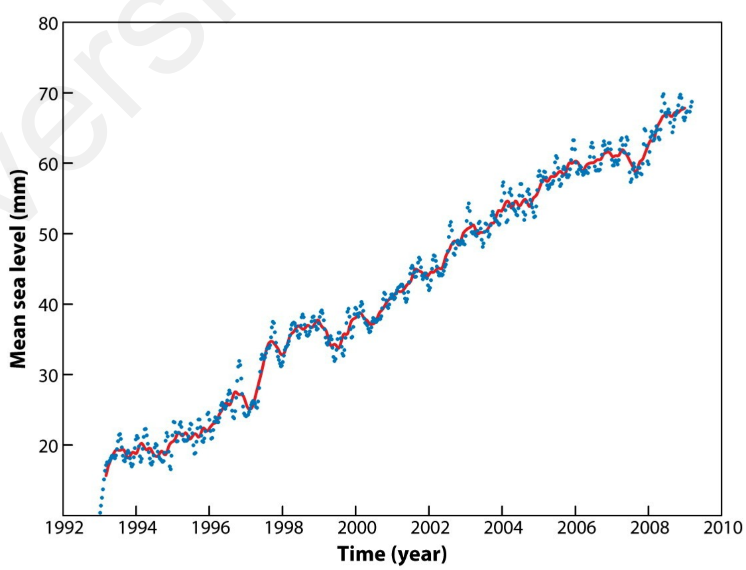

Figure 2.2: GMSL via satellite altimetry from 1993 to 2008. Red solid lines correlate with a 90-day data smoothing and blue dots represent 10-day raw data [from Cazenave and Llovel (2010)].

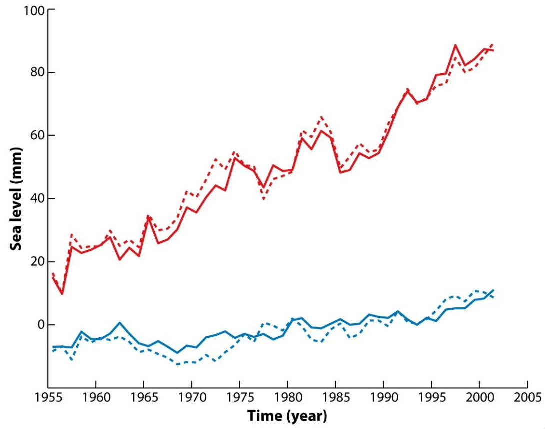

Figure 2.3: Ocean thermal expansion over the last six decades. Ishii and Kimoto (2009), and Levitus et al. (2009) reported the thermosteric SL in a time span from 1955 to 2001 that is shown by Blue solid lines and Blue dashed line,respectively. Also, the value observed GMSL from Church et al., (2004) minus thermosteric SL (*Residual SL*) is depicted by Red-dashed and Red-solid lines referring to the thermosteric SL data published by Levitus et al. and Ishii and Kimoto, respectively [adapted from Cazenave and Llovel (2010)].

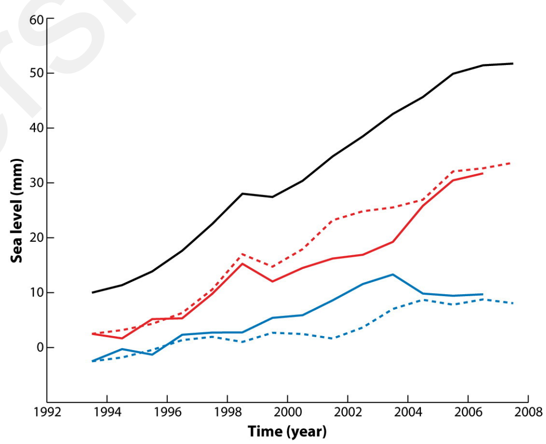

Figure 2.4: The global thermostatic SL curves from 1993. Ishii and Kimoto (2009) thermosteric SL data from 1993 to 2006 is shown in Blue-dashed lines and the Blue-dashed lines depicts the same data by Levitus et al. (2009) until 2007. The mean annual altimetry-based GMSL is illustrated in Black lines. Residual SL is shown by solid-red lines for Ishii and Kimoto, and dashed-red lines for Levitus et al. (2009) [adapted from Cazenave and Llovel (2010)].

2.3.1 (a) Extreme storms

Extreme storm events may create storm surges at the coastal waters. The magnitude of the storm surges is dependent on wave parameters, near-shore hydrodynamics, local bathymetric characteristics and storm track (Cahoon, 2006). The reliability of historical records of tropical cyclone activities during the 20th century is minimal. However, enhancements of the measurement tools since the second half of the previous century has made it possible to virtually trace an increase in the rate of occurrence and the severity of tropical cyclones (Emanuel, 2005).

2.3.1 (b) Extreme sea levels

Many factors contribute to the occurrence of extreme sea levels (ESL). These may include wind waves and swell, storm surges, inter-annual fluctuations in the sea levels, and astronomical tides (Menandez & Woodworth, 2010). Up to the present, the observed trends in the ESL have matched the direction of MSL (Cayan et al., 2008). Thus, the coastal environments are at ultimate risk, because the observations of MSL and expected projections show a clear upward trend.

ESLs are not likely to attend a simple extreme value distribution (Lewandowsky, Risbey, Smithson, Newell, & Hunter, 2014). However, such an assumption may potentially be considered as an adaptive mitigation measure to cope with the unexpected catastrophes.

2.3.1 (c) Winds and waves

The change in the wind climate significantly influences the wave climate in the large-scale. In addition, wind affects the long-shore current processes and upwelling systems (Huthnance, 1995).

The coastal sea level can also be raised via beach erosion, wave setup and run-up, all of which occur due to energy fluxes after wave breaking processes that generate currents at near-shore regions (Basco, 1985). Therefore, wind climate through wave interactions may affect the coastal geomorphology and shoreline responses (Davis & Hayes, 1984).

The direction and period of waves together with the coastline shape are other important factors in the wave climate change. For example, surface gravity waves that hold a dominant energy source, put the coastal structures at a significant risk (Hemer, Fan, Mori, Semedo, & Wang, 2013). They are also the main cause of flooding at the coastal areas with steep shelf in the absence of coastal management plans (Young, Zieger, & Babanin, 2011).

2.3.1 (d) Sea Surface temperature

In the past three decades, the sea surface temperature (SST) has increased significantly with an uneven spatial and temporal distribution. The mean rate of SST change per annum was $0.18 \pm 0.16°$ C and the mean seasonal change was -3.3 ± 4.4 days over one decade (Lima & Wethey, 2012). According to Lima and Wethey (2012), the SST observations are higher than those reported between 1971 and 2010 for the mean global ocean temperature change at 0.11 per 10 years in the upper 75 meters of the ocean area. To conclude, an increasing trend in the SSTs of global waters is observed, which is highly likely to continue in the future.

2.4 Coastal protection

The main objectives of coastal protection are to: (1) defend neighboring areas at the coasts against flooding (e.g., Nicholls, 2004), and (2) hamper erosion at the beaches (e.g., Allan & Komar, 2006). In the utmost environment, flooding occurs in wide spatial and temporal scales (Pirazolli, 2000), especially this is more significant during short term events. This indicates that the entire stretch of coastlines must be protected against flooding events. On the contrary, the erosion happens in smaller spatial and temporal space (Phillips & Jones, 2006). This indicates the effect of erosion in a more restricted temporal and spatial space.

Coastal erosion is related to storms events. They cause short-term erosion events after seasonal fluctuations that are not recovered through long-term natural processes (Dawson et al., 2009). Coastal structures are aimed to mitigate imbalances that occur in the inter-diurnal time span. Thus, mitigation of coastal erosion is somehow highly dependent on the storm damage reduction.

Coastal protection structures help reduce the damage of storms. Over the years, various conventional coastal protection techniques have been developed to alleviate the risks of erosion and flooding. Most of these mitigation measures are aimed to solve the setbacks in a site-specific scale (Kabat et al., 2009). For example, revetments and groins are constructed to reduce small-scale erosion threats (temporal and spatial), and dams are usually implemented to protect the hinterland against flooding in larger temporal and spatial scales. The following subsection discusses some of the methods of coastal protection.

2.4.1 Methods of coastal protection

The methods of coastal protection are categorized into two classes: (1) armoring, and (2) mitigation. Hard engineering is usually classified under the armed protection class. In recent years, there has been a shift from adaptation of hard to soft engineering techniques in coastal protection (Temmerman et al., 2013). The following subsections discuss various methods of coastal protection in relation to hard and soft engineering approaches.

2.4.2 Hard engineering techniques

When flooding and erosion put the civilizations at risk, the construction costs of coastal structures can be justified. The followings are the details of various types of hard engineering approaches.

2.4.2 (a) Dikes and seawalls

Seawalls are massive concrete-based structures that heavily rely on their weights to counterbalance the overturning moments as well as sliding forces. Dikes are earth-dams that retain the elevated water levels from causing low-lying inland flooding. These are mainly used to avoid inland flooding due to dynamic forces of waves and extreme storm surges. The most important parameter for designing these structures is the crest height to avoid overtopping and wave run-up.

They are classified into two groups: (1) energy absorbing, and (2) non-energy absorbing. The first class is termed after the vertical structures, whereas the second class indicates structures with a sloping surface. They usually fail to perform function in the case of following events: (a) corrosion of reinforcements, (b) toe scour followed by undermining, and (c) flanking, overtopping and rotational sliding along their front face and water-ward of the structure.

Tuan and Oumeraci (2010) performed a numerical study for hydrodynamics of wave overtopping on a dike crest. They found that dikes mostly fail due to wave overtopping as well as landward slope sliding. In another study, Schutrumpf and Oumeraci (2005) confirmed that those aspects must be incorporated in the design procedure. The authors suggested a set of verified theoretical formulas based on the small scale testing.

Hieu, Vinh, Toan, and Son (2014) numerically simulated the interaction between the wave and wind at a seawall. The authors reported that the wave overtopping rate is strongly influenced by the wind condition. Koraim, Heikal, and Zaid (2014) investigated the hydrodynamic response of a seawall protected by a breakwater system. The results indicated that the reflection coefficient and run-up at the seawall are decreased after increase in the wave steepness, relative seawall width, the seawall porosity and relative water depth.

2.4.2 (b) Nearshore breakwaters

Near-shore breakwaters are aimed to reduce the wave impacts on the coastal areas through shore-parallel detached structures. They also affect the rate of littoral drift after reduction of the wave energy; thereby deposition of sediments in the protected areas contribute to formation of shoreline bulge or salient features. Generally, the main objective of a near-shore breakwater is to provide protection against the storm damage. Sometimes this is possible by stabilization of beach front-face or creating low-lying lands (i.e., wetlands) in nearshore area.

Breakwaters are categorized into several types. They can be low-crested, preventing the heightened wave transmission while reducing the construction expenditures. In addition, they may be reef type, made of homogeneous same-size stone compared with the traditional multi-layer design.

Many studies were carried out to evaluate the efficiency of nearshore breakwaters to mitigate coastal related problems. For example, Sharifahmadian and Simons (2014) proposed a 3D numerical model for estimation of spatial transmission coefficient behind the submerged breakwaters. The authors used machine learning algorithms to validate and correlate the experimental data with the projected results. Also, Du, Pan, and Chen (2010) employed the wave overtopping modules for changes of the morphological and hydrodynamic characteristics around the installed breakwaters. The authors concluded that it is imperative to include the wave overtopping in the modeling of the near-shore breakwater.

2.4.2 (c) Revetments

Revetments are formed of erosion resistant materials placed on the existing dike, embankment or slope near the coastlines to protect them against wave impacts and storm surges. They are usually made up of three main layers; (1) armoring layer, (2) filter layer, and

(3) toe protection. The details of various aspects of revetment structures are discussed in section 2.5.

2.4.3 Integrated approach for coastal protection

Over the last decade, integration of ecology processes with coastal protection have been significantly developed (e.g., van den Hoek, Brugnach, & Hoekstra, 2012). This advancement is due to the emerging needs for sustainable, novel and cost-optimized coastal protection methods that attend to climatic change risks as well as the urgency to lessen the anthropogenic effects in the coastal environment as a result of installation of barrier structures. The latter also necessitates establishment of new methods to improve ecosystem function (Lewis III, 2005).

In order to meet these needs, two theoretical design platforms have been initiated by which the ecology is integrated into the coastal protection: (1) utilizing selected eco-engineering species that adjust to their surrounding environment to improve coastal protection methods in terms of expenditures (Day et al., 2007), and (2) adapting conventional coastal structures to reinforce ecosystem livelihood and regional biodiversity (Martin et al., 2005).

Eco-engineering species are able to amend their surrounding environment. Some examples of these species are oyster beds, mussel beds, mangroves and coral reefs (Borsje et al., 2011). For instance, these species are capable to net and preserve sediments at inter-tidal areas (Spalding et al., 2007). In addition, these species are conductive to function as effective coastal barriers. Coastal vegetations play an outstanding role when it comes to coping up with the sea level rise. They are effective measures for coastal protection by increasing the soil elevation. This signifies that they are practical, sustainable and cost-effective solutions for coastal protection (Beger, Jones, & Munday, 2003).

In the utmost environment conditions, these species are essential to alleviate the stress factors and enhance ecosystem function. They are known to be the host for micro-organism that would be incapable to bear nature brutality in any other way (D'Hondt, Rutherford, & Spivack, 2002). They are either utilized to fully substitute the unnatural coastal protection structures (e.g., Kamali & Hashim, 2011), or are employed as a foreland defense mechanism to curtail the imposed forces to the coastlines (R. Hashim, Kamali, Tamin, & Zakaria, 2010). Examples of such adaptations are breakwaters coupled with the coral reefs (e.g., Burt, Bartholomew, Usseglio, Bauman, & Sale, 2009), mangrove forests, reef-forming shell species or coral reefs (Sanford, 2009).

Increasing the recognition of local communities for using the eco-engineering species has been possible by pronouncing their financial profits (Hsieh, Chen, & Lin, 2004). Nonetheless, in the face of the growing academic literature emphasizing on the monetary worth and conceivable use of micro-organisms, natural habitats and landscaping elements in protection of coastal areas, practical implementation of the eco-engineering species is still lingering (Bulleri & Chapman, 2010). Perhaps, this may be associated with the absence of pilot projects and law enforcement on how to assimilate the eco-engineering species in the design of coastal protection structures.

At the present time, it would be unrealistic to propose replacement of conventional protection structures with the eco-engineering species (Adger, Hughes, Folke, Carpenter, & Rockstrim, 2005). Instead, embodiment of ecological elements into coastal protection structures may be an optimal solution. This can be done by enhancing the traditional engineering design through the adjustment of natural habitation (Boesch, 2006). Although this solution may not noticeably reduce expenditures, it diminishes the environmental footprints of these structures.

2.4.4 Ecosystem engineering species

Ecosystem engineering species are termed after the organisms that alter the abiotic or biotic substances in an environment, thereby balancing the availability of resources (Hastings et al., 2007). From a practical stand point, organisms in any system are potentially ecosystem engineers (Reichman & Seabloom, 2002).

A large number of academic studies focus on the organisms that have higher engineering capacity compared with their own families, in scales of time and space (Lange, Sala, Vighi, & Faber, 2010). Several examples can be considered on the role of aqua species on the evolution of coastal ecology and environment. For example, in case of larger vegetation cover, mangroves have a positive effect on protecting the hinterland against tsunami and massive wave impacts (Alongi, 2008). The results of a laboratory study by A. M. Hashim and Catherine (2013) proved that the wave height reduction in areas covered with mangroves is two times higher than the bare land. In another study, Horstman et al. (2014) found relationships between the wave attenuation rates and the sedimentation rates in mangroves. The authors investigated the sediment characteristics and vegetation densities at a mangroves fringing estuaries in the southern Andaman region of Thailand. They reported that the average wave attenuation rates increased up to 40% when traveling in sparse to dense mangrove cover. Also, it was found that the increase in wave attenuation rates in the mangrove forests leads to enhancement of sediment deposition and refinement of bed material. Consequently, this made the area to be conductive for establishment of mangrove restoration and rehabilitation projects in future attempts.

In a smaller scale, the oyster beds and mussel beds have the same impacts on the wave fluxes and sediment retention capacities of the coastal environment (Reise, 2002). They greatly enhance the regional water quality through filtering the water (Lindahl et al., 2005). This expedites a better living capacity for other coastal habitat along with the diversified community.

2.4.5 Incorporation of ecological engineering in coastal protection

Integration of ecosystem species and engineering methodologies in coastal protection necessitates drawing a distinction in relation to different spatial and temporal scales. In small scales, for instance, the breakwaters are aimed to defend the low-lying lands against erosion and flooding. Introducing the ecosystem engineering in the design of breakwaters may be beyond the bounds of possibility considering the imbalances induced by the hydrodynamical forces. Thus, modifications in the design of these structures in means of pattern and material must be implemented to adapt the engineering structure for providing a more suitable condition for settlement and growth of species while maintaining the stability (Borsje et al., 2011).

Whether the replacement of coastal protection measures in shallow water zone with ecological engineering is feasible or not, is still an open question. Recently, Schmitt, Albers, Pham, and Dinh (2013) reported efforts to prevent coastal erosion and restore the narrow mangrove belt located at the Soc Trang, Mekong Delta of Vietnam. The authors declared that utilization of Bamboo T-fences as a type of near-shore breakwater system can help the mangrove restoration projects and erosion control plans. They reported that the system is effective to dampen the wave energies and thereby increase the sedimentation rate.

In a larger scale, incorporation of eco-engineering species in the design of revetments can help alleviate the wave energies on coastlines and thereby prevent the possibility of erosion events. Oyster and mussel beds are known to be effective in attenuation of waves and stabilization of bed surface. Brinkman, Dankers, and van Stralen (2002) assessed the habitat suitability in Dutch Wadden Sea and attested that distribution of mussel beds is dependent on the sediment grain size at the bed, wave action and submerging time. In addition, mussel beds have a ceiling of 5-10% coverage on an inter-tidal flat system due to food competition (Hertweck & Liebezeit, 2002). Thus, oyster and mussel beds can be incorporated in the revetments to a limited scale, providing that the food competition criteria and adaptability of these species for site-specific conditions are met.

In a floodplain scale, dikes are used to protect the hinterland against flooding. These structures have to withstand wave impact during high water levels. High dikes can provide shelter for the inhabitants living near them. By constructing willow floodplains in front of these structures, their design can be lowered due to the wave damping by the vegetation. Compared to the mussel and oyster beds, the willow floodplain is less sensitive to physical conditions (Borsje et al., 2011).

On a landscape scale, it is possible to strengthen or partly replace engineering constructions by ecological elements (i.e.,creation of artificial dunes and wetlands). Establishment of artificial dune and wetland growths is known to be dynamic (e.g., Sun et al., 2010), requiring good monitoring and comprehensive understanding of the characteristics of these ecological elements.

2.5 Revetments

Revetments are often made up of resilient stones, rock and concrete blocks. They provide armoring layer for natural slopes at the shoreline. In general, the revetments are constructed in three layers: (1) armoring, (2) filter layer(s), and (3) toe protection against scouring.

The armor layer of these structures is made of concrete blocks or random mass of stone and rock. In the case of concrete blocks, these structural elements are sufficiently interlocked to create a geometric well-arrayed pattern (Hedar, 1986). The filter layers are aimed to drain the excess water from front-face and underlying substrates (Escarameia, 1998). Toe protection measures counterbalance the impacts of undermining and scouring at the toe of the revetments (Reeve, Chadwick, & Fleming, 2004).

Revetments provide a shelter for the hinterland, although they may behave as a wave reflector causing the neighboring and front side of shore to erode (Bezuijen, Klein, & Breteler, 1987). The inclination of the structure plays the key role in reflection of waves. The higher steepness contributes to more erosion, thereby less wave energy dissipation. The problem is less prevalent in stepped, curved or less inclined surfaces whereby excessive energy is either dissipated or absorbed (Kamphuis, 2010).

Quality of design for revetments depends largely on the scale of the project. If the objective is to estimate the costs and find alternative protection measures, preliminary design standards are sufficient. However, prior to implementation of final design, the performance of the structures must be verified using experimental and numerical studies (CEM, 2002). These would result in remarkable cost saving and refinement of the structure before construction.

In this section, the literature is compiled to address various aspects of revetments structures in the view of planning, design and construction.

2.5.1 Conventional revetment structures

In the following, various types of conventional revetment structures in relation to their armoring layers are discussed.

2.5.1 (a) Stone revetments

Stone revetments are easy and low-cost to construct and maintain. They are made of either quarry stone or riprap (Figure 2.5a). Quarry stones are large stone pieces of similar sizes, while ripraps are the stones in the intermediate scales of rock size classification. The construction of riprap revetments is more difficult as distribution of stone sizes should be accurate (CEM, 2002).

When wave impacts are low, the riprap revetments are considered as an economical alternative, enabling access to the material near to the site. Quarry stone revetments are more suitable for the coastal environment with higher wave energy owning to more stability (CEM, 2002).

Stone revetments can be easily constructed on almost any soil texture. The developed damages are minimal, thereby the structure can still function satisfactory if any malfunction is experienced. Owning to their rough surface, they are highly resistant against overtopping and wave runup (de Waal & van der Meer, 2011). Ahrens (2011) provided a complete review on the evolution of revetments, particularly the stone revetments. He conducted numerous laboratory studies using different configurations to predict the critical mass of the stone required for protection of shorelines when revetments are aimed to be installed. In another study, Kearney and Kobayashi (2000) performed 27 tests in 3 spectral wave peak periods and 9 depths of water at the bottom of a 1:2 revetment. The objective of the study was to investigate the probability distribution of the waterline elevation. The results indicated that at the bottom of the revetment where the water depth was shallow, the incident waves were dissipated and low-frequency waves were generated.

During the design stage, the recommended slope steepness is usually 1:2 (CEM, 2002). The steeper slopes provide a reduction in wave runup potency up to 50% of the slope inclination (Kamphuis, 2010). In general, the revetments, being non-vertical have very low susceptibility against the wave reflection. In practice, filter layer of proper size is provided to retain the slope materials that are vulnerable to wave impacts as a result of voids between the revetment stones (Vick, 2013).

Larger stones for the armoring layer may result in higher dissipation of wave energy as a function of the stone weight (Pilarczyk, 1998). The most important disadvantage of these structures is that they usually require heavy machinery for implementation. The filling activities are necessary to ensure a uniform slope profile. In these instances, compaction efforts are essential considering the exclusion of debris or large stones in the filling material (Pilarczyk, 2011).

2.5.1 (b) Field stone

Field stone revetments are constructed of massive sub-rounded to rounded boulders as the armoring layer. In these structures, the void between the stones is minimal to have a close-fitting cross section (Figure 2.5b). Accurate placement of absolute rounded shapes is difficult, although an acceptable performance is feasible if care is taken in placement of stones (CEM, 2002).

2.5.1 (c) Concrete armoring units

Concrete armor units are alternatives for stone pieces in the revetment construction (Figure 2.5c). Some commercial examples of these units are: Tribars (e.g., PIANC, 1987), Tetrapods (e.g., Danel, 2000), and Dolosse (e.g., Kana, Al-Sarawi, & Holland, 2011). Some of these units provide up to five times higher protection level against the wave impacts compared with the stone armoring units.

Prefabricated concrete blocks commonly replaced the conventional stone revetments. These structural elements are employed to enhance the interlocking features of the revetment system towards providing an extra protection level against the storm surges and wave impacts (CEM, 2002). They usually form a well-arrayed geometric pattern which increases the aesthetic view of the coasts.

The main problem in handling these blocks is that if a block is displaced or becomes damaged, other blocks may fail too. This is due to interlocking feature between the blocks. Another problem with these types of structures is that they have a relatively smoother surface compared with the stone revetment causing a higher potentials for wave run up and overtopping (Kamphuis, 2010).

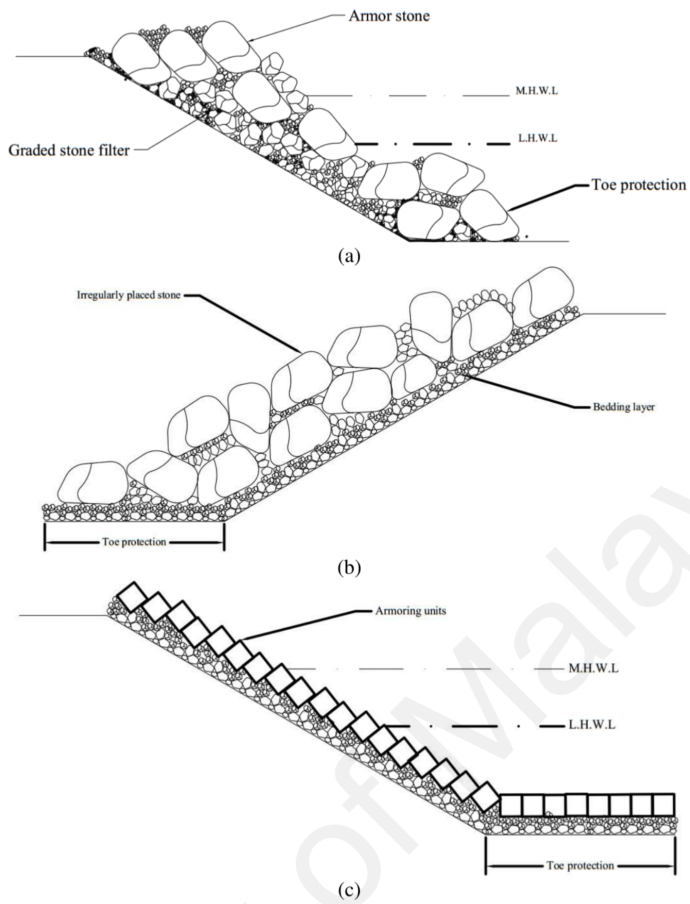

Figure 2.5: Cross section of typical (a) stone, (b) field stone, and (c) concrete armoring unit revetments.

2.5.2 Hydraulic stability of armoring units

Researchers proposed several empirical formula for predicting stability of armoring units (e.g., Koev, 1992). Although, these formula are suitable for preliminary design, on-site application of these need to consider uncertainties of physical conditions (CEM, 2002). Here, a review is delivered on some of these classical formula to identify the factors which affect the stability of armoring units.

2.5.2 (a) Formula for armoring units

Armoring units get their hydraulic stability from their weight. A stability formula determines the minimum weight of the armoring unit under extreme loading conditions. As a common practice, a qualitative stability ratio is defined as the ratio of wave force (lift force and drag force F_L and F_D) to the armoring unit buoyant force (restoring force, F_G) as in Equation 2.1.

$$\frac{F_D + F_L}{FG} \approx \frac{\rho_w D_n^2 v^2}{g(\rho_a - \rho_w) D_n^3} = \frac{v^2}{g \Delta D_n} \tag{2.1}$$

, where ρ_a is the density of armor unit and ρ_w is the density of water. D_n is the nominal diameter, v is the velocity of flow, and $\Delta = (\rho_a/\rho_w) - 1$ is the armor unit relative buoyant density. If H_b is the breaking wave height, the fluid velocity is computed using the shallow-water wave celerity, $v = (gH)^{0.5}$; hence, the stability ratio, (N_s), as it appears in most of the stability formula is given in Equation 2.2,

$$N_s = \frac{v^2}{g \Delta D_n} = \frac{H_b}{\Delta D_n} \tag{2.2}$$

For the first of its type, to calculate N_s, a formula was proposed by Iribarren Cavanilles (1938) using a simple relationship (Equation 2.3), where coefficient K depends on the shape of the unit and damage level, α is the slope of structure, and Φ is the response angle of slope.

$$\frac{H_b}{\Delta D_n} = K(tan\Phi cos\alpha \pm sin\alpha) \tag{2.3}$$

Further, Hudson (1959) introduced a formula after extensive testing with regular (monochromatic) wave (Equation 2.2). This relationship has been used widely due to its simplicity. In the Hudson formula, the phrase $cot\alpha^{1/3}$ replaces $cos\alpha - sin\alpha$ and introduces a constant K_D that is a combination of multiple parameters. In case of rubble mound structures, Φ is assumed the unity, and Equation 2.3 takes the form of Equation 2.4, where M_{50} represents medium mass of the unit. It should be noted that Equation 2.4 is valid only for the slopes that have steepness from 1:1.5 to 1:4.

$$N_s = \frac{H}{\Delta D_n} = (K_D cot\alpha)^{1/3} \rightarrow M_{50} = \frac{\rho_a H^3}{K_D \Delta^3 cot\alpha} \tag{2.4}$$

The Value of K_D was determined after a series of experiments and the recommended values were published in the Shore Protection Manual (SPM) (SPM, 1984) by the US Army Corps of Engineers (USACE). Initially, the SPM published a very small conservative value of K_D for the breaking waves. After many breakwater failures during 1970s, the USACE increased the safety margin for the armor layers.

Iribarren parameter, also known as the surf similarity parameter (ε_m), is used for defining different types of breakers in a beach (Equation 2.5). It describes the relationship between the slope of structure, $tan\alpha$, and steepness of wave; $S_{om} = \frac{2\pi H_g}{g T_m^2}$ (Battjes, 1974).

$$\varepsilon_m = \frac{tan\alpha}{\sqrt{S_{om}}} = \frac{T_m tan\alpha}{\frac{\sqrt{2\pi H_s}}{g}} \tag{2.5}$$

, where the mean wave period is represented by T_m, H_s represents the significant wave height, and g is the acceleration due to gravity.

J. Van der Meer (1988) developed an improved stability formula for breaking (Equation 2.6) and non-breaking (Equation 2.7) waves that considered the level of damage, number of waves, and structures permeability,

$$\frac{H_s}{\Delta D_{n50}} = 6.2P^{0.18}(\frac{S}{\sqrt{N}})^{0.2}\varepsilon_m^{-0.5} \tag{2.6}$$

$$\frac{H_s}{\Delta D_{n50}} = 1.0P^{-0.13}(\frac{S}{\sqrt{N}})^{0.2}\sqrt{cot\alpha}\ \varepsilon_m^{p} \tag{2.7}$$

, where P is the permeability coefficient, S is the level of damage, α is the slope of structure towards the seaward side, and N is the number of waves. Critical value of ε_{mc} is used for calculating the transition from breaking to non-breaking waves (Equation 2.8). This formula is valid for the slope angles with $cot\alpha$ ranging from 1.5 to 6. The significant wave height here is the average of one-third of the highest waves.

$$\varepsilon_{mc} = (6.2P^{0.31}\sqrt{tan\alpha})^{1/(P+0.5)} \tag{2.8}$$

In an another work Vidal, Medina, and Lomè´ŋaco (2006) suggested using H_{50} instead of significant wave height during the service life of structure for describing the damage level on the Rayleigh-distribution. Upon applying H_{50}, the Van der Meer formula converts to Equation 2.9 for breaking waves and Equation 2.10 for non-breaking waves as follows,

$$\frac{H_{50}}{\Delta D_{n50}} = 4.4P^{0.18}S^{0.2}\varepsilon_m^{0.5} \tag{2.9}$$

$$\frac{H_{50}}{\Delta D_{n50}} = 0.716P^{-0.13}S^{0.2}\sqrt{cot\alpha}\varepsilon_m^{-0.5} \tag{2.10}$$

Structures made of quarry stone have less steeper slopes due to their smaller size. On the other hand, concrete armoring units may have larger sizes. Therefore, there is no need to limit the steepness of slopes in armor layers of revetments which are formed by concrete units. Generally, the slope steepness in coastal protection structures made from interlocking concrete units ranges from 1:1.33 to 1:1.5 (CEM, 2002).

Over the years the design of concrete armoring units has been improved by enhancing their interlocking capability. For this, new armoring units are normally deployed in single layer. For example, the first single layer armor was designed in 1980 by the Sogreah Consultants (now known as Artelia Italy) (Arterlia, 2014) that was used in over 120 projects. The US Army Corps of Engineers introduced *Core-LOC* system in 1994, followed by the design introduced by the Delta Marine Consultants recently (DMC, 2014).

J. Van der Meer (1999) concluded that concrete armoring layers comprising of a single layer array of units are highly stable when compared with the double layer systems because of their high integrity. Based on these findings, *start of damage* for single layer armoring systems occurs at higher stability numbers, which is usually followed by the sudden failure. Generally, a safety coefficient, ranging from 1.3 to 1.5, is essential to obtain design stability number (J. Van der Meer, 1999).

2.5.3 Damage of armoring units

The external layers of revetments usually are formed from armoring units which are made of stones or precast concrete units. Armour layers usually are cast in-place to avoid erosion in the inner layers of revetment structures through dissipation of wave energy and countering runup and rundown (inflow and outflow) (Hazarika, Kasama, Suetsugu, Kataoka, & Yasufuku, 2013).

Coastal engineers are concerned with the damage of armoring layers. Determination of the damage level for the armoring layers is usually tied with uncertainty arises from the complexity of wave and near-shore currents, stochastic wave-structure interactions and diversity of affecting variables (Koc & Balas, 2012).

Predicting the degree of damage for armor layers largely depends on the designer's experience. Various experimental studies were conducted to enhance the design and analysis of armor layers in the coastal protection structures (e.g., J. Van der Meer, 1999; Vidal et al., 2006). The objectives of the studies were to reduce uncertainties and avoid underestimation and overestimation of armoring units weight which in turn change the degree of the expected damage of the armor layer.

Most of the equations in the literature are originally proposed for the stone armoring units. These relationships provide means for calculating the stability of the structures and evaluating the damage level. Knowing that concrete units almost similarly respond to the imposed loadings, the same equations can be used in the design of concrete armoring units (CEM, 2002).

Evaluation of the damage level for the stone armor layers can be done through: (1) surface profiling (e.g., Broderick, 1983) ,and (2) counting the number of displaced armoring units (e.g., Melby, 1999).

2.5.3 (a) Quantitative description of damage for stone armoring units

The armor layers are formed to protect the inner layers of revetments and decrease the wave energy. In order to achieve these goals, armoring units must provide sufficient hydraulic and structural stability to stay on initial position during and after extreme events. When wave forces displace certain numbers of armoring units, the underlying layer of revetment is exposed to the direct wave action. This leads to *progressive failure* of the structure depending on the duration of the sea state (CEM, 2002).

The damage of armoring units is defined as the amount of their individual displacement. Displacement of armoring units is described as shifting the mean position of armoring units when exceeding a certain distance (CEM, 2002). The evaluation of the damage level of particular armoring units is based on the type of material used in their texture. The following discusses this aspect of measuring the damage level.

2.5.3 (b) Explicit estimation of damage for stone armor layers (Surface Profiling)

Broderick (1983) introduced the S as a dimensionless *damage parameter* for stone armoring units. The damage parameter is described as in Equation 2.11.

$$S = \frac{A_e}{D_{n50}^2} \tag{2.11}$$

, where A_e is the mean eroded or eroding area of cross-section of the armor layer, and D_{n50} is the medium equivalent cubical length of stones as defined in Equation 2.12. In this equation, M_{50} is the median mass of stone grading given by 50% on the mass distribution curve and ρ_a is the mass density of stone armoring units.

$$D_{n50} = (\frac{M_{50}}{\rho_a})^{\frac{1}{3}} \tag{2.12}$$

If concrete units are used, there is no grading defined and only the mass of concrete unit is considered. Therefore, the nominal diameter of stone is denoted without the subscript 50, (D_n).

Equation 2.11 does not include the porosity of armoring units. The eroded area may be overestimated because of the porosity. In addition, the estimation of S is based on a comparison between the intact profile of the slope and the damaged profile after storm or after certain number of waves during the experiment. Thus, this leads to the assumption that the profile changes occur on the basis of erosion only. It is understood that the changes in profile of slope can also be caused by settlement (CEM, 2002).

2.5.3 (c) Implicit estimation of damage for stone armoring units (Counting)

When indirect assessment of damage for the armoring units is aimed, the damage is presented as *relative damage*, $D\%$. The relative damage is defined as the number of displaced units over the total number of units in the armoring layer or in a particular area around the SWL, known as the *active zone* (CEM, 2002).

The active zone is termed after the area between the middle of the crest to the vertical distance of significant wave height, H_s, below the SWL (CEM, 2002). In many of the existing structures, major displacement of armoring units occurred roughly in the spatial area of $SWL \pm H_s$, which is inclusive of the active zone. Therefore, the number of armoring units in the active zone is mostly taken as the reference number (total number of units) (SPM, 1984).

The available definitions of the active zone are not valid for submerged or low-crested structures (SPM, 1984). In addition, due to numerous approaches in the design of coastal protection structures, total number of armoring units is chosen differently for each structure (SPM, 1984). Thus, the estimated damage is subjective and can not be compared precisely between individual cases. The subjectivity of obtained results from the relative damage was overcome through introduction of *relative damage number*, N_{od}. This index is defined as the real number of the displaced units over the width of one nominal diameter, D_n (J. W. Van der Meer, 1988). The width is usually referenced along the longitudinal axis of the structure.

The relative damage number relates the actual displaced units in a cross-section with a width of D_n to the percentage of damage (J. Van der Meer, 1999). The enhanced definition of damage is still subjective in the sense that even though it avoids inclusion of the active zone, it is still dependent on the geometry of the cross-section and slope length (CEM, 2002).

The state of damage is largely dependent on the movement of individual units. Movement of the units can occur either as (1) total displacement out of the layer and being unstable outside the eroding or eroded area, or (2) relative displacement from the original position, reaching a stable position within the eroding or eroded area (two black units in Figure 2.6.b). In the latter case, the displaced units may still efficiently contribute to the stability of the structure. Table 2.1 presents a summary of widely accepted movement criteria for armoring units that associate the regime of movement with the S and N_{od}

Table 2.1: Displacement criteria modified after CEM (2006).

Movement Criteria	N_{od}	S_p
No movement	< 10	< 0.004
Limited movement during reshaping, eventual static stability	0.1 - 2	0.004 - 0.002
Relevant movement	> 2	> 0.002

To conclude, when implicit estimation of damage is applied (counting method), all the displaced units are considered as damaged regardless of their final position, whilst in

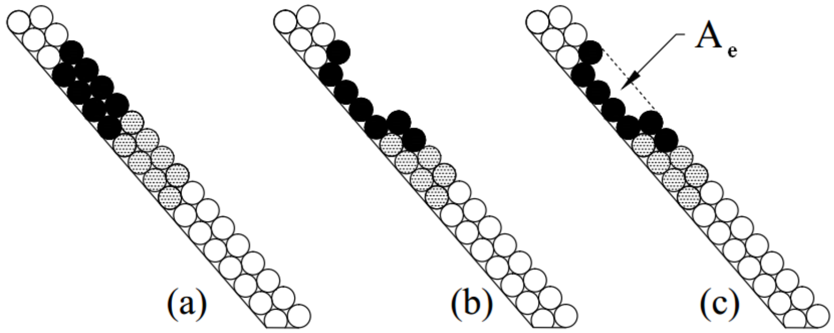

Figure 2.6: Methods of evaluation of damage in coastal structures: a) intact profile; b) damaged profile, counting method; c) damaged profile, measurement of eroded area.

explicit estimation of damage (profile measurement) only the units being unstable outside the eroding area are considered (Figure 2.6.c). Regardless of the type of movement, the integrity of armor layer is affected by displacement of units. The counting method results in overestimation of damage, and profiling measures lead to underestimation of damage.

2.5.3 (d) Damage of concrete armoring units

To evaluate the damage level of concrete armoring units, the counting method is preferred. In this regards, the number of displaced units out of the layer or the number of units displaced within a range of initial position are measured (e.g., 0.5 to 1 D_n) (Yagci, Mercan, Cigizoglu, & Kabdasli, 2005).

When concrete armoring units are of concern, a phenomenon termed as *rocking* can occur. Rocking is defined as a state of disturbance in which the armoring units move under wave action while maintaining their initial position (CEM, 2002). This phenomenon particularly can cause damage to the slender units (i.e., Dolosse and Tetrapods) (Yagci et al., 2005). Rocking is rarely recorded during small-scale studies, because the units rarely experience breakage during investigation; therefore, very few documents for rocking are available.

2.5.4 Bayesian definition of damage criteria for armor layers

The quantitative methods discussed in section 2.5.3 (a) can not associate the observed damages to the measured damages. Even though the damage parameters are able to quantify the degree of the damage, they fail to provide a physical interpretation of damage level (Vidal, Losada, & Mansard, 1995; Vidal et al., 2006).

To overcome this problem, Losada, Desire, and Alejo (1986) categorized the observed damage in to three classes namely, (1) the *initiation of damage*, (2) the *Iribarren damage*, and (3) the *destruction*. Further, Vidal, Losada, Medina, Mansard, and Gomez-Pina (1992) included an additional state of damage to the categories, termed as the *Start of Destruction* between the state of Iribarren damage and destruction. Thus, a widely accepted definition of damage criteria is as follows.

(a) Initiation of damage: this state of damage occurs when a certain number of armoring units is displaced to a distance longer than D_n from the initial position.

(b) Iribarren damage: this state of damage occurs when the units in the upper layer are cast away large enough that the units of lower armoring layer can be dislodged.

(c) Start of destruction: this state of damage occurs when the lower armoring layer experiences the initiation of damage in which a number of units are displaced through wave action.

(d) Destruction: this state of damage occurs when the armoring units continuously are displaced from the slope. Further, materials of the filter layer (secondary layer beneath the armour layer) are washed away. Eventually, if the severity of the sea state does not diminish in the course of time, the mound of the structure will gradually be destroyed.

2.5.4 (a) *Considerations in design of armoring units based on damage criteria*

It is important to consider an optimized solution to design the armoring units. If the solution incorporates a no-damage (*zero damage*) criterion, it is required to utilize a large number of massive armoring units. This turns into an uneconomical design approach. The no-damage criterion is typically termed after the condition in which the degree of damage is 2% by counting, or 5% by profiling (SPM, 1984). Thus, it is not reasonable to design armoring units for a no-damage level.

Based on J. W. Van der Meer (1988), the no-damage criterion is true when damage parameter, S, is within the range of 1 to 3. Similarly, in the case of failure (*Start of Destruction*), S exceeds 10. Thus, an optimized approach for the design of armoring units is based on the failure criteria that considers a value of S between 3 and 10.

2.6 Mangrove rehabilitation

Mangrove trees grow on a narrow interface between the land and sea. They are generally found between latitudes of 25 °N and 30 °S (Macnae, 1969), where they form a forest shelter for the complicated ecosystem dynamics and different salt water species (Ellison, 2000). Mangroves are currently being impacted globally, and the rising sea level can be directly linked to their degradation.

Mangroves provide an important level of protection in the coastal regions. They are various assemblages of trees and shrubs that are widely spread in tropical or subtropical coasts. The benefits of vegetation density have been studied extensively for years (e.g., R. Hashim et al., 2010). They have been known to have a positive impact on resolving common coastal problems such as erosion, structural inundation, and rising sea levels (Blasco, Aizpuru, & Gers, 2001).

The importance of mangroves as a coastal vegetation is well established. Mangroves are used throughout the tropics for their potential in terms of fishing, sheltering wildlife, human habitation, and aquaculture (Gedan, Kirwan, Wolanski, Barbier, & Silliman, 2011). In addition, mangroves are directly utilized in timber products (Brander et al., 2012).

Human interventions have remarkably decreased the number of mangroves in the coastal regions because of their conversion into agricultural zones and urban areas. For example, Kathiresan and Rajendran (2005) reported that mangroves had both saved lives and preserved resources during the massive tsunami on December 26th, 2004. In a more theoretical research, Alongi (2008) stated that mangroves can weaken the massive energy induced by tsunami before it hits the shoreline. In this view, mangroves are important for coastal ecology and they can be considered as a natural form of coastal protection.

Unfortunately, mangroves are perishing at a significant rate. Valiela, Bowen, and York (2001) reported that 35% of the total mangrove regions in the tropics has been lost in the last two decades. Mangrove re-plantation is the most common method for reducing the degradation trends; yet, the effectiveness of this method for restoring mangroves cover remains a subject of debate. Although replantation may be initiated at a particular threatened site, if the factors that disturb the ecological balance persist, this method will only perpetuates the cycle of failure.

Huge areas of mangroves have also been degraded by dredging, land-filling, and erosion due to storms (Brander et al., 2012). In this regards, development of techniques for their restoration and rehabilitation is necessary not only to maintain the biodiversity of the coastal areas but also for the monetary value and protective advantages they offer (Riley & Kent, 1999). In many of these restoration efforts, hard structures are still preferred. Despite the apparent beneficial outcome of these structures, their negative impacts on the ecological system are yet to be investigated.

2.6.1 Fundamentals of mangrove rehabilitation methodology

Restoration of mangroves is the reestablishment of mangroves to their trajectory original conditions whereby they have earlier grown (Ellison, 2000). These activities are funded on the ground of the restoration ecology discipline (Hobbs & Norton, 1996). This field aims to enhance the adaptive capacity and facilitate the resilient recovery of the ecosystems that have been degraded, damaged, or destroyed. Because environmental risk have ongoing impacts, to restore an ecosystem to the once-successful level, it is necessary not only to regenerate its former conditions, but also to enhance the adaptive capacity of the system against the negative human footprints in the course of time (Palmer, Ambrose, & Poff, 1997).

Rehabilitation or restoration should be considered an option when an ecosystem has undertaken changes to an extent that it cannot self-renew or self-correct (Kamali & Hashim, 2011). In these conditions, the ecosystem homeostasis reaches a permanent status of pause and the normal processes of natural recovery from destruction or secondary succession are inhibited in some way (Field, 1999a). Although, there is a significant number of literature providing great details about the rehabilitation of mangrove species (e.g., Bosire et al., 2008), practitioners in the field still emphasize on planting mangroves as the initial tool in rehabilitation activities. This approach, to a degree, may solve the problems of mangrove degradation at certain localities.

A better methodology in rehabilitation of mangroves would be to identify the causes of mangrove degradation or damage, remove the causes, and rely on the natural recovery potentials towards a successful rehabilitation of mangroves at the target site. In this respect, mangrove plantation as a tool for rehabilitation purposes, can only be effective when the natural recruitment mechanisms are inadequate for mangrove re-establishment, particularly after a suitable hydrological state is reached at the rehabilitation site (Lewis III, 2005).

Some functions of mangrove ecosystems can be restored even if crucial parameters, such as hydrological conditions and sediment characteristics, change (Kamali & Hashim, 2011). On the other hand, if the objective of restoration is to return the target area to a trajectory original condition, then the probability of failure for such expectations will increase (Schmitt et al., 2013). This implies that rehabilitation of selected ecosystem with distinguishing quality or characteristics has higher chance of success than a complete rehabilitation to original conditions (Lewis III, 2005). These facts should be strongly considered during the planning phase of any ecology rehabilitation activity.

Mangroves can reestablish themselves without plantation. In order for a non-planting rehabilitation project to be successful, a primary gear towards the possibility of a successful rehabilitation is to identify and remove the causes of environmental stressors (i.e., blocked tidal flow and inadequate sediment budget at the rehabilitation site) that may prevent mangrove recruitment (Lewis III, 2005). If there are no environmental stressors, or after they have been removed, monitoring programs should be conducted to determine the extent to which the propagules recruitment or seedlings growth occurs. At this stage, plantation of mangroves should only be considered as an alternative if natural recruitment does not occur.

As an incorrect practice, the majority of mangrove rehabilitation efforts are rerouted towards immediate plantation of mangroves without identifying the causes as to why the natural recovery did not occur. In the majority of cases, budget is spent on growing the seedlings in a nursery and planting them at rehabilitation sites even before removing the causes of environmental stressors. For example, Sanyal (1998) reported a survivability of 1.52% for the planted mangroves in India. On the other hand, provided that environmental stressors are removed from the rehabilitation site, the natural recruitment may lead to significant mangrove densities. For instance, Duke, Pinzan M., and Prada T. (1997)

reported that for a mangrove rehabilitation project in Panama, the densities of natural recruits far exceeded both the expected and the observed densities of planted seedlings in both sheltered and exposed sites.

Other factors that may influence the success of restoration strategies are the dominant and the existing ecological and physical attributes in the rehabilitation site. In this regard, site selection is the main factor that affects the success of the rehabilitation works. For selecting a suitable site for initiation of rehabilitation works, Turner and Lewis (1996) recommended that the following criteria should be considered: (a) avoid areas of high salinity, and (b) avoid areas of extreme inundation or submersion (>1.5 m) to minimize barnacle infestations, whereby a 80-100% mortality rate can be obtained; (c) avoid plantation on sea grass beds, which is important for overall maintenance of the productivity of the coastal zone; (d) avoid areas that are exposed to quick current; thus, shifting the substrates; (e) avoid open areas except when the objective is to stabilize the adjoining soil (planting on these sites should have a denser population); (f) avoid areas where the freshwater supply is scarce; (g) avoid areas with unstable soil substrate; (h) avoid areas that are highly affected by the tidal inundation, except for the daily submersion routine by the saline water; (i) consider the harmony of the target species with the existing species at the site; (j) consider the zonation (distribution) pattern for mangrove rehabilitation works and; (k) consider areas that are low energy (calm shorelines) in nature (i.e., lagoons, bays, riverine areas, and estuaries).

CHAPTER 3: MATERIALS AND METHODS

3.1 Introduction

This chapter deals with the materials and methods used in this research work. The main focus of this chapter is on design and implementation of two innovative eco-friendly revetments. For this purpose, first the empirical procedure for design of the revetments are discussed in section 3.2, 3.3, and 3.4. The preliminary design layouts were verified using laboratory experiments (section 3.5) and numerical modeling (section 3.6.4). The finalized design layouts were amended to incorporate local conditions for a pilot project at the Carey Island, Malaysia (section 3.6). The site and the proposed revetments undertook monitoring program to investigate the stability of the constructed revetments and the topographic and physical changes at the site. Finally, a series of mangrove rehabilitation works (section 3.7) and coastal flora plantation (section 3.8) were carried out at the site and the monitoring works were performed. In addition, the details for development of the eco-friendly concrete materials are discussed in section 3.9.

3.2 Considerations in design of revetments

The main considerations in the design of revetments are discussed in this section.

Shoreline Use: Shoreline use is an important element in the design of revetments (CEM, 2002). For example, stone revetments may make it difficult to access the shoreline. The revetments made of concrete armoring units usually make it impossible for the public to access the beach.

Serviceability of protection measures: Coastal protection structures are designed to safely undertake the most extreme condition at the shorelines. It is necessary that these structures experience no damage exceeding the ordinary maintenance during their life-time, or allowable safety margin is to be provided in the case of deterioration (SPM, 1984). The minimum design criteria must provide sufficient protection for at least 50% of event occurrence with the probability of being exceeded during the design life (CEM, 2002). Also, it must be assured that during extreme loading conditions, the failure does not involve loss of life or property.

Water level design: The maximum water level is required to predict the critical crest elevation of the revetment, the maximum wave height at the revetment, and the magnitude of wave runup (Kamphuis, 2010). In addition, determining this parameter contributes to prediction of the depth of armor layer as well as the extent of the toe scoring (Zanuttigh & van der Meer, 2008).

Estimation of wave height and design wave: Wave period and wave height are determined to predict the most critical impacts caused by the hydrodynamic forces on a structure (Goda, 2011). These parameters are estimated usually on the basis of visual observations, wave gauge data, maximum breaking wave, the published wave hindcast or wave forecast at the site. The critical design conditions can be derived by analyzing the extreme high and low design water levels and for single or multiple intermediate water levels.

The parameter, H_{mo}, known as the *energy-based height of the zeroth moment* provides the wave information. The value of H_{mo} and significant wave height in deep water, H_s, may be equal; however, in shallow water these might vary significantly due to the shoaling effect (Taylor & Yelland, 2001). According to Hughes and Borgman (1987), Equation 3.1 can be used to equate the significant wave height in deepwater from H_{mo}.

$$\frac{H_s}{H_{mo}} = exp\left[c_0\left(\frac{d_s}{gT_p{}^2}\right)^{-c_1}\right] \tag{3.1}$$

, where the period of the peak energy density of the wave spectrum is denoted by T_p and the c_0= 0.00089 and c_1 = 0.834 are the regression coefficients (CEM, 2002). If a conservative design is intended, the H_s can be estimated by assuming the c_0 = 0.00136 (Hughes & Borgman, 1987).

Height of protection: The height of the structure is perhaps the most significant design factor in the design of revetments. When estimating the height of design, contributing parameters, such as the maximum water level, overtopping and wave run-up, freeboard, and expected structural settlement must be taken into account (CEM, 2002).

The height of protection in reference to the MLLW (mean lower low water) can be derived from Equation 3.2.

$$h_e = \delta_t + \delta_z + \delta_w + H_d + F \tag{3.2}$$

, where δ_t is the spring tidal range, δ_s is the design storm surge, δ_w is the wave setup, H_d is the design wave height, and F is the freeboard width.

Wave Run-up: Wave run-up is the vertical distance between the SWL (still water level) and rise of the wave on the structure. According to Kobayashi and Jacobs (1985), for stone revetments the maximum wave runup due to irregular waves can be estimated from Equation 3.3.

$$\frac{R_{max}}{H_{mo}} = \frac{a\varepsilon}{1 + b\varepsilon} \tag{3.3}$$

, where the maximum run-up is denoted by R_{max} , two regression coefficients are defined as a = 1.022 and b = 0.24, and the surf zone parameter ε is calculated by Equation 3.4. In this equation, the slope angle of the revetment is denoted by θ.

$$\varepsilon = \frac{tan\theta}{(\frac{2\pi H_{mo}}{gT_p^2}^{1/2})} \tag{3.4}$$

Assuming the value of 1.286 for the regression coefficient results in a more conservative value of the maximum wave run-up (CEM, 2002). This yields a highly reasonable upper threshold limit for the data from which Equation 3.3 has been derived. Carstea (1975) proposed a correction factor for estimation of run-up for revetments with concrete armoring units. The authors suggested that should $1.3 < \cot\theta < 3$, then the correction factor that applies to the Equation 3.3 is between 0.45 to 0.5.

Overtopping: Revetments shall be built high enough to prevent overtopping. However, cost boundaries and bulkhead line limit the height of structures. In these cases, it is required to approximate the volume of water per unit time that might overtop the revetment. Equation 3.5 can be used to estimate the wave overtopping of revetments (Abdullah & Nakagoshi, 2007).

$$Q^{'} = \frac{Q}{\sqrt{gH_{mo}^2}} = C_0 exp(C_1 F^{'} + C_2 m) \tag{3.5}$$

, where non-dimensional freeboard, $F^{'} = F/(H_{mo}^2 L_0)^{\frac{1}{3}}$, F = structure freeboard, m = $cot\theta$, regression coefficients are C_0 = 0.4578, C_1=-29.45, C_2 = 0.8464.

Stability and flexibility: Well-arrayed large masses of stones or concrete units usually provide a higher strength, although they lack flexibility. This results in progressive failure associated with accommodation of differential settlement or toe scouring (SPM, 1984). On the contrary, randomly placed armoring units can tolerate the settlement under wave impacts. In this case, the consequences of failure are not catastrophic and minor damages can be rectified.

Stability of armoring layer: The well-known Hudson's formula as expressed in Equation 3.6 is used to estimate the number of required armoring units or riprap weight for stability of the revetments,

$$N_s = \frac{H_d}{\Delta D_n} = (K_D cot\alpha)^{1/3} \rightarrow M_{50} = \frac{\rho_a H_d^3}{K_D \Delta^3 \cot\alpha} \tag{3.6}$$

where N_s is the stability number, $\Delta = (\frac{\rho_a}{\rho_w}) - 1$, D_n is the unit nominal diameter width along the longitude axis, M_{50} is the medium mass of armoring units, ρ_a is the density of armors, H_D is the design wave height, K_D represents coefficient factor derived from a set of factors contributing to the stability, Δ is the relative buoyant density of the armoring units defined by $\Delta = (\rho_a/\rho_w) - 1$ and α is the angle of slope.

To estimate the required thickness for the armoring layer Equation 3.7 can be used, where typically n=2.

$$r = nk_\Delta(\frac{W}{\gamma_\alpha})^{\frac{1}{3}} \tag{3.7}$$

For estimation of the number for armoring number per surface area Equation 3.8 can be used, where typically n=2.

$$\frac{N_\alpha}{A} = nk_\Delta(1 - \frac{P}{100})(\frac{\gamma_\alpha}{W})^{\frac{2}{3}} \tag{3.8}$$

In the case of graded riprap, the minimum layer thickness (r_{min}) can be obtained from Equation 3.9 (Ahrens, 1975),

$$r_{min} = max[2.0(\frac{W_{50min}}{\gamma_r})^{\frac{1}{3}}, 1.25(\frac{W_{50min}}{\gamma_r})^{\frac{1}{3}}, 30cm] \tag{3.9}$$

Toe protection: Toe protection is auxiliary armoring at the toe of the structure that protects the systems from scoring and undermining that may lead to progressive failure. According to SPM (1984), the minimum required weight of toe protection in terms of armoring units can be estimated by Equation 3.10.

$$W_{min} = \frac{\gamma_S H_d^3}{K_{rr}(S_r - 1)^3 \cot\theta} \tag{3.10}$$

, where the K_{rr} is a stability coefficient for angular or graded riprap as shown in Table 7-8 of SPM (1984), γ_S is the unit weight of the armoring unit, H_d is the design wave height, S_r is the specific gravity of the unit, and $\cot\theta$ is the angle of revetment slope.

Design of filters: The filter layers are responsible for smooth transition of excess water on the structure to the underlying soil (CEM, 2002). They are usually made of small stone, gravel and graded rock.

Two types of filter materials are common, the graded rock filters as well as the riprap and stone armoring units (Bezuijen et al., 1987). Equation 3.11 can be used for the design of filter layers for the graded rock filters, riprap and stone armoring units (CEM, 2002).

$$\frac{d_{15\ filter}}{d_{85\ filter}} < 4\ to\ 5 < \frac{d_{15\ filter}}{d_{15\ soil}} \tag{3.11}$$

3.3 Design of LEco revetment for moderate wave condition

In this section, details for the design of LEco revetments in moderate wave conditions are discussed.

3.3.1 LEco armoring units

Concrete armoring units are commonly used to form the first forefront layer of the revetments. The main factors contributing to the hydraulic stability of structures employing these units are: (1) the weight of the units, (2) the interlocking capacity, and (3) the adhesion between the units that are placed at the neighboring position or the friction between the armoring units and the underlying soil or filter layer materials.

In the development of recent armoring units (e.g., Xbloc, Core-Loc and L-block), it has been tried to employ more sturdy geometries to overcome the weakness of the units against the tensile stresses (CEM, 2002). The new generation of armoring units shall provide an improved behavior against the hydraulic forces through the larger mass as well as better interlocking capacity. The newly-developed units shall be placed at a single layer rather than multiple layers, which has been the norm of practice in conventional armoring units. This will be resulted in reduced construction costs, because the minimum number of units required for armor layers of the coastal defense structures significantly declines.

The LEco armoring unit (LEco) is a hollow-shaped armoring units that were first developed at the University of Malaya in 2015. Figure 3.1(a) depicts a 3D view of the LEco armoring units (LEco).

Concrete armoring units are mostly designed for extreme wave conditions ($H_s >$ 4.00 m); thus, they usually have robust geometric shapes. However, the units can also be designed for moderate and low wave conditions at smaller scales. Hence, for the smaller scale units, it is not economical to design the units in complicated shapes. According to Short (2006), application of smaller scale units is limited to wave conditions where $H_S < 1.5$ m. This has led to the idea of developing LEco revetment that uses a single layer interlocking unit to counter the hydrodynamic forces at coastal areas.

The design of LEco was aimed to meet the following criteria: (1) simple geometry that is easy to maneuver and fabricate, (2) a relatively good interlocking capacity between the neighboring units, (3) potential to be placed within a single layer, (4) suitability for moderate to low wave conditions, and (5) cost-effectiveness and local availability of materials for fabrication of units.

3.3.1 (a) *Geometric shape of LEco armoring units*

The LEco is a solid armor unit made of concrete material. The unit is in rectangular shape with four legs, placed at each corner of the frame. As can be seen in Figure 3.1a, the frontier legs are longer than the rear legs such that the unit can be stable when placed on an inclined surface. The size of unit is a function of the length of the main frame, L. Figure 3.1b shows the geometric shape and dimension of the LEco.

The LEco are placed evenly in a single layer on armoring layers of the coastal protection structures. Figure 3.1c shows the suggested layout for the units. Implementing this layout, the packing density (φ) for the LEco which is the number of the armoring units in an nominal diameter of the unit (D_n) is obtained as follows.

$$D_n = V^{1/3} = (\frac{M}{\rho_c})^{1/3} \tag{3.12}$$

, where D_n is the nominal diameter of the units in m^2, V is the volume of the LEco in m^3, M is the weight of the units in kg, and ρ_c is the unit density of concrete in kg/m^3.

Weighing the LEco made of ordinary Portland cement fabricated through normal practices in construction industry shows that a unit of LEco armoring is nearly 98.6 kg when the concrete density is 2300 kg/m^3. By measurement, the volume is 0.064 m^3 and length of the frame (L) equals to 80 cm. Therefore, $D_n = 0.4m$.

The required number of LEco per unit area of 1 m^2 is equal to 4.07, thus:

$$\varphi = 4.07 \times 0.4^2 = 0.65 \tag{3.13}$$

The small size of unit resulted in a lower packing density ($\varphi = 0.65$) compared to other type of concrete armoring units (see Table 4.1). This is not a weak point, because the relative size of unit is comparatively very smaller than the robust units ($D_n = 0.4m$). The low nominal diameter can be considered as a benefit of the LEco, since the fabrication cost and time are significantly reduced while a reasonable interlocking capacity is developed.

3.3.1 (b) Placement of LEco on inclined surfaces

The LEco is designed to be placed at the inclined surfaces at a single layer. The units must be placed at the slopes with a small gap between the neighboring units ($< 5cm$). The direction of placement is from left-to-right and once the first row at the toe of the slope is completed, the subsequent rows are placed. It must be remembered that in order to develop interlocking between the neighboring units, longer legs of the units must face the beach-front and should be placed inside the lower unit frames (Figure 3.1c and Figure 3.1d).

3.3.2 Procedure of design for LEco revetment

The procedure of design for LEco revetment is discussed in the following sections.

Wave action: The required depth at which the waves break can be estimated by Equation 3.14 according to Solitary wave theory (SPM, 1984).

$$H_b = 0.78 d_b \tag{3.14}$$

, where H_b is the breaker height and d_b is the water depth at which the waves break. If $d_b < d_s$, the structure is subjected to non-breaking wave conditions. d_s is the depth of water at the toe of the structure considering the scouring depth as well as the eroded shoreline depth.

Crest elevation: Crest elevation of the structure is established based on the discussion provided in subsection 3.2. The calculated maximum wave run-up (R_{max}) is converted into a surplus height that must be added to the design height.

Slope of structure: The slope of structure is selected based on the existing condition at the rehabilitation site. To reduce the earth works and according to the site conditions, the

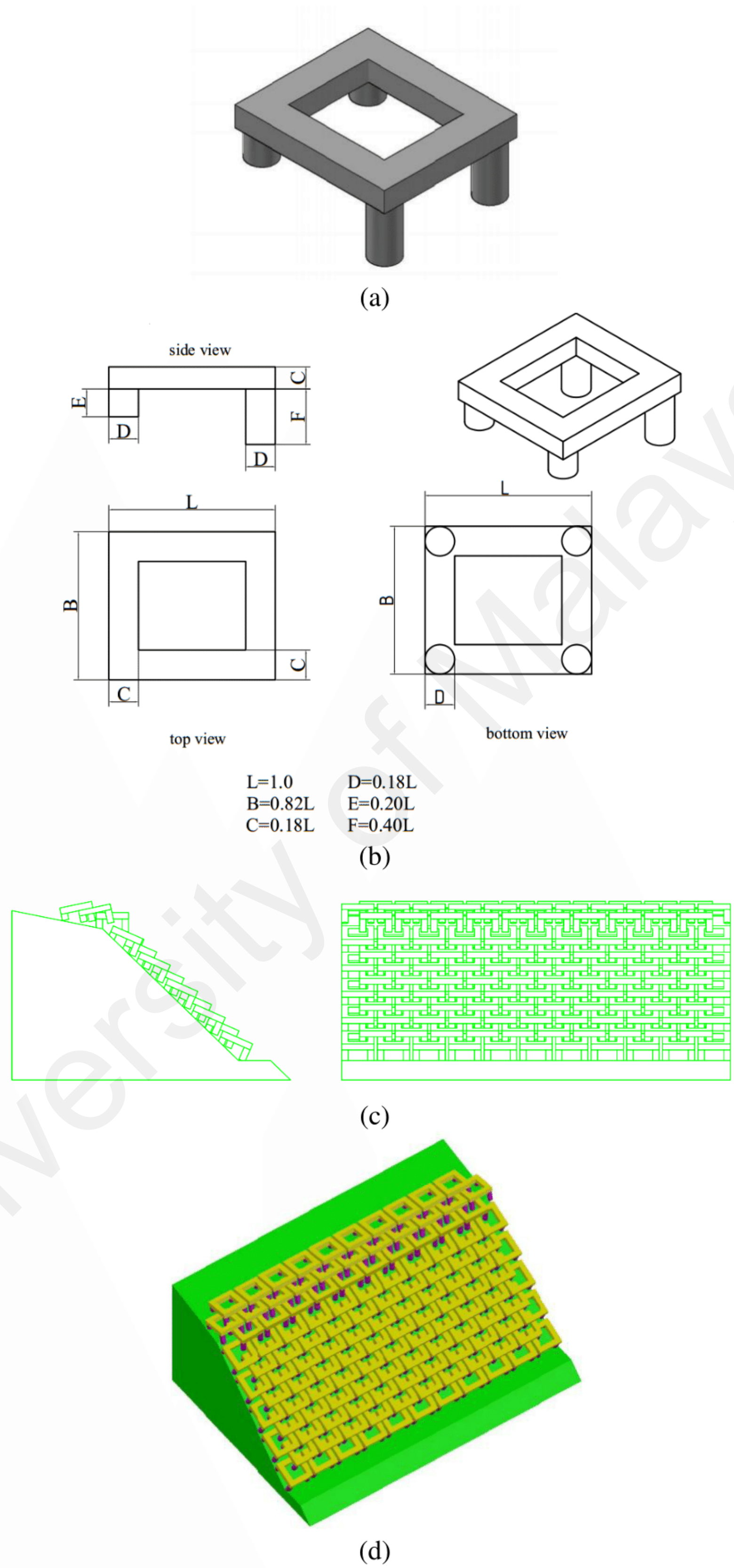

Figure 3.1: (a) A 3D view of LEco, (b) Geometric properties of the LEco, (c) Side and front view of the placement of the LEco on revetment structures, and (d) Pattern for placement of LEco.

angle of slope is within the range of 30°to 60°, which satisfies the criteria as described in CEM (2002).

Minimum weight of LEco armoring unit: The primary armoring layer of LEco revetment is made of LEco. The minimum weight of each LEco required for protection of slope (SPM, 1984) for non-breaking conditions is calculated as follows:

$$W_L = \frac{\rho_c H_d^3}{g K_D (S_r - 1)^3 \cot\theta} \tag{3.15}$$

, where W_L is the mass of armoring unit in kg, ρ_c is the unit density of the concrete in kg/m^3, H_d is the design wave height in m, θ is the slope of the structure in *degree*, S_r is the unit density of the concrete over the unit density of the water, and the K_D is the the stability coefficient, which is a factor of wave action, slope of the structure and other stability parameters.

Design of secondary cover layer: The minimum weight of the secondary cover layer (W_S) is a function of the weight of the LEco if assumed to be rock (W_R). It can be calculated as follows:

$$W_R = \frac{w_r H_d^3}{g K_D (S_r - 1)^3 \cot\theta} \tag{3.16}$$

, where W_R is the unit weight of the LEco armoring layer in *tons* if it is made of rock, w_r is the unit weight of rock in kN/m^3, and K_D is equal to 4.00 for rock (CEM, 2002).

Then, the minimum weight of the secondary cover layer (W_S) in *tons* is as follows:

$$W_S = \frac{W_R}{10} \tag{3.17}$$

The thickness of the secondary cover layer ($T_s e$) in *meters* is calculated as follows:

$$T_s e = n k_\Delta \left(\frac{g W_R}{10 w_r}\right)^{\frac{1}{3}} \tag{3.18}$$

, where the T_se is the thickness of the cover layer in meters, n is the number of armoring units that form the layer, w_r is the unit weight of the rock approximately equal to 25.00 in kN/m^3, and k_Delta is the layer coefficient of stone structure ((SPM, 1984)).

The number of layers required for the secondary cover layer is as follows:

$$n = \frac{T_S}{K_\Delta}(\frac{10w_r}{gW_R})^{\frac{1}{3}} \tag{3.19}$$

The number of stones in the secondary cover layer (N_S) is,

$$N_S = \frac{6.3AT_S w_r}{gW_R} \tag{3.20}$$

$$A_{ro} = \frac{(H_{design} + H_{crest})100}{\sin\theta}$$

, where T_S is the thickness of the second cover layer in *meters*, w_r is the unit weight of the rock approximately equal to 25.00 in kN/m^3, W_R is the unit weight of the LEco in *tons*, and A_{ro} is the area per 100 meters of the structure if it is made of rock.

Finally, weight of the required rock in the secondary cover layer in *tons* is calculated as follows:

$$W_S = \frac{gW_R}{10}N_S \tag{3.21}$$

Design of filter layer: Use of granular filters is common in revetment structures that are at risk of soil erosion. It is commonly accepted that a thicker granular filters is more stable in geotechnical view, but it yields a lower hydraulic stability in terms of uplift of the armoring units (CEM, 2002).

Filters have two functions in the revetments structure: (1) providing drainage, and (2) erosion prevention. In conventional design of revetments, the filter layers are believed to have higher permeability compared with the base soil. This causes the negative consequence of multiple filter layers that are uneconomical and not timely. A more reasonable approach toward a better design of filters is to apply the concept of *geometrically tight granular filters*.

This concept works well when granular filter is so small that the soil particles can not pass through the voids. The basic rules that govern the design of *geometrically tight granular filters* for the LEco revetments are as follows:

$$\frac{D_f\,15}{D_b 85} \leq 4 \; to \; 5 \tag{3.22}$$

, where Equation 3.22 refereed to as the *interface stability criterion*, D_f 15 is the grain size of the filter layer in meters which is larger than 15% of the whole material by weight and D_b 85 is the grain size of the base layer in meters, which is larger than 85% of the whole material by weight.

Design of toe protection: Toe protection must be provided for the LEco revetment to protect the structure against toe scouring and undermining. For a moderate wave condition, suggestions for the toe protection by the SPM (1984) and CEM (2002) were reviewed and suitable geometry for the LEco was selected.

Geometry of LEco revetment: The schematic geometry of the LEco revetment is shown in Figure 3.2a. The thickness of layers as well as the *design water level* were calculated in accordance with the criteria discussed in subsection 3.3. The LEco revetment is flexible so that it adapts to any coastal environment with moderate to low wave conditions. In this view, the design of LEco revetment is site-specific.

3.4 Design of Double-Layer revetment for moderate wave condition

In this section, the details for the design of Double-Layer revetment in moderate wave conditions are discussed.

Design of cover layer: Design of the cover layer for the Double-Layer revetment follows the same procedure as discussed in subsection 3.3.2.

Design of first filter layer: Design of the first filter layer using wide-graded materials follows the same procedure as discussed in subsection 3.3.2.

Design of second filter layer: CEM (2002) proposed Equation 3.23 for small-graded materials to be used in filter layer .

$$\frac{D_{f\ 50}}{D_{b\ 50}} < 6\ to\ 10 \tag{3.23}$$

, where $D_{f\ 50}$ is the grain size of the filter layer in meters, which is larger than 50% of the whole material by weight and $D_{b\ 50}$ is the grain size of the base layer in meters which is larger than 50% of the whole material by weight.

Design of toe protection: Toe protection must be provided for the Double-Layer revetment to protect the structure against toe scouring and undermining. For a moderate wave condition, suggestions for toe protection by the SPM (1984) and CEM (2002) were reviewed and suitable geometry was selected.

Geometry of Double-Layer revetment: The schematic geometry of Double-Layer revetment is shown in Figure 3.2b. The thickness of layers as well as the *design water level* were calculated in accordance with the criteria discussed in subsection 3.4. The Double-Layer revetment can be adapted for the coastal environments with moderate to low wave conditions.

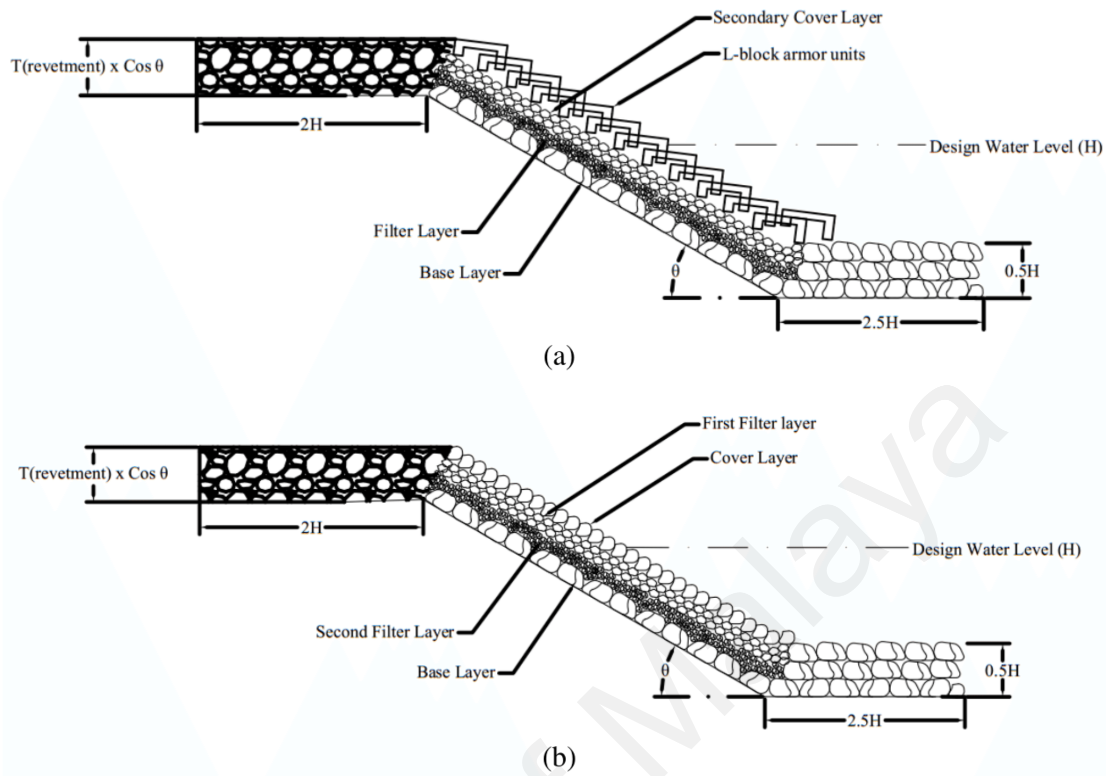

Figure 3.2: Schematic geometry of (a) LEco, and (b) Double-Layer revetments.

3.5 Physical modeling: Experiments

To evaluate the hydraulic stability of the LEco armoring unit (LEco), stone armoring units, and geotechnical stability of the proposed revetment structures, 2D physical models of the LEco revetment and Double-Layer revetment with a slope in front of the model representing the actual foreshore were simulated for the model tests. The details of the geometry of the structures, the materials and the testing configurations are discussed in the following sections.

3.5.1 Wave flume

The physical experiment was carried out in the 2D flume channel at the Hydraulic Laboratory, Department of Civil Engineering, University of Malaya. The flume channel was equipped with measurement tools for the purpose of this study with an approximate budget of RM 500,000 (see Figure 3.3). The flume is 16 m in length, 1 m in width and 1 m in height. In addition, a flexible dissipative slope was incorporated in the flume channel and a wave damper was located at the other side of the flume near the wave generator to absorb the reflected waves.

The wave generator system includes a steel connecting hydraulic jack controlled by a servo hydraulic valve and a hydraulic power pack. The waves of different frequencies and energies, both in regular and irregular shapes, can be simulated through the computer software (equipped with the package to generate waves via the *JONSWAP* spectrum) and a console panel connected to the hydraulic pack. The measurement system is flexible for both vertical and horizontal direction through wire-hinge rollers that can slide in X and Y directions. The measurement system incorporates the wave gauge, turbidity and temperature meter, video recording camera, Laser CNC profiler, and peizo pressure sensors.

3.5.2 Revetment models

3.5.2 (a) Scaling

To obtain efficient results from the physical models, it was important to scale the geometry of the model based on the local site conditions (see subsection 4.2.1). If the *scale effect* applies, the results were not useful for the analysis (CEM, 2002). The problems arising from the scale effect in coastal engineering application is often experienced when it is aimed to simultaneously deal with the fluid-viscosity related phenomena and gravity-driven forces (Kamphuis, 2010). It is accepted that since the waves and currents are gravity-driven forces, simulations are more accurate on gravity rather than viscosity (CEM, 2002).

According to SPM (1984), the similarity between model and prototype can be evaluated in three classes, (1) the geometric similarity, (2) the kinematic similarity, and (3) the

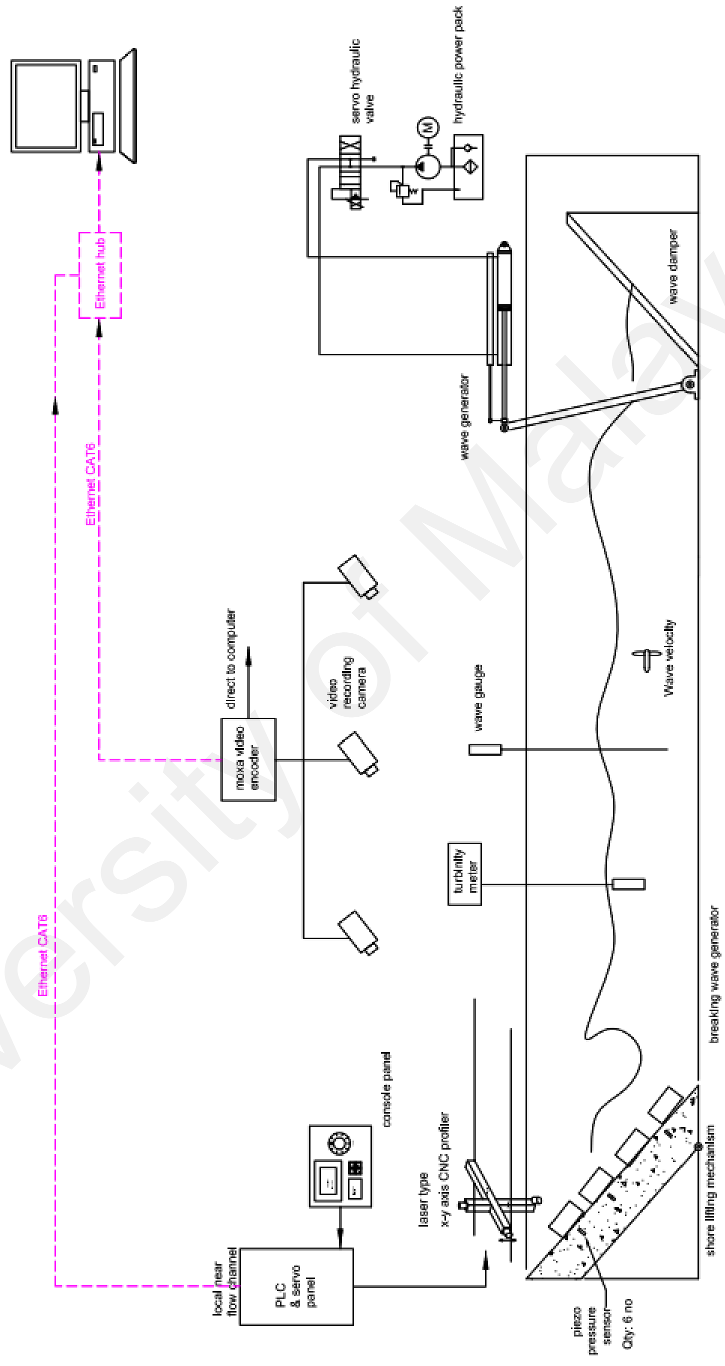

Figure 3.3: The 2D flume channel at Hydraulic Labratory, University of Malaya equipped with wave generator system and measurements.

dynamic similarity. To satisfy the geometric similarity Equation 3.24 applies.

$$N_L = \frac{x_p}{x_m} = \frac{y_p}{y_m} = \frac{z_p}{z_m} \tag{3.24}$$

In this study, a geometric linear scale factor of $N_L = 5$ was used in the experiment.

To meet the *Froude* criterion, the *Froude number* (F_r) must be similar for the model and the prototype. To satisfy this condition, Equation 3.25 must govern.

$$F_r = \frac{U_p}{\sqrt{gL_p}} = \frac{U_m}{\sqrt{gL_m}} \rightarrow \ if \ g \ = \ cte \ : \ \sqrt{\frac{L_m}{L_p}} = \frac{U_m}{U_p} \rightarrow \ N_L = N_U^2 \rightarrow \ N_T^2 = N_L \tag{3.25}$$

, where U is velocity of the fluid in m/sec, g is the gravitational acceleration of the earth in m/sec^2, L is the length of flow in m, and N_T is the time scale factor.

The *Froude* and the *Raynolds* scaling laws can not be satisfied at the same time (CEM, 2002). According to Heller (2011), the effect of *Reynolds* number for a coastal protection structure at the laboratory scales is small, thus can be neglected. In this experiment, the *Froude* scaling law was more suitable for the similarity verification purposes.

The mass of LEco can be estimated through Equation 3.6, and it can be applied to calculate the scale for the LEco mass according to Equation 3.26. The model is a smaller scale of the prototype with the seawater density of $\rho_w = 1035kg/m^3$, the concrete density of the model and prototype are respectively equal to $(\rho_a)_m = 2250\ kg/m^3$ and $(\rho_a)_p = 2300\ kg/m^3$, and if K_D and θ are the same in the model and prototype, the following calculation for the scale for the LEco mass is valid.

$$N_{M_a} = \frac{N_{\rho_a} N_{H_s}^3}{N_{K_D} N_\Delta^3 N_{\cot\theta}} \rightarrow \ N_{M_a} = \frac{1.022 N_L^3}{(1)(0.987)^3(1)} = 1.0925(5^3) \approx \ 137 \tag{3.26}$$

The same procedure for the stone armoring units yields the value of $N_{M_a} \approx\ 92$, assuming that $(\rho_a)_p = 1600\ kg/m^3$, $(\rho_a)_m = 1500\ kg/m^3$ averaged for the dry gravel sized between 1/4" to 2", and the seawater density of $\rho_w = 1035kg/m^3$.

3.5.2 (b) Geometry and materials of the revetment models

The 2D model of the revetments was built on the basis of 1:5 Froude scale matching with the suitable size of the prototype and the dimension of the Flume channel at the Civil Engineering Department, University of Malaya (see subsection 3.5.1). The largest feasible dimension of the armoring units was selected in accordance with the CEM (2002) guidelines for the modeling of coastal structures as well as the wave conditions in the flume.

Depending on the angle of the revetment model ($\theta = 37\ \deg\ or\ 53\ \deg$), the depth of water was kept between 30-40 cm (see section 4.2.1. In this case, it can be assured that the wave energy largely affects the armoring units on the top of the revetment. This can be considered as an extreme loading condition in which the wave height exceeds the wave design condition for the west Peninsular Malaysia. If the structures can successfully stand this extreme case, moderate to low loading conditions also can be dampened. A common scale effect that was expected to happen is that in the actual condition, the armoring units may be displaced due to rocking, whereas in the physical model such a damage would not happen (SPM, 1984).

The details of models for each proposed structures in terms of material and geometry are as follows:

The LEco revetment model was made of a armor layer, a secondary cover layer, a filter layer, and a base layer. The model of LEco for the armoring layer were fabricated using concrete of $\rho_a = 2250 kg/m^3$. The length of the main frame denoted by L was 14.5 cm and weight of each armoring unit was on average 862.9 $\pm$16.3 grams with a nominal diameter of 7.25 cm (see Figure 3.1a and Figure 3.1b). The secondary cover layer was made of crushed stone with $D_{n50} = 0.037$ and $\rho_a = 1500 kg/m^3$. The filter layer was built of crushed stone with $D_{n50} = 0.027$ and $\rho_a = 1700 kg/m^3$ and the base layer was crushed stone with $D_{n50} = 0.047$ and $\rho_a = 1600kg/m^3$. This large value of D_{n50} is to ensure sufficient permeability of the structure; thus, a turbulent flow could be assumed as when used in the prototype revetment. The $\frac{D_{85}}{D_{15}} < 2$ satisfied the grading criterion for stones as suggested by der Meer (1987). Other details related to the LEco revetment model are presented in Figure 3.4a and Table 3.1. The Double-Layer revetment was made of a cover

Table 3.1: The geometry configurations for the LEco revetment model.

Number	Item	Config.1	Config.2
1	Layer thickness- Second cover layer (cm)	15	18
2	Layer thickness- Filter layer (cm)	15	18
3	Layer thickness- Base layer (cm)	15	18
4	Deck Length (cm)	20	20
5	Slope angle (degree)	37	53

layer, two filter layers and a base layer. The details for the geometry and material of this revetment was the same as the LEco revetment, except that there was no LEco in the armoring layer. The replacement of crushed stone with $D_{n50} = 0.042$ and $\rho_a = 1650kg/m^3$ is the point of difference between the LEco and Double-Layer revetments. Other details related to the Double-Layer model are presented in Figure 3.4b and Table 3.2.

Table 3.2: The geometry configurations for the Double-Layer revetment model.

Number	Item	Configuration 1	Configuration 2
1	Layer thickness- cover layer (cm)	12.5	15
2	Layer thickness- First Filter layer (cm)	12.5	15
3	Layer thickness- Second Filter layer (cm)	12.5	15
4	Layer thickness- Base layer (cm)	12.5	15
5	Deck Length (cm)	20	20
6	Slope angle (degree)	37	53

3.5.3 Hydraulic stability

3.5.3 (a) Wave spectrum

Tests were conducted with 2D irregular waves generated using a *JONSWAP* spectrum with the γ (peak enhancement factor) of 3.3. The tests were considered completed after the damage is occurred. Each step had a total of 3,000 waves.

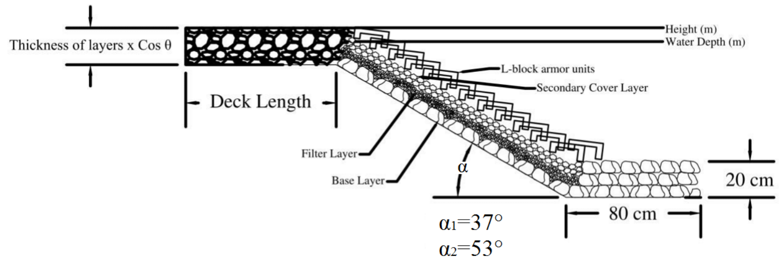

(a)

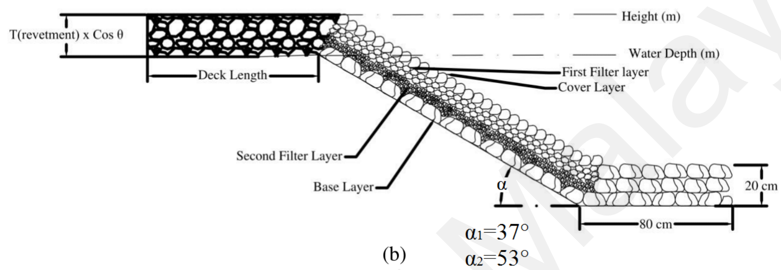

(b)

Figure 3.4: Schematic cross-section of (a) LEco, and (b) Double-Layer revetment models.

For the pilot project in this study the average wave periods ranged from 2 to 8 seconds (see section 4.2.1). The wave steepness is known as the ratio of the wave height to the wave length ($S_0 = \frac{H_0}{L_0}$). Under shallow water condition, $L = (gh)^{1/2}T$, Hence L is proportional to T; if h=constant. The H_s at site conditions ranged from 1.5-1.8 m. Therefore, in this experiment the wave steepness is from 0.02 to 0.2.

Considering the scale factor, in the experiments the significant wave depth ranged from 0.30 to 0.40 m (Table 3.3). It is well-known that movement of concrete armoring units is highly dependent on whether breaking occurs or not. According to observation on-site, the waves break before reaching the location of the installed revetments. This is perhaps due to low to moderate wave conditions at the site, and the positioning of foreshore slope. Therefore, in the experiments the effect of wave breaking was not considered. Referring to *small amplitude*, the wave period (T_0) was determined. The wave length (L) as a function of the depth and wave period was calculated from Equation 3.27

$$L = \frac{gT^2}{2\pi} \tanh \frac{2\pi d}{L} \tag{3.27}$$

From Equation 3.27, the wave periods were found to be in the range of 2.15 to 2.85 seconds. Based on the Equation 3.25, the time scale was $N_T = N_L^{1/2} = 2.24$. Therefore, in the prototype it was expected that the wave periods ranged from 4.5 to 6.5 seconds. The majority of waves at the west Peninsular Malaysia have periods of 2 to 8 seconds (see Subsection 4.2.1). Thus, the selected wave heights and periods were appropriate for the modeling. In addition, the corresponding wave height and periods in the experiment agree with the condition of non-breaking waves at on-site observations.

The spectral peak period (T_p) is defined as the peak period of the spectrum. In general, the value is used as the representative period. On the basis of the suggestion by the SPM (1984), $T_s = 0.95T_p$ and thus the peak period in this experiment ranged from 2.15 to 2.85 seconds. The parameters that were used for each test run are shown in Table 3.3.

Table 3.3: Wave spectrum setup for the experiment.

Paremeter	Config 1	Config 2	Config 3	Config 4	Config 5	Config 6
Hs (cm)	30	32	34	36	38	0.40
Tp(Sec)	2.15	2.29	2.43	2.57	2.71	2.85
N	3000	3000	3000	3000	3000	3000

3.5.3 (b) Displacement of LEco armoring units

To monitor the damage of the armoring units in terms of displacement, three points were marked on the target LEco. During the displacement survey, the wave generation was stopped. Measurement of displacement was carried out for four LEco at different locations of the armoring layer as depicted in Figure 3.5. Each unit was marked with three points on the surface. Point 1 was located at the right-middle side of the units, point 2 was located at the bottom-middle side of units and point 3 was located at the left-middle side of the units (see Figure 4.5). The rationale behind selecting these target units was that it was observed during the experiment that the units located at these positions are more likely be subjected to displacement. Such an observation also agrees with the theoretical evidences of developing LEco because the interlocking features are the lowest at these locations.

An automatic Laser type CNC profiler (Figure 3.6) was used to record the orthogonal coordinates X, Y and Z of each reference point before and after each test run. When an observable displacement occurred, the data was graphed for each of the four target LEco based on the marked points on them. The results of the displacement survey is discussed in section 4.3.1.

Figure 3.5: The location of target LEco for displacement survey.

Figure 3.6: Laser type CNC profiler used in this study.

3.5.3 (c) measurement of damage progression

Damage of the armoring units was measured in the event of their displacement due to wave impact. In case of total removal of the units from the armoring layer which leads to no contribution of the units to the stability of the armoring layer, damage is worth measuring. After the wave cycles were completed in each configuration (Table 3.1 and Table 3.2), the displaced armoring units were counted. Since the scale of the models were sufficiently large, counting could have been taken place with ease.

3.5.3 (d) Evaluation of damage level

To evaluate the level of damage (see section 2.5.3), the relative damage number (N_{od}) was calculated. The value is defined as the actual number of displaced units after each test run relative to a width of the nominal diameter (D_n) along the longitudinal axis of the structure.

3.5.4 Slope stability

Using the slope analysis as discussed in SPM (1984), the factor of safety must be more than 3 to ensure that the slope is safe against sliding. Since numerical models were carried out for this study and the minimum factor of safety under the defined loading conditions was considered to be highly lower than the SPM (1984) criterion, it is sufficient to refer to the results of the numerical models for the purpose of slope stability analysis.

3.5.5 Damage level of armoring units

Damage of an armoring unit is measured when a unit is displaced due to wave forces. The displacement is defined as being measurable when a unit is noticeably removed from the system, whereby there is no contribution of the unit in protection of the structure. Visual observation of sufficiently large models through counting can be used to enumerate the number of displaced armoring units (i.e., stone or concrete units).

Relative damage number, N_{od}, is defined as real number of the units which are displaced relative to the width of 1D diameter D_n. The width is measured along the longitudinal axis of the structure. In concept (subsection 2.5.3 (a)), N_{od} is the percentage of damage in which the actual damage of armoring units in a cross section with a width of D_n is measured. $N_{od} = 0$ is defined as the *start of damage* and $N_{od} = 0.5$ is considered as the *failure* criterion (CEM, 2002). It is not reasonable to design armoring units for no-damage criterion because it would lead to massive amount of armoring units.

As discussed in section 2.5 and section 2.5.4, the damage level of the armoring units is measured either via a Bayesian approach through defining the N_{nod} or based on the *dimensionless damage parameter* (S). The former is usually designated to identify the damage of concrete armoring units and the latter is utilized for stone or rock armoring units. According to J. W. Van der Meer (1988), the no-damage criterion is defined as $1 < S \leq 3$. Similarly, in case of failure, $S \geq 10$. Thus, a possible optimized scenario for the design of armoring layers would consider $3 \leq S < 10$. For the concrete units, N_{od} indicates the *start of damage* when $N_{od} = 0$, and the *failure* when $N_{od} = 0.5$.

In this study, the parameter S is calculated after Burcharth, Kramer, Lamberti, and Zanuttigh (2006) (see Equation **??**). They introduced an empirical relationship to link the damage given as the number of displaced stone armoring units, N, to the S parameter (Broderick, 1983).

$$S = \frac{A_e}{D_{n50}^2} \tag{3.28}$$

$$D_{n50} = \frac{M_{50}}{\rho_a}$$

, where A_e is the average of eroded cross-sectional area of the armoring layer, D_{n50} is the nominal diameter of stone armoring units, M_{50} is the median mass of rock grading given by 50% on the mass distribution curve, and ρ_a is the mass density of armor units.

In order to design the LEco revetment and select necessary stone grading for Double-Layer revetment, which satisfy the above criteria with respect to the acceptable damage level, two graphs were drawn: a) N_{od} versus stability number, N_s, and b) S versus stability number, N_s. The design criteria for the acceptable damage level in the LEco and stones armoring units were identified, and further were used to design, select and fabricate each armoring unit (see section 4.5 and section 4.6.1). The stability number N_s was calculated in accordance with the Hudson's formula (see Equation 3.6).

3.6 Pilot project: Carey Island, Klang, Malaysia

In June 2014, a pilot project was started in the Carey Island (CI) located in the Banting district in Selangor, Malaysia. The project aimed to evaluate the efficiency of the proposed revetment structures for the purpose of coastal protection. The cohesive beach of CI has experienced a tremendous environmental degradation and erosion events to the extent that the natural ecosystem capability to restore the imbalances could no longer be relied on. In fact, many areas within the west coast of Malaysia Peninsula has gone through the same scenario over the past few decades. In this respect, the Carey Island can be considered as a suitable representative of the eroded beaches around the west coast for the aim of this pilot project.

Earlier between 2008 and 2010, a mangrove rehabilitation project was conducted in the target area. In this study, it was aimed to assess the current condition of the Carey Island in terms of geotechnical characteristics, topography of beach at the target site, and the coastal flora. In addition, six slots of revetments in three configurations (see subsection 3.6.2) were constructed at the site to prevent the continual erosion. Also, new mangrove rehabilitation works were attempted during the completion of this study. Perhaps due to the incorrect plantation techniques and ongoing stressors, earlier attempts to restore the mangroves at the site were unsuccessful (Motamedi et al., 2014).

3.6.1 Description of the site

Malaysia is located in the southeast Asia, near the equator with a total landmass of 329,847 km^2. The country is comprised of 13 states and three federal territories divided by the South China Sea into two equally regions, known as the *East Malaysia* and *Peninsular Malaysia*. East Malaysia shares land and maritime border with Indonesia and Brunei and a maritime border with the Philippines. Peninsular Malaysia shares maritime border with Vietnam, Indonesia and Singapore and a land and maritime border with Thailand. To a large extent, it is encircled by the seas, the South China Sea to east, the Straits of Malacca to west of Peninsula, the South China Sea to north of Borneo Island, and the Celebes Sea and the Sulu Sea to east of the East Malaysia.

Figure 3.7 shows the location of Carey Island in Peninsula Malaysia. Carey Island is located within the Klang Isle (03°38’ N and 101°00’ E), which is one of the most famous mangrove forests in the Strait of Malacca alongside the west coast of Peninsula Malaysia. Klang Isle is composed of eight small islets, and the Carey Island is the largest of those, separated from the Selangor coast by the Langat River on the east and the Kelang River on the north. The total area of the Carey Island is 161.87 km^2 and nearly 65% of its total area is covered with palm oil trees (Tajul Baharuddin, Taib, Hashim, Abidin, & Rahman, 2013). The island’s elevation is lower than the mean high tide level indicating a possible excessive seepage or overtopping when a coastal protection structure is deemed to be installed at the coastline. Consequently, to protect the upper land from the effect of higher waves, *coastal dikes*, a network of drainage canals and water control systems was constructed at the beach-side of the site in 1995 (Tamin, Zakaria, Hashim, & Yin, 2011). The details of wave/climatic properties, and the geologic/sediment stratigraphy of at the study site is delivered in section 4.2.

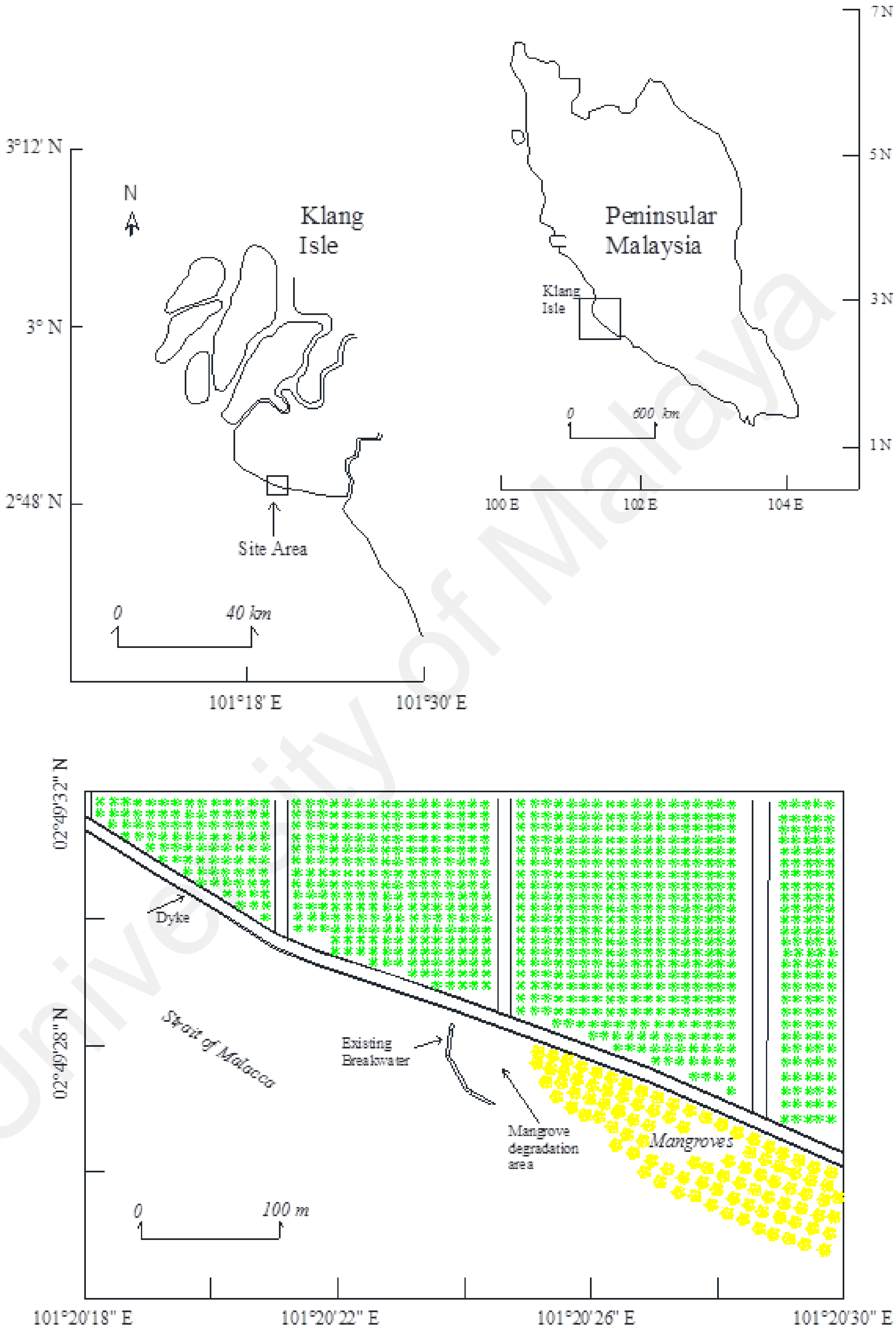

Figure 3.7: The geographical position of Carey Island. Gray-shaded hatch denotes the thin mangrove cover.

3.6.2 Placement of revetments at the site

In the following, the placement of revetment structures and the construction details for the LEco, Double-Layer and Abstention revetment are discussed. In this study, six units of revetments were constructed at the Carey Island study site. These included two LEco revetment structures and two Double-Layer revetments (see section 3.6.3 (a), as well as two Abstention revetments (see section 3.6.3 (b)). The abstention revetment is basically an inclined filled area (in a shape of revetment) that was used as an index to evaluate the performance of the other developed structures.

Table 3.4 summarizes the configuration of the revetments that were constructed at the site. One LEco revetment (L1) and one Double-Layer revetment (D1) were constructed in the area behind the breakwater system and other two slots (L2 and D2) were installed on the east of breakwater system in an area that is not protected by the breakwater. The basic idea behind such a placement was to understand the effect of the existing breakwater on the performance of the revetments. Two 5-m length of the shoreline (A1 and A2) were engineered though no protection layer was incorporated in the scheme so that the performance of the other proposed revetment structures against erosion could be evaluated. Figure 3.8a illustrates the positioning of the revetment structures at the Carey island site.

Table 3.4: Configuration for the placement of revetment systems at the Carey island site.

Number	Type of protection	Index letter	Location of placement
1	LEco revetment	L1	Behind the breakwater
2	Double-Layer revetment	D1	Behind the breakwater
3	Abstention	A1	Behind the breakwater
4	LEco revetment	L2	To the east of the breakwater
5	Double-Layer revetment	D2	To the east of the breakwater
6	Abstention	A2	To the east of the breakwater

3.6.3 Preliminary design of the proposed revetments

3.6.3 (a) LEco revetment and Double-Layer revetment

Using the empirical approaches as discussed in sections 3.2, 3.3 and 3.4, preliminary layouts were designed for the LEco and Double-Layer revetment. These design layouts are demonstrated in Figure 3.8a and Figure 3.8b, respectively.

These layouts were aimed to serve as preliminary design so it was necessary to verify the performance of the actual structures using numerical (section 3.6.4) and physical (section 3.5) models prior to their construction. When these modeling works were completed, necessary amendments were incorporated in the final design to include local site conditions in relation to climate, geometry and dimension. The final design of the proposed structures are discussed in section 4.5.

3.6.3 (b) Abstention revetment

Initially, the Abstention revetment was aimed to provide an index for measuring the efficiency of the other proposed revetments (LEco and Double-Layer). For this, the preliminary layout of these revetments was designed such that their dimension and geometry could match the other revetments. Basically, the Abstention revetment is made of local soft clay material which could be easily found at the coastal bank of the study area. Further, the revetment was engineered to form the geometry and dimension as shown in Figure 3.8d.

The physical properties of the soil material used for construction of these revetments are summarized in Appendix B. The material was compacted to attain the OMC condition. Also, a toe protection was incorporated in the design layouts. The efficiency of the constructed revetments was monitored in terms of any observable erosion for one year into their construction. The results of these monitoring works are discussed in section 4.7.5.

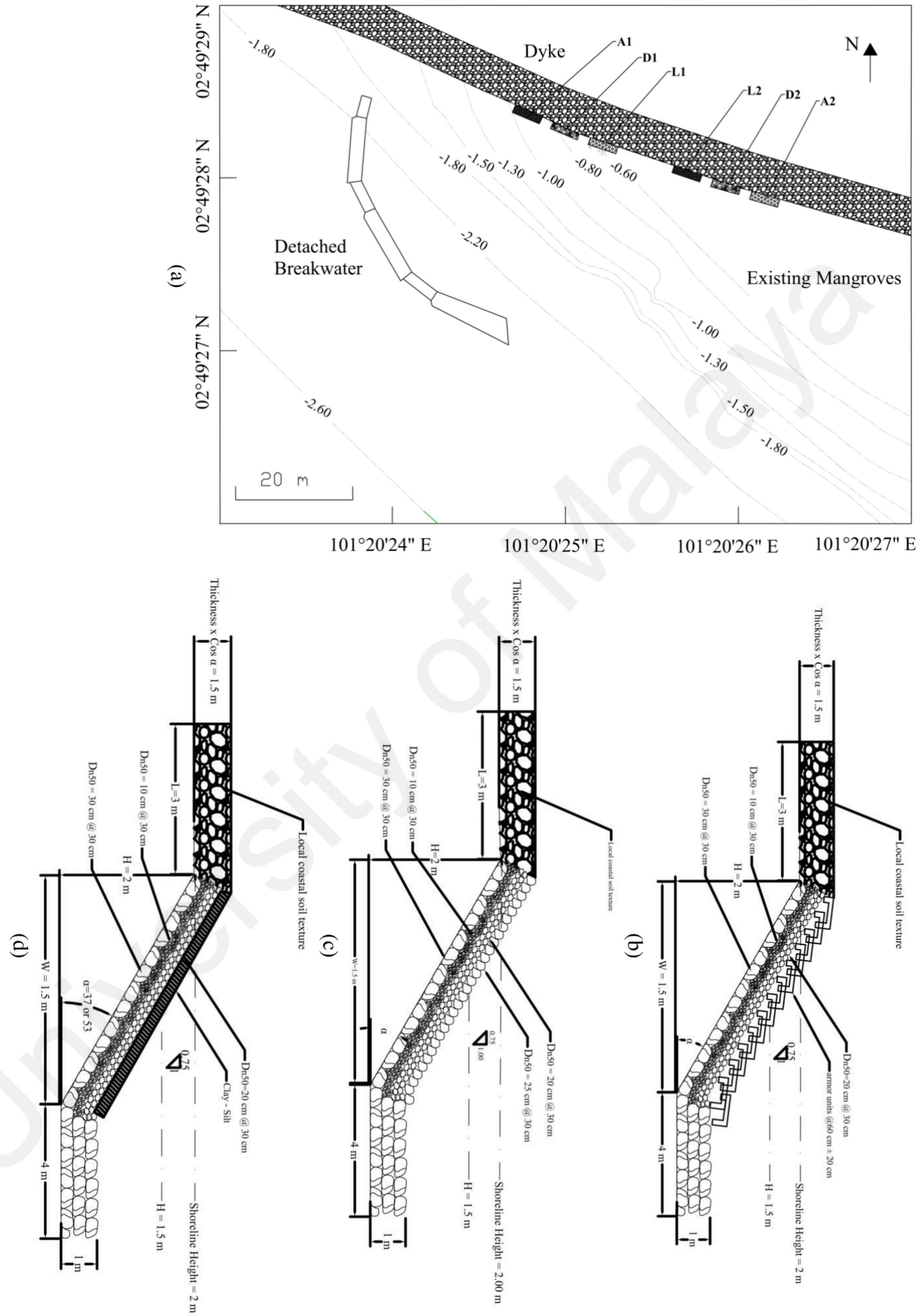

Figure 3.8: (a) Positioning of the revetments at the Carey island site; and preliminary design layouts of (b) LEco, (c) Double-Layer, and (d) Abstention revetments at the Carey island site.

3.6.4 Design verification by computer model

3.6.4 (a) General

When a geotechnical structure fails, most of the times the causes can be attributed to the design insufficiencies; either a lack of understanding of geological and geotechnical conditions of the site or inadequate design considerations (Meyerhof, 1956). When predicting the future response of a geotechnical structure to both hypothetical and factual loading conditions is of concern, it is important to delicately evaluate the soil strength parameters. In addition, a thorough stress-strain analysis of the structure under the imposed or postulated loading shall be conducted to ensure that any abnormal behavior of structure is detected prior to any possible failure scenarios.

3.6.4 (b) Input parameter selection in this study

In this study, the site investigation works were done in accordance with the *BS 5930: 1999* "*Code of Practice for Soil*" and "*HongKong Geotechnical Office Guidelines* (Office, 2000). Three boreholes were drilled using a hydraulic feed rotary boring machine. The drilling operation for the boreholes namely BH1, BH2 and BH3, were terminated at a depth three times the SPT N value (100 blows per 100 mm). The drilling advanced in a total depth of 102.9 m. The location of boreholes is shown in Figure 3.10 and borehole logs can be found in Appendix B.

In this investigation, a total of 34 Standard Penetration Tests (SPT) were taken to understand the engineering properties and type of soil. The SPT was conducted based on the *BS 1377: 1990 Part 9* (see Table 3.5 and Table 3.6).

A total of five undisturbed samples and 19 disturbed samples were derived from different boreholes depth (see Table 3.6). Further, four types of laboratory tests were carried out for the undisturbed samples in accordance with the *BS 1377*. These tests were the moisture content (*BS 1377:1990 Part2: Test no. 3*), the bulk and dry density determination test (*BS 1377: 1990 Part 2: Test no. 7:2*), the atterberg limits test (*BS 1377:1990 Part2: Test no. 4.5 and no. 5.3*), and the unconsolidated undrained triaxial compression test (*BS 1377:1990 Part 7: Test no. 9*). The results of laboratory testing are presented in Appendix B.

Table 3.5: Summary of quantity for site sampling works.

No.	Start	Finish	Depth	Coring	SPT	DS	UD
BH 1	11/1/2015	13/1/2015	45.31	45.31	15	8	3
BH 2	12/1/2015	14/1/2015	104.02	36.27	12	6	0
BH 3	13/1/2015	15/1/2015	103.88	21.32	7	5	2

Table 3.6: Sumamry of quantity for laboratory works.

No.	Bulk/Dry Density	Moisture Content	Atterberg Limit	Triaxial UU test
BH 1	3	3	3	3
BH 2	0	0	0	0
BH 3	2	2	2	2

3.6.5 Analysis for excessive seepage potential

In this study, for analyzing the seepage, the *SEEP/W-2007* software was employed to simulate the revetment structures under steady-state flow. The features of the software are necessary to solve the conventional problems associated with the unconfined flow through a revetment. Also, since no piezometer was installed at the site, the computer-generated phreatic line was used for slope stability analysis (subsection 3.6.6). The possibility of high exit gradients and uplift pressure was checked for various loading conditions as described in subsection 3.6.5.

The seepage analysis in this study was done to confirm that the preliminary design layouts were safe against potential seepage at the site. The results of the seepage analysis are discussed in section 4.4.1.

During the preliminary design using the empirical methods (see section 3.6.3), the design height was chosen such that overtopping at the structures was prevented. Thus, the extreme loading of 100% out of total height of the structure would be an imaginary condition. If the structures would be stable under higher water elevations at the structure (i.e., 100% of total height of structures), then it should be conservative enough to claim that structures remain stable under lower water elevations at the structure (i.e., 70% of total height of structures). The seepage analyses for revetments were conducted in accordance with the guidelines as described by the USBR, 2014b; MWLA, 2003; SPM, 1984; CEM, 2002.

Condition of flow: According to the DID (2010), three-dimensional modeling of geotechnical problem is not required in geotechnical projects in Malaysia. In addition, according to the USBR (2014b), the most common analysis performed for potential seepage problems includes modeling of on-the-soil mass on slopes, assuming a steady state water body at operation. The basic assumption for this condition is that the variable of time is not included in the analysis. Based on the discussion in section 4.2.1, for the study site, periodic changes in water head remain constant for most of the time that result in a stable flow regime. Given the uncertainties about assigning permeability for modeling seepage behavior, any inherent conservative approach in the assumption of steady-state condition is usually considered acceptable.

Loading scenarios: The seepage analysis considered four scenarios including a) no loading (0% water at the height of structure), b) quarter loading (25% water at the height of structure), c) Maximum Controllable Level (CRL) (75% water at the height of structure), and d) Maximum Flood Level (at crest Level; 100% water at the height of structure). Based on the discussion in section 4.2.1, fluctuations of the tidal table at the determined locations of revetment structures were lower than the proposed height for the revetment structures (4.5 meters above the most frontier point of revetment placement). According to DID (2010), the effect of wave breaking was not considered in the numerical analysis.

Hydraulic conductivity: Table 3.7 presents the hydraulic conductivity of the materials used in the modeling. The hydraulic conductivity (K [m/sec]) of the materials was chosen based on the SI reports from the site (Appendix B) and matching them with the DID guidelines (2010). The hydraulic conductivity is denoted by K (m/sec).

Factor of safety: Assessment of pore pressure and seepage forces at the upstream of slopes and toe areas of revetments is complicated; thus it needs a careful consideration of the site conditions. In this view, simplified formula to estimate safety factors and exit gradients can be misused if the failure mechanism is not fully understood. The Following conditions were checked for the factor of safety.

High exit gradients in a cohesionless soil: Exit gradients are known as the hydraulic gradients at a free face or into more pervious materials. Quick ground conditions at the seepage locations are believed to be associated with high upward exit gradients in cohesionless soils, that are sometimes accompanied by presence of sand boils. In a soil mass consisting of cohesionless material with a narrow distribution of fine sand and silt grain sizes (the case in the study site), the soil body may be vulnerable to be fluidized, because the water body exceeds the hydraulic head that is required to generate the critical gradient.

When the objective is to determine the critical gradients for a soil mass, an evaluation of effective stress conditions is necessary. The critical gradient occurs when the effective stress is zero. Under this circumstance, a *quick* condition happens in the cohesionless mass of soil, and the underlying materials may heave or boil.

After construction of revetment structures and during the monitoring period, no sand boil or heave were observed. In this regards, the factor of safety against excessive exit hydraulic gradient was calculated using the numerical model as described in the following.

The critical gradient ($I_c = \frac{\gamma_b}{\gamma_w}$) is commonly defined as the ratio of the buoyant unit weight of the soil (γ_b) to the unit weight of water (γ_w). For the case of cohesionless soils, the factor of safety against boiling or heave ($FOS = \frac{I_c}{I_e}$) with respect to vertical exit gradients is expressed as the ratio of the critical gradient (I_c) to the predicted or measured exit gradient (I_e).

According to the USBR (2014b), the above calculated FOS is not a factor against the creation of an unfiltered exit or start of internal erosion. In instances of low safety factor, or even when the $FOS < 1$, there is no certainty that an internal erosion or failure mechanism is definite to start or develop. As a conservative approach, according to USBR (2014b) $FOS > 3$ was used for assessing any threat of high exit gradients.

Uplift pressure: Dangerous high pressure develops if pervious soil lays over less pervious soil. Uplift of confined layer may occur if seepage forces in a given layer becomes higher than the pressure from the confining layer. In such a situation, the confined layer may blow out leading to quick condition and even sand boils. This situation increases cohesion of the confined layer and formation of fine grained soils or clay. Here, one should note that the concept of critical gradient does not hold for cohesive soil. Therefore, FOS needs to be calculated with the concept of effective stress ($FOS = \frac{\gamma_b \times t}{\gamma_w \times \Delta h}$). Here, γ_b is the confined layer's buoyant weight; t is the thickness of confined layer; Δ_h is the piezometric reading; and γ_w is the unit weight of water. The effective stress method uses the concept of seepage forces and buoyant forces. It was used for calculating the factor of safety for the study site.

According to the USBR (2014b), using the effective stress method, $FOS > 1.5$ was considered to be sufficient for the study site that compensates for insufficient data on water table.

Boundary conditions: For seepage problems, the boundary conditions are in terms of total head or its gradient in a direction normal to the boundary conditions. In this study, boundary conditions were fixed in accordance to the recommendations presented by the USBR (2014b).

3.6.6 Analysis of slope stability

In this study, for analyzing the stability of the seaside and leeward slopes of the revetments, the *SLOPE/W 2007* software was employed to simulate the structures. The possibility of slope failure has been checked against various loading conditions as elaborated in subsection 3.6.6. This subsection deals with description of a 2D stability model based on the *Limit Equilibrium* analysis for the developed revetments using the SLOPE W/2007. The analysis was carried out under the static loading condition that resulted in calculating the factor of safety values based on a) the *Morgenstern-Price* (MP) method, and b) the *Spencer* methods.

The water table in this analysis was selected based on the input generated from the *SEEP/W* software. The location of potential circular arc slip surfaces and safety map of the model was also reported after the analysis. Using the power of the *SLOPE/W*, for accurate results, several automatic slope surface searches were performed to select the potential slip surface through different starting points. The slope analysis in this study was conducted in accordance with the guidelines in the USBR (2014a) and the CEM (2002). The results of the stability analysis are discussed in section 4.4.2. The followings are the details of the stability analysis.

Loading scenarios: The definition of loading scenarios for stability analysis are the same as those described in subsection 3.6.5.

Material properties: One needs to carefully select shear strength that most accurately represents material property. Laboratory experiments are required to determine shear strength for stability analysis. Material obtained from the study site were subjected to laboratory tests to determine soil distribution and other material properties.

As suggested by the USBR (2014a), effective shear strength parameters were used for steady state condition. The adapted shear strength parameters and saturated densities used in the stability analysis were derived from the SI reports, and then matched with the acceptable range as suggested by the USBR (2014a) and DID (2010). These values rely on the lower bound effective friction angle rather than the cohesion values as the recent investigation on the shear strength of the soil material with respect to Mohr-Coulomb circle indicates a curve-linear behavior rather than a perfectly linear response (Zhang et al., 2014). In addition, for rock material, the Mohr-Coulomb (MC) criterion values were derived based on the methods of converting Hoek-Brown parameters (HB) to MC as indicated by DID (2010).

Table 3.7: Material properties for numerical model.

Material	C' (kPa)	phi (deg)	gamma (kN/m3)	K (m/sec)	Model
Sandy Silt	8	25.5	20	4.80E-09	MC
Clay	9	20.5	17	5.10E-10	MC
Medium Sand	0	28.5	16	5.00E-04	MC
Large Stone	0	47.5	53	2.00E-01	HB-MC
Permeable Stone and Concrete	0	43	48	1.00E-02	HB-MC

Required factor of safety: Factor of safety (FOS) is defined as the total shear strength of soil required to keep equilibrium at the surface of sliding. FOS gives the approximate stability of the embankment at different loading conditions. A large FOS suggests low shear stress or small deformation in the embankment.

The USBR (2014a) recommends the Spencer's procedure for slope stability analysis to determine FOS. A minimum FOS of 1.3 is considered adequate for analyzing the undrained shear strength (USBR, 2014a).

Computer-generated pore-water pressure: The USBR (2014a) highlights that 2D numerical methods are only ways to compute pore water pressure for a steady-state and operational condition for complex geometry. In this study, the seepage model was based on the assumptions mentioned before and yielded satisfactory results. Since the numerical model was based on a conservative FOS, the computer generated pheratic surface would never occur in real conditions. The conservative approach helped evaluate embankment condition under the extreme elevation conditions (loading case a and loading case b).

Slip surface configuration: This study incorporated the circular arc slip surface in the 2D model. The USBR (2014a) also suggests that the circular arc slip surface is for analyzing homogeneous or zoned structures. As suggested by USBR (2014a), a comprehensive automation search for different starting points was conducted.

3.6.7 Evaluation of topography changes and soil properties

In this subsection, the methods of evaluating the coastal rehabilitation used in this project are discussed.

3.6.7 (a) Surface elevation measurement

The surface elevation data was collected using a *TOPCON* Total Station. The Temporary Bench Mark (TBM) is located at 2°49’28" N, 101°20’25" E. Further, surface profiling was conducted in accordance with the TBM along axis AA to FF (X-direction) and KK to HH (Y-direction) as shown in Figure 3.9, from 0 to 80 m seaward of the existing dike (Y-direction) and -20 to 80 m along the horizontal coastline stretch (X-direction). Along the defined axis as shown in Figure 3.9, the survey data was collected in an interval of 5 m. The survey was conducted during low tide exposure with the reference to datum defined

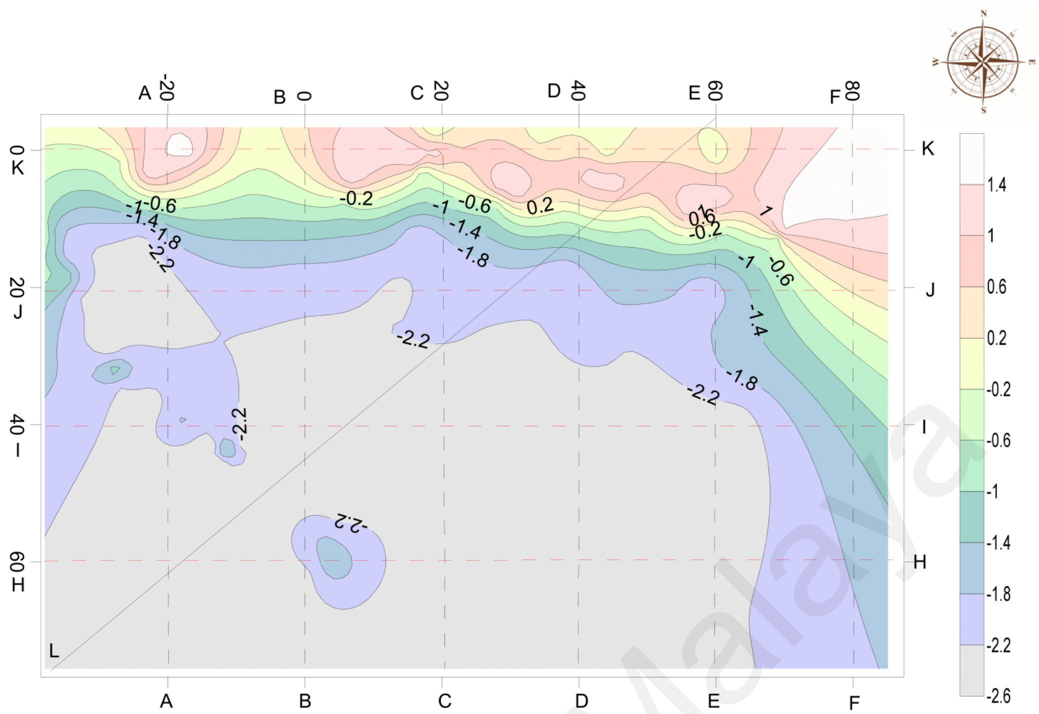

Figure 3.9: Location of topographic data collection is along the direction of X-Y axis in Cartesian coordinate system. Note: all dimensions are in meter and the scale is true for the dimensions depicted along X axis and Y axis.

by the Department of Survey and Mapping Malaysia (B 5345 and B 63083). Finally, the data was corrected in relation to the coordinates taken from the TBM.

The topography data from the study site at the Carey island were collected in seven rounds: (1) January 2011 (24 months after installation of the breakwater); (2) January 2012; (3) January 2013; (4) January 2014; (5) June 2014 (before the installation of the revetments), (6) December 2014 (6 months after installation of the revetment), and (7) June 2015 (12 months after installation of the revetments). The analysis of topographic data along the axis in Figure 3.9 was graphed in various temporal periods to evaluate the performance of the revetments for identifying erosion and accretion trends (see section 4.7).

3.6.7 (b) Monitoring the shoreline elevation change

As discussed in section 3.6.7 (a), changes in the elevation before and after construction of the revetments were measured between 2008 and 2015. Elevations at each subsequent survey round were interpolated using the *Kringing* method in the the *Surfer* software. In addition, other interpolation techniques, such as the *nearest neighbor*, *nearest Shephard*, *minimum curvature*, *radial basis function*, and *inverse distance to a power* were undertaken. A comparison of the *Root Mean Square Error* (RMSE) was carried out for each interpolation technique to determine which method could provide a more accurate surface shape result. The interpolation method with the lowest value of RMSE (the *Kringing* method) was used to generate topography map of the site and other measurements associated with the topography map. This process was undertaken to increase the accuracy of the generated map, which in turn enhanced calculation of the changes in elevation for the study area.

3.6.7 (c) Displacement of the structures along the Cartesian axis for the LEco Revetment

The same method as explained in section 3.6.7 (a) was used to investigate the displacement for the LEco used in LEco revetment. For this purpose, after the installation of the revetment, the LEco placed at the borders of the system were marked and further their vertical displacement were measured (X, Y and Z-axis). The monitoring was conducted in June 2014 and continued in September and December 2014 as well as March and June 2015. Due to design integrity of the LEco revetment, there was little expectation for the displacement along X and Y axes.

3.6.7 (d) Geotechnical characterization of the site

Subsurface soil material characterization: As discussed in section 3.6.4 (b), in this study site investigation works were conducted in accordance with **BS 5930: 1999** "*Code of Practice for Soil*" and Office (2000). The details of subsurface characterization techniques and the results of the laboratory testing are presented in Appendix B.

Near surface sediment characterization: For this study, a stainless steel soil sampler was used to collect 20 soil samples from the Carey Island shoreline along the six axes as shown in Figure 3.10 from the predetermined data points. The logic behind the selection of these data points was that the sample data points were scattered between two main areas, a) behind the breakwater protection and b) outside the area where the breakwater could protect (see details in section **??**). The soil sampling was carried out in accordance with the *ASTM International's Standard Practice for the Field Collection of Soil Samples for the Subsequent Lead Determination* (ASTM E 1727). In this respect, sediment samples were obtained using a hand augur to a depth of 20 to 30 cm (on average) and the disturbed samples were taken to laboratory for testing. The sampling activities was conducted five times between June 2014 and June 2015 (see section 4.7.2).

In this study, sieving and hydrometer methods were employed to obtain the particle size distribution of the soil samples. The tests were performed in accordance with the *Standard Test Method for Particle-Size Analysis of Soils* (ASTM D 422). According to the prerequisite criteria of the *ASTM D 422*, this test is applicable only to the sediment including fine sand, silt, and clay particles that are larger than 0.075 mm. Before carrying out the test, it was assured that carbonates, soluble salts, organic matter, and iron oxides were removed from the samples. For all samples, the soil mass was dried and sieved.

3.6.7 (e) Monitoring of armoring unit damage

Monitoring the integrity and the health of the coastal structures is an essential part of any coastal protection project. Evaluating the structure condition is highly opinion-based. Factors such as the operator's experience and the previous site visits may have influence on the evaluation results. In this study, monitoring of the damage for the armor units was carried out according to the discussion delivered in subsection 3.5.5.

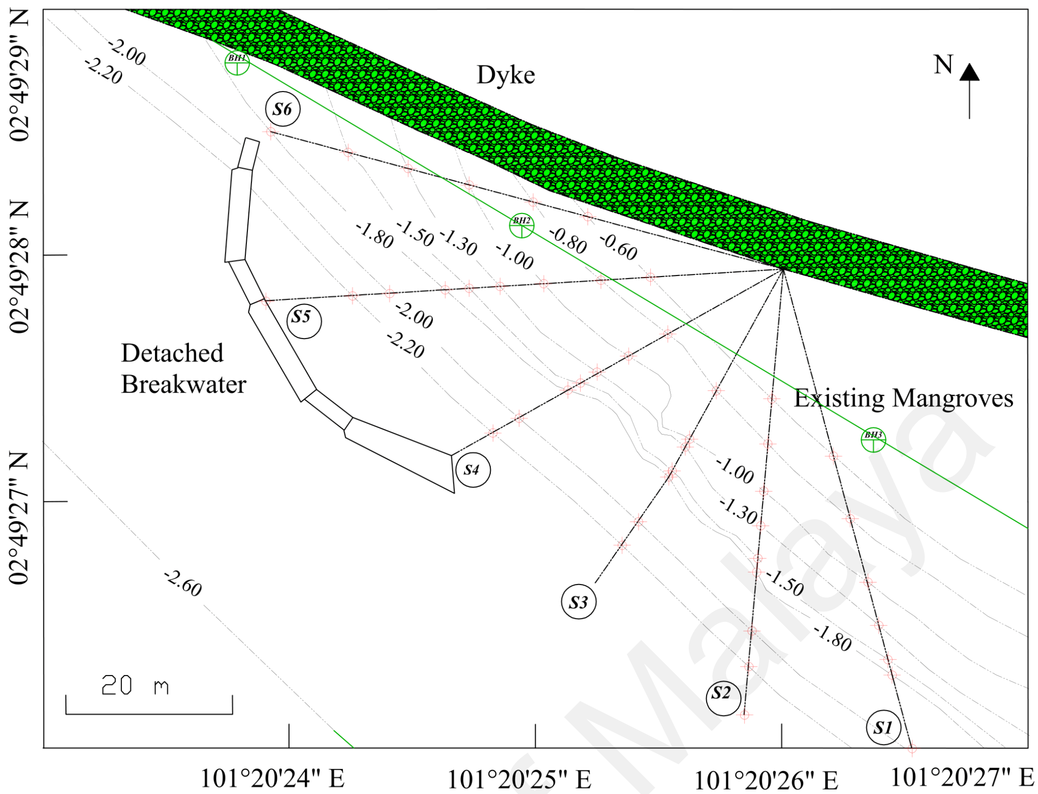

Figure 3.10: Location of data points for the collection of sediment samples and location of boreholes.

3.7 Mangrove rehabilitation

An important factor in the design and implementation of the mangrove rehabilitation projects at coastal areas is the definition of time and the extend of success for projects. This involves setting objectives, goals and performance standards for the project before initiation of attempts. In this section, the methodologies for implementation of mangroves rehabilitation are described. Figure 3.11 shows the flow of mangrove rehabilitation activities in this study.

3.7.1 Mangrove distribution at the site

According to Rozainah, Redzwan, and Wati (2008), the remaining mangrove species on the Carey island (CI) included 31 species. Based on the results of the study conducted by Saraswathy, Rozainah, and Redzwan (2009), *Avicenna alba* is the dominant species on the CI, followed by *Avicenna marina*, *Rhizophera mucronata*, *Rhizophora apiculata* and

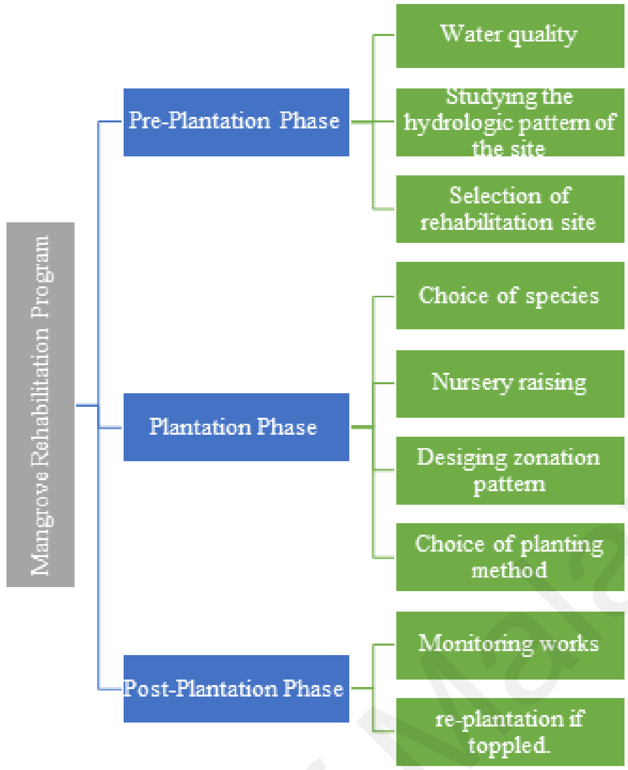

Figure 3.11: Flow of rehabilitation works in this study.

minor cover of *Sonneratia alba*. Thus, the zone pattern of mangroves is dominated by *Avicenna* species (in Malay language known as *Api-Api*), Rhizophora species (in Malay language known as *Bakau Kurap*), and Sonneratia species (in Malay language known as *Perepat*) (Affandi, Kamali, Mz, Tamin, & Hashim, 2010).

3.7.2 Hydrogeochemical assessment for site selection

In this study, hydrogeochemical properties of soil-water samples taken from the Carey Island's coastal zone were investigated before the commencement of revetment construction in June 2014. The main objective of this assessment was to investigate whether future mangrove rehabilitation project at the site in terms of hydrogeochemical parameters could be successful or not.

In this regard, twenty water samples were collected along axis S1 through axis S6 as shown in Figure 3.10 using a split-barrel sampler attached to the hand augur. The samples were obtained from a depth of 20 to 30 cm from the ground surface. The depth of sampling was selected in accordance with the assumption that the sapling roots could be planted in that depth. The S1, S2, and S3 axes denote the area of existing mangroves (natural habitat) and the S4, S5, and S6 axes represent the rehabilitation site. The natural habitat was considered as the control site and the rehabilitation site was considered as the experimental site. The pH value, salinity index, nutrient concentration, and heavy metal content of the samples were measured.

The pH value was assessed for each of the 36 water samples using a multi-probe apparatus according to the *Standard Test Methods for pH of Water* (ASTM D 1293).

The salinity of samples was assessed using a *Atago Hand-Held Refractometer* in accordance with the *Standard Methods for the Examination of Water and Wastewater* (American Water Pollution Control Federation).

The nutrient concentrations were measured via the *ICP* (the 861-Advanced Compact; Australia/Switzerland) in accordance with the *ASTM Water Testing Standards in the "Inorganic Constituents in Water"* series. In this study, the concentrations of nitrogen, sulfur, chlorine, calcium, manganese, and copper were evaluated.

3.7.3 Planting methods

In this study, the main goal of the mangrove rehabilitation project was to have an acceptable trend in successful growth of saplings at the study site to an extent that, natural recovery could take place, and no further plantation was required. In this view, the objective of the mangrove rehabilitation works in this study was to provide shoreline protection and increase the productivity of nearby coastal waters. In this respect, the following five steps were considered to achieve the objective,

(a) The existing mangrove species at the site (see section 3.7.1) were studied with regards to the individual species ecology. In particular, this preliminary assessment included identifying the signs of successful natural mangrove establishment, pattern of reproduction, and propagules distribution.

(b) The current hydrologic pattern of the study area was studied to control the distribution and successful establishment and growth of the targeted mangrove species.

(c) The reasons behind the continuing loss of mangroves at the site were investigated. Also, the environmental modification induced by hard engineering (the breakwater) was assessed to verify the success of engineering measures in removing stressors and unsuitable conditions (see section 4.7 and section 4.9).

(d) The rehabilitation program was designed to incorporate hard and soft engineering concepts (see section 4.9).

(e) Once it was proved that the site is conductive for re-establishment of mangroves (steps a-d), the replanting works were commenced.

3.7.3 (a) Nursery site selection

The target mangrove species (see section 3.7.3, and section 3.7.3 (c)) were first planted in a temporary nursery site, and further upon acceptable growth, the species were transported to the rehabilitation site for replanting. Figure 3.12 shows two views of the nursery site which was located near the rehabilitation site. Figure 3.13 shows the establishment of target species at the nursery prior to transferring to the rehabilitation site.

After the acceptable establishment of mangroves, transportation of species from the nursery to the rehabilitation site was done with maximum care so that the seedlings could be kept healthy before replanting at the rehabilitation site. The nursery ground had enough drainage and was relatively flat. This decision was made, because when standing water is present, the plants become waterlogged and working in the nursery area could be troublesome. The size of the nursery area was selected to be adequate for exposure to sunlight and avoiding problems arising from overcrowding of the saplings.

Figure 3.12: View of the nursery site which was near to the rehabilitation site.

(a) *Avicennia marina* **(b)** *Rhizophora mucronata* **(c)** *Sonneratia alba*

Figure 3.13: Establishment of target species at the nursery prior to transferring to the rehabilitation site.

3.7.3 (b) Selection of rehabilitation site and design of zonation pattern

Suitable location of the rehabilitation site is a key factor to avoid plantation failure. In this study, the care was taken to select the suitable rehabilitation site, which is governed by proper local parameters, such as a) type and quantity of existing species (see section 3.7.1), b) tidal regime (see section 4.2.1), c) extent of wave action (see section 4.2.1), and d) sedimentologic type of substrate (see section 4.7.2). These are crucial for successful establishment of planted mangroves (see section 4.9).

According to the works of Primavera and Esteban (2008), Snedaker (1982), and Watson (1928), for muddy rehabilitation site at the Carey island, the zonation patterns of target planting species (see section 3.7.1) were planned (see section 3.7.3 (d)) based on the criteria provided in Table 3.8.

Figure 3.14 shows the location of planted species at the rehabilitation site with respect to the existing hard engineering features. In June 2014, approximately around 2,000 seedlings of target species were planted at the designated locations. The rehabilitation zones were grouped in to two zones: a) *Zone A* and b) *Zone B*. *Zone A* is located behind the existing breakwater at the rehabilitation site, which is protected directly by the breakwater, and *Zone B* is placed outside the area that is not protected by the breakwater.

Table 3.8: Zonation pattern of target species at the rehabilitation site. Note 1: A. alba, R. mucronata, R. apiculata, A. marina, and S. alba are abbreviations for *Avicenna alba*, *Rhizophera mucronata*, *Rhizophora apiculata*, *Avicenna marina*, and *Sonneratia alba*, respectively. Note 2: S, Si, Cs, C, Sl denote Sand, Silt, silty Clay, Clay, and Sandy loam, respectively. Note 3: HACD is *Height Above Chart Datum*.

Zone	Soil type	Flooded by	HACD (m)	Selected species
Landward	S, Si, Cs, C	All hight tides	0 - 2.09	A. alba, R. mucronata
Middle	Si, Cs,	All medium hight tides	2.10 - 4.10	A. alba, R. apiculata
Seaward	S, Sl	Spring high tides	4.11 - 5.08	A. marina, S. alba

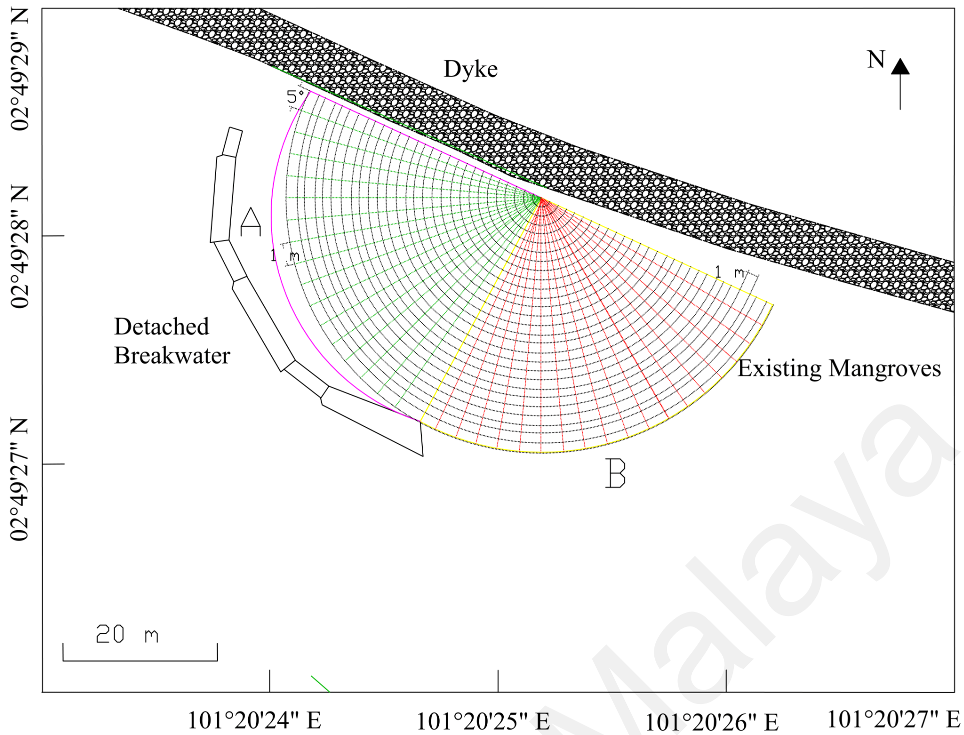

Figure 3.14: Location of planting the target species at the site two month into construction of revetments.

3.7.3 (c) Choice of species

Although making decision about the suitable species can be considered a complex task, the finite objective of mangrove replantation works (i.e., protection or production) and local biophysical characteristics of the rehabilitation site are crucial factors to determine the success of the plantation. The discussions provided in sections 3.7.3 and 3.7.3 (b) explained the reason as to why the target species were chosen for replantation purposes at the rehabilitation site.

3.7.3 (d) Planting techniques and monitoring works

Planting and monitoring works were carried out in different phases at the rehabilitation site. The following is a summary of the planting and monitoring works in this study.

In nursery, the target species were prepared as plant plugs. The selected target sapling for transplanting on average was 31.7 $\pm$ 1 cm in height and 8 mm in diameter. After establishing in the nursery for nearly two months, the saplings were hardened and reached an average height of 80 $\pm$ 5 cm and a diameter of 10 mm. Further, the saplings were transported to the rehabilitation site.

In nursery, the saplings were exposed to gradual direct sunlight before transporting to the rehabilitation site. The micromole daylight intensity at the study site measured by a Lux meter ranged from approximately 250 $\mu molem^{-2}s^{-1}$ at the natural habitat (existing mangroves area) to approximately 1,500 $\mu molem^{-2}s^{-1}$ at the rehabilitation area.

Prior to plantation at the rehabilitation, preparation activities were done at the site. These included the removal of debris, clearance of *Achrosticum* fern or other brush from the area, and clearing the dead woods that could potentially shade out the area.

The plantation works were carried out in several rounds until an acceptable survivability rate of the planted mangroves was reached (see section 4.8). The location for direct plantation of plant plugs of the target species is shown in Figure 3.14. An innovative plantation layout was designed in line with the guidelines in Turner and Lewis (1996) and Lewis (2009) to provide a non-grid plantation scheme.

As can be seen in Figure 3.14, the two quadrant areas between the breakwater and the beach were divided into 18 pieces each rotating from the center location of the circle at 5°. The center of the circle was considered fixed, thus rotating clock-wise in increment of 5° forms the zone A and in the same manner, the rotation in direction of counter-clockwise forms the zone B.

Zone A was planned behind the breakwater so that the wave energy could be dampened before reaching the saplings, and the zone B was placed outside the area in which the breakwater could directly protect it. The rationale behind such plantation layout was to investigate the effect of existing breakwater on the success of rehabilitation works. Each rotational line was crossed with a perpendicular line with an interval of 1 m to generate rectangular inter-blocks. The location of the planted saplings was at corners of each inter-block.

From Figure 3.14, it is obvious that the density of mangrove in the leeward of zone A and zone B was higher. The reason for such an arrangement is that the wave energy flux was lower in the leeward of the rehabilitation site (see section 4.9). This would enhance the survivability of the replanted mangroves, because main stressor at the site is the wave energy. In addition, in that time, considering the scenario of a successful rehabilitation of mangroves, justified that natural recovery could be enhanced providing that the replanted species at the leeward started to generate propagules.

After few days into the construction of the revetments, in June 2014, the first phase of replantation was commenced. The plantation for each class of species at the plantation zones was carried out randomly. In the first plantation phase, 2,000 saplings of the target species were planted at zone A (1000 saplings) and zone B (1,000 saplings). The consequent phases of plantation were carried out each subsequent two months to replace the lost replanted mangroves. The saplings were monitored each month for their survival rates, height increments, and diameter increments.

3.8 Planting coastal vegetation on the revetments

In this study, the main objective of the rehabilitation of coastal vegetation project was to maximize the vegetation cover at the site so that: (1) enhance the biodiversity of the coast, (2) restore the degraded coastal flora at the site , and (3) improve aesthetic view of the proposed revetment structures installed at the coast for providing protection against erosion.

In this view, two coastal flora species were planted at the site: *Cynodon dactylon* (Figure 3.15a) and *Ipomoea pes-caprae* (Figure 3.15b). Hereafter, these species are denoted as *S1* and *S2*, respectively. These were planted at specific location in reference to the developed revetments as summarized in Table 3.9 and Table 3.10. Figure 3.16a shows the plan location of planting S1 species on the deck of all the revetments. In addition,

(a) *Cynodon dactylon*

(b) *Ipomoea pes-caprae*

Figure 3.15: The sample of the coastal flora species used for the rehabilitation project.

Figure 3.16b shows the plan location of planting S1 and S2 species only at the slope of the Abstention revetment.

After the plantation phase was completed, the survivability of the plants were observed for a period of six month. Whenever a significant loss had been observed, the rate of survivability, and the number of the alive species over the total planted species, was graphed against the time unit (month) for evaluating the success of the project.

Table 3.9: Plantation setup for rehabilitation of the *Cynodon dactylon* (S1) and *Ipomoea pes-caprae* (S2) species for all types of the proposed revetments.

Number	Type of structure	Type of species	Location of plantation
1	L1	S1	Revetment deck
2	L1	S1	Revetment deck
3	D1	S1	Revetment deck
4	D1	S1	Revetment deck
4	A1	S1	Revetment deck and slope
5	A1	S2	Revetment deck and slope
6	A2	S1	Revetment deck and slope
7	A2	S2	Revetment deck and slope

Table 3.10: Plantation setup for rehabilitation of the *Cynodon dactylon* (S1) and *Ipomoea pes-caprae* (S2) species at the site using abstention approach.

Number	Type of structure	Type of species	Location of plantation
1	A1	S1	Revetment deck and slope
2	A1	S2	Revetment deck and slope
3	A2	S1	Revetment deck and slope
4	A2	S2	Revetment deck and slope

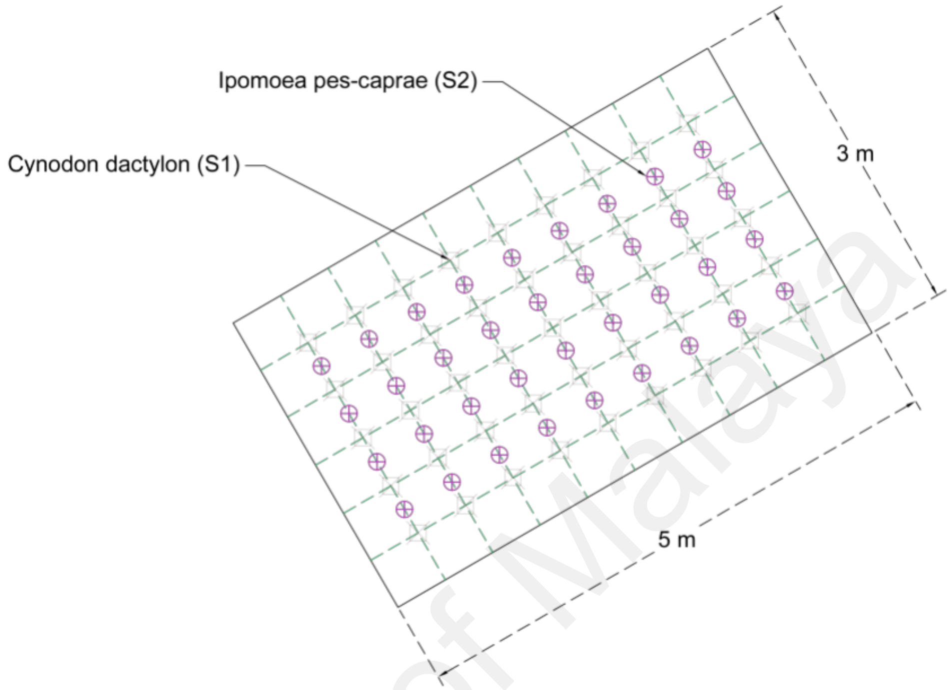

(a)

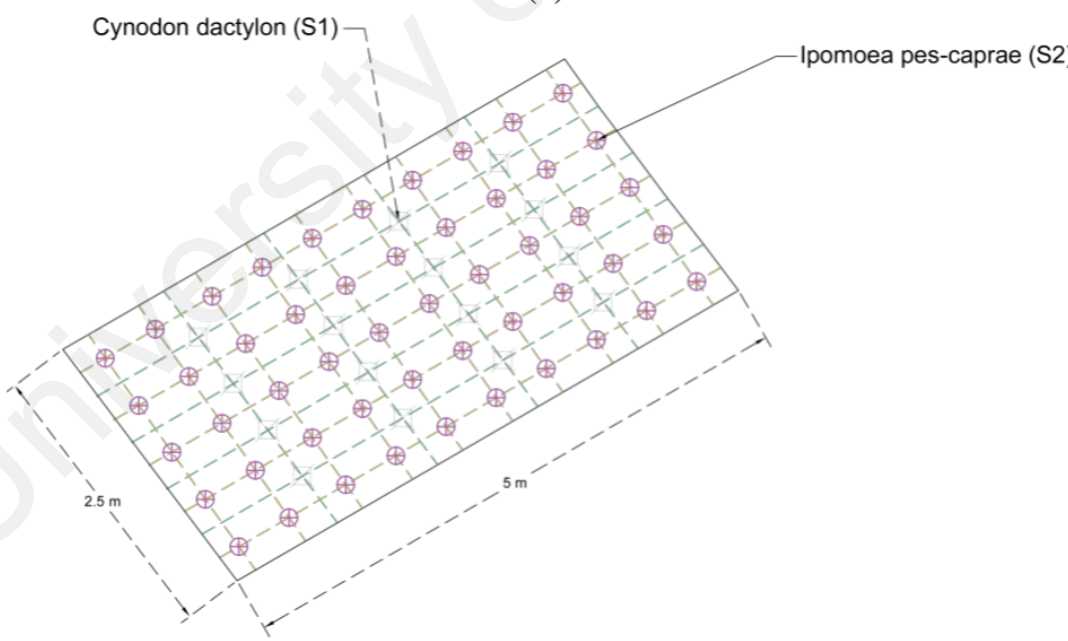

(b)

Figure 3.16: Plan of planting at the (a) deck of the revetments, and (b) at the slope of the abstention revetment.

3.9 Sustainable concrete material for LEco armoring units

In this study, development of eco-friendly revetment structures were one of the main objective. Thus, it was important to ensure that the concrete material used for fabrication of the LEco armoring units is sustainable and eco-friendly. In this respect, series of unconfined compressive tests were performed on various loading conditions for a set of varying parameters on composition materials as well as curing period. These parameters were Pulverized Fuel Ash (PFA) content (%), cement content (%), sand inclusion (%) and curing period (days). In addition, for the alternative material cockle shell powder replaced the PFA.

3.9.1 Development of PFA-cement-sand composite material

A series of unconfined compressive tests (UCT) were conducted for various mixtures of PFA, aggregate and cement; the tests considered both the optimum moisture content (OMC) and the curing period. The total number of tested samples was 91 and for each of them, the PFA content, cement content, and density were measured. The diameter and the length of each sample were 5 cm and 10 cm, respectively. The samples were cured for 1, 7, 14, and 28 days prior to testing. The cement content was 5-25% of the total weight of the sample, whereas the PFA content was 5–40 %. More detailed findings of these researches are found in Motamedi, Song, and Hashim (2015), Motamedi, Shamshirband, Petkovic, and Hashim (2015) and Motamedi, Shamshirband, Hashim, Petkovic, and Roy (2015).

3.9.2 Development of Cockle shell-Cement-Sand composite material

A series of unconfined compressive tests (UCT) were conducted for various mixtures of PFA, aggregate and cement; the tests considered both the optimum moisture content (OMC) and curing period. The total number of tested samples was 810, and for each of them, the cockle-shell content, cement content, and density were measured. The diameter and the length of each sample were 5 cm and 10 cm, respectively. The samples were cured for 1, 7, 14, and 28 days prior to testing. The cement content was 0-50% of the total weight of the sample, whereas the cockle-shell content was 0–25 %. More detailed findings of these researches can be found in Motamedi, Shamshirband, Hashim, et al. (2015).

CHAPTER 4: RESULTS AND DISCUSSIONS

4.1 Introduction

This chapter is comprised of two main components. First, results and discussions in relation to the design, construction and monitoring of the proposed revetments are elaborated. For this, section 4.3 , section 4.4 and section 4.5 deal with the verification of the preliminary design layouts of the proposed revetments. Further, in section 4.6 the details for construction of the proposed revetments are presented. In addition, a series of monitoring works for the stability of the proposed revetments are delivered in section 4.7. Further, the second component of this chapter deals with the results and discussions in relation to a series of mangrove rehabilitation works (section 4.8) and plantation of coastal flora at the site (section 4.8.4). Finally, a thorough discussion is delivered in section 4.9 including the details of the proposed integrated coastal rehabilitation program in this study.

4.2 Wave/climatic properties and geological conditions of the site

In this section, the findings from desktop study in relation to wave/climatic properties and geological conditions of the site is discussed.

4.2.1 Climatic conditions and tide/wave properties

The climatic data were provided by the Malaysian Meteorological Department (MMD) at the range of 2°-3° latitude and 101°-102° longitude for a period between 1950 to 2014. The following is the list of key findings based on the statistical analysis of the climatic data for the study site.

Tropical climate characteristics are widely found within the target site, and the climatic properties in this zone are tied to the Northeast and Southwest monsoonal regimes. During the inter-monsoon season, the weather is highly unpredictable (R. Hashim et al., 2010). The Southwest monsoon occurs between May to September annually and the

Northeast monsoon takes place from November to March. From April to October is a transition period or inter-monsoon which happens between the Southwest and Northeast monsoons.

In terms of temperature, humidity, and annual precipitation, based on the analysis of data from the Malaysian Meteorological Department (MMD) between the year 1950 and 2014, the temperature at the vicinity of the site has been fluctuated on average between 22 ± 0.65°C and 32 ± 0.65°C (Figure 4.1) with an average maximum relative humidity of 84 to 92% since 2000 (Muzathik, Nik, Samo, & Ibrahim, 2011). In addition, annual precipitation data indicates that, on average, the mean monthly precipitation (mm) at the vicinity of the site is 201 ± 15 mm between the year 1950 and 2014 (Figure 4.2). The results almost matched with the measured average annual precipitation (approximately on average 2,220.51 mm) by the West Estate Office, Sime Darby Sdn. Bhd. in 2012.

The coast of Carey Island is influenced by significant local currents generated by vessle transition, waves and tides. In addition, the coast is influenced by insignificant deep water wind-generated waves. According to the analysis of tide data obtained from the Department of Survey and Mapping Malaysia (JUPEM) from 2004 to 2014, the coast of Carey Island has a semi-diurnal tidal regime with an average low tide (MLW) of +2.09 m above the MSL, an average high tide of +5.08 m above the MSL, and it receives daily tidal inundation that the average range of tides is +2.99 m above the MSL.

The direction of wind at the Carey Island alters in accordance with the monsoon seasons. Based on a report from the MMD between the year 2004 and 2014, prevailing wind direction during the Northeast monsoon, measured in the range from lat 2.0 °N to 3.0 °N and long 101.0 °E to 102.0 °E, comes from 130 °SE to 160 °SE with an average velocity of 2 m/s (the highest recorded in July 2011 at 17 m/s). Based on the JUPEM report, during November and January, these winds generate monthly local waves with significant heights of 1.5-1.8 m on the coasts of Carey Island with wave periods of 2-8 s

(Muzathik et al., 2011). Figure 4.3 shows the significant wave height for a period between January 2009 and November 2013. The strongest waves at the site are those from the SW. Thus, the positioning of the proposed revetments at the site was planned so that they were almost perpendicular to the prevalent wave direction.

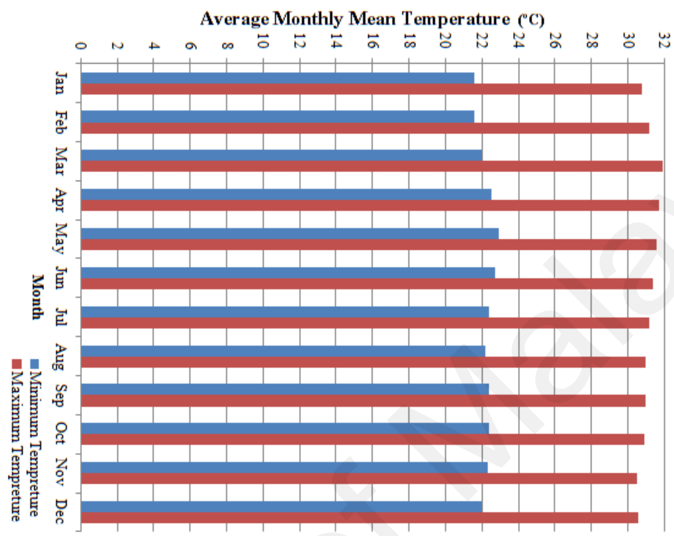

Figure 4.1: The average monthly temperature at the vicinity of the study site between the years 1950 and 2014.

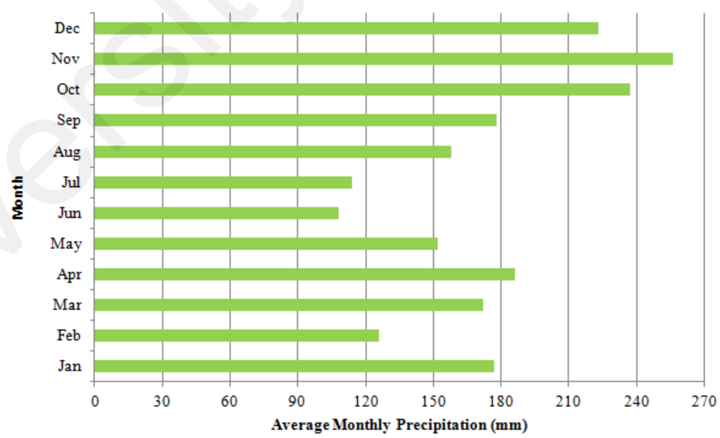

Figure 4.2: The average monthly precipitation at the vicinity of the study site between the years 1950 and 2014.

4.2.2 Geology and Sediment Stratigraphy

The Carey Island is located next to the wider channel of the Strait of Malacca. Previous geological studies at the Carey Island demonstrated the existence of alluvial textures

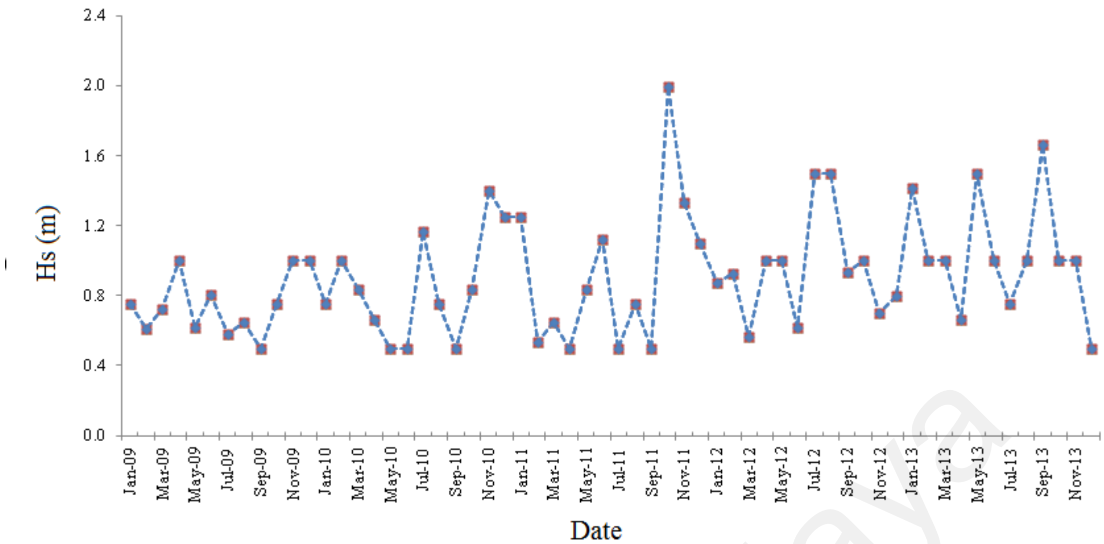

Figure 4.3: Monthly significant wave height that is measured in the vicinity of the site at Carey island for a period between January 2009 and November 2013.

(Baharuddin, Ismail, Othman, Taib, & Hashim, 2013). Bathymetry studies in the Strait of Malacca reveal complicated characteristics, and the area is interpreted as a "*Pleistocene lowered-sea-level alluvial-delta-fan*" with sediments underlies by old alluvium texture dated back from 36,420 to 41,500 BP (Kamaludin, Nakamura, Price, Woodroffe, & Fujii, 1993).

Approximately 70% of the Carey Island is composed of Holocene deposits of clay, silty clay, peat and minor sand formations that with the foundations of Pleistocene deposits of gravel, sand, clay and silt (Baba, 2003). The bedrock at the Carey Island mainly constituted of sedimentary rocks such as inter-bedded shale, siltstone, and sandstone (Nawawi, Harith, Ayub, Ibrahim, & Alphonse, 2001).

The subsoil at the site from samples collected at the range of 10 to 40 cm depth indicated the existence of stiff clay covered by a thin layer of silt loam (see subsection 3.6.7 (d)). Also, during the study muddy depositions were observed at the site during the North-East monsoon indicating that these sediments could have been carried from the deep water to the beach by strong currents and waves.

4.3 Verification of preliminary design using 2D physical model

The physical model in this study was performed at the hydraulic laboratory of the Civil Engineering Department, University of Malaya. The followings are the results and discussion related to the physical modeling for the LEco revetment and Double-Layer revetment.

4.3.1 Hydraulic stability of LEco armoring units

Based on the methods in section 3.5, the hydraulic stability of LEco armoring units (LEco) was assessed. When $\theta = 37°$, no displacement of the LEco was observed, whereas when $\theta = 53°$ (Figure 4.4a and Figure 4.4b), minor displacement occurred. The following elaborates on these findings.

Figure 4.5b to Figure 4.5d show the results of the recorded displacements for three points located on four representative blocks (Figure 4.5a) for $\theta = 53°$ under various wave set-up no. 6 as in Table 3.3. In these figures, point 1 is located at the right-middle side of the blocks, point 2 is located at the bottom-middle side of the blocks and point 3 is located at the left-middle side of the blocks (Figure 4.5a). For other configurations as stated in Table 3.3, no displacement occurred, or the values were small enough to be negligible.

From Figure 4.5b to Figure 4.5d, it can be seen that block 2 and block 4 located at the bottom-left and the bottom right side of the model, had undergone the maximum observed displacement at 6.3 ± 0.1 mm (Y-direction) and 7.8 ± 0.1 mm (Z-direction), respectively. The minimum values of displacement observed for these two blocks were 3.4 ± 0.1 mm (Y-direction) and 2.9 ± 0.1 mm (Y-direction), respectively. In the meantime, the average values of displacement irrespective of the direction for block 2 and block 4 were 4.9 ± 0.1 mm and 5.7 ± 0.1 mm, respectively.

The recorded displacement for block 1 and block 3, located at the top-right and top-left side of the model was lower than those observed for block 2 and block 4. For example, the maximum values of displacement for block 1 was 3.8 ± 0.1 mm (Z-direction) and 2.5 ± 0.1 mm (Z-direction) for block 3. In addition, minimum displacements for block 1 and block 3 were 1.9 ± 0.1 mm (X-direction) and 1.0 ± 0.1 mm (Y-direction), respectively. Also, the mean values of the displacement, for blocks 1 and 3, irrespective of the direction were 2.7 ± 0.1 mm and 1.8 ± 0.1 mm, respectively. Therefore, it can be stated that the blocks located at the bottom part of the model were more vulnerable to displacement compared with those located on the top of the model.

The values recorded for all directions were all lower than 7.8 ± 0.1 mm, which is considered very small compared with the length of the model (see section 3.5) and therefore can be negligible. Although the measured displacement was negligible, for nearly all the points at these four blocks, the highest displacement occurred in Z-direction; except in a few instances where the recorded displacement along the X-direction was slightly higher compared with the displacement recorded for the Z-direction (i.e., point 2 at block 3 and point 3 at block 3).

Due to great interlocking capabilities of the LEco, within the tested range of wave events (see Table 3.3), they were not removed or toppled from the armoring layer. Nevertheless, in the rare probable occurrence of an extreme event on actual site conditions, a failure would statistically happen due to removal of armoring units on the upper row of the armoring layer. This is because of the loosening the interlocking capacity of units on upper row of the armoring layer, which then may result in malfunction of lower raw armoring units. This can lead to possible catastrophic failure of the armoring layer. However, in the tested range of wave, during the experiments in this study, no damage was observed for the wave set-up when $\theta = 37°$ and $\theta = 53°$.

Although during the experimental study, rocking was not found to cause damage to the model, it is probable that if the units are not reinforced with steel bars, the rocking can result in damage (see section 2.5.3 (d)). In this respect, for the adaptation of the LEco for the pilot project, reinforcement was used in the fabrication of the LEco (see section 3.3).

The LEco are modified version of L-blocks developed at the University of Malaya. For instance, the reinforcement layout for the LEco was totally rearranged compared with L-blocks. In addition, the material used in fabrication of the LEco was eco-friendly and resistant to higher loading conditions (see section 3.9). These improvements were planned so that the LEco could be placed on the revetments even with higher slope angle (see section 3.3.1 (b)).

Previously, the L-blocks were designed and tested for breakwater applications. Based on the previous studies on hydraulic stability of L-blocks (Kamali & Hashim, 2011), $N_{od} = 0$ was recorded at the $N_s = 2.98$. In addition, $N_{od} = 0.5$ was observed at $N_s = 3.8$ which replicates the $K_D \sim 20$. In this respect, given the enhancement incorporated in design and fabrication of the LEco, the stability number (N_s) obtained for L-blocks was conservative. According to the CEM (2006), it is necessary to ensure that during the life time of the coastal protection structures, the damage risk is minimized as much as possible. Thus, incorporating safety in the design of revetment structures towards reducing the consequences of unforeseen events yielded a ration for selecting $K_D = 20$ in the final design of the LEco. Table 4.1 summarizes the data for commonly used armoring units and LEco. As can be seen, the LEco provides a reasonable stability while being easy to fabricate and simple in geometry.

During the experiment, when $\theta = 53°$, a slide was observed on the sides of the model perpendicular to the wave direction (Figure 4.4c). The incident was due to the limitation of laboratory model, because the sides of the model were constrained by flume walls. When the waves hit the wall, they were reflected back to the model leading to progression of the slide. Such an incident was not expected to occur in the field condition, because in actual condition, the flow of water can seep through the main body of revetments and then be dissipated. In order to mitigate against the effect of $H_s > H_d$, the final design of revetments (see section 4.5) incorporated a transverse arrangement of stone pieces with $D_{n50} = 30cm$. As a check, the model was reconstructed and re-tested using stone pieces with $D_{n50} = 6cm$. Upon re-testing the model using the revised configurations, no sliding was observed.

Table 4.1: Comparison between LEco and other conventional armoring units (data derived from SPM (1984). Note: The KD parameter is for non-breaking waves and no-overtopping criteria.)

Unit	Dolos	Tribar	Tetrapod	LEco
Country	RSA	USA	FR	MY
Year	1963	1958	1950	2015
Geometry	Double Anchor	Slab Type	Thetraedon	Hollow Shape
Shape	Complex	Complex	Complex	Simple
Placement	Double-Layer	Double-Layer	Double-Layer	Single-Layer
KD	25	11	9	20
Fabrication	Difficult	Difficult	Difficult	Easy
Φ	0.83	0.938	0.97	0.65

4.3.2 Hydraulic stability of stone armoring units

Based on the methodology discussed in section 3.5, hydraulic stability of the Double-Layer revetment system was evaluated. When $\theta = 37°$ and $\theta = 53°$, no major displacement were observed in the stone armoring units. Figure 4.6 and Figure 4.7 show the condition of the models for $\theta = 53°$ and $\theta = 37°$, before and after the test run for wave configuration no. 6 as in Table 3.3.

Based on the explicit quantitative assessment of damage parameter (section 2.5.3 (a)), for all the wave configurations, the $A_e = 0$. Therefore, $S = 0$.

Based on the implicit estimation of damage for stone armoring units (section 2.5.3 (c)), the N_{od}, was calculated. Table 4.2 shows the results of the calculated N_{od} for the test run after wave configuration no. 6 as in Table 3.3. For other wave configurations, no movement was observed in the stone armoring units (see Table 2.1). From this table, for both $\theta = 37°$ and $\theta = 53°$, the type of movement criteria was *limited movement during reshaping, with eventual static stability*.

(a)

(b)

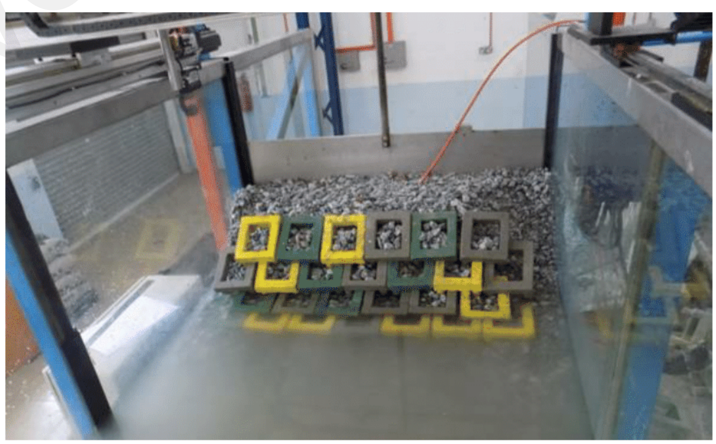

(c)

Figure 4.4: The physical model of LEco-revetment when $\theta = 53°$ (a) before the experiment, (b) after the experiment; and (c) the minor sliding observed at filter layer of the model due to flume wall constraints leading to re-testing using larger stone pieces.

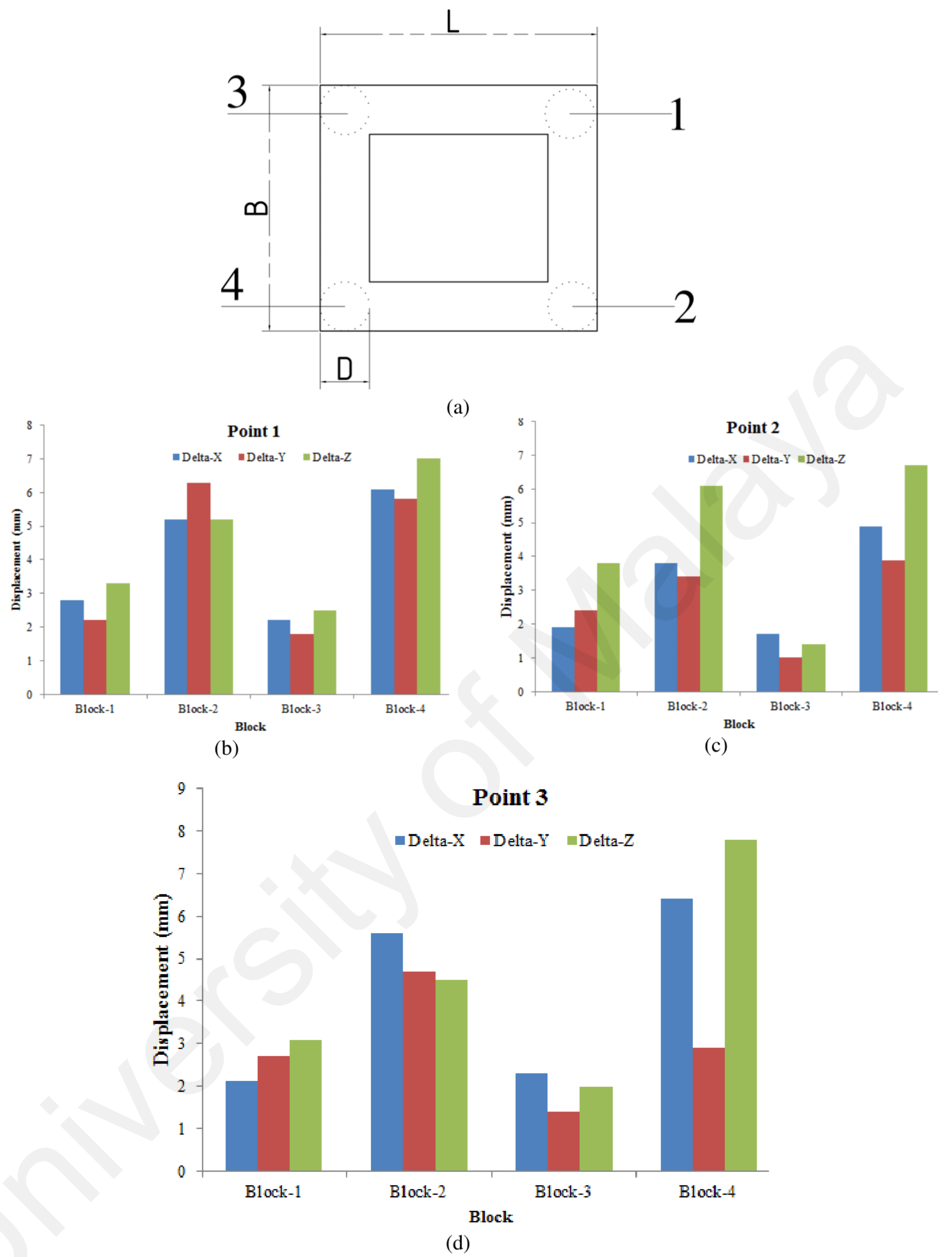

Figure 4.5: (a) The location of displacement measurement points on selected LEco; and the displacement observed at (b) point 1, (c) point 2, and (d) point 3 for representative LEco on LEco revetments when $\theta = 53°$ after the experiment.

Table 4.2: Calculated N_{od} for the test run after wave configuration no. 6

Angle	Displaced stones	D_n	N_{od}	Movement Criteria
53	18	100 cm	0.18	Type 2
37	12	100 cm	0.12	Type 2

(a) (b)

Figure 4.6: When $\theta = 53°$ for (a) before and (b) after the test run, no major displacement was observed for Double-layer revetment.

(a) (b)

Figure 4.7: When $\theta = 37°$ for (a) before and (b) after the test run, no major displacement was observed for Double-Layer revetment.

4.4 Verification of preliminary design layouts using numerical model

Being located at the coastal area, the study site at the Carey island was potentially vulnerable to excessive seepage problems. The existence of pervious sandy layers in the subsurface soil at the identified locations below the revetments could be the main cause of seepage problem. In addition, the underlying soil material was found to be highly pervious. Therefore, prior to finalizing the design layouts for revetments, it was necessary to verify their safety against sliding and excessive seepage potential. The results of the numerical analysis were incorporated in validating the preliminary design layouts of the revetments.

4.4.1 Seepage analysis

This subsection deals with the results of 2D seepage analysis for revetment structures using the *SEEP/W* software (subsection 3.6.5). The seepage is believed to come through and under the revetment structures. The analysis was a unconfined flow analysis that consists of steady state condition.

Figure 4.8 shows 2D numerical model developed for loading case of 100% water at the height of the developed revetments. Figure **??** depicts the predicted seepage (lit/min) for different loading scenarios at the point located in the back side of the revetments. According to the defined loading conditions (subsection 3.6.5), the predicted seepage was highest at 6.8×10^{-8} lit/min for Double-Layer revetment when the loading case a was assumed. Lowest value of predicted seepage was found at 9×10^{-9} lit/min for Absentation revetment when loading case c was assumed. In general, for all the revetments, the predicted seepage at the point located in the back side of the revetments followed a decreasing trend from 0% towards 75% of water at the height of the structures. Subsequently when the water level reached 100% of the height of the structure, the predicted seepage increased. The highest predicted seepage values were found for the Double-Layer, the LEco and the Abstention revetments, respectively. This can be explained from the perspective that higher porosity of materials of the Double-Layer compared to other modes of the developed revetments resulted in higher hydraulic conductivity.

Figure 4.9b shows the predicted seepage (lit/min) for different loading scenarios in the point located in the middle of the revetment structures. From this figure, similar to the case of seepage values predicted at the back of revetments, the predicted seepage values for the points located in the middle of the revetments, resulted in a higher seepage values for the Double-Layer revetments, followed by the LEco and the Absentation revetments. This can be attributed to the fact that higher porosity of materials of the Double-Layer resulted in a higher hydraulic conductivity.

Unlike the case of the revetments' back, when the values at the middle of the revetments was predicted, a consistent decreasing trend was found. This difference is to the existence of material barrier between the cases in back and middle of revetments, which resulted in the variation between the predicted seepage values.

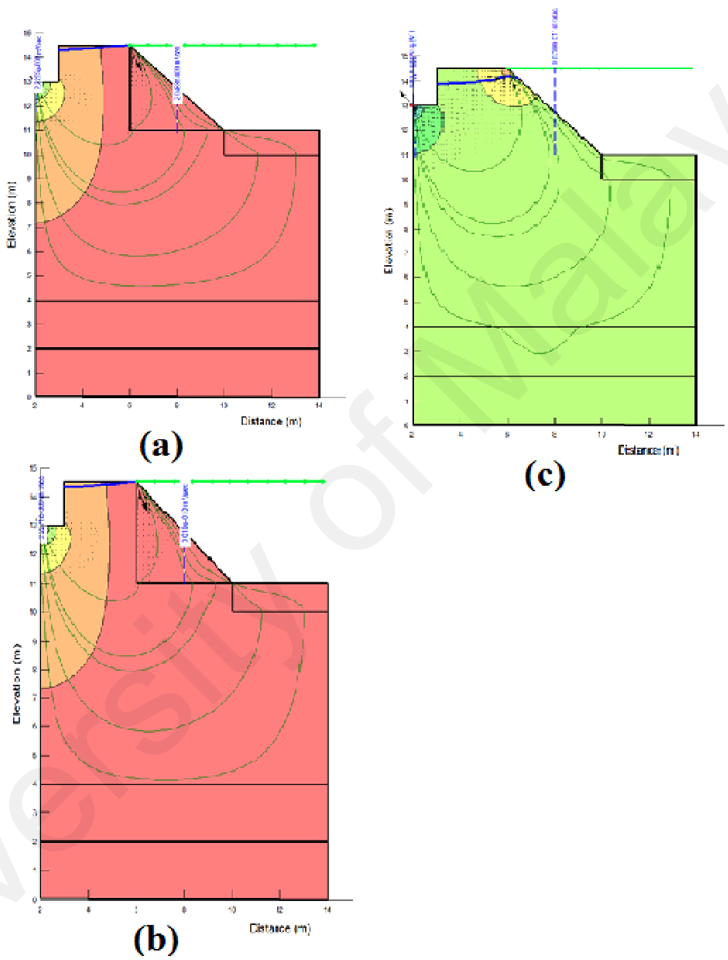

Figure 4.8: 2D seepage numerical model developed for loading case of 100% water height: (a) Double-Layer, (b) LEco, and (c) Absentation revetments.

According to section 3.6.4, the minimum factor of safety shall be so that hydraulic exit gradients are within the range (FOS>3). Figure 4.10b shows the calculated FOS against the high exit gradients that could lead to quick condition in the back of the revetments. It is evident that all the calculated FOS for four loading scenarios (i.e., water level at height of the structure (%) = 0, 25, 50, and 100) result in higher FOS than 3. The high-

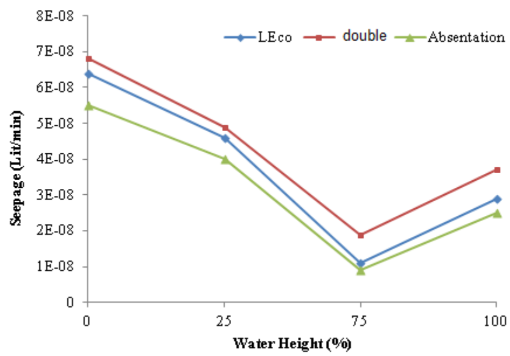

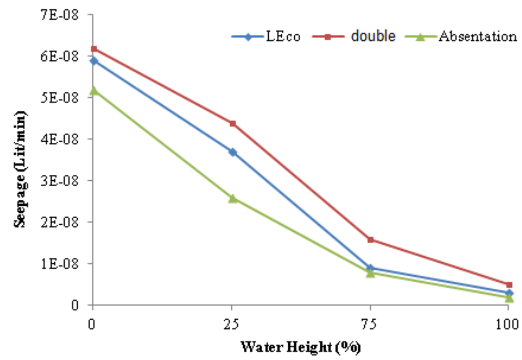

(a) **(b)**

Figure 4.9: Predicted seepage (lit/min) for different loading scenarios at the point located at the (a) back and (b) middle of the developed revetments.

est FOS values were calculated when the value (%) was 50. This indicates that presence of the revetments significantly contributed to the safety of coastline by reducing the risk of quick condition.

Although the calculated FOS values decreased when the water level reached 100% compared to 50%, the values are relatively higher than that calculated for cases of water levels 0% and 25%. This supports the conditions by which the presence of the revetments contribute to the safety of coastline against quick condition.

The calculated FOS for the Abstention are higher than the Double-Layer and LEco revetments. This is attributed to the fact that due to the porous nature of the materials used in the construction of LEco and Double-Layer, the hydraulic conductivity of the materials used are somehow higher than the intact soil used in Abstention revetment.

In conclusion, all three types of the developed revetments under the loading conditions, material and geometric properties used in the numerical modeling are considered safe against the high exit hydraulic gradients. Thus, quick condition would not be highly likely to occur for these structures.

As presented in section 3.6.4, the minimum factor of safety against uplift pressure shall be higher than 1.5 ($FOS > 1.5$). Figure 4.10 shows the calculated FOS against the uplift pressure at the base of the confining layer below the revetment structures. It is evi-

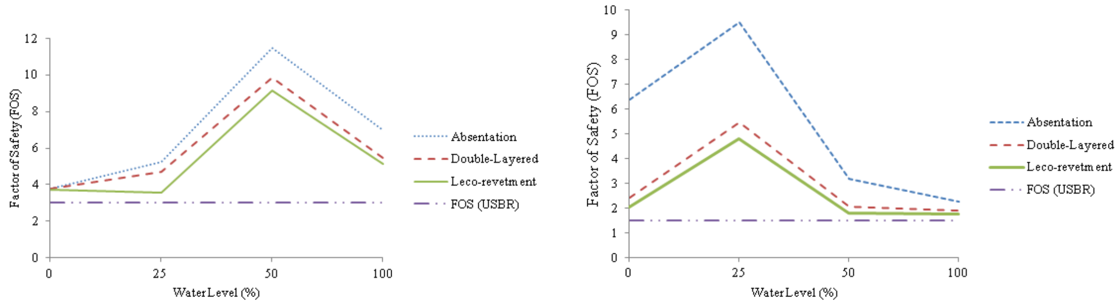

(a) **(b)**

Figure 4.10: Calculated FOS against (a) high exit gradients and (b) uplift that might lead to quick condition in the back of the proposed revetment structures.

dent that all the calculated FOSs for four loading conditions result in FOS higher than 1.5. The highest FOS values were calculated when water level (%) was 25. In this respect, increasing the water level (%) resulted in lower FOS against the uplift pressure. Therefore, the obtained results follow the expected scenarios as indicated by the USBR (2014b). On the other hand, elevation of the water level from 0 to 25% resulted in increased FOS. This is because when water level is 0%, the revetment structures are not functional to the modeling conditions. Thus, these results are considered normal.

Based on the above discussions, all three types of the developed revetment structures under the loading conditions, material and geometric properties used in the numerical modeling are considered safe against the uplift pressure at the base of the confining layer and thus, it is highly unlikely that uplift pressure occurs.

4.4.2 Stability analysis

This section presents the results of 2D numerical model for analysis of stability for the proposed revetments. Based on the method of analysis discussed in subsection 3.6.6, the 2D numerical models were developed using the SLOPE/W software.

Figure 4.11 shows the 2D stability numerical models developed for loading case of 100% water height for the developed revetments. Figure 4.12 shows the graph of FOS against sliding versus water levels at height of the structures (loading scenarios). The highest FOS was found at 1.741 for the LEco revetment using the Spencer method when the water level was 0%. The lowest FOS of 1.156 was found for the Abstention revetment when the water level was 100% using *Morgenstern-Price* (MP) method.

For both MP and Spencer methods, the predicted FOS was higher in case of LEco compared to Double-Layer and Abstention revetments. In addition, for all the cases, as the water level increases, the FOS decreases. For example, using Spencer method, the FOS of 1.496 predicted for the water level at 75% for the LEco revetment dropped to 1.429 when the water level reached 100%.

Except for the case of Abstention , the predicted FOS for the Double-Layer and LEco revetments satisfies the criteria explained in the USBR (2014a), whereby the predicted FOS shall be above 1.3. However, for the Abstention revetment when the water level reaches 100%, the predicted FOS using both M-P and Spencer methods is lower than 1.3 (1.156 for the M-P and 1.163 for the Spencer).

In conclusion, for the LEco and Double-Layer revetments under all the loading scenarios, material and geometric properties used in the numerical modeling are considered safe against sliding. However, care should be taken when the Abstention revetment is designed, because it is vulnerable to sliding when $h_e = 100\%$ of the design water height.

4.5 Finalized design layouts of the proposed revetments

Based on the methods in section 3.6.3, the preliminary design layouts for all the proposed revetments were verified in accordance with the physical model (section 4.3), and the numerical study (section 4.4) and . In this view, the final design layouts of revetments that considered the dimensions, geometry, climate and environmental conditions of the site were finalized. The final design layout of the proposed revetments are shown in Figure 4.13a, Figure 4.13b and Figure 4.13c for the LEco, the Double-Layer and the

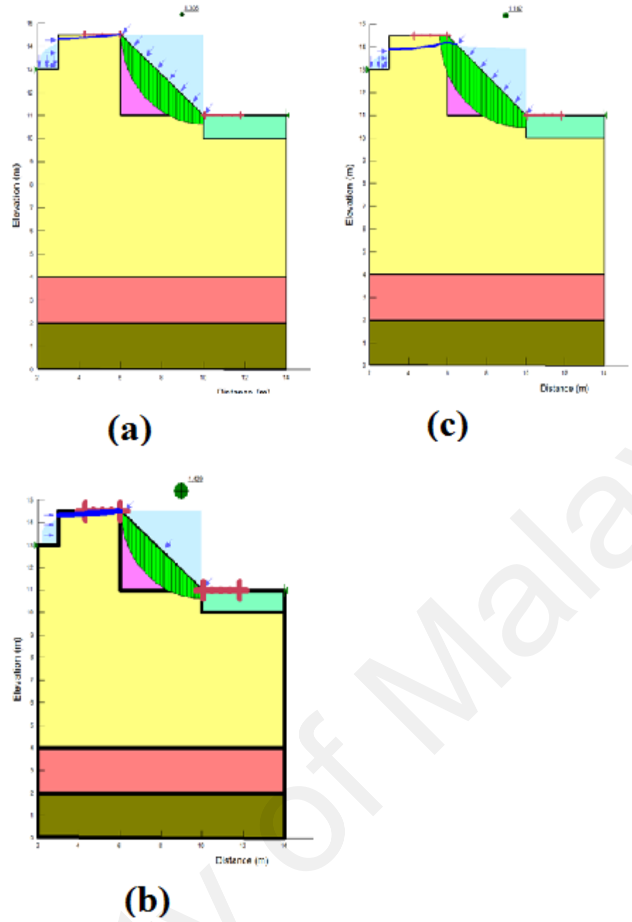

Figure 4.11: 2D stability numerical model developed for loading case of 100% water height: (a) Double-Layer revetment, (b) LEco revetment, and (c) Absentation revetment.

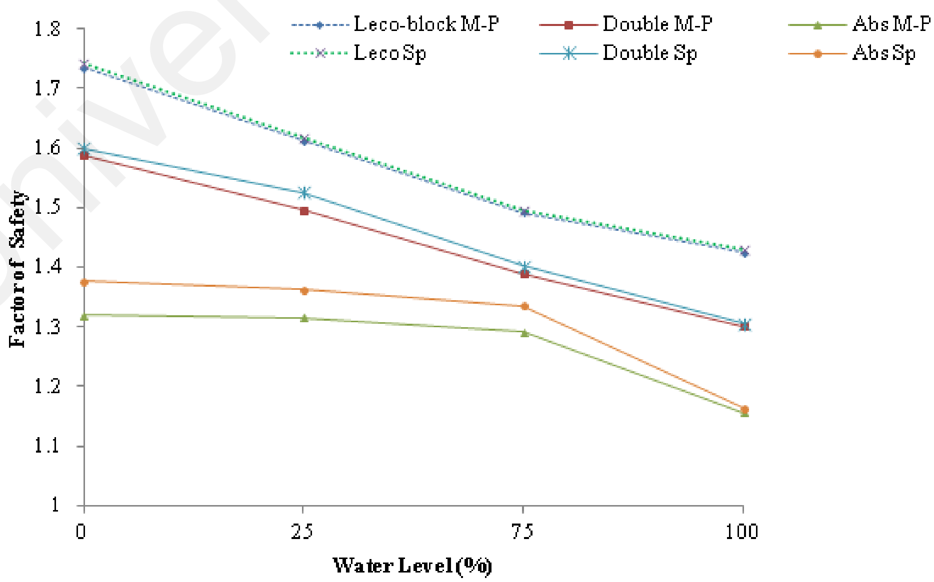

Figure 4.12: Factor of Safety against sliding using MP and Spencer methods for the proposed revetments.

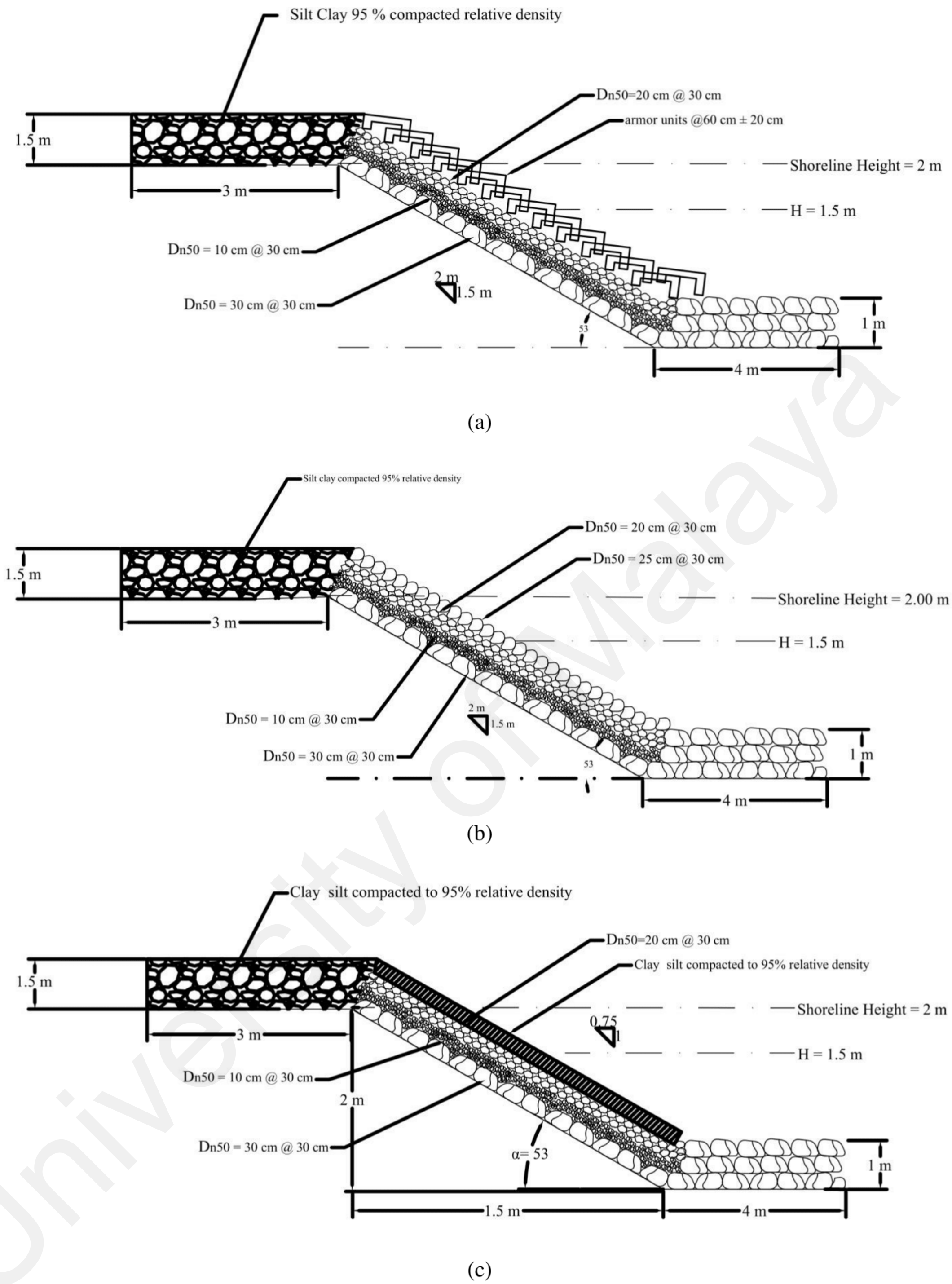

Figure 4.13: Final design layout of (a) LEco, (b) Double-Layer, and (c) Abstention revetments for construction at the study site.

Abstention revetments. Section 4.6 discusses the details of the construction procedure for the revetments at the site.

4.6 Construction of revetment structures at Carey Island

The following section discusses the detailed information on the extent of construction activities pertaining to completion of the proposed revetments.

4.6.1 Sequence of construction activities

The construction works in this study were carried out in six steps. These works were carried out in line with the guidelines provided in the CEM (2002) and SPM (1984). Figure 4.14 depicts the massive erosion at the site before commencement of coastal protection project. The sequence in which the construction activities were conducted is shown in Figure 4.15.

Figure 4.14: The massive erosion at the site before commencement of the coastal protection project (August 2014).

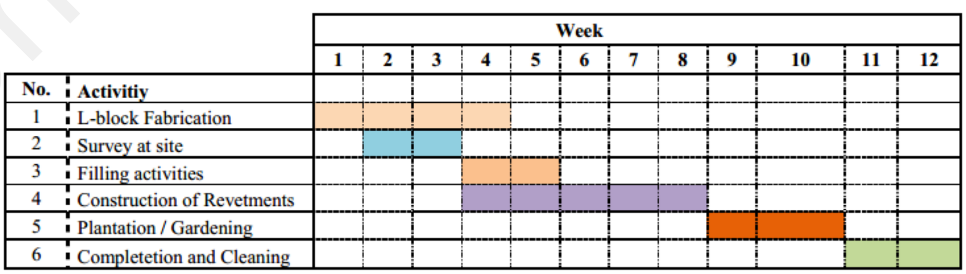

Figure 4.15: The gantt chart shows the sequence of construction activities for the Carey island project.

4.6.2 Fabrication of LEco armoring units

As discussed in section 3.3.1, one of the objectives of this study was to develop a sustainable cement-based material for the fabrication of LEco. Thus, two alternative materials were used, namely a) Pulverized Fuel Ash (PFA), and b) cockle shell (CS) powder to reduce the amount of cement used in the production of concrete. The LEco that were used in the LEco revetment behind the existing breakwater (L1) were fabricated using the PFA mixture material and the other revetment used the LEco that were formed using the CS mixture. Comparison between the on-site performance of the LEco made of different material mixtures was not the primary objective of this study.

For the purpose of this study, it was sufficient that each material mixture could provide a satisfactory performance for purposing armoring layer layout under the loading conditions. Figure 4.16 depicts the actual shape and dimension of the LEco used to form the LEco revetment.

4.6.2 (a) Final geometry of LEco armoring units

The fundamental of design for the LEco was discussed earlier in subsection 3.3.1. Based on the site conditions (i.e., moderate steepness of the slope, moderate to low wave conditions and volume of earthworks) and practical construction simplifications, the parameters of LEco dimension (Figure 3.1) were chosen. Afterwards, the design layout of the LEco

Figure 4.16: The actual shape and dimension of LEco armoring units.

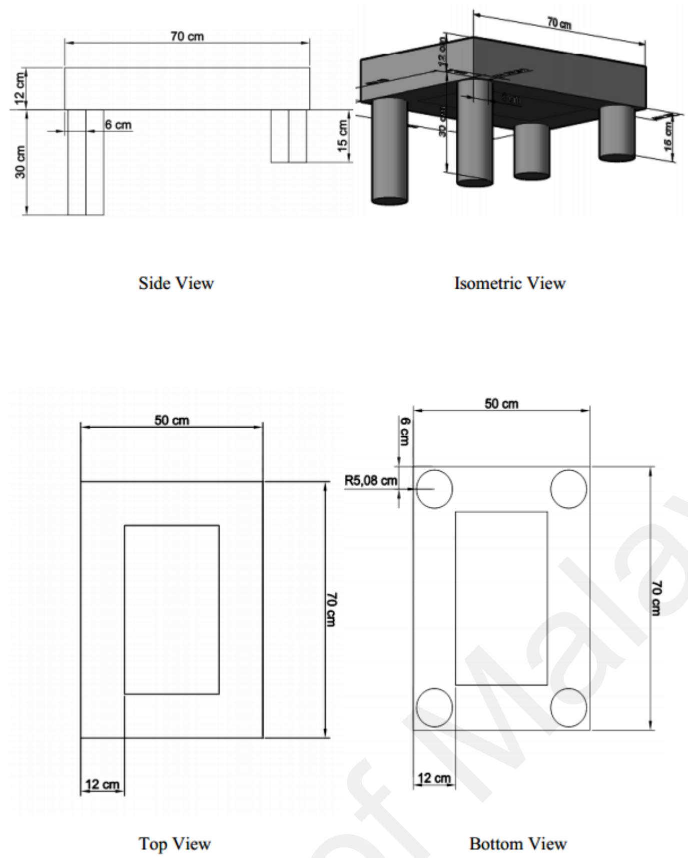

Figure 4.17: The finalized geometry of LEco armoring units proposed for the Carey island project.

for the Carey island coastal protection project was finalized (Figure 4.17). The final design layout also incorporated reinforcement using steel bars to counter the inherent low tensile strength of the cement-based mixtures. Figure 4.18 depicts the reinforcement design for the rectangular slab of the LEco, and Figure 4.19 shows the reinforcement design for short and long legs of the LEco.

4.6.2 (b)   Fabrication material

In this study, two alternative eco-friendly cement-based materials were developed for fabrication of the LEco.

PFA-cement-sand composite material   A series of unconfined compressive tests (UCT) were conducted for various mixtures of PFA, aggregate and cement; the tests considered both the optimum moisture content (OMC) and the curing period. The total number of

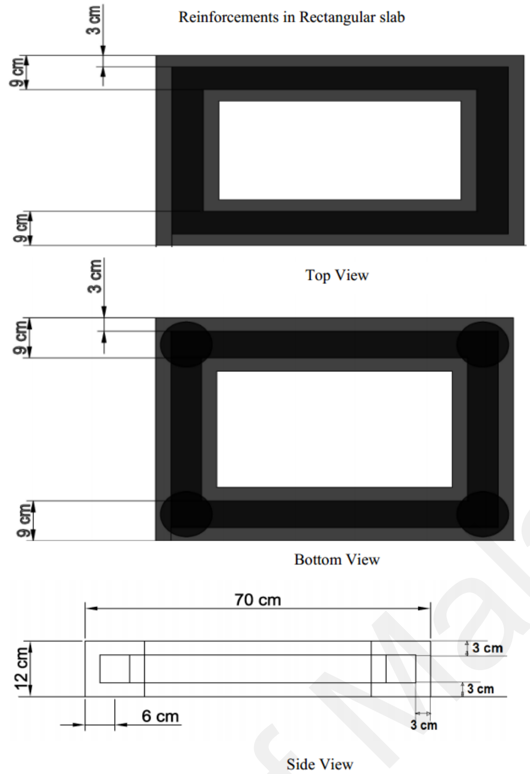

Figure 4.18: The design of reinforcement steel bars for the rectangular slab of LEco armoring units.

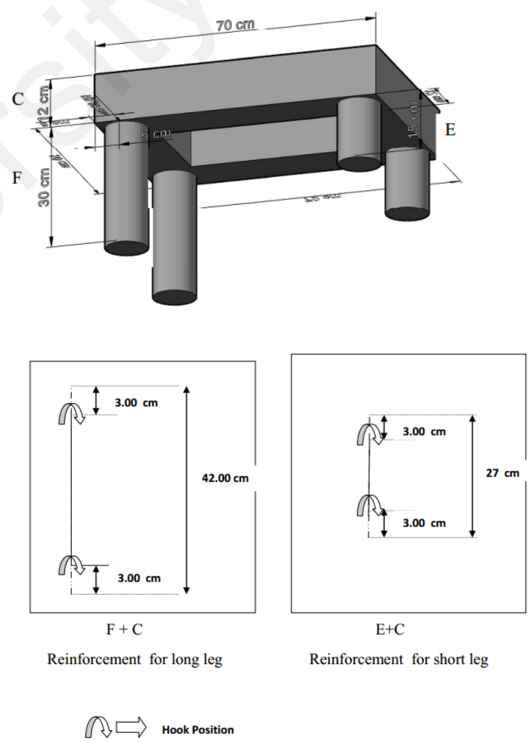

Figure 4.19: The design of reinforcement steel bars for the short and long legs of the LEco armoring units.

tested samples was 91 and for each of them, the PFA content, cement content, and density were measured. The diameter and the length of each sample were 5 cm and 10 cm, respectively. The samples were cured for 1, 7, 14, and 28 days prior to testing. The cement content was 5-25% of the total weight of the sample, whereas the PFA content was 5–40 %. Table 4.3 summarizes the percentage of materials used for the mixture design. The following observations and conclusions are based on the findings of this research. More detailed findings of these researches are found in Motamedi, Song, and Hashim (2015), Motamedi, Shamshirband, Petkovic, and Hashim (2015) and Motamedi, Shamshirband, Hashim, et al. (2015).

Based on the results of this study, the cement content had a significant effect on the UCS of the PFA-cement based mixtures. When the PFA inclusion was kept constant at 30%, increasing the cement inclusion increased the UCS up to 13.22 MPa after a curing period of 28 days. The results also indicated that the PFA content had an optimum value. In this respect, an excessive amount of PFA in a material matrix could reduce the UCS. When the cement content was 25% of the total weight of the medium, the optimum content of the PFA was 20%. The OMC also plays a vital role in obtaining higher UCS values; thus it is important to ensure that the OMC condition is reached via providing enough compaction.

Cockle shell-cement-sand composite material A series of unconfined compressive tests (UCT) were conducted for various mixtures of PFA, aggregate and cement; the tests considered both the optimum moisture content (OMC) and curing period. The total number of tested samples was 810, and for each of them, the cockle-shell content, cement content, and density were measured. The diameter and the length of each sample were 5 cm and 10 cm, respectively. The samples were cured for 1, 7, 14, and 28 days prior to testing. The cement content was 0-50% of the total weight of the sample, whereas the cockle-shell content was 0–25 %. Table 4.4 summarizes the percentage of materials used for mixture design. The following observations and conclusions are based on the findings of this research. More detailed findings of these researches can be found in Motamedi, Shamshirband, Hashim, et al. (2015).

Based on the results of this study, the cement content had a significant effect on the UCS of the cockle shell-cement based mixtures. Generally, the UCS was decreased for all the samples with the increase in the cockle shell content. However, the UCS increased for all the samples with aging. The UCS increases non-linearly as the cement content increases. Additionally, the UCS increases with aging for all the samples.

Table 4.3: Percentage of PFA, cement and aggregate for fabrication of LEco units.

Material	Pulverized Fuel Ash	Cement	Aggregate
Percentage	20%	25%	55%

Table 4.4: Percentage of cockle-shell, cement and aggregate for fabrication of LEco units.

Material	Cockle-shell (CS)	Cement (C)	Aggregate
Percentage	0-25%	0-50%	100-(CS+C)%

4.6.3 Installation of the developed revetments

Six slots of revetments in three configurations were installed at the site (see subsection 3.6.2). Prior to installation, necessary fill works were carried out to ensure that the ground was level (see Figure 4.20a). This was important to ensure consistency in elevation for the ground, where the revetments were aimed to be installed. The fill works concentrated in three zones: a) upstream slope, b) crest, and c) downstream slope. The ground was compacted using manual tools and machinery to reach a satisfactory compaction condition. Further, the base layer of the revetments was formed using granitic rock pieces with D_{n50} of 20 to 30 cm (Figure 4.20b).

Based on the methodology explained in subsection 3.6.2, the construction works for six slots of revetments (see Table 3.4) were carried out. Figure 4.21 and Figure 4.22 show the progress of construction activities for the revetments in November 2014. Figure 4.23 depicts the completed revetments in December 2014. Comparing the site condition before (Figure 4.14) and after the construction of revetments is an obvious indication of the enhancement of the site in means of coastal protection, aesthetic view and erosion prevention functions. Further monitoring works were carried out to assure the satisfactory functioning of the proposed revetments (see section 4.7).

(a) **(b)**

Figure 4.20: (a) Fill works activities were carried out using heavy machinery at the site, and (b) The granitic rock pieces used for forming the base layer of the revetments.

Figure 4.21: Construction progress for the revetments on 11 November 2014.

(a) LEco **(b)** Double-Layer **(c)** Abstention

Figure 4.22: Construction progress for each type of the revetments on 11 November 2014.

Figure 4.23: Completed construction for the revetments on 11 December 2014.

4.6.4 Landscaping and cleaning works

Ten weeks into the commencement of project, the landscaping and cleaning activities started. These works were carried out in two weeks. The main objective was to increase the total aesthetics view of the site and non-structural components of the systems. The scope of works in this part of the project consisted of a) installation of wooden fence, b) leveling the dike downstream, c) compacting the access road and spreading cobbles along the leeward of the dike, and d) removing the debris and waste construction materials from the site. Figure 4.24a illustrates the stretch of wooden fence that was installed along the crest of the dike. Figure 4.24b shows the leveled downstream side of the dike (green arrow) and compacted access road (red arrow).

(a) **(b)**

Figure 4.24: Landscaping and cleaning works: (a) Wooden fence along the crest of the dike, and (b) Leveled downstream side of the dike (green arrow) and compacted access road (red arrow).

4.6.5 Vandalism

Few month into the completion of construction activities, it was observed that some part of the wooden fence on the deck were displaced. Perhaps, this was due to lack of security check at the study site. The area is located in a remote place, whereby sufficient light was not available at night time. For future research works, it is advised that the wooden fence is replaced with bricks made of sustainable material. For example, using the cement stabilized peat during this research work, an eco-friendly brick has been developed. The details of the study can be found in Motamedi, Roy, et al. (2015).

4.7 Monitoring the proposed revetment systems and the surrounding environment

In this section, the results and discussions are provided in relation to the monitoring of revetment systems performance and the surrounding environment.

4.7.1 Investigating the shoreline elevation changes at the site

Based on the methodology in subsections 3.6.7 (a) and 3.6.7 (b), the topography data from the study site at Carey island were collected in seven rounds (Figure 4.25).

The analysis of topography data along the axis in Figure 3.9 was graphed in various temporal periods to evaluate the performance of the revetments for identifying erosion and accretion trends. The followings are the results and discussions related to the analysis of temporal and spatial topographic data.

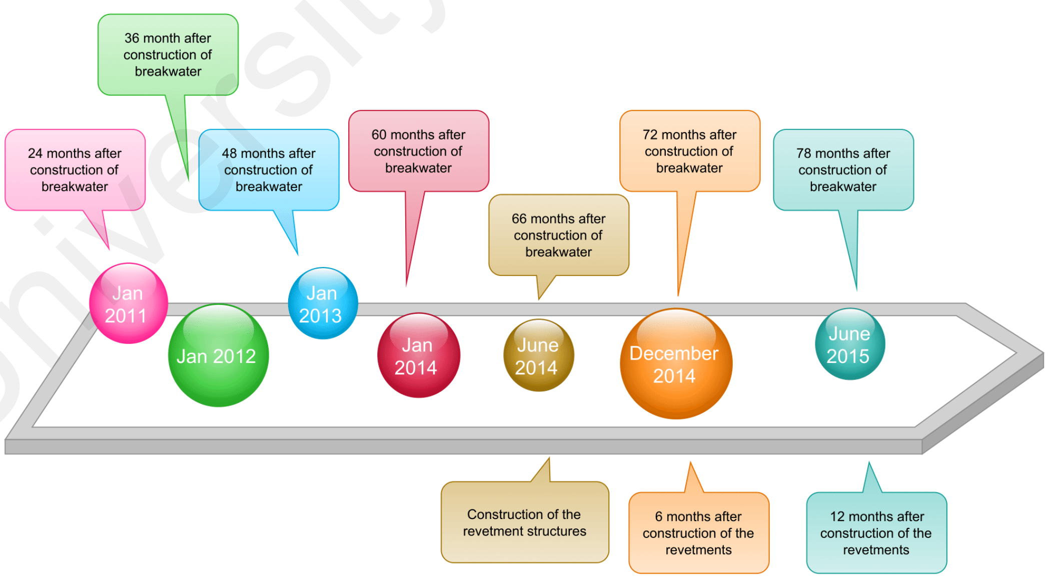

Figure 4.25: The collection of topographic data were carried out in seven rounds between the years 2011 and 2015.

4.7.1 (a) Topography of the site before June 2014

Figure 3.9 shows the spatial distribution of topographic data in Y-Z plane for six cross-sections taken along X direction in respect to the TBM. Figure 4.26 shows the elevation (m) of topographic features along the cross-section E-L for 5 temporal periods namely, (a) January 2011, (2) January 2012, (3) January 2013, (4) January 2014, and (5) June 2014.

According to Figure 4.26, it is evident that traveling from the landwards (point E) to the waterbody, the elevation for all the monitoring periods are almost the same until the distance of approximately 38.5 m from the land. Further, until the point L (nearly 125.6 m), the elevation is higher for the most recent monitoring period (June 2014), followed by January 2014.

Table 4.5 summarizes the average elevation (m) from the distance 38.5 m towards 125.6 m along the E-L cross-section. From this table, it can be stated that the elevation of the bed level has consistently increased since January 2011.

Figure 4.27 shows the graph of relative topographic change (%) over total topographic change (%) (hereafter $\frac{RTC}{TTC} = RTT$) versus diagonal distance along the cross-section E-L. RTC is the change of elevation between subsequent temporal period over the TTC that is the the change of elevation during the measuring periods. From this figure, the highest RTT was observed during January 2011 at 78.49 %, and the lowest RTT was for June 2014 (P4) at 0.01 % (Table 4.6). The fluctuation of RTT values can be attributed to the seasonal effect of wave regime as a result of variance in celerity, height, and direction of waves in north and south monsoon.

Figure 4.28 shows the variation of RTT along the cross section E-L for monitoring period before and during June 2014. From this graph, the rate of accumulation of sediments after installation of the breakwater at the site decreased from January 2011 (P1) to

June 2014 (P4). The trend line in Figure 4.28 was higher in P1 and P2 and lower in P4 and P3, respectively. This decrease in the elevation of bed level (Figure 4.28) is an indication that an equilibrium condition has been reached at the site which in turn provides insight into the fact that as the elevation of bed increased from P1 to P4, the natural trends in deposition of sedimentations slowed. Thus, it is evident that installation of the breakwater could increase the bed level at the site, and that further mangrove rehabilitation works were worthwhile.

A significant volume of sediments was deposited on the site between January 2011 and June 2014 (see Table 4.7). In particular, a high volume of deposition was found in the leeward of the breakwater. The analysis of bathymetric data proved that in line with the results shown in Figure 4.28, between January 2012 and January 2013 the highest volumetric deposition of 0.129 $\pm$ 0.36 m^3/m^2 was observed on the site before the construction of revetment systems. The lowest volumetric deposition was recorded between January 2014 and June 2014 at 0.04 $\pm$ 0.27 m^3/m^2. This is an indication that after few years into construction of the breakwater, an equilibrium state reached at the site.

Generally, during all monitoring periods, the volumetric deposition had a decreasing rate; except between January 2012 and January 2013 in which a sharp positive increment was observed compared with the previous monitoring period (January 2011 to January 2012). This sudden change could be attributed to the initiation of the breakwater positive performance at the site after one year into its construction.

Table 4.5: Average elevation (m) from the distance 38.5 m towards 125.6 m along the E-L cross-section.

Monitoring period	2014 June	2014 Jan	2013 Jan	2010 Jan	2008 Dec
Average elevation (m)	-2.19488	-2.2028	-2.29002	-2.33138	-2.82706

Table 4.6: The minimum and maximum values of RTT versus diagonal distance along the cross section E-L for monitoring period before June 2014.

Monitoring Period	P1	P2	P3	P4
Maximum	78.49	75.87	75.95	49.15
Minimum	0.41	0.055	0.5	0.01

Table 4.7: The volumetric sediment accretion (m^3/m^2) within the study area between January 2011 and June 2014.

Monitoring Period	Average Volumetric Sediment Accretion (Mean+SD) (m^3/m^2)
Jan 2011 - Jan 2012	0.095 ± 0.43
Jan 2012 - Jan 2013	0.129 ± 0.36
Jan 2013 - Jan 2014	0.069 ± 0.31
Jan 2014 - June 2014	0.04 ± 0.27

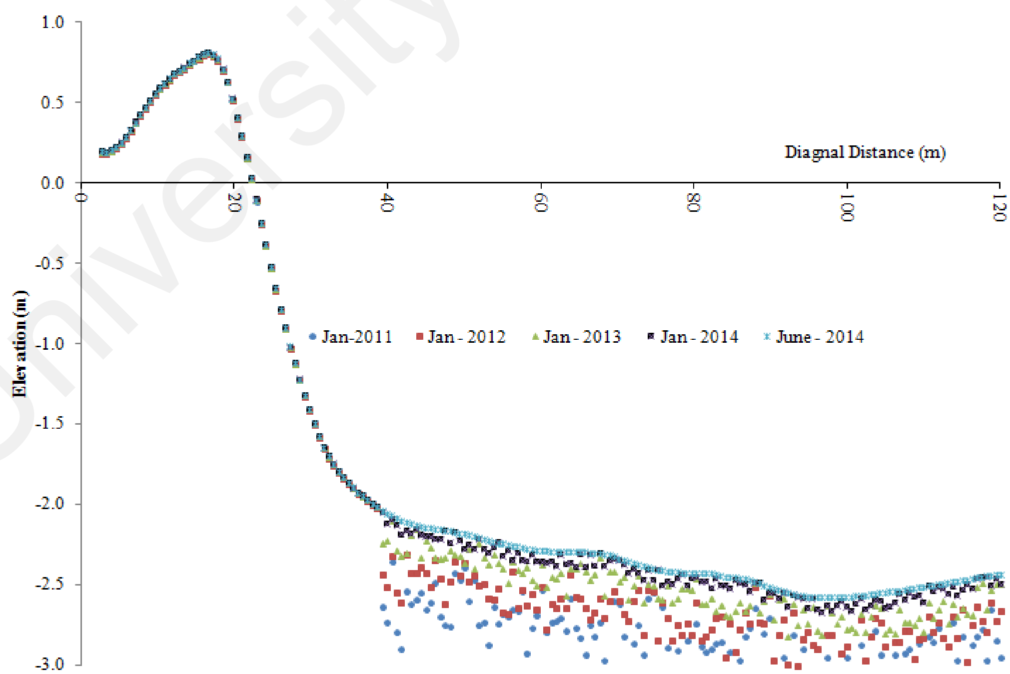

Figure 4.26: Elevation of topographic features (m) along the cross section E-L for monitoring period before June 2014.

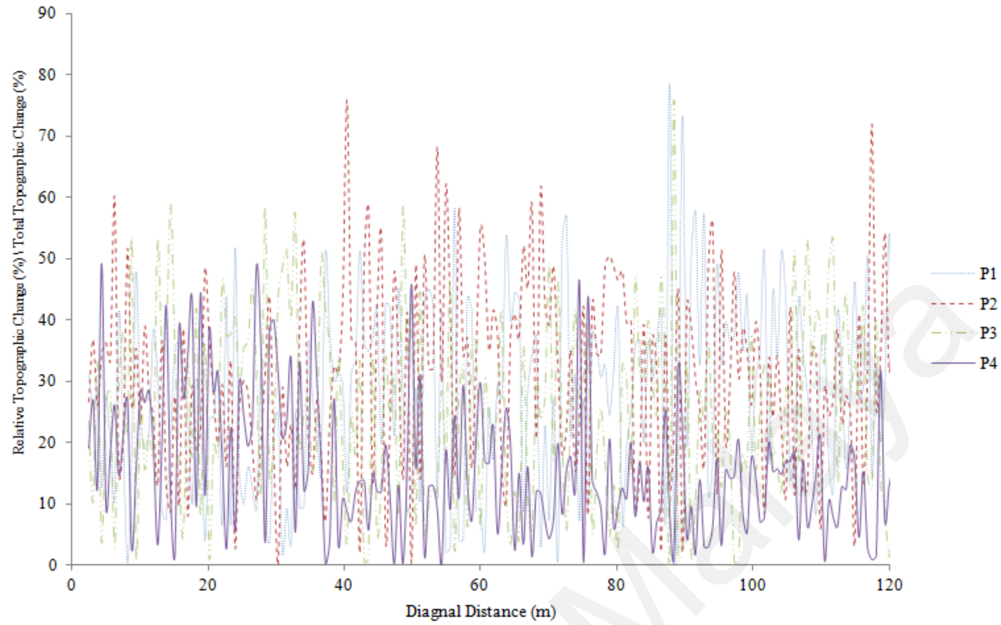

Figure 4.27: RTT values versus diagonal distance along the cross section E-L for monitoring period in and before June 2014.

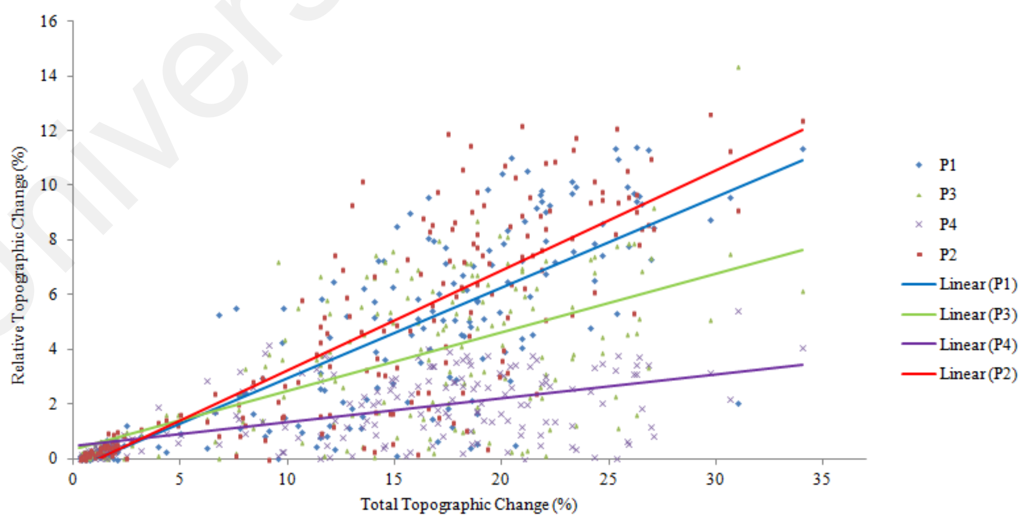

Figure 4.28: RTT values along the cross section E-L for monitoring period in and before June 2014.

4.7.1 (b) Topography of the site in June 2014

Figure 3.9 shows the spatial distribution of topographic data in Y-Z plane for six cross-sections taken along X direction in respect to TBM. Along cross-section F-F the elevation remained negative in respect to TBM, whereas along all other cross section namely A-A, B-B, C-C, D-D and E-E, the elevation was positive (see Figure 4.29a). Figure 4.29c shows the profile of cross-sections CC and FF. The topographic data collected in June 2014 as well as other profiles for cross section along X-direction can be found in Appendix C.

For cross section A-A, from the distance 3.24 m to 10.12 m, the elevation increased from +1.48 m to +1.55 m, which is approximately 5% higher (Figure 4.29a). Further, the elevation decreased almost 5% (elevation= +0.89 m) when the distance from the TBM was 20.25 m. When the distance from the TBM was 30 m, the elevation reached -0.27 m that was 1.75 m below the elevation that was recorded when the distance from the TBM was 3.24 m. The existing breakwater at the site was approximately located at 40 m distance from the TBM along AA cross-section which had the elevation of -0.96 m and was almost 2.44 m below the distance 3.24 from the TBM, where the elevation was 1.48 m.

The highest elevation was recorded along the cross section A-A at +1.55 m (Figure 4.29a) and the lowest elevation was recorded along the cross-section FF at elevation -2.57 m (Figure 4.29a). For other cross sections, similar trends in variation of cross sections were observed for cross sections B-B, C-C, D-D and E-E.

The topography of the site along the transverse section (increasing distance along Y-axis in Figure 3.9), increased until the distance of approximately on average 8 m from the TBM. Despite the existence of slight fluctuation in elevation departing from the distance of 8 m towards 79 m from the TBM in direction of Y-axis, there was an almost consistent gradual decrease in elevation (Figure 4.29c).

In general, the topography of the site along the transverse sections (increasing distance along Y-axis in Figure 3.9) had similar decreasing elevation trends. That is an indication that traveling from the north to the south of the site, the elevation has decreased.

Figure 4.29b shows the spatial distribution of topographic data in X-Z plane for six cross-sections taken along Y direction as shown in (Figure 3.9). For almost all the instances along the cross-section KK, the elevation remained positive with respect to the TBM, whereas in many instances along all other cross sections (HH, II and JJ), the elevations were lower than the TBM (negative). The topographic data collected on June 2014 as well as other profiles for cross section along Y-direction can be found in Appendix C.

As depicted in Figure 4.29b, for the cross section KK, from the distance 0.6 m to 4.33 m, the elevation consistently decreased from -0.23 m to -0.27 m with respect to the TBM. Further, the elevation increased about 600% as the distance from the TBM increased from 4.33 m to 20.43 m. Similar fluctuations were observed in the topography along the KK axis and in general the elevations were kept above the TBM for other topographic points.

The highest elevation was recorded along the cross-section KK at + 1.52 m (Figure 4.29b) and the lowest elevation was recorded along the cross section HH at elevation -2.57 m (Figure 4.29d). For other cross sections, similar trends in variation of topography were observed for the cross sections II and JJ.

In general, the topography of the site along the longitudinal sections (increasing distance along X-axis in Figure 3.9), had similar trends of fluctuations and at the distance of approximately 97 m, all the cross sections had a steep increase in elevation. That is an indication that traveling from the west to the east of the site, the elevation has increased. Figure 4.30 shows the 3D spatial distribution of study site in June 2014 and the profile of topography along the cross-section E-L.

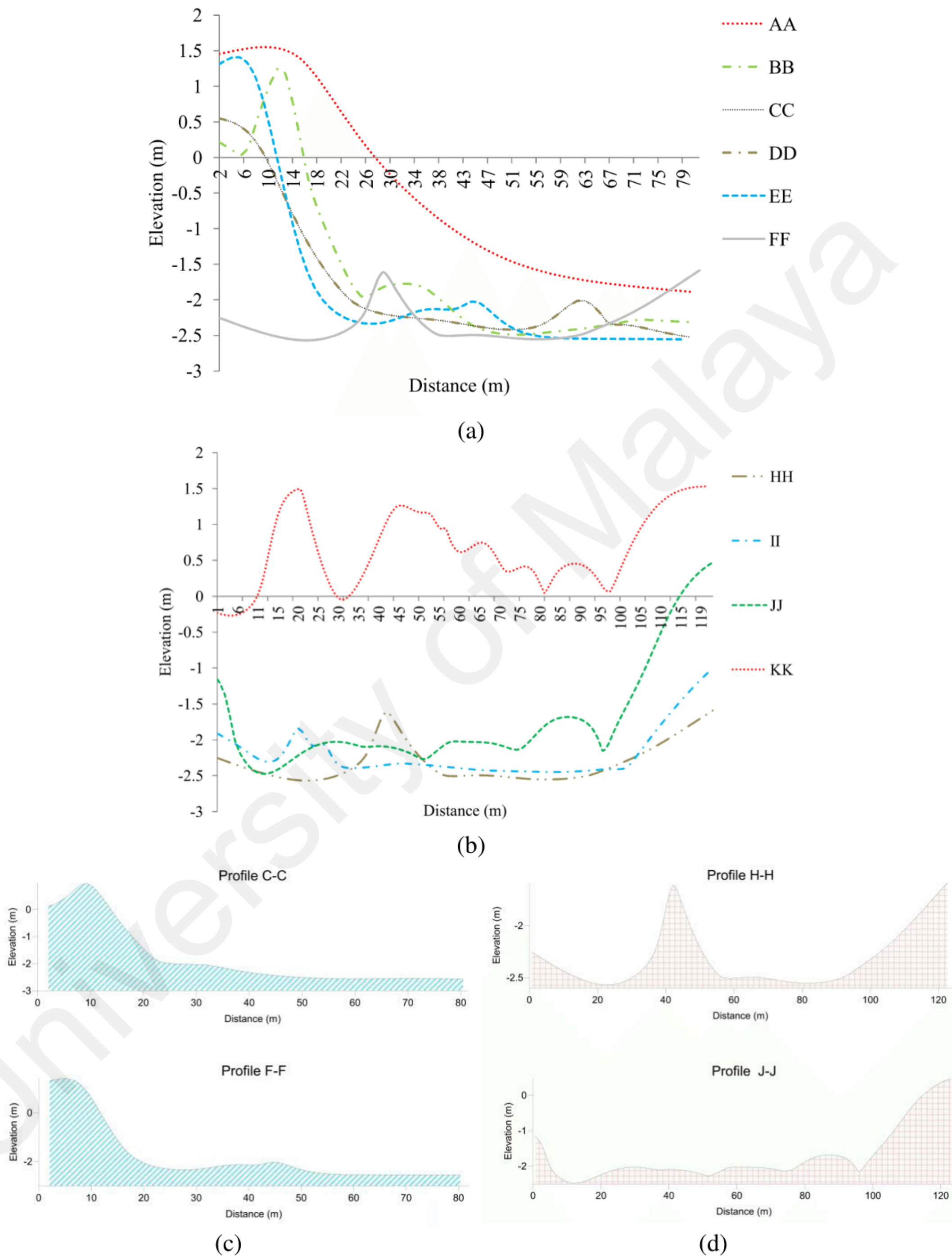

Figure 4.29: Variation of elevation along cross-sections (a) AA, BB, CC, DD, EE, and FF; (b) HH, II, JJ, and KK placed along X-axis; and Profile of cross-sections (c) CC and FF, and (d) HH and JJ in June 2014.

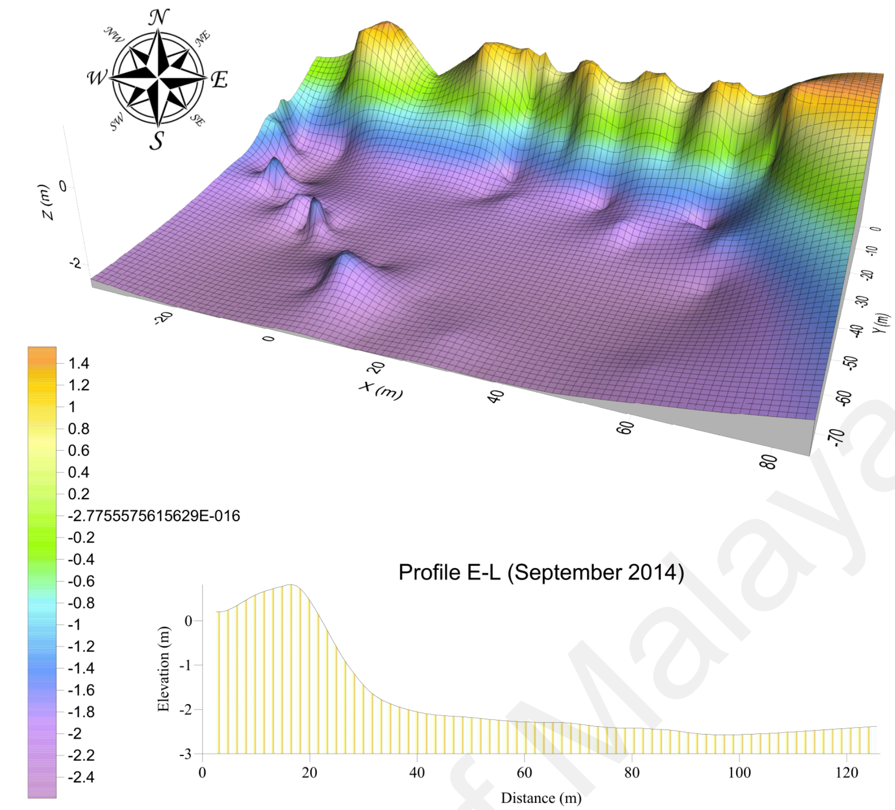

Figure 4.30: 3D spatial distribution of study site June 2014 and the profile of topography along cross-section E-L.

4.7.1 (c) Topography of the site in December 2014 and June 2015

Table 4.8 summarizes the average elevation (m) from the distance 38.5 m towards 125.6 m along the E-L cross section. From this table, it can be stated that the elevation of the bed level were consistently increasing since June 2014. Figure 4.31 shows the graph of RTT versus diagonal distance along the cross-section E-L between June 2014 and June 2015.

Based on the findings, it can be stated that the highest RTT was observed between December 2014 and June 2015 at 23.30 and the lowest RTT was for the period between June 2014 and December 2014 (P2) at 0.01 (Table 4.8). The fluctuation of RTT can be attributed to the seasonal effect of wave regime as a result of variance in celerity, height, and direction in North and South monsoon.

Figure 4.32 shows the variation of RTT along the cross section E-L for monitoring period between June 2014 and June 2015. From this graph, it can be observed that the rate of accumulation of sediments after installation of the revetment at the site decreased from June 2014 (P2) to June 2015 (P1). The trend line in Figure 4.32 was higher for P2 and P1. Further, the decrease in the elevation of bed level (Figure 4.32) is an indication that an equilibrium condition reached to the site, which in turn provides insight into the fact that as the elevation of bed increased from P2 to P1; thus, natural trends in the deposition of sedimentations slowed.

From the above discussions, it is evident that the integration of revetment and breakwater structures was successful to increase the bed level at the site and further mangrove rehabilitation works were worthwhile.

Figure 3.9 shows the spatial distribution of topographic data in Y-Z plane for six cross-sections taken along X direction with respect to the TBM. Figure 4.33 shows the elevation (m) of topographic features along the cross section E-L for three temporal periods, namely, (a) June 2014, (2) December 2014, and (3) June 2015. According to Figure 4.33, it is evident that traveling from the landwards (point E) to the waterbody, elevation for all the monitoring periods is almost the same until the distance of approximately 32.2 m from the land. Further to this point until the point L (nearly 125.6 m), the elevation was higher for June 2015 and then followed by December 2014.

Figure 4.34 and Figure 4.35 depict the 3D spatial distribution and 2D topography map of the study area in the monitoring periods between June 2014 and June 2015. These figures show that accumulation of sediments continued on the site between June 2014 and June 2015 (Table 4.9). In particular a high volume of deposition was found in the leeward of the breakwater as well as in the vicinity of the revetment structure in zone A. The analysis of bathymetry data proved that in line with the results shown in Figure 4.28, between June 2014 and December 2014, a total highest volumetric deposition of 0.11

$\pm$ 0.06 m^3/m^2 was observed on the site in the monitoring period after construction of the revetment systems. Also, the lowest volumetric deposition was recorded between December 2014 and June 2015 at 0.03 $\pm$ 0.76. This indicates that after one year into construction of the revetments, an equilibrium state reached at the site.

Similar to the previous monitoring periods shown in Table 4.7, during both monitoring periods the volumetric deposition had a decreasing rate. This indicates that construction of the revetment systems did not interfere with the ongoing natural sediment recovery processes.

Table 4.8: The minimum and maximum values of RTT versus diagonal distance for monitoring period June 2014 and June 2015.

Monitoring Period	P2	P1
Maximum	15.26	23.30
Minimum	0.01	0.09

Table 4.9: The volumetric sediment accretion (m^3/m^2) within the study area between January 2011 and June 2014.

Monitoring Period	Average Volumetric Sediment Accretion (m^3/m^2)
June 2014 - December 2014	0.11 $\pm$ 0.06
December 2014 - June 2015	0.03 $\pm$ 0.76

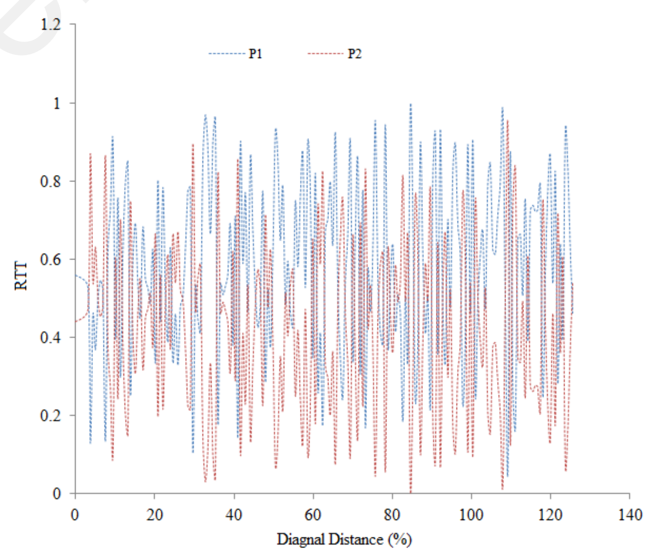

Figure 4.31: Variation of RTT values versus diagonal distance for monitoring period between June 2014 and June 2015.

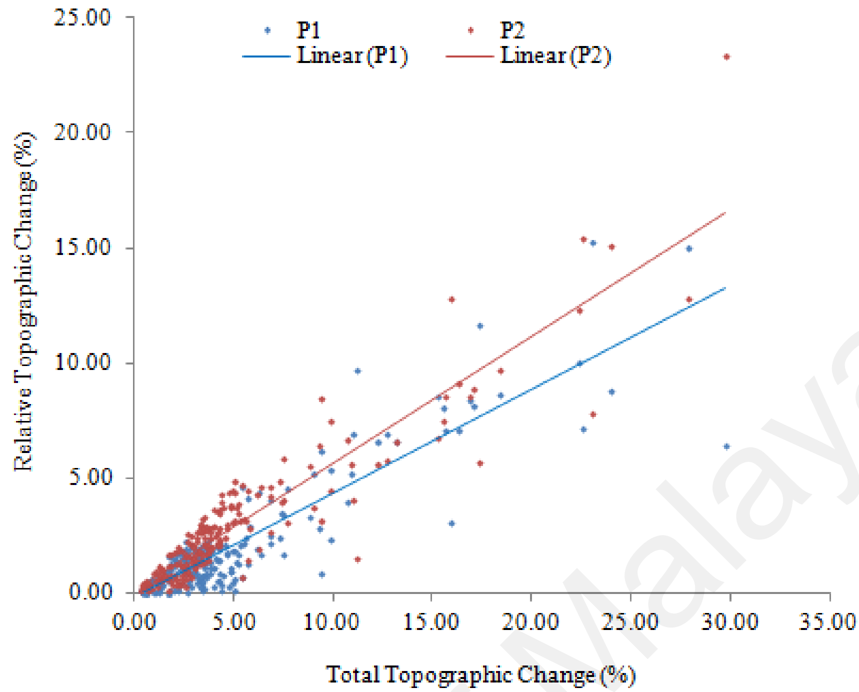

Figure 4.32: Variation of RTT for monitoring period between June 2014 and June 2015.

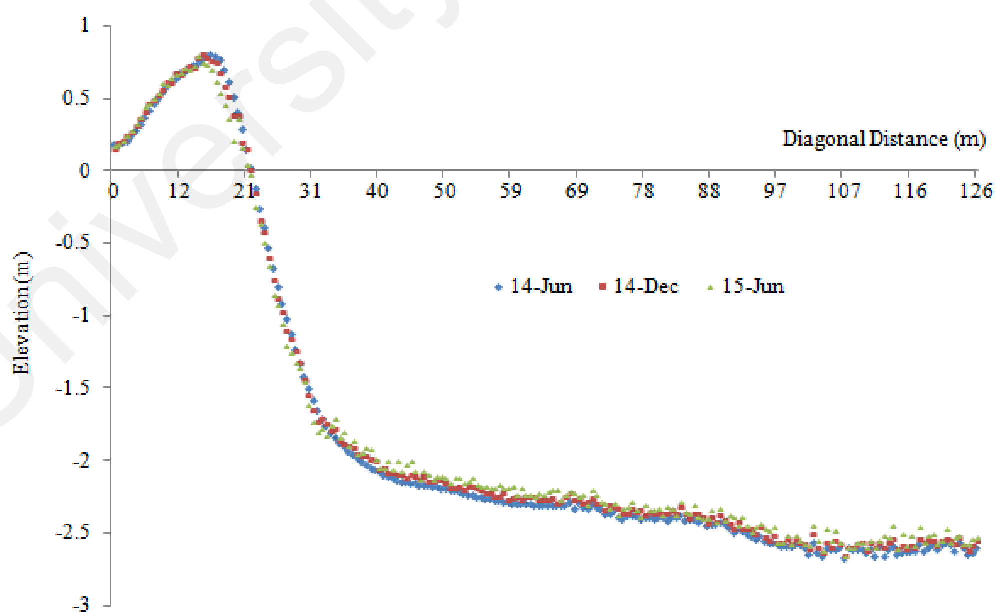

Figure 4.33: Elevation of topographic features (m) for monitoring period between June 2014 and June 2015.

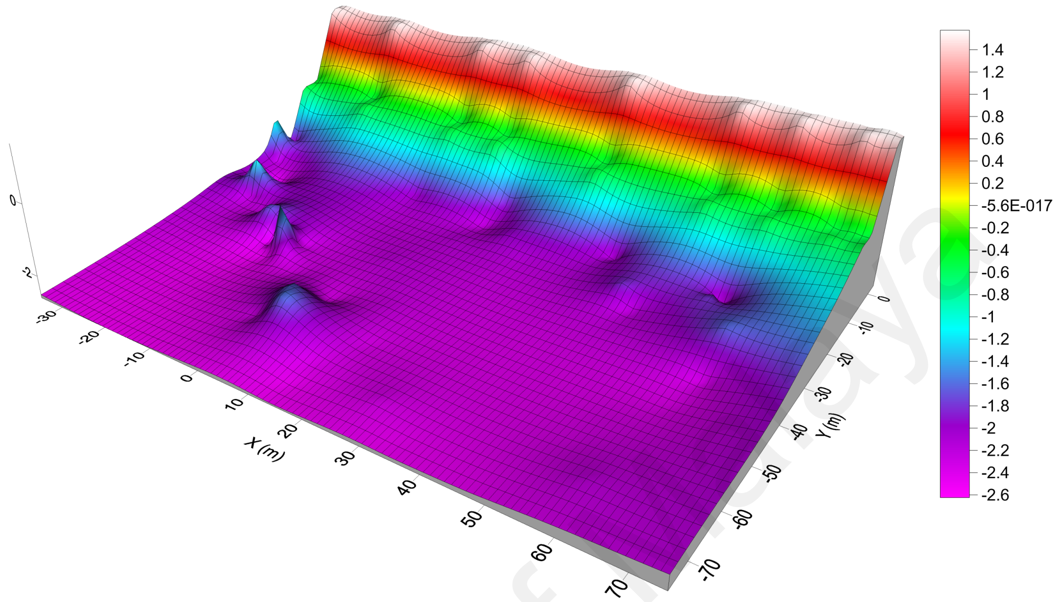

(a)

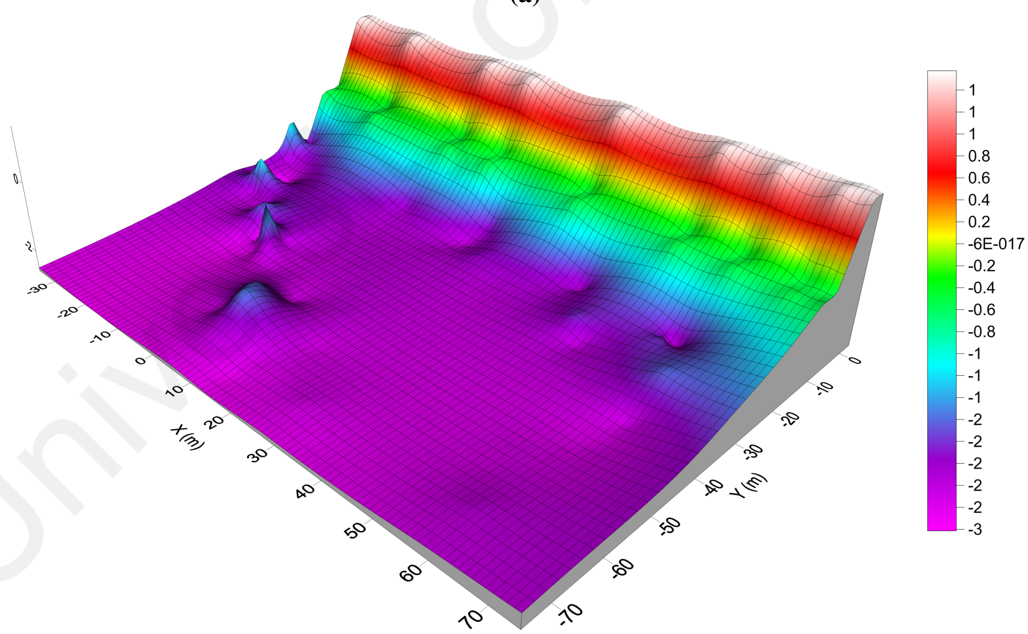

(b)

Figure 4.34: 3D spatial distribution of the study site in (a) December 2014 and (b) June 2015.

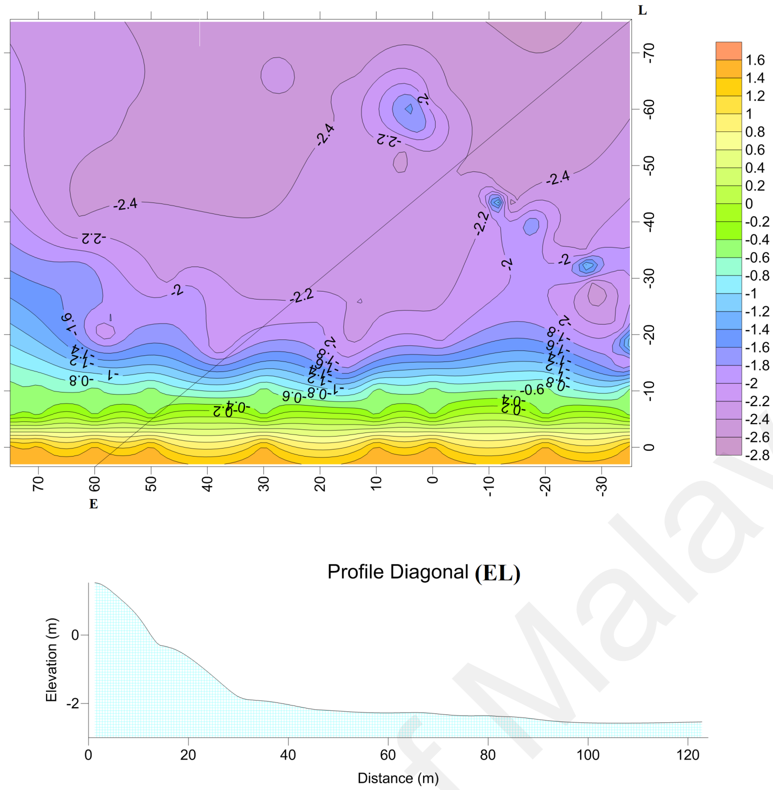

(a)

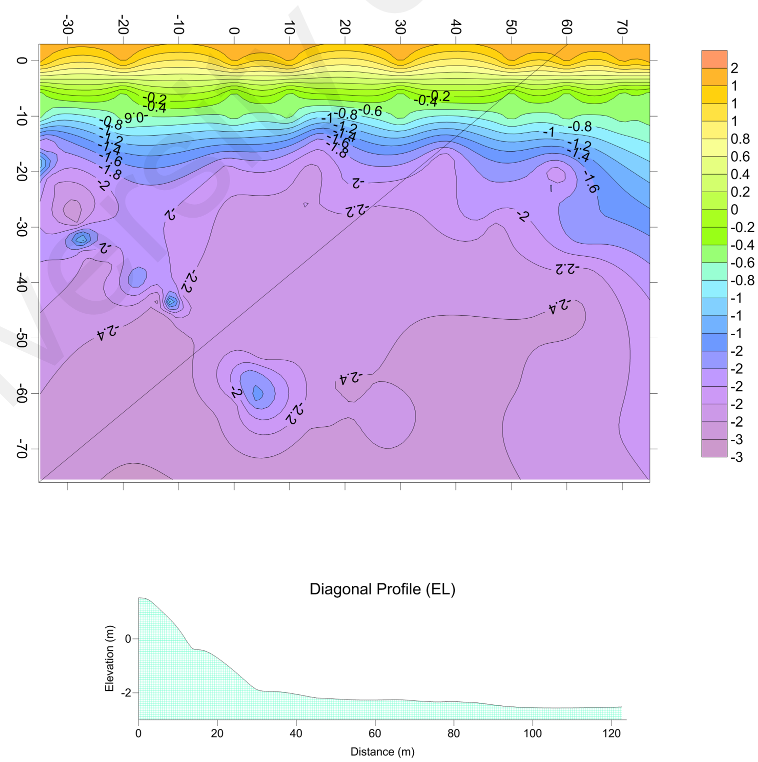

(b)

Figure 4.35: 2D spatial distribution of the study site and the profile of topography along cross-section E-L in (a) December 2014 and (b) June 2015.

4.7.1 (d) Implications of the findings

The Carey island is considered as a cohesive shore (see section 4.7.2). In essence, the extend of physical forces (i.e., tidal currents and waves) and sediment characteristics significantly affect the accretion and erosion trends in cohesive shores (CEM, 2002). Unlike the non-cohesive shorelines, cohesive shorelines are composed of cohesive sediments (i.e., clay and silt) that have cohesive characteristics as a result of electrochemical forces acting on inter-particle spaces that in long term would cause consolidation and flocculation phenomena (van Maren & Winterwerp, 2013). In this respect, the cohesiveness of the sediments can contribute to a great level of resistance to erosion which can be beneficial for bed load transport prevention (SPM, 1984)

Wave and tidal currents have major roles in the sediment dynamics in inter-tidal flats. Strong waves re-suspend the sediment and generate cross-shore and long-shore currents, which are actively involved in transportation of sediments from seaward of the shore toward the on-shore region. In the cohesive shores, the wave height at the inter-tidal regions are highly lower than the off-shore. This is because as the waves travel towards the shoreline, the wave attenuate due to friction effect of the increasing viscosity by the soft fluid mud (CEM, 2002).

Tide is the most important process in the inter-tidal regions. The wave height at these areas are comparatively smaller than the tidal range; thus, the tidal forcing appears to be dominant over the wave forcing in inter-tidal regions (CEM, 2002). In this respect, as the tide rise and falls at the flat, the tidal forces generate currents that further involve in suspension of sediments from upstream during flood tide and from downstream during ebb tide.

The attenuation of waves, as well as presence of dynamic condition for accretion and erosion trends are also affected by the presence of barrier coastal structures on-shore

(CEM, 2002). For example, installation of breakwater would potentially cause dissipation of wind-generated waves prior to reaching coastline in which the condition of on-shore currents may be positively affected when the aim is to increase the accretion rate.

In this study, based on the results described in section 4.7.1 (a), the increasing trend in the elevation of bed at inter-tidal flat of the wave attenuate Carey Island between January 2011 (12 months after installation of breakwater system) and June 2014 (before installation of revetment systems) is a proof to success of the breakwater system in preventing the erosion at the site and increasing the accretion trends in inter-tidal flat resulting in a suitable morphodynamic regime for rehabilitation of mangroves.

4.7.2 Geotechnical characterization of the site

4.7.2 (a) Subsurface material

Based on the methodology discussed in section 3.6.7 (d), the subsurface soil at the study site was characterized. The borelogs and results of soil laboratory testings can be found in Appendix B.

Based on the collected data from boreholes BH1, BH2 and BH3, the soil strata at the site consists of four major soil types which are dominantly distributed at the study site. These soil types are: a) Clay and Sandy Clay, b) Clayey Sand, c) Sandy Silt, and d) Silty Sand.

The Clay and Sandy Clay were consistently found in all boreholes at the surface level. This soil strata is composed of soft to firm, light gray to black or light yellowish brown particles of Clay or Sandy Clay with organic matter (i.e., wood pieces). The thickness of this layer varies between 3.0 to 6.0 meters with the SPT N-value ranging from 1 to 5 blows.

The Clayey Sand is a minor soil layer, which is overlain by clay and sandy clays. In general, the material texture was loose to medium dense, and occasionally very dense.

The texture color of the material varies between gray to greenish grey Clayey, fine to medium Sand with some gravels. The thickness of this layer varies between 3.0 to 6.0 meters with the varying SPT N-value of 1 to >50 blows.

The Sandy Silt material was majorly found at the middle part of the boreholes. The material was composed of white to light gray to light bluish gray, hard texture. The thickness of the layer ranged from 8.0 m to slightly over 14.0 m and the SPT N-value ranged from 35 blows to >50 blows.

The Silty Sand material covered the bottom of the boreholes. The material is generally composed of dense to very dense, light yellow to dark reddish brown, Silty Sand. The thickness of the layer is approximately 18 meters and the SPT N-values ranges from 40 to >50 blows.

Based on the borelogs, the site has a thick alluvial deposit of silt, clay and sand. Generally, sandy silty Clay with wood pieces and fragmented stone exist from ground level to depths of about 9 meters. These layers are occasionally followed by Clayey Sand layers with stone and decayed wood pieces. Immediately, the soil stratum composed of Sandy Silt with decayed vegetation and wood appears to a depth of approximately 30 m. Further, the most dominant layer is Silty Sand layers to a depth of approximately 45 m. These layers occasionally consist of Clayey Sand, Sand and Sandy Clay with various thickness. Gravels, decayed wood pieces and fragmented rocks are also found randomly in some layers.

4.7.2 (b) Near-surface material

Based on the methodology discussed in section 3.6.7 (d), the disturbed soil samples collected from the rehabilitation site were tested to obtain the particle size distribution curve for each sample at different spatial location. The soil samples were collected at predetermined locations along the axis S1 to S6 as depicted in Figure 3.10. The data collection was conducted for five times in: a) June 2014, b) September 2014, c) December 2014, d) March 2015, and e) June 2015.

Figure 4.36 to 4.37 depict the grain size distribution of the sediments on higher and lower elevation areas at zones A and B of the rehabilitation site (Figure 3.14). In general, the average clay percentage at lower elevation (LE) is higher than that observed in higher elevation (HE) areas. For example, in September 2014, the average clay percentage for collected data points at zone A for the LE areas was 12.14 ± 0.23, which was higher than the clay percentage at the HE areas of zone A (3.78 ± 0.38). Also, in December 2014, the average clay percentage for collected data points at zone B for the LE areas was 19.91 ± 0.12 which was higher than clay percentage at HE areas of zone B (5.65 ± 0.43). These observations are due to slower settling of clay particles at lower elevations compared to the sand and silt particles.

Generally, the clay and silt percentages for both HE and LE at zone A were higher than those observed at zone B, whilst the sand percentage for both HE and LE was slightly higher at zone B in comparison to zone A. Further, for both zone A and zone B, the silt formed the highest percentage of near-surface soil for all the monitoring periods.

Figure 4.38 shows the graph of clay percentage (%) versus month of monitoring for the HE and LE areas of zone A and zone B. Generally, at LE areas of both zone A and zone B, the average clay percentage was higher than that observed for the associated HE areas. For example, in June 2015, the average clay percentage of LE areas at zone A (11.54 ± 0.26) and at zone B (9.81 ± 0.15) was higher than that observed for the HE areas at zone A (7.62 ± 0.57) and zone B (5.46 ± 0.47), respectively.

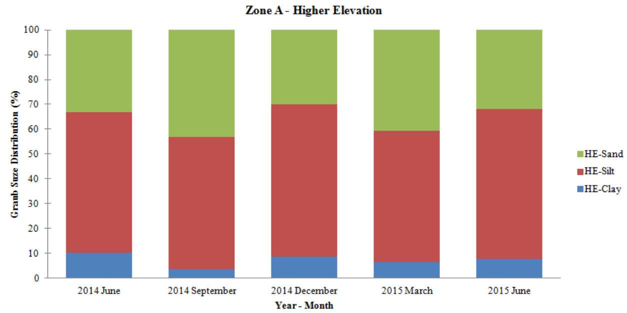

(a)

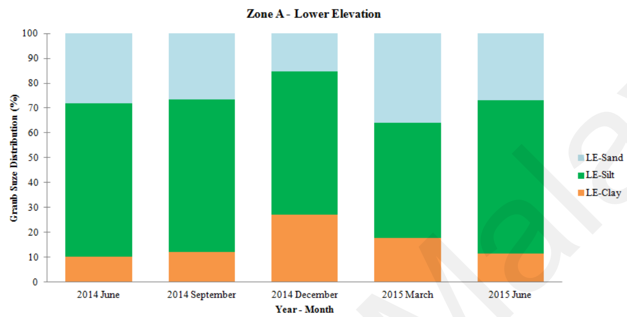

(b)

Figure 4.36: Grain size distribution of the sediments on (a) higher and (b) lower elevation areas at zone A of the rehabilitation site.

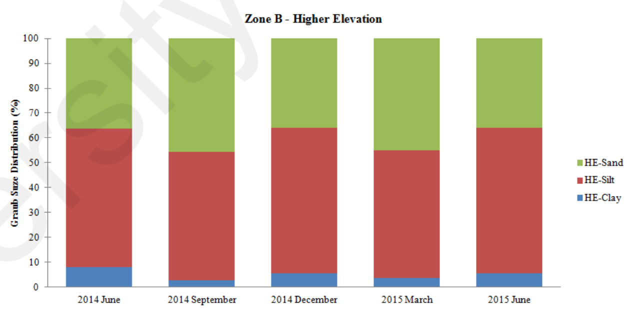

(a)

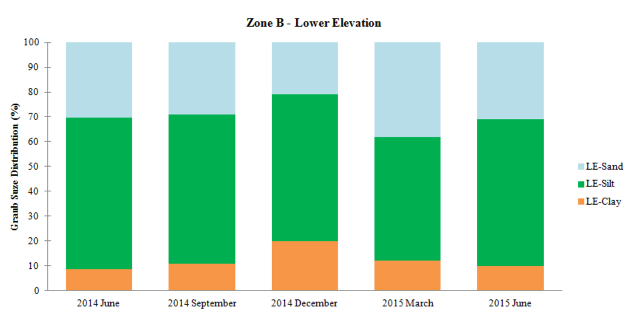

(b)

Figure 4.37: Grain size distribution of the sediments on (a) higher and (b) lower elevation areas at zone B of the rehabilitation site.

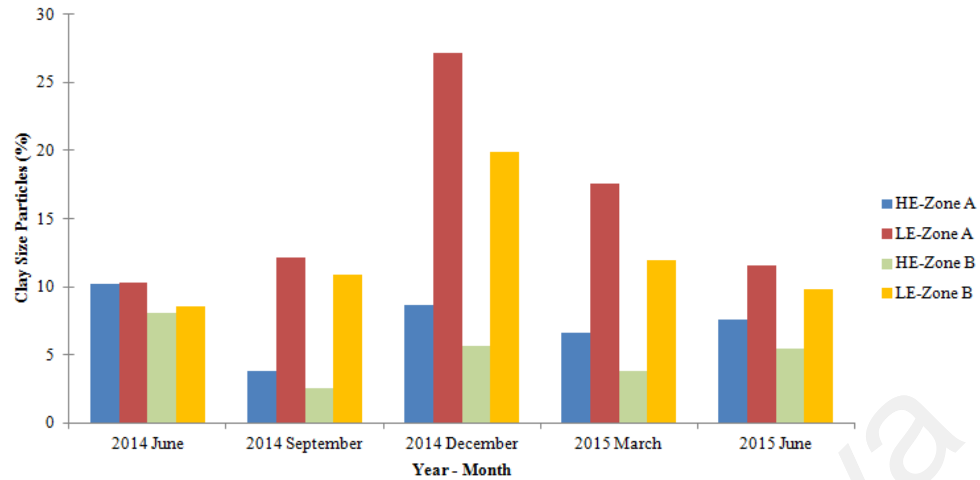

Figure 4.38: The sediments had higher clay percentage at LE for both zone A and zone B.

4.7.3 Post-construction monitoring for LEco revetments

As explained in subsection 2.5.3 (d), to evaluate the damage level of concrete armoring layers, counting method is preferred. The number of displaced units out of the layer or the number of units displaced within a range of initial position were considered (e.g. 0.5 to 1 D_n) (Yagci et al., 2005). Profile measurement is not typically practical for concrete armoring layers. In relation to this, the performance of L1 and L2 revetments (see Table 3.4) was assessed by investigating the number of units that were potentially displaced from their initial position on a monthly basis from June 2014 to June 2015 for a total of 12 times (Figures 4.39a to 4.39e).

Based on the results of these investigations, for both L1 and L2 revetments, the LEco were not displaced significantly. Thus, it can be stated that both L1 and L2 had a satisfactory performance, and both of LEco revetments including the one protected behind the breakwater (L1) and the other one, which is not protected behind the breakwater (L2) are considered suitable solutions to protect the shoreline against erosion.

Considering the implicit estimation of damage for concrete armoring units, the N_{od} is almost zero for L1 and L2 revetments, since the real number of the displaced stones over the width of D_n was negligible (subsection 2.5.3 (c)). Therefore, based on the Bayesian definition of damage criteria for armoring layers (see section 2.5.4), for both L1 and L2 revetments, the damage state did not reach the *Initiation of damage*. Also, no rocking was observed for both L1 and L2 revetments.

[hb!]

Figure 4.39: (a) Condition of LEco revetment L1 in June 2014, (b) Condition of LEco revetment L1 and L2 in September 2014, (c) Condition of LEco revetment L2 in December 2014, (d) Condition of LEco revetment L1 condition in March 2015, (e) Condition of LEco revetment L2 in June 2015.

4.7.4 Post-construction monitoring for Double-Layer revetments

Based on the methodology in subsections 3.6.7 (a) and 3.6.7 (b), the displacement of the system in accordance with the Cartesian axis for the Double-Layer revetments (D1 and D2) (Table 3.4) were collected in three rounds in: (1) July 2014 (1 month after the revetment systems were constructed); (2) October 2014 (4 months after the revetment systems were complete); and (3) January 2015 (7 months after the revetment systems were installed). Figures 4.40 and 4.44e depict the condition of D1 and D2 revetments at the site in July 2014 and January 2015, respectively.

The analysis of topography data along the Cartesian axis was conducted in various temporal periods to explore performance of the Double-Layer revetments for evaluating the performance of D1 and D2. The followings are the results and discussions related to the analysis of temporal/spatial topographic data.

Figures 4.42a to 4.42c show the 3D spatial distribution of Double-Layer revetments (D1 and D2) in July 2014, October 2014 and January 2015. In addition, Figures 4.43a to 4.43c depict the topographic map of the revetments at the same monitoring time. From these figures, it can be observed that although changes in topography were not significant for both D1 and D2 revetments, variations in elevation had an increasing trend over time.

Figure 4.44a shows the graph of relative elevation change (%) over the initial elevation change in July 2014 (%) (hereafter RTT_i) versus total elevation change between the observation periods at the center line along Y-axis for D1 revetment. P1 and P2 are the absolute values of relative topographic change (%) between October 2014 and July 2014, as well as January 2015 and October 2014, respectively; over total initial elevation change (%) in July 2014. Based on the findings, it can be stated that the highest RTT_i was observed during P2 period at 14.82% and the lowest RTT_i was for P1 at 0.75%. The fluctuation of RTT_i can be attributed to the seasonal effect of wave regime as a result of variance in celerity, height, and direction in North monsoon and South monsoon.

Having said that, it can be observed that rate of displacement of D1 slightly increased in P2 compared to P1 (Figure 4.44a). This is an expected condition due to displacement of the underlying components as a result of continuous wave action and occurrence of primary and secondary settlement.

Figure 4.44b shows the graph of RTT_i versus total elevation change between the observation periods at the center line along Y-axis for D2 revetment. P3 and P4 are the absolute values of relative topographic change (%) between October 2014 and July 2014, and January 2015 and October 2014 over the total initial elevation change (%) in July 2014. Based on the findings, it can be stated that the highest RTT_i was observed during P4 period at 15.20% and the lowest RTT_i was for P3 at 0.82%. The fluctuation of RTT_i can be attributed to the seasonal effect of wave regime as a result of variance in celerity, height, and direction in North and South monsoon.

Comparing Figures 4.44a and 4.44b, it can be concluded that the displacement rate was slightly higher in D2 revetment. This can be associated with the fact that the D2 revetment is not protected directly by the existing breakwater at the site. A less energy dissipation could have resulted in more displacement for D2 revetment.

Figures 4.44c to 4.44e compare the elevation with respect to distance across Y-axis (i.e., see Figure 4.43a) of D1 and D2 revetments in July 2014, October 2014, and January 2015, respectively. Based on these figures, it can be observed that in general the D2 revetment had undergone a higher decrease in elevation compared to D1. For example, at the distance of approximately 4 m along Y-axis at the center line of both revetments, for D1 revetment in July 2014, the elevation was higher at -1.43 ± 0.1 m compared to D2 revetment in the same period at -1.47 ± 0.1 m. Similar trends were also observed in October 2014 and January 2015. In addition, from these figures it can be observed that the revetments had an decreasing trend of elevation for both revetments D1 and D2 over time. For example, In October 2014 at the distance of approximately 4 m along Y-axis at the center line of both revetments on D1 revetment, the elevation was at -1.49 ± 0.1 m whereas in January 2015 for the same point, the elevation was recorded at $-1.52.1$ m.

Although based on the above discussions, the revetments have undertaken a minor settlement, their armoring units have not been displaced significantly. According to Equation 2.11, the damage parameter (S) is negligible since A_e variable is almost zero. In addition, considering the implicit estimation of damage for stone armoring units, N_{od} is also very small, because for D1 and D2 revetments, the real number of the displaced stones over the width of one D_n, is negligible (subsection 2.5.3 (c)). Therefore, considering the Bayesian definition of damage criteria for armoring layers (section 2.5.4), for both D1 and D2 revetments, the damage state has not reached the *Initiation of damage*.

Figure 4.40: Double-Layer revetments in July 2014.

Figure 4.41: Double-Layer revetments in January 2015.

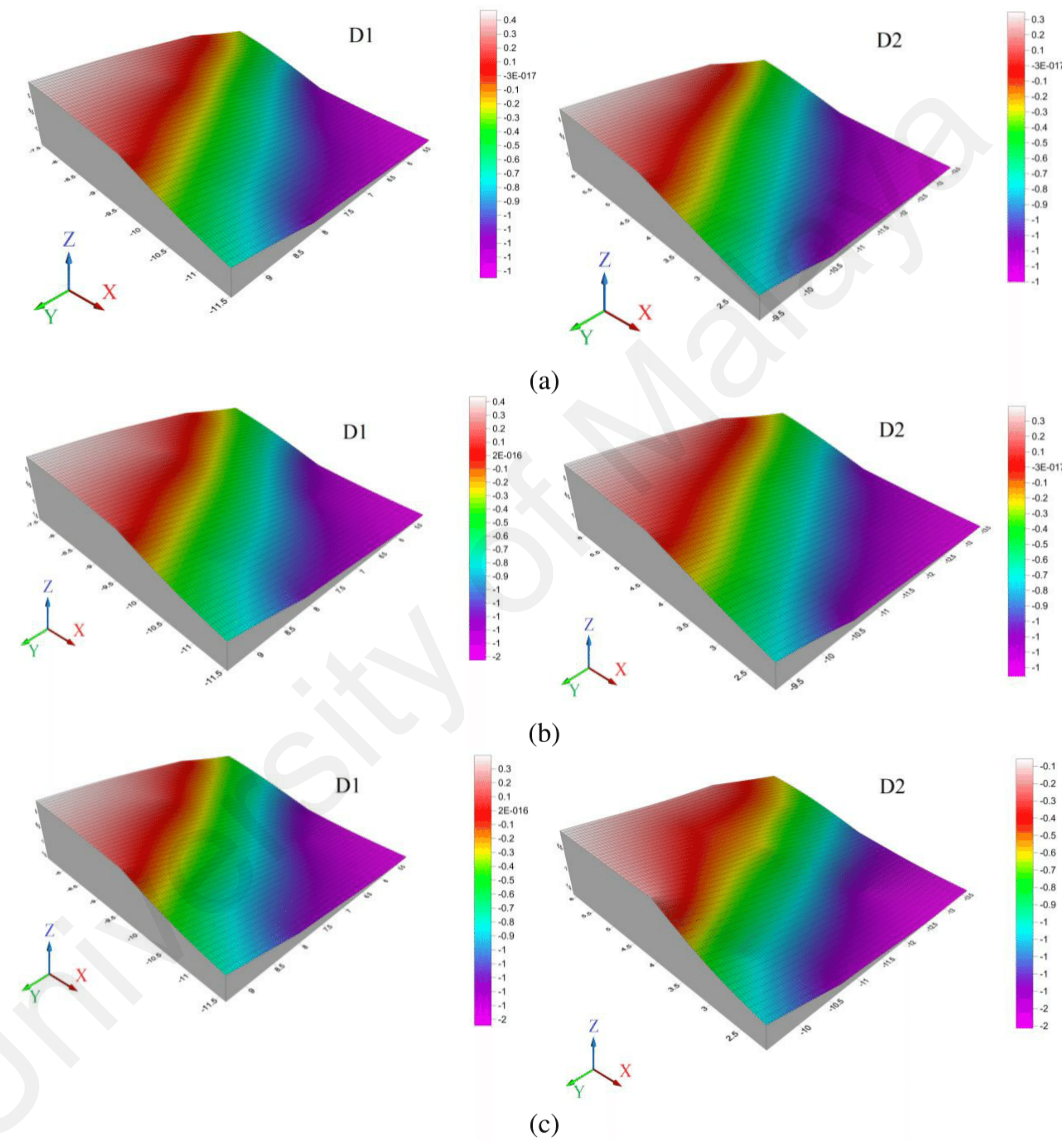

Figure 4.42: 3D spatial distribution of D1 and D2 revetment in (a) July 2014, (b) October 2014, and (c) January 2015.

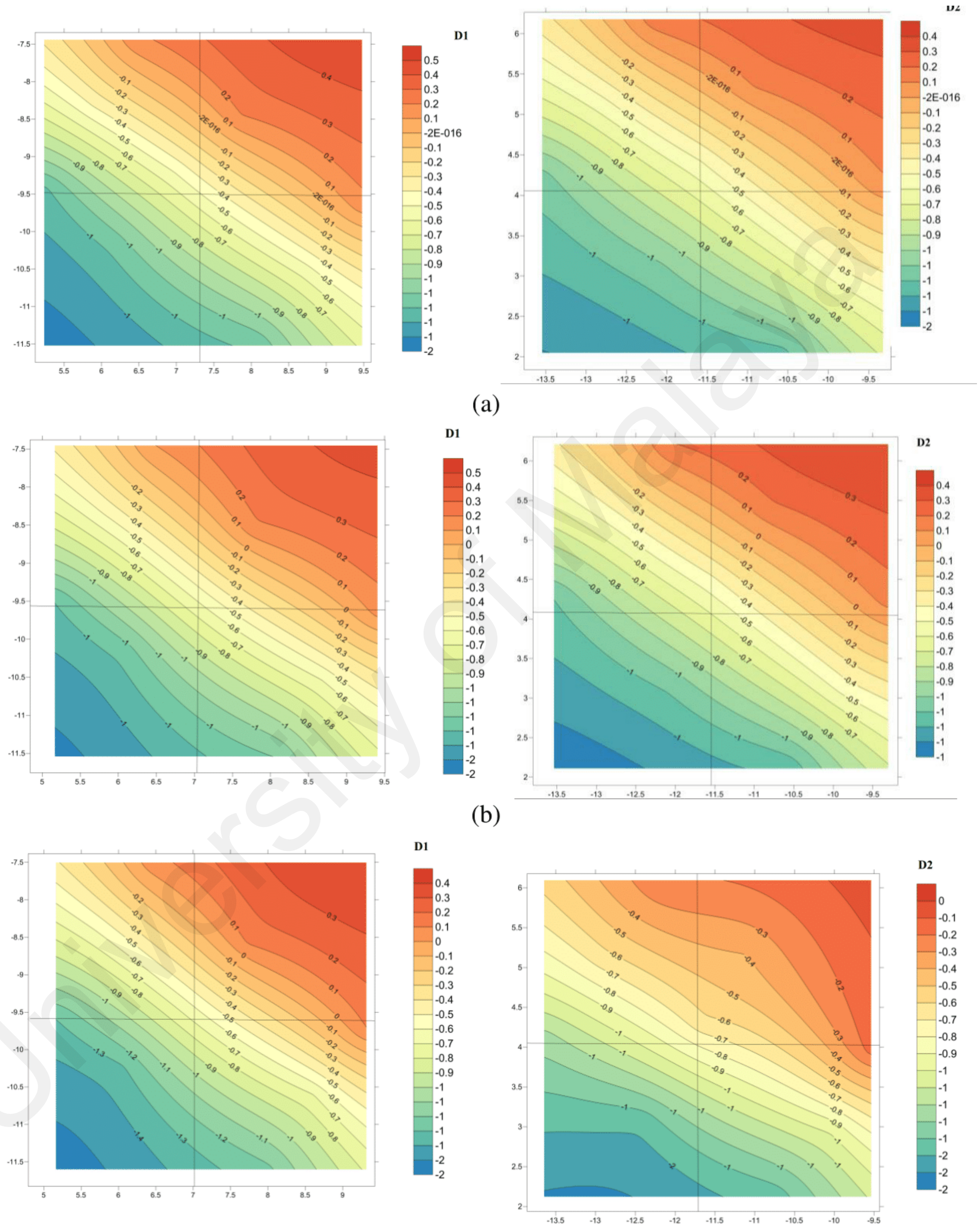

Figure 4.43: Topographic map of D1 and D2 revetments in (a) July 2014, (b) October 2014, and (c) January 2015.

4.7.5 Post-construction monitoring for Abstention revetment

According to the discussions in section 3.6.3 (b), the abstention revetments were monthly monitored for a period of six months from June 2014 to December 2014. During this period, any significant and observable erosion was identified. Further, the extent of the erosion was described using the measuring the eroded area. Figure 4.45 shows the A1 and A2 revetments (see Table 3.9) in June and December 2014. In addition, The coastal flora species were planted on the inclined surfaces of A1 and A2 two weeks after installation of the revetments (section 3.8). From the figure it can be observed that over the six months of monitoring, very minor erosion occurred at both A1 ($A_e \approx 0.02\ m^3$) and A2 ($A_e \approx 0.05\ m^3$).

Figure 4.46 shows the condition of the revetments in June 2015. From this figure, it can be found that a significant erosion occurred on the inclined surface of A2 ($A_e \approx 0.4\ m^3$). Perhaps, this was due to an unforeseen wave impact at the study site between December 2014 and June 2015. Thus, it can be stated that the Abstention method would be unsafe with regards to local erosion under the extreme wave impacts. It is not advised to use this method for the coastal areas with medium to high wave regime. If this technique is to be used for a certain area, it must be ensured that necessary maintenance works are carried out for rectifying the probable instances of erosion. A separate discussion on the growth of coastal vegetation when used on the Abstention revetments are delivered in section

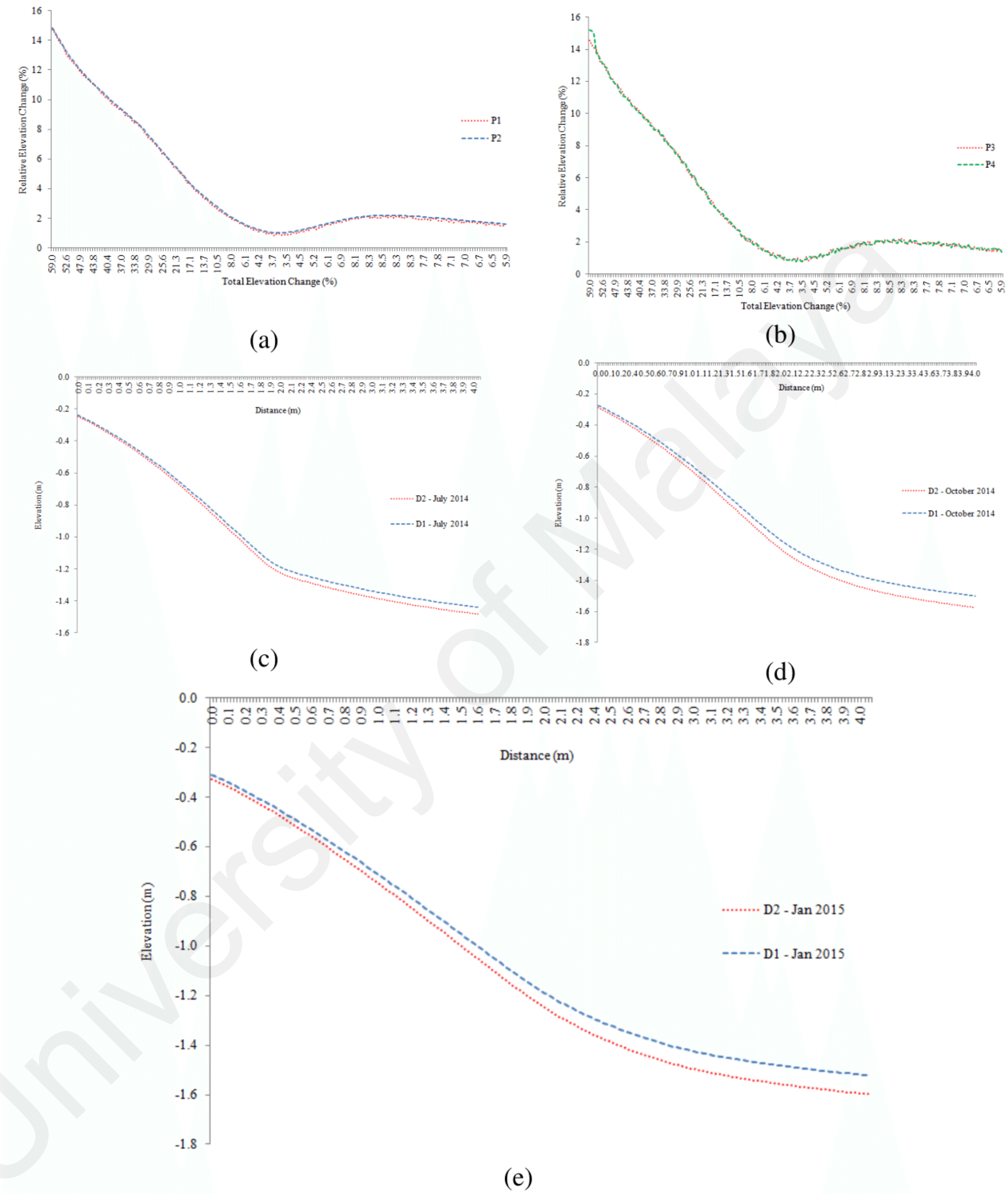

Figure 4.44: (a) Relative topographic change (%) over initial elevation change (%) versus total elevation change (%) at the most left side of the D1 revetment, (b) Relative topographic change (%) over initial elevation change (%) versus total elevation change (%) at the centerline along Y-axis of the D2 revetment; and Comparison of elevation in respect to distance across Y-axis of D1 and D2 revetments in (c) July 2014, (d) October 2014, and (e) January 2015.

(a) (b)

(c) (d)

Figure 4.45: Condition of A1 (a-b) and A2 (c-d) revetments in June and December 2014.

Figure 4.46: Condition of A2 revetment in June 2015.

4.8 Survival of replanted mangroves and coastal vegetation

4.8.1 Previous mangrove rehabilitation works at the site

For centuries, the cohesive coast of the Carey island (CI) has been a natural habitat for various species of mangroves. Large areas of mangroves in this area have been degraded and then converted to agricultural areas since 1950. In 1995, a dike system (Figure 4.47a) was constructed along the CI coastline to shelter the low-lying agricultural land (Tajul Baharuddin, Othman, et al., 2013). As a national strategy, the Department of Irrigation and Drainage (DID), Malaysia, built hundreds of kilometers of these coastal dikes to protect agricultural lands from massive wave energy induced by storms and tidal inundation (Affandi et al., 2010; Baharuddin et al., 2013). Mangroves were left as a safety shield between the dike and the sea to provide a second level of protection (Othman, 1994). However, in that era, the environmental value of mangroves was ignored which led to catastrophic negative consequence. As a result, massive retreat of the mangrove trees has been observed over the last two decades (see Figure 4.47b and Figure 4.47c).

With increasing research on the ecology of mangroves, it is clear that the dikes behind the mangrove forests can enclose water, creating ponds between the mangroves and the dike (Kamali & Hashim, 2011). Also, altitude of the silt-clay flat on the beach front of the CI has decreased. The reason for this remains unknown and requires further study. One possible reason is that the decrease in the morphological elevation leads to scouring of the soil underneath mangroves (R. Hashim et al., 2010). This can be observed through repositioning of mangroves to a hydrology regime more favorable for their survival (Kamali & Hashim, 2011). These, in turn caused depletion of the mangroves at the site.

Between 2008 and 2010, the first mangrove rehabilitation project was carried out at the southern part of CI which faces the Strait of Malacca (see Figure 3.7). The geograph-

Figure 4.47: (a) The existing dike system at the site from 1995, (b) The loss of mangroves at Carey Island in 2008, (c) The loss of mangroves at Carey Island in before construction of revetments, and (d) Natural recruits at the rehabilitation site after construction of revetments.

ical location of the rehabilitation site was selected in that part of the Carey Island because of the sustained forest degradation and serious erosion. The rehabilitation site was degraded to an extent that natural recovery processes were unable to restore the mangroves to their trajectory dense vegetation cover. This was determined based on the trends of massive mangroves degradation at the site (see Figure 4.47b and Figure 4.47c).

The rehabilitation site was considered suitable to carry out the pilot project because of the existing natural mangroves, which could be an indication that the area is a ground for re-establishment of mangroves, assisting the nature to reactivate its recovery processes. The existing mangroves at the rehabilitation site might have shed light on the hope that the area still possess the requisite biological, physical, and chemical environment that could contribute to the nurturing new generations.

Hard engineering intervention became an option once the designated area was failed to recover naturally, and there was fear of its further deterioration. The rehabilitation site was locally subjected to high and strong waves; thus as a phase of the proposed coastal rehabilitation framework (see R. Hashim et al. (2010) and Kamali and Hashim (2011)), a 80-m long detached breakwater system was installed at the rehabilitation site to provide a calm perimeter that could ensure and maintain the growth of seedlings that were planned to be planted, or occurring naturally through waterborne seeding from the nearby natural mangroves.

After identifying the major environmental stressors at the rehabilitation site, detached breakwater system was constructed at the site with the aim of (a) reducing the wave energy; thus creating a calm hydrologic regime for rehabilitation of mangroves, and (b) increasing the sediment deposition rate; thus countering the erosion trends at the site and enhancing the accretion trends behind the breakwater, where the rehabilitation area was located. The hard engineering system consisted of a submerged breakwater with three segments separated by 2.5 m to allow for water circulation to avoid forming stagnant water (R. Hashim et al., 2010). In addition, Kamali and Hashim (2011) stated that the average structural height at the crest of the breakwater was 1.8 m above the MSL. Further detailed information on the breakwater design and its construction sequence is found in R. Hashim et al. (2010) and Kamali and Hashim (2011).

Upon completion of the breakwater installation in early 2009, a series of several planting phases that employed few different techniques of plantation was tested. This was to verify whether the rehabilitation area was conductive to re-establishment of mangroves (see details in R. Hashim et al. (2010) and Tamin et al. (2011)). Selecting the planting species at the rehabilitation site was based on a fundamental concept reported by Primavera and Esteban (2008). The authors declared that the choice of mangrove species for rehabilitation purposes must have a harmony with the dominant naturally occurring mangroves species.

Nursery-raised 20-cm-tall seedlings of *Avicennia marina* and *Rhizophora apiculata* were selected for planting. This decision was made because *Rhizophora apiculata* is the major species at the rehabilitation site and *Avicennia marina* is the most dominant species on the Carey island (Saraswathy et al., 2009). Both species were planted in a grid system behind the breakwater using coir logs and conventional planting methods.

Unfortunately, in that time, after one year into the plantation efforts, a survivability index = 5% was recorded and the planted seedlings only survived a few months before they succumbed. The high mortality rate in the rehabilitation project could be attributed to the following: a) it is evident that after few month into plantation activities, a high sedimentation rate occurred at the site due to intervention of the breakwater. This could be potentially a contributing factor to the increasing loss of planted mangroves due to the positive increment in the burial depth (Kamali & Hashim, 2011); b) the coir logs were not suitable for the degraded coasts, because they could be displaced or disturbed by the current-induced drag forces. Even if they are appropriately installed at the exposed coastal areas, they cause stress to the seedlings due to their large dimensions (Kamali & Hashim, 2011).

On the basis of the observation at the rehabilitation site, in June 2014, before construction of the proposed revetment systems, a few new natural recruits were identified (Figure 4.47d). Being nearly 1-m tall with well-developed spreading root systems, the natural recruits are the *Avicennia marina* and *Rhizophora apiculata*. The growth of natural recruits was an indication that the breakwater could have successfully rehabilitate the bathymetric and hydrological site conditions (see section 4.9), and the site was biologically ready for further mangrove rehabilitation. Based on the findings of the present study, it is worthwhile rehabilitating the mangrove forest at the target site.

4.8.2 Hydrogeochemical assessment before rehabilitation of mangroves

In this subsection, based on the methodologies described in subsection 3.7.2, the results of the analysis for hydrogeochemical properties of soil-water samples at coastal zone of the Carey Island (Figure 3.10) are presented.

In this study, hydrogeochemical properties of soil-water samples taken from the Carey Island's coastal zone were identified prior to commencement of the mangrove rehabilitation. Overall, 36 water samples were collected along the axis S1 through the axis S6 as can be seen in Figure 3.10. Along each axis, six samples were taken at the longitudinal distance of 10 m. The S1, S2, and S3 axes denote the area of existing mangroves (natural habitat), while the S4, S5, and S6 axes represent the rehabilitation site. The natural habitat was considered as the control site and the rehabilitation site was considered as the experimental site. The pH value, salinity index, nutrient concentration, and heavy metal content of the samples were measured.

4.8.2 (a) pH Value

The results of the investigation for the pH values of the soil-water samples did not differ significantly between the natural habitat and the rehabilitation site. The average and standard deviation of pH value for the natural habitat, pH is 7.14 $\pm$ 0.21; for the rehabilitation site is 7.23 $\pm$ 0.19. This proves that the pH values at both rehabilitation site and natural habitat are slightly alkaline. Thus, the pH level at this site was appropriate for planting mangroves, because mangroves are able to survive in medium to high pH conditions (Wakushima, Kuraishi, & Sakurai, 1994).

When the pH value is lower than 7, the metal availability in the soil is increased since the hydrogen ion (H+) has a higher tendency for attracting negative charges and thus releasing the metals to the environment. On the contrary, when the pH value is higher than 7, it decreases the metal availability of the medium since the hydroxyl ion (OH-) has high affinity to attract positive charges and thus lowers the availability of metals in the soil-water (Jing, He, & Yang, 2007). The measured pH values in this study show that soil-water samples were slightly alkaline, which is an indication of reduction in the concentration of heavy metal ions along the study site.

4.8.2 (b) Salinity Index

Based on the results of this study, the mean value of salinity for the natural habitat ranged between 25.7 $\pm$ 0.57 ppt and 28.3 $\pm$ 0.74 ppt; an average of 26.3 $\pm$ 0.62 ppt. The values for the rehabilitation site ranged from 24.3 $\pm$ 0.43 part per thousand (ppt) to 29.2 $\pm$ 0.12 ppt; an of average = 26.9 $\pm$ 0.15. Thus, it can be concluded that the salinity in the soil-water samples did not vary significantly between the natural habitat and the rehabilitation site.

Depending on the region, the same mangrove species may have different tolerances to salinity. Aziz and Khan (2001) claimed that, in india, *Avicennia marina* can survive in semiarid to saline deserts and it is highly salt-tolerant up to 35 ppt. However, it was found in Hong Kong that Avicennia marina can barely survive in a salinity higher than 15 ppt (Ye, Tam, Lu, & Wong, 2005). In the Malaysian coastal zones, mangroves were reported to have the potency to survive in a salinity between 20 ppt and 30 ppt (Affandi et al., 2010). In this study, it was found that the salinity ranged from 24.3 ± 0.43 to 29.2 ± 0.12 ppt (average = 26.9 ± 0.15 ppt) on the Carey Island. Thus, it can be concluded that the site was suitable for natural recruits of *Avicennia marina*.

4.8.2 (c) Nutrient Concentrations

The Carey island is a wide area of palm cultivation. It is inevitable that for the commercialized production of palm oil a large amount of fertilizers are used. The site selection of mangrove rehabilitation plays a major role in having confidence in the positive outcomes of the project. According to Duarte et al. (1998), the growth of mangroves is essentially more successful near wetlands and riverine flats where the nutrients can be transported. In this study, the location of rehabilitation project was selected near three rivers: a) Air Hitam, b) Judah, and c) Keluang (Suntharalingam & Teoh, 1985) as well as also in the vicinity of palm cultivation areas. In this respect, the runoff of surface water could potentially transport the remnant of fertilizers into the study site, which in turn might imbalance the success of mangrove rehabilitation activities. Because mangrove seedlings could use the abundant nutrients in the sediment deposits to establish themselves, quantifying the nutrient content at the site was worthwhile.

Nutrient is a vital chemical element that is required for the life-cycle completion and growth of plant. The rate of growth for mangrove seedlings can increase when sufficient nutrient-rich sediments are available (Duarte et al., 2013). Non-organic nutrients are classified into two types: a) micronutrients and b) macronutrients. In general, plants need larger volume of macronutrients for their growth (Ye et al., 2005), whilst smaller amounts of micronutrients are needed in the regulatory and catalytic mechanisms (Ye et al., 2005). The plants will be imposed to the risk of toxification if the micronutrients reach above an acceptable level, where they are called *heavy metals* (Jing et al., 2007).

In the following, based on the methodology presented in subsection 3.7.2, a quantitative assessment of non-organic nutrients from the soil-water samples collected from the study site is presented and discussed. Table 4.10 summarizes the nutrient concentrations from the collected soil-water samples that are discussed in detail as follows.

Table 4.10: The range of nutrient concentration at reforestation site. Note 1: Nutrient Concentration (NC), Rehabilitation Site (RS), Natural Habitat (NH), Concentration Considered Toxic (CCT). Note 2: [a] Gong and Ong (1990), [b] Clemens (2006), [c] Reddy and DeLaune (2008), and [d] Hopkins and Huner (2004).

NC (ppm)	RS (ppm)	NH (ppm)	CCT (ppm)
Macronutrient			
Nitrogen (N)	22.69 – 57.39	0	10 – 60 [a]
Calcium (Ca)	260.28 – 314.81	151.60 – 311.47	<500 [b]
Magnesium (Mg)	265.47 – 325.71	209.00 – 255.77	<300 [b]
Sulphur (S)	1.56 – 4.01	1.78 – 4.39	>2 [c]
Micronutrients			
Manganese (Mn)	0.09 – 0.78	0.01 – 0.38	0.01 – 0.8 [c]
Chlorine (Cl)	15.46 – 32.84	12.08 – 27.91	120 - 300 [d]
Copper (Cu)	0.01 – 0.02	0.02 – 0.04	0.02 – 0.05 [d]

Nitrogen is considered a basic ingredient for the growth of plants. Nitrogen in the soil has organic and inorganic forms. In the organic form, nitrogen comprises of residues from plant, living organisms and other organic matters in the decomposed form. On the other hand inorganic nitrogen are found either as nitrate (NO_3^-) or ammonium (NO_4^+) (Meyer, Kelley, & Vignais, 1978). In this study, Nitrogen in the range of 10 ppm to 60 ppm is acceptable in the soil (Gong & Ong, 1990). Table 4.10 shows the concentration of nitrogen at the reforestation site ranges from 22.69 ± 0.19 ppm to 57.39 ± 0.33 ppm (average = 42.1 ± 0.27 ppm). This implies that the nitrogen content is in the acceptable range. On the other hand, no nitrogen was found at the natural habitat due to natural processes such as, the bacterial nitrification, de-nitrification, and ammonia valorization

(Meyer et al., 1978). At the natural habitat the above mentioned processes consumed nitrogen from the soil. Therefore, it can be concluded that rehabilitation site had enough nitrogen to support mangroves.

Sulfur plays an important role for growing plants and other biological processes. It should be noted that for plants sulphate is the usable form of sulphur (Hopkins & Huner, 1995). In this respect, a minimum sulfate of 2 ppm is considered acceptable for the coastal area (Reddy & DeLaune, 2008). It was observed that sulfate ranges from 1.56 $\pm$ 0.38 ppm to 4.01 $\pm$ 0.12 ppm (average = 2.71 $\pm$ 0.51 ppm), and 1.78 $\pm$ 0.58 ppm to 4.39 $\pm$ 0.86 ppm (average = 2.73 $\pm$ 0.62 ppm) at the reforested and natural sites, respectively. It can be concluded from the above discussion that sufficient sulfate was present for establishing mangroves at both sites namely at the rehabilitation and natural coastal regions.

Chlorine is an essential chemical for photosynthesis (Hopkins & Huner, 1995). It is abundant in nature. Plants use chlorine in the form of chloride (CL^{-}). Mangroves can take chloride up to 106 ppm (Meyer et al., 1978). It was found that concentration of chloride was higher at the reforested site than at the natural habitat. At the rehabilitation site, concentration of chloride was 15.46 $\pm$ 0.41 – 32.84 $\pm$ 0.76 ppm with an average value of 26.76 $\pm$ 0.84 ppm, while at the natural habitat the concentration of chloride ranged from 12.08 $\pm$ 0.37 to 27.91 $\pm$ 0.54 ppm with an average value of 19.32 $\pm$ 0.41 ppm. Thus, it can be concluded that chloride at the rehabilitation area was in the acceptable range.

Magnesium and calcium are vital for growth of plants (Meyer et al., 1978). Based on the research work of Clemens (Clemens, 2006), calcium and magnesium contents below 500 ppm are considered non-critical, or are acceptable for growth of plants. In this regard, a similar concentration of calcium and magnesium at the rehabilitation and natural habitats was found. At the rehabilitation site the concentration of calcium and magnesium were in the range of 260.28 $\pm$ 0.79 to 314.81 $\pm$ 0.11 ppm (average = 281.16 $\pm$ 0.36 ppm), and 265.47 $\pm$ 0.94 to 325.71 $\pm$ 0.21 ppm (average = 291.23 $\pm$ 0.36 ppm), respectively.

However, at the natural habitat the concentration of calcium and magnesium 260.28 $\pm$ 0.79 to 314.81 $\pm$ 0.11 ppm (average = 281.16 $\pm$ 0.36 ppm) and 209.00 $\pm$ 0.49 ppm to 255.77 $\pm$ 0.87 ppm (average = 283.34 $\pm$ 0.36 ppm), respectively. The above discussion suggests that reforestation site was suitable for establishing mangroves.

Manganese acts as a catalyst to enzymes of plant responsible for respiration, photosynthesis, and protein synthesis (Otero et al., 2009). An acceptable range of manganese falls in the range of 0.01 ppm to 0.8 ppm (Reddy & DeLaune, 2008). Concentration of manganese at the rehabilitation and natural habitat was from 0.09 $\pm$ 0.29 to 0.78 $\pm$ 0.74 ppm (average = 0.36 $\pm$ 0.31 ppm) and from 0.01 $\pm$ 0.06 to 0.38 $\pm$ 0.24 ppm (average= 0.29 $\pm$ 0.44 ppm), respectively. Thus, manganese concentration was favorable at both sites.

Reddy and DeLaune (2008) described copper as highly toxic for plants. Copper causes yellow coloration, retardation, and chlorosis in plants, when present in soil or water (Hopkins & Huner, 1995). Amount of copper in soil and plant should be lower than 0.05 ppm and 0.02 ppm (Reddy & DeLaune, 2008). It was found that reforestation reduced the amount of copper. The Copper concentration at the reforested and natural habitat ranged from 0.01 $\pm$ 0.63 to 0.02 $\pm$ 0.27 ppm (average = 0.031 $\pm$ 0.68 ppm) and 0.02 $\pm$ 0.53 to 0.04 $\pm$ 0.17 ppm (average = 0.037 $\pm$ 0.31 ppm), respectively. Though copper concentration was reduced at the reforested area, both sites had copper concentration below the danger level.

Based on the above discussion, it can concluded that the rehabilitation site was suitable for rehabilitating mangroves, because the nutrient content increased in the rehabilitation area. In addition, rehabilitation of mangroves could be further ensured by reducing the impact of wave energy; and increasing sedimentation in the region under rigorous anthropogenic control.

4.8.3 Survival of planted mangrove species

Based on the methodology described in section 3.7.3, the target mangrove species (Table 3.8) were planted at the site in accordance with the planting layout shown in Figure 3.14. The monitoring program after planting the nursery-raised seedlings was carried out in line with the methods described in section 3.7.3 (d). Figures 4.48 and 4.49 show the mortality of mangroves for each subsequent two months after the initial plantation activities from late June 2014 to December 2014. It should be noted that upon death of seedlings in each monitoring period, the lost mangroves were replaced with new seedlings to accommodate the initial total planted species in June 2014.

In general, it is observed that mortality rate of the planted mangroves had a decreasing trend with time. For example, within zone A, for *Avicenna marina* species that were planted in the seaward of the rehabilitation area, the mortality of the species dropped from 7% in the late June 2014 to 1.5% in the late October 2014 (Figure 4.48). For the same conditions, the mortality of the *Avicenna alba* species decreased from 3% in late June 2014 to 0.5% in late October 2014. In zone B, the mortality rates of *Avicenna marina* (84.5%) and *Sonneratia alba* (90.5%) were comparatively higher than other target species (Figure 4.49). This high mortality observed in zone B can be associated with the fact that zone B was not protected by the existing breakwater; thus, higher wave energy exposed the planted species at the risk of death.

Figure 4.50 depicts the results of analysis for the mortality rate of target mangrove species at zone A and zone B of rehabilitation site for 6 months. Based on the results, the rate of mangrove loss was higher for zone B compared to zone A. For example, over the monitoring period at zone B, *Sonneratia alba* species had the highest rate of mortality at 12%, followed by 10.5% mortality rate recorded for *Avicenna marina* species. Both of these species were planted at seaward of the rehabilitation site, which could be a reason for their high mortality rate. Meanwhile, for same species at the zone A of the rehabilitation site, the mortality rate was 0.83% and 1% for *Sonneratia alba* and *Avicenna marina*, respectively. The same conclusion can be made for other species planted at zone A and zone B.

Figures 4.51 to **??** illustrate different views of the rehabilitation site before, during and after plantation activities. The average monthly rate of relative increment in height for both zones was 43 ± 3 mm per month. In addition, the average number of leaves that each seedlings at zone A and zone B could produce during the monitoring periods was 4 leaves per month. From these figures, it can be observed that the rehabilitation project during the six months of monitoring period was successful in establishing conductive conditions for further growth of mangroves at the rehabilitation site. Details on the extend of the success are discussed in section 4.9.

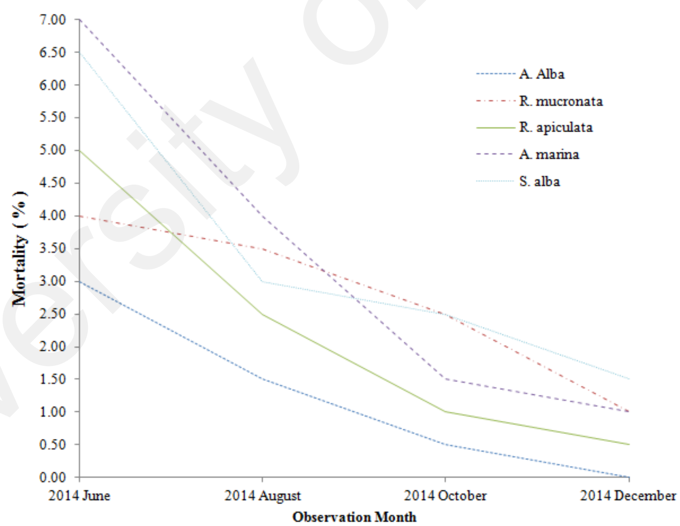

Figure 4.48: The mortality of planted mangrove species at the site in zone A.

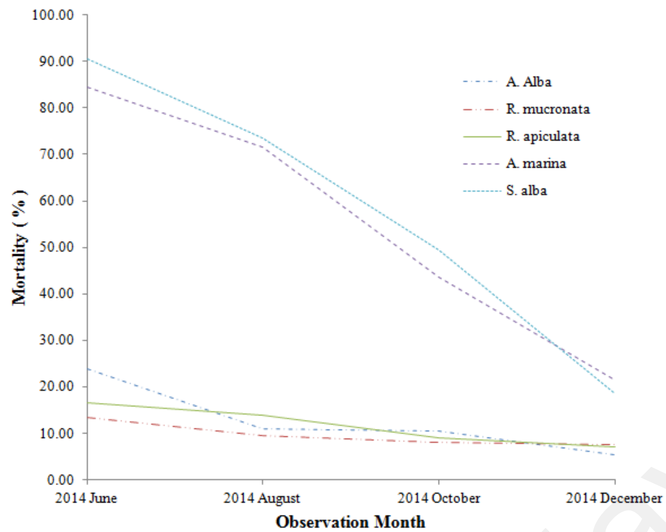

Figure 4.49: The mortality of planted mangrove species at the site for different monitoring periods in zone B.

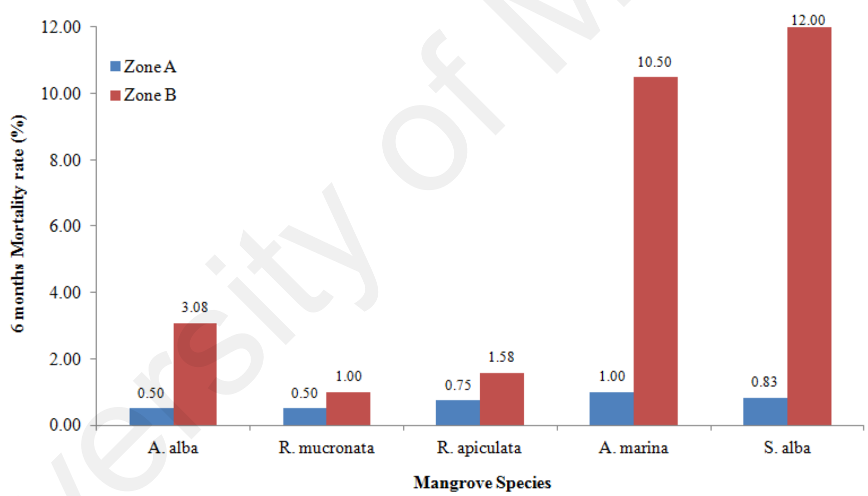

Figure 4.50: The mortality rate of planted mangrove species at the site in 6 months monitoring period.

(a) (b)

Figure 4.51: A view of the rehabilitation site before plantation activities in (a) zone A and (b) zone B.

(a) **(b)**

(c)

(d)

Figure 4.52: A view of the rehabilitation site a) during the plantation activities (June 2014), b) July 2014, c) October 2014, and d) December 2014.

4.8.4 Survival of planted coastal vegetation

Based on the methodology described in section 3.8, 3,000 species of two coastal flora species, *Cynodon dactylon* (Figure 3.15a) and *Ipomoea pes-caprae* were planted at the site in accordance with the planting layout shown in Figure 3.16. Hereafter, these species are denoted as *S1* and *S2*, respectively. The monitoring program after planting the species was carried out in line with the methods described in section 3.8. Figures 4.53 and 4.54 show the mortality of S1 and S2 for each subsequent two months after the initial plantation activities from late June 2014 to December 2014. It should be noted that upon death of species in each monitoring period, the lost flora species were replaced with new seedlings to accommodate the initial total planted species in June 2014.

In general, it is observed from these figures that the mortality rate of the planted species had a decreasing trend over time. For example, within zone A, for S1 species that were planted on the deck and the inclined surface of the revetments, the mortality of the species dropped from 1.84% in late June 2014 to 0.31% in late October 2014 (Figure 4.53) For the same conditions, the mortality of S2 species decreased from 2.12% in late June 2014 to 0.35% in late October 2014. In zone B, the mortality of S2 (6.58%) in June 2014 was comparatively higher than S1 (5.07%) (Figure 4.54). In addition, the average observed mortality rate for both zones was higher in zone B (3.38%) compared to zone A (1.13%). For S2 species planted in zone B, a sudden increase of mortality rate (8.34%) was observed in August 2014. This high mortality observed in zone B can be associated with the fact that zone B was not protected by the existing breakwater; thus, higher wave energy impose the planted species at the risk of death. Also, perhaps the vandalism (section 4.6.5) can be another reason for higher rate of mortality of planted species especially for the species planted on the deck of the revetments.

Figures 4.55 illustrates different views of the rehabilitation site before, during and after plantation activities. From these figures, it can be observed that the rehabilitation project during the six months of monitoring was successful in providing a the objectives proposed for increasing the aesthetic features of the site as well as incorporating the eco-friendly elements into the revetment systems. Details on the extent of success are discussed in section 3.8.

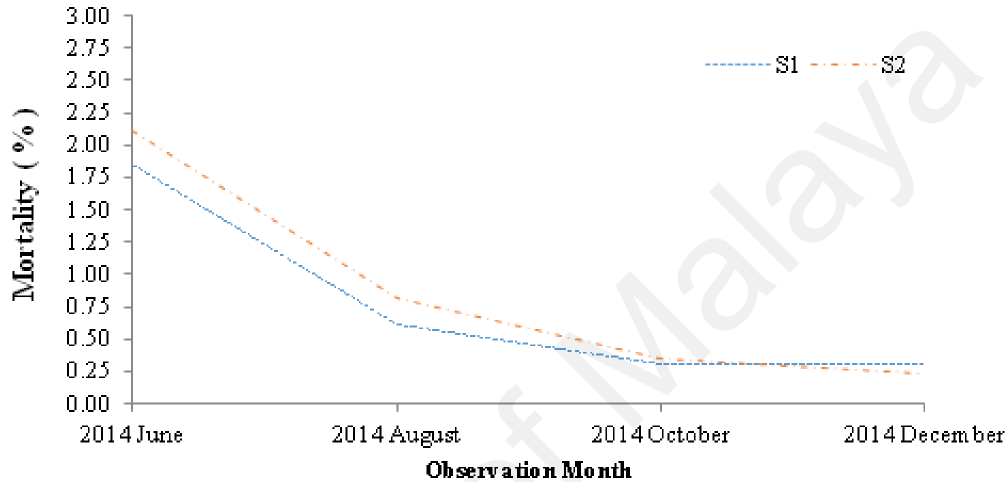

Figure 4.53: The mortality of planted flora species at the site for different monitoring periods in zone A.

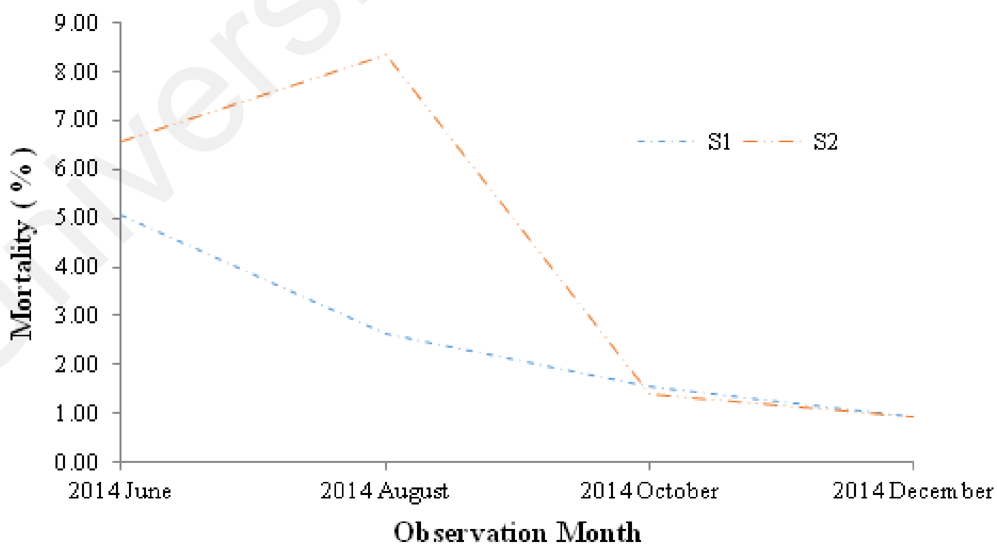

Figure 4.54: The mortality of planted flora species at the site for different monitoring periods in zone B.

(a)

(b)

(c)

Figure 4.55: A view of the rehabilitation site (a) before, (b) during, and (c) after plantation of S1 and S2.

4.9 Coastal rehabilitation under the proposed protection program

This section looks into the implications of findings in this study in relation to the rehabilitation works under the protection of the proposed integrated coastal rehabilitation program.

4.9.1 Mitigation of erosion using mangroves

The intensity of coastal erosion is directly associated with the magnitude of degradation in coastal ecosystem. For example, at the Carey island, the deforestation of mangrove forests as a result of mismanagement in land development strategies has led to retardation of natural recovery of the coastal zone. To a significant degree, irreversible coastal erosion made it necessary to employ engineering measures to speed up natural processes and rehabilitate the site to an acceptable level through engineering solutions.

Although the first step towards conducting coastal rehabilitations works is to prevent further erosion events, human intervention in the name of engineering mitigation measures may lead to intensified erosion and even increase the magnitude of ecosystem degradation. Therefore, it is necessary to be careful for selecting a mitigation or prevention strategy for the coastal erosion through minimizing the future negative consequences. For example, in the Carey island, a dike system was built along the coastline to provide the so-called *solution* to protect the cultivation lands in close vicinity of shoreline. Unfortunately, greater deterioration of mangroves was reported after few years into the construction of the dike system. The dike system was built on the leeward of the coast to provide protection for low-lying coastal areas against the inundation. Even though the dike was efficient to provide protection for the low-lying lands, at the same time it disconnected the ecological link between the mangroves and the backshore. This resulted in aggravation of erosion seawards of the coastline.

An integrated coastal rehabilitation program not only should provide structural measures (hard engineering) to reduce stresses on the coastal environment, but also shall employ ecological features (soft engineering). The latter is of special importance because a key element when incorporating ecological engineering concepts into programs of coastal rehabilitation is to bring the focus on utilizing the power of nature to release the disturbance factors in the coasts. In this context, replacing a portion of engineering works with relying on the natural recovery processes can be an option. For example, a magnificent example for adaptation of ecosystem in coastal protection is the role of coastal wetlands. Generally, wetlands decrease the wave energy, reduce erosion and increase the sedimentation at the coasts (Barbier, 2012).

4.9.2 The proposed coastal rehabilitation program

The proposed program is inclusive of three phases. The First phase is to alleviate the erosion rate until an equilibrium state be reached; leaving a confident margin of safety for further phases of the program. For example, the bed level at the study site experienced a history of continuous erosion before installation of the breakwater in 2009. After installation of the breakwater, the approach was successful to trap fine sediments (section 4.7.1 (a)). The bed level experienced a positive dynamic morphophonemic changes resulting in elevation of the bed level in nearshore. The increase in bed level at the lee-ward of the breakwater is an indication of the success for the breakwater in dampening of local wave energy.

The eroded zone at the coastline of the study area (see Figure 4.14) was under progressive failure due to existing of stressors. Figure 4.56 shows the existing breakwater in June 2014. The red arrow shows the original location of few armoring units that were displaced during the construction of the revetments. Therefore, it was necessary to move forward to the second phase of rehabilitation program.

The Second phase of the rehabilitation program is to restore the shoreline to its tra-

Figure 4.56: The existing breakwater at the site in June 2014.

jectory stable condition. Although the breakwater was successful in dampening the wave energy and elevating the bed level, it could not completely reduce the exposure of the hydraulic forces to the shoreline. Massive erosion was found behind the breakwater at the natural shoreline. Construction of the revetments at the eroded coastline was successful in preventing further erosion. Also, the revetments alleviated the ongoing erosion and restored the aesthetic features of the study site.

These revetments were placed at the eroded coastline of the Carey island so that the performance of each system could be evaluated in the presence and the absence of the existing breakwater. The discussions in section 4.7 proved that revetments were more efficient when they were sheltered with the breakwater. Although, breakwater was successful in providing balance for erosion and accretion trends at the bed level, the area behind the breakwater at the shoreline was left unprotected. This implies that there was an immediate need for employing mitigation measures for rehabilitation of shoreline mass movement to stable condition by construction of revetments. It can be concluded that an integration of few hard engineering solutions to address a wider range of problems at the coastal zones is an option.

The third phase of the rehabilitation program is to incorporate the power of nature in the design of the hard engineering solutions. This phase should only be implemented after the stressors are removed. In this phase, four main objectives are pursued: a) to restore the biotic features at degraded site, b) to facilitate the conditions for natural recovery processes to reach a long-term stable state, c) to increase the aesthetic view of degraded site by relying on ecological features, and d) to establish an ecological link between soft engineering and hard engineering methods of coastal protection for enhancing the aquaculture services. For example, at the study site, a series of mangrove rehabilitation works and re-plantation of coastal flora species were carried out to enhance the quality of the coastal environment by increasing the survivability of coastal habitat and the associated biota.

Breakwaters are successful in dampening the wave energy and elevating the bed level, but they may not completely remove the stressors from the coasts. Therefore, massive erosion is commonly found behind the breakwaters, where the natural shoreline soft is located. It is viable to adapt hard engineering measures as a secondary level of protection to alleviate the erosion rate at these regions. In this context, revetments are suitable to provide such preventive measures against erosion. If the aim is to minimize the environmental risks arising from the implementation of these structures, soft engineering concepts can be adapted in the design layouts. Incorporating biotic features such as vegetation cover and enhancing the armor layer components using eco-friendly materials can be considered as an alternative soft engineering solution.

The proposed coastal rehabilitation program (Figure 4.57) provides a comprehensive platform that integrates a range of hard engineering measures and soft engineering techniques. Rigid one-dimensional techniques solely rely on incorporation of man-made structures to protect the coastal environment. At the study site, the area behind the break-

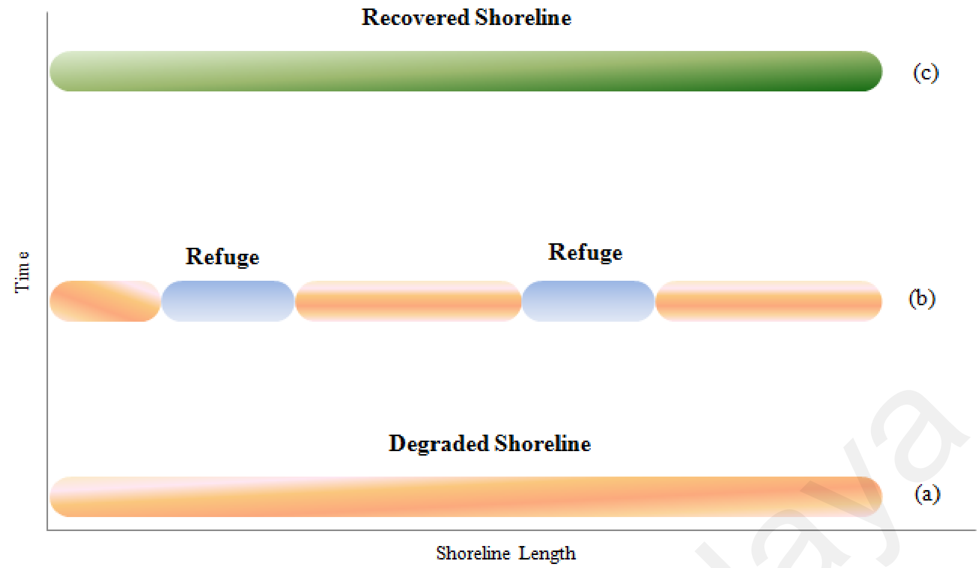

Figure 4.57: The conceptual scheme for the proposed coastal rehabilitation program; (a) degraded shore before rehabilitation works; (b) providing refuge using innovative hard engineering measures (i.e., revetment system and breakwater); (c) Possible natural mangrove rehabilitation of full length of shoreline in long-term.

water is sheltered from the extreme coastal forces that is in a conductive ground for rehabilitation of mangroves and other coastal flora (Kamali & Hashim, 2011). Adaptation of hard engineering concepts was proved to form a refuge on the eroding coast that is attractive for natural recruits.

At the study site, a refuge was formed by the breakwater and revetments. The approach rather than promoting a full intervention of artifacts, encourages the repairing of degraded coastal ecosystem through natural recovery. A larger stretch of the coastal area is expected to be rehabilitated by providing a few number of refuges along the coastlines instead of installation of hard structures at the full length of the coasts.

4.9.3 Success of mangroves rehabilitation program

Evaluating the success of a coastal rehabilitation project is subjective and challenging. This is because there are no universally accepted criteria for measuring the success of such projects. In a coastal rehabilitation project, various methods of soft and hard engineering techniques with a wide range of objectives are employed. These goals may be unachievable or even unrealistic due to the inherent uncertainties arising from such methods (Lewis III, 2000). For example, success of hydrogeologic for rehabilitation of coastal wetlands is site-dependent. The mathematical formulation of wetland rehabilitation works are mostly empirical rather than scientific which makes them inefficient to generalize the findings for different local conditions (Turner & Lewis, 1996).

The conventional concepts in assessing the success of mangrove rehabilitation programs are on the view that a particular project is considered successful when a full recovery of the targeted degraded species is reached. For example, Krauss et al. (2008) defined the success of mangrove rehabilitation as the stage in which the replanted seedlings become rooted, survived and developed to the sapling phase. Other such definitions recommended production of flowers and viable fruits as indicators of long-time sustainable success of mangrove rehabilitation (Primavera & Esteban, 2008).

The plantation of mangroves at the rehabilitation site started after the construction of revetments in June 2014 (see section 4.6.1). R. Hashim et al. (2010) stated that when volumetric sedimentation rate is relatively high, there is a high probability that increasing the sediment burial depth has a direct relationship with the increasing replanted saplings mortality. Based on the discussions provided in section 4.7.1 (a), the volumetric sediment accretion at the study area decreased from 0.129 ± 0.36 m^3/m^2 between January 2012 and January 2013 to 0.04 ± 0.27 m^3/m^2 between January 2014 and June 2014. This is an indication that, overall, the rate of volumetric sediment accretion, after around 5 years into the construction of the breakwater, decreased significantly and the shoreline reached a nearly stable equilibrium state.

Based on the results of this study (section 4.8 and section 4.7.1), the sedimentation rate at the site has significantly alleviated since 2009, after the implementation of the first phase of the proposed coastal rehabilitation program. In areas where relative annual positive topographic change at the bed level (see Figure 4.27 and Figure 4.28) was higher, a higher mortality rate was observed for the replanted mangroves.

In this study, long-term monitoring was essential in the Carey Island rehabilitation site to evaluate the success of mangrove rehabilitation. According to the discussion in section 4.8, based on the results of short-term monitoring, the mangrove rehabilitation efforts are successful at the Carey Island site. In addition, in line with the discussions in section 4.7, it is highly probable that the proposed rehabilitation program is successful in providing protection against erosion and other hydraulic forces at the site. Therefore, it is recommended that a 3 to 5 years long-term monitoring program is conducted at the site to assess the success of the mangrove rehabilitation.

CHAPTER 5: CONCLUSION AND RECOMMENDATION

In this study, a novel approach for the coastal rehabilitation works was developed and examined. The main component of this research work was design, construction and monitoring of the developed eco-friendly revetment systems. In addition, an integrated coastal protection program was proposed and implemented at the eroding coastline of Carey Island, Malaysia. The program was successful in providing protection at the coastline against erosion. Also, it may promote natural colonization of mangroves and coastal flora through integration of hard and soft engineering techniques. It is expected that the shelter formed by this approach contributes to improving the process of repairing the degraded ecosystems at the coastal regions.

5.1 Conclusion

Based on the results of the experiments and field monitoring works presented in this study, the following conclusions can be drawn in relation to design, construction and monitoring of the developed eco-friendly revetment systems, the developed armoring unit, success of the proposed coastal protection program, and rehabilitation of coastal vegetation.

5.1.1 Developed armoring unit: material and hydraulic stability

- In this study, a novel armoring unit termed as the LEco was developed. This highly interlocking unit (packing density:ϕ=0.65) is simple and cheap to fabricate. The unit is adaptable to areas that experience low to medium wave climate regime. To fabricate the unit, two cement-based mixtures were developed using the Pulverized Fuel Ash (PFA) and the cockle shell powder (CS). Both of these mixtures were successfully tested and used for fabrication of the unit. The optimal contents of PFA (20% of the total weight) and CS (25% of the total weight) were found for cement-aggregate mixtures in order to obtain the maximum unconfined compressive strength (UCS) of the developed composite materials. Therefore, in terms of eco-friendliness, using the developed mixture of PFA-Cement-Sand for fabrication of the armoring units, a 20% reduction in use of cement was achieved.

- Based on the laboratory experiments, when the LEco armoring unit shielded the revetment with a slope (θ) of 37°, no displacement was observed; whereas when $\theta = 53°$a maximum displacement of 7.8 $\pm$ 0.1 *mm* was measured. The recorded displacement is negligible when compared to the dimensions of the model. This is due to high interlocking capacity of the unit ($\phi = 0.65$). In addition, the obtained stability number of $N_s = 3.8$ equals to $K_D = 20$ at $N_{od} = 0.5$ shows the great hydraulic stability of the unit.

5.1.2 Developed eco-friendly revetment systems

- All the developed revetments remained stable ($N_{od} < 0.5$) after series of laboratory experiments under various loading conditions. In addition, applying numerical modeling for all the developed revetments under the maximum loading condition ($h_e = 100\%$ of design water level), the calculated FOS met the *USBR (2014)* criteria of safety against high exit gradient (>3), and uplift pressure (>1.5). Besides, for local conditions of the study site, the LEco and Double-layer revetments are safe against sliding under the maximum loading condition ($FOS_{LEco} = 1.429 > 1.3$ and $FOS_{Double-Layer} = 1.362 > 1.3$). However, Abstention revetment for local conditions of the study site is vulnerable to sliding when subjected to maximum loading condition ($FOS_{Abstention} = 1.163 < FOS_{USBR} = 1.3$).

- Based on the field monitoring of the LEco revetment systems, it was found that both L1 and L2 did not experience any displacement of the LEco armoring units (LEco) ($N_{od} = 0$). L1 is the LEco revetment protected behind the existing breakwater at the site and L2 is the one not protected behind the breakwater. In this relation, according to the Bayesian definition of damage criteria for armor layers, L1 and L2 did not reach the state of *initiation of damage*.

- Based on the field monitoring of the Double-Layer revetments, it was found that the displacement of D1 and D2 was not significant ($RTT_{Average} = 0.5\%$). D1 is the Double-Layer revetment protected behind the existing breakwater at the site and D2 is the one not protected behind the breakwater. However, an increasing trend in displacement of both D1 and D2 revetments with respect to time was observed. Comparing the temporal changes in elevation for D1 ($RTT_{Oct14-Jan15} = 0.75$) and D2 ($RTT_{Oct14-Jan15} = 0.82$) revealed that D2 has experienced a higher decrease in elevation compared to D1. This is due to protection of D1 behind the existing breakwater system.

- The stone armoring units used in D1 and D2 experienced a very minor displacement under low to moderate wave conditions ($N_{od} \approx 0$). For both D1 and D2, the N_{od} was negligible, since A_e was almost zero. Based on the Bayesian definition of damage criteria, D1 and D2 did not reach the state of *initiation of damage*.

- Based on the field monitoring of the Abstention revetments, a minor erosion occurred at A1 ($A_e = 0.02\ m^3$). A1 is the Abstention revetment protected behind the existing breakwater at the site and A2 is the one not protected behind the breakwater. In case of A2, a significant erosion ($A_e = 0.0.4\ m^3$) occurred at its inclined surface. In this view, the Abstention revetment may be unsafe when exposed to high wave impacts. This type of revetment is not advised for the coastal areas with medium to high wave regime.

5.1.3 The proposed coastal protection program

- Before construction of the developed revetments, the bed level at the area protected by the existing breakwater consistently increased over time. The highest and lowest values of RTT were observed in January 2011 and June 2014 at 78.49% and 0.01%, respectively.

- After installation of the breakwater, the elevation rate of the bed level decreased from January 2011 to June 2014. This rate of elevation was higher in the monitoring period between January 2011 and January 2012 (P1) ($RTT_{P1} = 0.41\%$), and between January 2012 and January 2013 (P2) ($RTT_{P2} = 0.55\%$) compared to the monitoring period between January 2013 and January 2014 (P3) ($RTT_{P3} = 0.50\%$), and between January 2014 and June 2014 (P4) ($RTT_{P4} = 0.01\%$). This decrease in the bed level is an indication that an equilibrium condition was reached at the site.

- A significant volume of sediments was deposited between January 2011 and June 2014. During the monitoring period of P2, a total highest volumetric deposition of 0.129 ± 0.36 m^3/m^2 was observed at the site before the construction of the revetment systems. In addition, the lowest volumetric deposition was recorded during P4 at 0.04 ± 0.27 m^3/m^2. This is an indication that after few years into the construction of the breakwater, an equilibrium state was reached at the site.

- The volumetric deposition at the study area had a decreasing rate in all the monitoring periods, except for P2 (0.129 ± 0.36 m^3/m^2) in which a sharp positive increment for the volumetric deposition was observed compared to P1 (0.095 ± 0.43 m^3/m^2). This sudden change could be attributed to the initiation of the breakwater positive performance in alleviating the erosion at the site after one year into its construction.

- Accumulation of sediments decreased between June 2014 (after construction of the developed revetments) and June 2015 (one year into the construction of the developed revetments). In the first six-months periods into the construction of the revetments, a total highest volumetric deposition of 0.11 $\pm$ 0.06 m^3/m^2 was observed after construction of the revetments. In addition, the lowest volumetric deposition of sediments was recorded in the second six months into the construction of the revetments at 0.03 $\pm$ 0.76 m^3/m^2. This indicates that after one year into the construction of the developed revetments, an equilibrium state was established at the site.

- Based on borelogs, the study site sits on a tick alluvial deposit consisting of silt, clay and sand. For both zone A and B, the average clay percentage at the lower elevation (LE) was higher than that observed in the higher elevation (HE) areas. Three months into the construction of the revetments, the average clay percentage at zone A for the LE areas was 12.14 $\pm$ 0.23 which was higher than that observed for zone A for the LE areas (3.78 $\pm$ 0.38). In addition, six month into the construction of the revetments the average clay percentage at zone B for the LE areas was 19.91 $\pm$ 0.12 which was higher than the clay percentage at the HE areas of zone B (5.65 $\pm$ 0.43). Also, in June 2015 the average clay percentage of the LE areas at zone A (11.54 $\pm$ 0.26) and at zone B (9.81 $\pm$ 0.15) was higher than that observed for the HE areas at zone A (7.62 $\pm$ 0.57 and zone B (5.46 $\pm$ 0.47), respectively. This is due to slower settling of clay particles at lower elevations compared to the sand and silt particles. For both zone A and B, the silt formed the highest percentage of near-surface soil (60-70%).

5.1.4 Rehabilitation of mangroves and planting of coastal flora species

- The mortality rate of the planted mangroves had a decreasing trend over time. Within zone A, for *Avicenna marina* species that were planted on the seaward of the rehabilitation area, the mortality dropped from 7% in late June 2014 (completed construction of the revetments) to 1.5% after four months into the construction of the revetments). For the same conditions, the mortality of *Avicenna alba* species decreased from 3% after construction of the revetments to 0.5% in four month into the construction of the revetments. In zone B, the mortality of *Avicenna marina* (84.5%) and *Sonneratia alba* (90.5%) was comparatively higher than other target species. This high mortality in zone B could be associated with the fact that zone B was not protected by the existing breakwater; thus, higher wave energy was imposed to the planted species, which increased the rate of their death.

- The rate of mangrove loss was higher for zone B compared to zone A. At zone B, *Sonneratia alba* species had the highest rate of mortality at 12%, following by 10.5% mortality rate recorded for *Avicenna marina* species. Both of these species were planted at the seaward of the rehabilitation site, which could be a reason for their high mortality rate. Meanwhile, for the same species at zone A, the mortality rate was 0.83% and 1% for *Sonneratia alba* and *Avicenna marina*, respectively.

- Based on the short-term field monitoring, the mangrove rehabilitation efforts were successful in establishing conductive conditions for the establishment of mangroves at the study site. The average monthly rate of the relative increment in height for the planted mangroves at both zones was on average 43 $\pm$ 3 mm per month. In addition, the average number of leaves that each seedlings at zones A and B could produce during the monitoring periods was 4 leaves per month.

- The mortality rate of the planted coastal flora species had a decreasing trend over time. Within zone A, for *Cynodon dactylon* (S1) species that were planted on the deck and the inclined surface of the revetments, the mortality of the species dropped from 1.84% in late June 2014 to 0.31% in late October 2014. For the same conditions, the mortality of *Ipomoea pes-caprae* (S2) species decreased from 2.12% in late June 2014 to 0.35% in late October 2014. In zone B, the mortality of S2 (6.58%) in June 2014 was comparatively higher than S1 (5.07%). In addition, the average observed mortality rate for both zones was higher in zone B (3.38%) compared to zone A (1.13%). For S2 species planted in zone B, a sudden increase of mortality rate (8.34%) was observed two months into the construction of the revetments. This high mortality of species in zone B might be associated with the fact that zone B was not protected by the existing breakwater; thus, higher wave energy was imposed to the planted species at the risk of decease.

5.2 Recommendations for future research works

This study presented a new model of integrated coastal rehabilitation program. The model can be implemented in other sites that face the similar ecosystem degradation problems. In the following several recommendations are made for future research works.

- Over the last two decades, there has been an on-going decrease in the elevation of mudflats along the coastlines of west peninsular Malaysia. The reflective effect of the dikes plays a role in erosion of mudflats. Therefore, it is necessary to carry out research works to understand why elevation of mudflats along the coastlines of the west peninsular Malaysia has been decreased. Perhaps, a study incorporating larger temporal and spatial variations of the mudflat geo-hydro-morphology of the area would provide a better picture of the problem.

- To enhance the findings of this study for fabrication of the LEco, it is recommended that the developed units are tested for resistance to shear loadings. This is because reinforcement in the design layouts of the units may experience saline water and can be subjected to rusting. In addition, it is suggested that a thicker concrete cover (approximately 2.5 inches) is used for fabrication of the units.

- Mangroves are vulnerable to erosion which weakens their root structures and supporting stratum. Future works are necessary to quantitatively investigate the resistance of mangroves to erosion.

- A useful research work would be to look into the impacts of revetment structures on the soft bottom assemblages of the mudflats. In this study, no attempt was made to investigate the possible changes that could be resulted after the construction of the revetments on the human activities at the mudflat (i.e., fishing, sea food collection). In this view, it would be a useful to look into the the effect of the structures on the surrounding environment where human intervention is observed.

REFERENCES

Abdullah, S. A., & Nakagoshi, N. (2007). Forest fragmentation and its correlation to human land use change in the state of selangor, peninsular malaysia. *Forest Ecology and Management*, *241*(1â“3), 39 - 48.

Adger, W. N., Hughes, T. P., Folke, C., Carpenter, S. R., & Rockstrim, J. (2005). Social-ecological resilience to coastal disasters. *Science*, *309*(5737), 1036-1039.

Affandi, N. A. M., Kamali, B., Mz, R., Tamin, N. M., & Hashim, R. (2010). Early growth and survival of avicennia alba seedlings under excessive sedimentation. *Scientific Research and Essays*, *5*(18), 2801–2805.

Ahrens, J. (2011). Dynamic revetments. *Coastal Engineering Proceedings*, *1*(22).

Alexander, K. S., Ryan, A., & Measham, T. G. (2012). Managed retreat of coastal communities: understanding responses to projected sea level rise. *Journal of Environmental Planning and Management*, *55*(4), 409-433.

Allan, J. C., & Komar, P. D. (2006, May). Climate controls on us west coast erosion processes. *Journal of Coastal Research*, 511–529.

Allen, J. (1998). Mangroves as alien species: the case of hawaii. *Global Ecology & Biogeography Letters*, *7*(1), 61–71.

Alongi, D. M. (2008). Mangrove forests: Resilience, protection from tsunamis, and responses to global climate change. *Estuarine, Coastal and Shelf Science*, *76*(1), 1 - 13.

Anderson, J., Wallace, D. J., Simms, A. R., Rodriguez, A. B., & Milliken, K. T. (2014). Variable response of coastal environments of the northwestern gulf of mexico to sea-level rise and climate change: Implications for future change. *Marine Geology*, *352*(0), 348 - 366. (50th Anniversary Special Issue)

Arterlia. (2014). Arterlia consultant. *Retrieved from http://www.it.arteliagroup.com.*

Aziz, I., & Khan, M. (2001). Experimental assessment of salinity tolerance of ceriops tagal seedlings and saplings from the indus delta, pakistan. *Aquatic Botany*, *70*(3), 259 - 268.

Baba, M. (2003). Geology quaternary at teluk datuk area, state of selangor (sheet 101). *Geology Quaternary Report, Department of Mineral and Geoscience Malaysia, Ministry of Natural Resources and Environment Malaysia*, 1–32.

Baharuddin, M. F. T., Ismail, Z., Othman, S. Z., Taib, S., & Hashim, R. (2013). Use of time-lapse resistivity tomography to determine freshwater lens morphology. *Measurement*, *46*(2), 964 - 975.

Balmford, A., Fisher, B., Green, R., Naidoo, R., Strassburg, B., Kerry Turner, R., & Rodrigues, A. (2011). Bringing ecosystem services into the real world: An operational framework for assessing the economic consequences of losing wild nature. *Environmental and Resource Economics*, *48*(2), 161-175.

Barbier, E. B. (2012). Progress and challenges in valuing coastal and marine ecosystem services. *Review of Environmental Economics and Policy*, *6*(1), 1-19.

Basco, D. (1985). A qualitative description of wave breaking. *Journal of Waterway, Port, Coastal, and Ocean Engineering*, *111*(2), 171-188.

Beger, M., Jones, G. P., & Munday, P. L. (2003). Conservation of coral reef biodiversity: a comparison of reserve selection procedures for corals and fishes. *Biological Conservation*, *111*(1), 53 - 62.

Bellwood, D. R., Hughes, T. P., Folke, C., & Nystrom, M. (2004). Confronting the coral reef crisis. *Nature*, *429*(6994), 827–833.

Bezuijen, A., Klein, M., & Breteler, B. (1987). *Design criteria for placed block revetments and granular filters* (Tech. Rep.). Amsterdam, Netherlands: TuDelft.

Blasco, F., Aizpuru, M., & Gers, C. (2001). Depletion of the mangroves of continental asia. *Wetlands Ecology and Management*, *9*(3), 255-266.

Boesch, D. F. (2006). Scientific requirements for ecosystem-based management in the restoration of chesapeake bay and coastal louisiana. *Ecological Engineering*, *26*(1), 6 - 26. (Advances in coastal habitat restoration in the northern Gulf of Mexico)

Borsje, B. W., van Wesenbeeck, B. K., Dekker, F., Paalvast, P., Bouma, T. J., van Katwijk, M. M., & de Vries, M. B. (2011). How ecological engineering can serve in coastal protection. *Ecological Engineering*, *37*(2), 113 - 122.

Bosire, J., Dahdouh-Guebas, F., Walton, M., Crona, B., III, R. L., Field, C., … Koedam, N. (2008). Functionality of restored mangroves: A review. *Aquatic Botany*, *89*(2), 251 - 259. (Mangrove Ecology â“ Applications in Forestry and Costal Zone Management)

Brander, L. M., Wagtendonk, A. J., Hussain, S. S., McVittie, A., Verburg, P. H., de Groot, R. S., & van der Ploeg, S. (2012). Ecosystem service values for mangroves in southeast asia: A meta-analysis and value transfer application. *Ecosystem Services*, *1*(1), 62 - 69.

Brinkman, A., Dankers, N., & van Stralen, M. (2002). An analysis of mussel bed habitats in the dutch wadden sea. *Helgoland Marine Research*, *56*(1), 59-75.

Broderick, L. (1983). Riprap stability a progress report. In *Coastal structuresâ™ 83* (pp. 320–330).

Bulleri, F., & Chapman, M. G. (2010). The introduction of coastal infrastructure as a driver of change in marine environments. *Journal of Applied Ecology*, *47*(1), 26–35.

Burcharth, H. F., Kramer, M., Lamberti, A., & Zanuttigh, B. (2006). Structural stability of detached low crested breakwaters. *Coastal Engineering*, *53*(4), 381 - 394.

Burt, J., Bartholomew, A., Usseglio, P., Bauman, A., & Sale, P. (2009). Are artificial reefs surrogates of natural habitats for corals and fish in dubai, united arab emirates? *Coral Reefs*, *28*(3), 663-675.

Cahoon, D. (2006). A review of major storm impacts on coastal wetland elevations. *Estuaries and Coasts*, *29*(6), 889-898.

Cardinale, B. J., Duffy, J. E., Gonzalez, A., Hooper, D. U., Perrings, C., Venail, P., ... Naeem, S. (2012, June). Biodiversity loss and its impact on humanity. *Nature*, *486*(7401), 59–67.

Carstea, D. (1975). *Guidelines for the environmental impact assessment of small structures and related activities in coastal bodies of water*. Mitre Corporation.

Cayan, D., Bromirski, P., Hayhoe, K., Tyree, M., Dettinger, M., & Flick, R. (2008). Climate change projections of sea level extremes along the california coast. *Climatic Change*, *87*(1), 57-73.

Cazenave, A., & Llovel, W. (2010). Contemporary sea level rise. *Annual Review of Marine Science*, *2*(1), 145-173. (PMID: 21141661)

CEM. (2002). *Coastal engineering manual. engineer manual 1110-2-1100*. Washington, D.C: U.S. Army Corps of Engineers.

Chambers, D. P., Merrifield, M. A., & Nerem, R. S. (2012). Is there a 60-year oscillation in global mean sea level? *Geophysical Research Letters*, *39*(18), n/a–n/a.

Church, J., & White, N. (2011). Sea-level rise from the late 19th to the early 21st century. *Surveys in Geophysics*, *32*(4-5), 585-602.

Clemens, S. (2006). Toxic metal accumulation, responses to exposure and mechanisms of tolerance in plants. *Biochimie*, *88*(11), 1707 - 1719. (Facets of Environmental Nuclear Toxicology)

Costanza, R. (2012). Ecosystem health and ecological engineering. *Ecological Engineering*, *45*(0), 24 - 29. (Ecological Engineering–Its Development, Applications and Challenges)

Coverdale, T., Bertness, M., & Altieri, A. (2013). Regional ontogeny of new england salt marsh die-off. *Conservation Biology*, *27*(5), 1041–1048.

Danel, P. (2000). Tetrapods. *Coastal Engineering Proceedings*, *1*(4).

Davis, R., & Hayes, M. (1984). What is a wave-dominated coast? *Marine Geology*, *60*(1â“4), 313 - 329. (Hydrodynamics and Sedimentation in Wave-Dominated Coastal Environments)

Dawson, R., Dickson, M., Nicholls, R., Hall, J., Walkden, M., Stansby, P., ... Watkinson, A. (2009). Integrated analysis of risks of coastal flooding and cliff erosion under scenarios of long term change. *Climatic Change*, *95*(1-2), 249-288.

Day, J. W., Boesch, D. F., Clairain, E. J., Kemp, G. P., Laska, S. B., Mitsch, W. J., … Whigham, D. F. (2007). Restoration of the mississippi delta: Lessons from hurricanes katrina and rita. *Science*, *315*(5819), 1679-1684.

der Meer, V. (1987). Stability of breakwater armour layers: design formulae. *Coastal Engineering*, *11*(3), 219 - 239.

de Waal, J., & van der Meer, J. (2011). Wave runup and overtopping on coastal structures. *Coastal Engineering Proceedings*, *1*(23).

D'Hondt, S., Rutherford, S., & Spivack, A. J. (2002). Metabolic activity of subsurface life in deep-sea sediments. *Science*, *295*(5562), 2067-2070.

DID. (2010). *Did manual - chapter 6: Geotechnical manual, site investigation and survey, chapter 7: Engineering modelling, chapter 9: Dam safety, inspections and monitoring.*

DMC. (2014). Delta marine consultants. *Retrieved from http://www.dmc.nl/*.

Du, Y., Pan, S., & Chen, Y. (2010). Modelling the effect of wave overtopping on nearshore hydrodynamics and morphodynamics around shore-parallel breakwaters. *Coastal Engineering*, *57*(9), 812 - 826.

Duarte, C., Geertz-Hansen, O., Thampanya, U., Terrados, J., Fortes, M. D., Kamp-Nielsen, L., … Boromthanarath, S. (1998). Relationship between sediment conditions and mangrove rhizophora apiculata seedling growth and nutrient status. *Mar Ecol Prog Ser*, *175*, 277–283.

Duarte, C., Hendriks, I., Moore, T., Olsen, Y., Steckbauer, A., Ramajo, L., … McCulloch, M. (2013). Is ocean acidification an open-ocean syndrome? understanding anthropogenic impacts on seawater ph. *Estuaries and Coasts*, *36*(2), 221-236.

Duke, N. C., Pinzan M., Z. S., & Prada T., M. C. (1997). Large-scale damage to mangrove forests following two large oil spills in panama1. *Biotropica*, *29*(1), 2–14.

Ellison, A. (2000). Mangrove restoration: Do we know enough? *Restoration Ecology*, *8*(3), 219–229.

Emanuel, K. (2005). Increasing destructiveness of tropical cyclones over the past 30 years. *Nature*, *436*(7051), 686–688.

Erlandson, J. M. (2008). Racing a rising tide: Global warming, rising seas, and the erosion of human history. *The Journal of Island and Coastal Archaeology*, *3*(2), 167-169.

Escarameia, M. (1998). *River and channel revetments: a design manual*. Thomas Telford.

FAO. (2007). *The worlds mangroves 1980-2005.* FAO Rome, Italy.

Feagin, R. A., Mukherjee, N., Shanker, K., Baird, A. H., Cinner, J., Kerr, A. M., ... Dahdouh-Guebas, F. (2010). Shelter from the storm? use and misuse of coastal vegetation bioshields for managing natural disasters. *Conservation Letters*, *3*(1), 1–11.

Field, C. (1999a). Mangrove rehabilitation: choice and necessity. In R. Dodd (Ed.), *Diversity and function in mangrove ecosystems* (Vol. 145, p. 47-52). Springer Netherlands.

Field, C. (1999b). Rehabilitation of mangrove ecosystems: An overview. *Marine Pollution Bulletin*, *37*(8â“12), 383 - 392.

Firth, L., Thompson, R., Bohn, K., Abbiati, M., Airoldi, L., Bouma, T., ... Hawkins, S. (2014). Between a rock and a hard place: Environmental and engineering considerations when designing coastal defence structures. *Coastal Engineering*, *87*(0), 122 - 135. (Coasts@Risks: THESEUS, a new wave in coastal protection)

FitzGerald, D. M., Fenster, M. S., Argow, B. A., & Buynevich, I. V. (2008). Coastal impacts due to sea-level rise. *Annual Review of Earth and Planetary Sciences*, *36*(1), 601-647.

Gedan, K., Kirwan, M., Wolanski, E., Barbier, E., & Silliman, B. (2011). The present and future role of coastal wetland vegetation in protecting shorelines: answering recent challenges to the paradigm. *Climatic Change*, *106*(1), 7-29.

Ghazali, N. H. M. (2006). Coastal erosion and reclamation in malaysia. *Aquatic Ecosystem Health & Management*, *9*(2), 237-247.

Giri, C., Long, J., Abbas, S., Murali, R., Qamer, F. M., Pengra, B., & Thau, D. (2014). Distribution and dynamics of mangrove forests of south asia. *Journal of Environmental Management*, *148*(2014).

Giri, C., Ochieng, E., Tieszen, L. L., Zhu, Z., Singh, A., Loveland, T., ... Duke, N. (2011). Status and distribution of mangrove forests of the world using earth observation satellite data. *Global Ecology and Biogeography*, *20*(1), 154–159.

Goda, Y. (2011). On the methodology of selecting design wave heighst. *Coastal Engineering Proceedings*, *1*(21).

Gong, W.-K., & Ong, J.-E. (1990). Plant biomass and nutrient flux in a managed mangrove forest in malaysia. *Estuarine, Coastal and Shelf Science*, *31*(5), 519 - 530. (Mangrove Oceanography)

Graham, N., Nash, K., & Kool, J. (2011). Coral reef recovery dynamics in a changing world. *Coral Reefs*, *30*(2), 283-294.

Grinsted, A., Moore, J., & Jevrejeva, S. (2010). Reconstructing sea level from paleo and projected temperatures 200 to 2100 ad. *Climate Dynamics*, *34*(4), 461-472.

Hashim, A. M., & Catherine, S. M. P. (2013). A laboratory study on wave reduction by mangrove forests. *Procedia*, *5*(0), 27 - 32. (4th International Conference on

Environmental Science and Development- {ICESD} 2013)

Hashim, R., Kamali, B., Tamin, N. M., & Zakaria, R. (2010). An integrated approach to coastal rehabilitation: Mangrove restoration in sungai haji dorani, malaysia. *Estuarine, Coastal and Shelf Science*, *86*(1), 118 - 124.

Hastings, A., Byers, J. E., Crooks, J. A., Cuddington, K., Jones, C. G., Lambrinos, J. G., … Wilson, W. G. (2007). Ecosystem engineering in space and time. *Ecology Letters*, *10*(2), 153–164.

Hazarika, H., Kasama, K., Suetsugu, D., Kataoka, S., & Yasufuku, N. (2013). Damage to geotechnical structures in waterfront areas of northern tohoku due to the march 11, 2011 tsunami disaster. *Indian Geotechnical Journal*, *43*(2), 137-152.

Hedar, P. (1986). Armor layer stability of rubble-mound breakwaters. *Journal of Waterway, Port, Coastal, and Ocean Engineering*, *112*(3), 343-350.

Heinimann, H. R. (2010). A concept in adaptive ecosystem management :an engineering perspective. *Forest Ecology and Management*, *259*(4), 848 - 856.

Heller, V. (2011). Scale effects in physical hydraulic engineering models. *Journal of Hydraulic Research*, *49*(3), 293-306.

Hemer, M. A., Fan, Y., Mori, N., Semedo, A., & Wang, X. L. (2013). Projected changes in wave climate from a multi-model ensemble. *Nature Clim. Change*, *3*(5), 471–476.

Hertweck, G., & Liebezeit, G. (2002). Historic mussel beds (mytilus edulis) in the sedimentary record of a back-barrier tidal flat near spiekeroog island, southern north sea. *Helgoland Marine Research*, *56*(1), 51-58.

Hieu, P. D., Vinh, P. N., Toan, D. V., & Son, N. T. (2014). Study of wave-wind interaction at a seawall using a numerical wave channel. *Applied Mathematical Modelling*, *38*(21-22), 5149 - 5159.

Hobbs, R. J., & Norton, D. A. (1996). Towards a conceptual framework for restoration ecology. *Restoration Ecology*, *4*(2), 93–110.

Hoegh-Guldberg, O., Mumby, P. J., Hooten, A. J., Steneck, R. S., Greenfield, P., Gomez, E., … Hatziolos, M. E. (2007). Coral reefs under rapid climate change and ocean acidification. *Science*, *318*(5857), 1737-1742.

Hopkins, W. G., & Huner, N. P. (1995). *Introduction to plant physiology* (Vol. 355). Wiley New York.

Horstman, E., Dohmen-Janssen, C., Narra, P., van den Berg, N., Siemerink, M., & Hulscher, S. (2014). Wave attenuation in mangroves: A quantitative approach to field observations. *Coastal Engineering*, *94*(0), 47 - 62.

Houston, J. R., & Dean, R. G. (2011, February). Sea-level acceleration based on u.s. tide gauges and extensions of previous global-gauge analyses. *Journal of Coastal Research*, 409–417.

Hsieh, H.-L., Chen, C.-P., & Lin, Y.-Y. (2004). Strategic planning for a wetlands conservation greenway along the west coast of taiwan. *Ocean & Coastal Management*, *47*(56), 257 - 272.

Hudson, R. Y. (1959). Laboratory investigation of rubble-mound breakwaters. In *Proc. asce* (Vol. 85, pp. 93–121).

Hughes, S. A., & Borgman, L. E. (1987). Beta-rayleigh distribution for shallow water wave heights. In *Coastal hydrodynamics* (pp. 17–31).

Huthnance, J. M. (1995). Circulation, exchange and water masses at the ocean margin: the role of physical processes at the shelf edge. *Progress in Oceanography*, *35*(4), 353 - 431.

IPCC. (1990). *Climate change 1990: the ipcc scientific assessment (prepared by houghton, jt and jenkins, gj and ephraums, jj).* Cambridge University Press, Cambridge.

IPCC. (1996). *Climate change 1995: the science of climate change. contribution of working group i to the second assessment of the intergovernmental panel on climate change (prepared by: Houghton, john t and meira filho, lg and callender, ba and harris, neil and kattenberg, a and maskell, kathy).* Cambridge University Press Cambridge, United Kingdom.

IPCC. (2001). *Climate change 2001: the scientific basis (prepared by houghton, john theodore and ding, ydjg and griggs, david j and noguer, maria and van der linden, paul j and dai, xiaosu and maskell, kathy and johnson, ca)* (Vol. 881). Cambridge university press Cambridge.

IPCC. (2007). *Intergovernmental panel on climate change, climate change 2007: The physical science basis. contribution of working group i to the fourth assessment report of the intergovernmental panel on climate change (prepared by solomon, susan and qin, dahe and manning, martin and chen, z and marquis, m and averyt, kb and tignor, m and miller, h).* Cambridge University Press, Cambridge.

IPCC. (2013). Climate change 2013: The physical science basis (prepared by stocker, thomas f and qin, dahe and plattner, gian-kasper and tignor, m and allen, simon k and boschung, judith and nauels, alexander and xia, yu and bex, vincent and midgley, pauline m). *Intergovernmental Panel on Climate Change, Working Group I Contribution to the IPCC Fifth Assessment Report (AR5)(Cambridge Univ Press, New York)*.

Iribarren Cavanilles, R. (1938). A formula for the calculation of rock fill dikes. *Revista de Obras Publicas*.

Jacob, T., Wahr, J., Pfeffer, W. T., & Swenson, S. (2012, February). Recent contributions of glaciers and ice caps to sea level rise. *Nature*, *482*(7386), 514–518.

Jing, Y., He, Z., & Yang, X. (2007). Effects of ph, organic acids, and competitive cations on mercury desorption in soils. *Chemosphere*, *69*(10), 1662 - 1669.

Kabat, P., Fresco, L. O., Stive, M. J. F., Veerman, C. P., van Alphen, J. S. L. J., Parmet, B. W. A. H., … Katsman, C. A. (2009, July). Dutch coasts in transition. *Nature Geosci*, *2*(7), 450–452.

Kamali, B., & Hashim, R. (2011). Mangrove restoration without planting. *Ecological Engineering*, *37*(2), 387 - 391.

Kamaludin, H., Nakamura, T., Price, D. M., Woodroffe, C. D., & Fujii, S. (1993). Radiocarbon and thermoluminescence dating of the old alluvium from a coastal site in perak, malaysia. *Sedimentary Geology*, *83*(3 - 4), 199 - 210.

Kamphuis, W. (2010). *Introduction to coastal engineering and management* (Vol. 30). World Scientific.

Kana, T., Al-Sarawi, M., & Holland, M. (2011). Design and performance of artificial beaches for the kuwait waterfront project. *Coastal Engineering Proceedings*, *1*(20).

Kathiresan, K., & Rajendran, N. (2005). Coastal mangrove forests mitigated tsunami. *Estuarine, Coastal and Shelf Science*, *65*(3), 601 - 606.

Kearney, P. G., & Kobayashi, N. (2000). Time-averaged probabilistic model for irregular wave runup on coastal structures. In *Coastal engineering 2000* (p. 2004-2017).

Kelly, P., & Adger, W. (2000). Theory and practice in assessing vulnerability to climate change andfacilitating adaptation. *Climatic Change*, *47*(4), 325-352.

Kemp, A. C., Horton, B. P., Donnelly, J. P., Mann, M. E., Vermeer, M., & Rahmstorf, S. (2011). Climate related sea-level variations over the past two millennia. *Proceedings of the National Academy of Sciences*, *108*(27), 11017-11022.

Kirshen, P., Watson, C., Douglas, E., Gontz, A., Lee, J., & Tian, Y. (2008). Coastal flooding in the northeastern united states due to climate change. *Mitigation and Adaptation Strategies for Global Change*, *13*(5-6), 437-451.

Kobayashi, N., & Jacobs, B. (1985). Riprap stability under wave action. *Journal of Waterway, Port, Coastal, and Ocean Engineering*, *111*(3), 552-566.

Koc, M. L., & Balas, C. E. (2012). Genetic algorithms based logic-driven fuzzy neural networks for stability assessment of rubble-mound breakwaters. *Applied Ocean Research*, *37*(0), 211 - 219.

Koev, K. (1992). Statistical analysis of formulas for breakwater armor layer design. *Journal of Waterway, Port, Coastal, and Ocean Engineering*, *118*(2), 213-219.

Koraim, A., Heikal, E., & Zaid, A. A. (2014). Hydrodynamic characteristics of porous seawall protected by submerged breakwater. *Applied Ocean Research*, *46*(0), 1 - 14.

Krauss, K., Lovelock, C., McKee, K., Lapez-Hoffman, L., Ewe, S., & Sousa, W. (2008). Environmental drivers in mangrove establishment and early development: A review. *Aquatic Botany*, *89*(2), 105 - 127.

Lange, H. D., Sala, S., Vighi, M., & Faber, J. (2010). Ecological vulnerability in risk assessment â" a review and perspectives. *Science of The Total Environment*, *408*(18), 3871 - 3879.

Leatherman, S. P., Zhang, K., & Douglas, B. C. (2000). Sea level rise shown to drive coastal erosion. *Eos, Transactions American Geophysical Union*, *81*(6), 55–57.

Lee, S. Y., Primavera, J. H., Dahdouh-Guebas, F., McKee, K., Bosire, J. O., Cannicci, S., ... Record, S. (2014). Ecological role and services of tropical mangrove ecosystems: a reassessment. *Global Ecology and Biogeography*, *23*(7), 726–743.

Lewandowsky, S., Risbey, J., Smithson, M., Newell, B., & Hunter, J. (2014). Scientific uncertainty and climate change: Part i. uncertainty and unabated emissions. *Climatic Change*, *124*(1-2), 21-37.

Lewis, R. (2009). Methods and criteria for successful mangrove forest restoration. *Coastal Wetlands: An Integrated Ecosystem Approach. Amsterdam: Elsevier*, 787–800.

Lewis III, R. (2000). Ecologically based goal setting in mangrove forest and tidal marsh restoration. *Ecological Engineering*, *15*(3-4), 191 - 198.

Lewis III, R. (2005). Ecological engineering for successful management and restoration of mangrove forests. *Ecological Engineering*, *24*(4), 403 - 418. (Wetland creation)

Lima, F. P., & Wethey, D. S. (2012). Three decades of high-resolution coastal sea surface temperatures reveal more than warming. *Nat Commun*, *3*, 704.

Lindahl, O., Hart, R., Hernroth, B., Kollberg, S., Loo, L.-O., Olrog, L., ... Syversen, U. (2005, March). Improving marine water quality by mussel farming: A profitable solution for swedish society. *AMBIO: A Journal of the Human Environment*, *34*(2), 131–138.

Losada, M., Desire, J., & Alejo, L. (1986). Stability of blocks as breakwater armor units. *Journal of Structural Engineering*, *112*(11), 2392-2401.

Lotze, H. K., Lenihan, H. S., Bourque, B. J., Bradbury, R. H., Cooke, R. G., Kay, M. C., ... Jackson, J. B. C. (2006). Depletion, degradation, and recovery potential of estuaries and coastal seas. *Science*, *312*(5781), 1806-1809.

Macnae, W. (1969). A general account of the fauna and flora of mangrove swamps and forests in the indo-west-pacific region. In F. S. Russell & M. Yonge (Eds.), (Vol. 6, p. 73 - 270). Academic Press.

Martin, D., Bertasi, F., Colangelo, M. A., de Vries, M., Frost, M., Hawkins, S. J., ... Ceccherelli, V. U. (2005). Ecological impact of coastal defence structures on sediment and mobile fauna: Evaluating and forecasting consequences of unavoidable modifications of native habitats. *Coastal Engineering*, *52*(1011), 1027 - 1051. (Low Crested Structures and the Environment)

Mase, H., Kimura, Y., Yamakawa, Y., Yasuda, T., Mori, N., & Cox, D. (2013, March). Were coastal defensive structures completely broken by an unexpectedly large tsunami? a field survey. *Earthquake Spectra*, *29*(S1), S145–S160.

McKee, K., Rogers, K., & Saintilan, N. (2012). Response of salt marsh and mangrove wetlands to changes in atmospheric co2, climate, and sea level. In B. A. Middleton (Ed.), *Global change and the function and distribution of wetlands* (Vol. 1, p. 63-96). Springer Netherlands.

McLeod, E., Moffitt, R., Timmermann, A., Salm, R., Menviel, L., Palmer, M. J., ... Bruno, J. F. (2010). Warming seas in the coral triangle: Coral reef vulnerability and management implications. *Coastal Management*, *38*(5), 518-539.

Melby, J. (1999). *Damage progression on rubble-mound breakwaters* (Tech. Rep.). DTIC Document.

Menandez, M., M.ndez, & Woodworth, P. L. (2010). Changes in extreme high water levels based on a quasi-global tide-gauge data set. *Journal of Geophysical Research: Oceans*, *115*(C10), n/a–n/a.

Meyer, J., Kelley, B. C., & Vignais, P. M. (1978). Nitrogen fixation and hydrogen metabolism in photosynthetic bacteria. *Biochimie*, *60*(3), 245 - 260.

Meyerhof, G. (1956). Penetration tests and bearing capacity of cohesionless soils. *Journal of the Soil Mechanics and Foundations Division*, *82*(1), 1–19.

Mitsch, W. J. (2012). What is ecological engineering? *Ecological Engineering*, *45*(0), 5 - 12. (Ecological Engineering–Its Development, Applications and Challenges)

Montagne, A., Naim, O., Tourrand, C., Pierson, B., & Menier, D. (2013). Status of coral reef communities on two carbonate platforms (tun sakaran marine park, east sabah, malaysia). *Journal of Ecosystems*, *2013*, 15.

Motamedi, S., Hashim, R., Zakaria, R., Song, K.-I., & Sofawi, B. (2014). Long-term assessment of an innovative mangrove rehabilitation project: Case study on carey island, malaysia. *The Scientific World Journal*, *2014*, 12.

Motamedi, S., Roy, C., Shamshirband, S., Hashim, R., Petković, D., & Song, K.-I. (2015). Prediction of ultrasonic pulse velocity for enhanced peat bricks using adaptive neuro-fuzzy methodology. *Ultrasonics*, *61*, 103-113.

Motamedi, S., Shamshirband, S., Hashim, R., Petkovic, D., & Roy, C. (2015). Estimating unconfined compressive strength of cockle shell-cement-sand mixtures using soft computing methodologies. *Engineering Structures*, *98*, 49-58.

Motamedi, S., Shamshirband, S., Petkovic, D., & Hashim, R. (2015). Application of adaptive neuro-fuzzy technique to predict the unconfined compressive strength of pfa-sand-cement mixture. *Powder Technology*, *278*, 278-285.

Motamedi, S., Song, K.-I., & Hashim, R. (2015). Prediction of unconfined compressive strength of pulverized fuel ash-cement-sand mixture. *Materials and Structures*, *48*(4), 1061-1073.

Muzathik, A., Nik, W. W., Samo, K., & Ibrahim, M. (2011). Ocean wave measurements and wave climate prediction of peninsular malaysia. *J. Phys. Sci*, *22*(1), 77–92.

MWLA. (2003). *Dike design and construction guide (best management practices for british columbia).*

Nawawi, M., Harith, Z., Ayub, M., Ibrahim, A., & Alphonse, A. (2001). Modeling of an undergroundwater aquifer using 2-d electrical imaging technique in brooklands plantation, selangor, malaysia. In *Proceedings of the second international symposium on geophysics, egypt* (pp. 293–297).

Nicholls, R. J. (2004). Coastal flooding and wetland loss in the 21st century: changes under the sres climate and socio-economic scenarios. *Global Environmental Change*, *14*(1), 69 - 86.

Nicholls, R. J., Marinova, N., Lowe, J. A., Brown, S., Vellinga, P., de Gusmao, D., ... Tol, R. S. J. (2011). Sea-level rise and its possible impacts given a 'beyond 4c world' in the twenty-first century. *Philosophical Transactions of the Royal Society A: Mathematical, Physical and Engineering Sciences*, *369*(1934), 161-181.

Odum, H. T. (1962). Man in the ecosystem in: Proceedings of lockwood conference on the suburban forest and ecology. *Bulletin of the Connecticut Agricultural Station*, *652*, 75-75.

Odum, H. T., & Odum, B. (2003). Concepts and methods of ecological engineering. *Ecological Engineering*, *20*(5), 339 - 361.

Office, G. E. (2000). Guide to site investigation (2nd ed.) [Computer software manual]. Geotechnical Engineering Office, Civil Engineering Department, Civil Engineering Building, 101 Princess Margaret Road, Homantin, Kowloon, Hong Kong..

Olsen, S. B. (2003). Frameworks and indicators for assessing progress in integrated coastal management initiatives. *Ocean & Coastal Management*, *46*(34), 347 - 361.

Oreiro, F. A., D'Onofrio, E., Grismeyer, W., Fiore, M., & Saraceno, M. (2014, March). Comparison of tide model outputs for the northern region of the antarctic peninsula using satellite altimeters and tide gauge data. *Polar Science*, *8*(1), 10–23.

Otero, X., Ferreira, T., Huerta-Daaz, M., Partiti, C., Jr., V. S., Vidal-Torrado, P., & Macaas, F. (2009). Geochemistry of iron and manganese in soils and sediments of a mangrove system, island of pai matos (cananeia sp, brazil). *Geoderma*, *148*(3-4), 318 - 335.

Othman, M. (1994). Value of mangroves in coastal protection. In A. Sasekumar, N. Marshall, & D. Macintosh (Eds.), *Ecology and conservation of southeast asian marine and freshwater environments including wetlands* (Vol. 98, p. 277-282). Springer Netherlands.

Palmer, M. A., Ambrose, R. F., & Poff, N. L. (1997). Ecological theory and community restoration ecology. *Restoration Ecology*, *5*(4), 291–300.

Parmesan, C., & Yohe, G. (2003, January). A globally coherent fingerprint of climate change impacts across natural systems. *Nature*, *421*(6918), 37–42.

Pethick, J. (2001). Coastal management and sea-level rise. *CATENA*, *42*(2 - 4), 307–322.

Phillips, M., & Jones, A. (2006). Erosion and tourism infrastructure in the coastal zone: Problems, consequences and management. *Tourism Management*, *27*(3), 517 - 524.

PIANC. (1987). *Guidelines for the design and construction of flexible revetments incorporating geotextiles for inland waterways: Report of working group 4 of the permanent technical committee i.* Permanent International Association of Navigation Congresses. Permanent Technical Committee I. Working Group 4.

Pilarczyk, K. (1998). *Dikes and revetments: design, maintenance and safety assessment*. CRC Press.

Pilarczyk, K. (2011). Design aspects of block revetment. *Coastal Engineering Proceedings*, *1*(21).

Pirazolli, P. A. (2000). Surges, atmospheric pressure and wind change and flooding probability on the atlantic coast of france. *Oceanologica Acta*, *23*(6), 643 - 661.

Piwowarczyk, J., Kronenberg, J., & Dereniowska, M. A. (2013). Marine ecosystem services in urban areas: Do the strategic documents of polish coastal municipalities reflect their importance? *Landscape and Urban Planning*, *109*(1), 85 - 93. (Special Issue: Urban Ecosystem Services)

Polidoro, B. A., Carpenter, K. E., Collins, L., Duke, N. C., Ellison, A. M., Ellison, J. C., ... Yong, J. W. H. (2010, 04). The loss of species: Mangrove extinction risk and geographic areas of global concern. *PLoS ONE*, *5*(4), e10095.

Primavera, J., & Esteban, J. (2008). A review of mangrove rehabilitation in the philippines: successes, failures and future prospects. *Wetlands Ecology and Management*, *16*(5), 345-358.

Rashid, T. (2014). Global sea-level changes scenarios during the holocene. In *Holocene sea-level scenarios in bangladesh* (p. 35-50). Springer Singapore.

Reddy, R., & DeLaune, R. (2008). *Biogeochemistry of wetlands: science and applications*. CRC press.

Reeve, D., Chadwick, A., & Fleming, C. (2004). *Coastal engineering: processes, theory and design practice*. CRC Press.

Reichman, O., & Seabloom, E. W. (2002). The role of pocket gophers as subterranean ecosystem engineers. *Trends in Ecology & Evolution*, *17*(1), 44–49.

Reise, K. (2002). Sediment mediated species interactions in coastal waters. *Journal of Sea Research*, *48*(2), 127 - 141. (Structuring Factors of Shallow Marine Coastal Communities, Part I)

Riley, R., & Kent, C. (1999). Riley encased methodology: principles and processes of mangrove habitat creation and restoration. *Mangroves and Salt Marshes*, *3*(4), 207-213.

Rosenzweig, C., Karoly, D., Vicarelli, M., Neofotis, P., Wu, Q., Casassa, G., … Imeson, A. (2008, May). Attributing physical and biological impacts to anthropogenic climate change. *Nature*, *453*(7193), 353–357.

Rozainah, Z., Redzwan, G., & Wati, H. (2008). Diversity of mangrove plants of carey island. In *Paper presented ar the proceeding of the conference biodiversity and national development: Achievements, opportunities and challenges.*

Sakho, I., Mesnage, V., Deloffre, J., Lafite, R., Niang, I., & Faye, G. (2011). The influence of natural and anthropogenic factors on mangrove dynamics over 60 years: The somone estuary, senegal. *Estuarine, Coastal and Shelf Science*, *94*(1), 93 - 101.

Sanford, M. P. (2009, January). Valuating mangrove ecosystems as coastal protection in post-tsunami south asia. *Natural Areas Journal*, *29*(1), 91–95.

Sanyal, P. (1998). Rehabilitation of degraded mangrove forests of the sunderbans of india. In *Program of the international workshop on rehabilitation of degraded coastal systems, phuket marine biological center* (pp. 19–24).

Saraswathy, R., Rozainah, M., & Redzwan, G. (2009). Diversity and biomass estimation of mangrove trees on carey island, malaysia. *Ecology, Environment and Conservation*, *15*(2), 205–211.

Schmitt, K., Albers, T., Pham, T., & Dinh, S. (2013). Site-specific and integrated adaptation to climate change in the coastal mangrove zone of soc trang province, viet nam. *Journal of Coastal Conservation*, *17*(3), 545-558.

Schutrumpf, H., & Oumeraci, H. (2005). Layer thicknesses and velocities of wave overtopping flow at seadikes. *Coastal Engineering*, *52*(6), 473 - 495.

Seddon, P. J. (2010). From reintroduction to assisted colonization: Moving along the conservation translocation spectrum. *Restoration Ecology*, *18*(6), 796–802.

Sharifahmadian, A., & Simons, R. R. (2014). A 3d numerical model of nearshore wave field behind submerged breakwaters. *Coastal Engineering*, *83*(0), 190 - 204.

Sheaves, M., Brookes, J., Coles, R., Freckelton, M., Groves, P., Johnston, R., & Winberg, P. (2014). Repair and revitalisation of australias tropical estuaries and coastal wetlands: Opportunities and constraints for the reinstatement of lost function and productivity. *Marine Policy*, *47*(0), 23 - 38.

Short, F. T., Coles, R., Fortes, M. D., Victor, S., Salik, M., Isnain, I., … Seno, A. (2014). Monitoring in the western pacific region shows evidence of seagrass decline in line with global trends. *Marine Pollution Bulletin*, *83*(2), 408 - 416. (Seagrass meadows in a globally changing environment)

Short, F. T., Polidoro, B., Livingstone, S. R., Carpenter, K. E., Bandeira, S., Bujang, J. S.,

… Zieman, J. C. (2011). Extinction risk assessment of the worlds seagrass species. *Biological Conservation*, *144*(7), 1961 - 1971.

Siddall, M., Stocker, T. F., & Clark, P. U. (2010, March). Retraction: Constraints on future sea-level rise from past sea-level change. *Nature Geosci*, *3*(3), 217–217.

Small, C., & Nicholls, R. J. (2003). A global analysis of human settlement in coastal zones. *Journal of Coastal Research*, *19*(3), 584-599.

Snedaker, S. (1982). Mangrove species zonation: why? In D. Sen & K. Rajpurohit (Eds.), *Contributions to the ecology of halophytes* (Vol. 2, p. 111-125). Springer Netherlands.

Snedaker, S. (1984). The mangroves of asia and oceania: status and research planning. In *Proceedings of the asian symposium on mangrove environment: Research and management. percetakan ardyas, kuala lumpur, malaysia* (pp. 5–15).

Spalding, M. D., Fox, H. E., Allen, G. R., Davidson, N., Ferdaza, Z. A., Finlayson, M., … Robertson, J. (2007). Marine ecoregions of the world: A bioregionalization of coastal and shelf areas. *BioScience*, *57*(7), 573-583.

SPM. (1984). *Shore protection manual*. US Army Corps of Engineers.

Stive, M. (2004). How important is global warming for coastal erosion? *Climatic Change*, *64*(1-2), 27-39.

Stokes, A., Barot, S., Lata, J.-C., Lacroix, G., Jones, C. G., & Mitsch, W. J. (2012). Ecological engineering: From concepts to applications. *Ecological Engineering*, *45*(0), 1 - 4.

Sun, Z., Mou, X., Lin, G., Wang, L., Song, H., & Jiang, H. (2010). Effects of sediment burial disturbance on seedling survival and growth of suaeda salsa in the tidal wetland of the yellow river estuary. *Plant and Soil*, *337*(1-2), 457-468.

Suntharalingam, T., & Teoh, L. (1985). Quaternary geology of the coastal plains of taiping. *Quaternary Geology Report. Geological Survey Malaysia. Ministry of Primary Industries Malaysia*.

Tajul Baharuddin, M., Othman, A., Taib, S., Hashim, R., Zainal Abidin, M., & Radzuan, M. (2013). Evaluating freshwater lens morphology affected by seawater intrusion using chemistry-resistivity integrated technique: a case study of two different land covers in carey island, malaysia. *Environmental Earth Sciences*, *69*(8), 2779-2797.

Tajul Baharuddin, M., Taib, S., Hashim, R., Abidin, M., & Rahman, N. (2013). Assessment of seawater intrusion to the agricultural sustainability at the coastal area of carey island, selangor, malaysia. *Arabian Journal of Geosciences*, *6*(10), 3909-3928.

Tamin, N. M., Zakaria, R., Hashim, R., & Yin, Y. (2011). Establishment of avicennia marina mangroves on accreting coastline at sungai haji dorani, selangor, malaysia. *Estuarine, Coastal and Shelf Science*, *94*(4), 334 - 342.

Taylor, P. K., & Yelland, M. J. (2001, February). The dependence of sea surface roughness on the height and steepness of the waves. *J. Phys. Oceanogr.*, *31*(2), 572–590.

Temmerman, S., Meire, P., Bouma, T. J., Herman, P. M. J., Ysebaert, T., & De Vriend, H. J. (2013, December). Ecosystem-based coastal defence in the face of global change. *Nature*, *504*(7478), 79–83.

Tuan, T. Q., & Oumeraci, H. (2010). A numerical model of wave overtopping on seadikes. *Coastal Engineering*, *57*(8), 757 - 772.

Turner, R., & Lewis, I., R.R. (1996). Hydrologic restoration of coastal wetlands. *Wetlands Ecology and Management*, *4*(2), 65-72.

Unsworth, R. K., & Cullen, L. C. (2010). Recognising the necessity for indo-pacific seagrass conservation. *Conservation Letters*, *3*(2), 63–73.

USBR. (2014a, January). *Embankment dams (chapter 4: Static stability analysis).*

USBR. (2014b, January). *Embankment dams (chapter 8: Seepage).*

Valiela, I., Bowen, J. L., & York, J. K. (2001). Mangrove forests: One of the world's threatened major tropical environments: At least 35decades, losses that exceed those for tropical rain forests and coral reefs, two other well-known threatened environments. *BioScience*, *51*(10), 807-815.

van den Hoek, R., Brugnach, M., & Hoekstra, A. (2012). Shifting to ecological engineering in flood management: Introducing new uncertainties in the development of a building with nature pilot project. *Environmental Science & Policy*, *22*(0), 85 - 99.

Van der Meer, J. (1988). Deterministic and probabilistic design of breakwater armor layers. *Journal of Waterway, Port, Coastal, and Ocean Engineering*, *114*(1), 66-80.

Van der Meer, J. (1999). Design of concrete armour layers. In *Proceedings of the coastal structures* (Vol. 99, pp. 213–221).

Van der Meer, J. W. (1988). Rock slopes and gravel beaches under wave attack.

van Maren, D., & Winterwerp, J. (2013). The role of flow asymmetry and mud properties on tidal flat sedimentation. *Continental Shelf Research*, *60, Supplement*(0), S71 - S84. (Hydrodynamics and sedimentation on mesotidal sand- and mudflats)

van Rijn, L. (2011). Coastal erosion and control. *Ocean & Coastal Management*, *54*(12), 867 - 887. (Concepts and Science for Coastal Erosion Management (Conscience))

Vick, D. (2013, April). Concrete revetment mat systems for shore erosion control on offshore embankments. In *Offshore technology conference.* Offshore Technology Conference.

Vidal, C., Losada, M., & Mansard, E. (1995). Suitable wave-height parameter for characterizing breakwater stability. *Journal of Waterway, Port, Coastal, and Ocean Engineering*, *121*(2), 88-97.

Vidal, C., Losada, M., Medina, R., Mansard, E., & Gomez-Pina, G. (1992). A universal analysis for the stability of both lowcrested and submerged breakwaters. *Coastal Engineering Proceedings*, *1*(23).

Vidal, C., Medina, R., & Lomè´¸naco, P. (2006). Wave height parameter for damage description of rubble-mound breakwaters. *Coastal Engineering*, *53*(9), 711 - 722.

Wakushima, S., Kuraishi, S., & Sakurai, N. (1994). Soil salinity and ph in japanese mangrove forests and growth of cultivated mangrove plants in different soil conditions. *Journal of Plant Research*, *107*(1), 39-46.

Watson, J. G. (1928). *Mangrove forests of the malay peninsula* (No. 6). Fraser & Neave.

White, A. T., AliÃ±o, P. M., Cros, A., Fatan, N. A., Green, A. L., Teoh, S. J., ... Wen, W. (2014). Marine protected areas in the coral triangle: Progress, issues, and options. *Coastal Management*, *42*(2), 87-106.

Wunsch, C., Ponte, R. M., & Heimbach, P. (2007). Decadal trends in sea level patterns: 1993-2004. *Journal of Climate*, *20*(24), 5889–5911.

Xu, H., Zhang, K., Shen, J., & Li, Y. (2010). Storm surge simulation along the u.s. east and gulf coasts using a multi-scale numerical model approach. *Ocean Dynamics*, *60*(6), 1597-1619.

Yagci, O., Mercan, D., Cigizoglu, H., & Kabdasli, M. (2005). Artificial intelligence methods in breakwater damage ratio estimation. *Ocean Engineering*, *32*(17-18), 2088 - 2106.

Ye, Y., Tam, N. F.-Y., Lu, C.-Y., & Wong, Y.-S. (2005). Effects of salinity on germination, seedling growth and physiology of three salt-secreting mangrove species. *Aquatic Botany*, *83*(3), 193 - 205.

Young, I. R., Zieger, S., & Babanin, A. V. (2011). Global trends in wind speed and wave height. *Science*, *332*(6028), 451-455.

Zanuttigh, B., & van der Meer, J. W. (2008). Wave reflection from coastal structures in design conditions. *Coastal Engineering*, *55*(10), 771 - 779.

Appendices

APPENDIX A : LIST OF PUBLICATIONS AND PAPERS PRESENTED

List of publications and papers presented

1. **Motamedi, S.**, Shamshirband, S., Petković, D., & Hashim, R. (2015). Application of adaptive neuro-fuzzy technique to predict the unconfined compressive strength of PFA-sand-cement mixture. Powder Technology, 278, 278–285.

2. **Motamedi, S.**, Song, K.-I., & Hashim, R. (2015). Prediction of unconfined compressive strength of pulverized fuel ash–cement–sand mixture. Materials and Structures, 48(4), 1061–1073.

3. **Motamedi, S.**, Shamshirband, S., Hashim, R., Petković, D., & Roy, C. (2015). Estimating unconfined compressive strength of cockle shell–cement–sand mixtures using soft computing methodologies. Engineering Structures, 98, 49–58.

4. **Motamedi, S.**, Shamshirband, S., Petković, D., & Hashim, R. (2015). Application of adaptive neuro-fuzzy technique to predict the unconfined compressive strength of PFA-sand-cement mixture. Powder Technology, 278, 278–285.

5. **Motamedi, S.**, Hashim, R., Zakaria, R., Song, K. I., and Sofawi, B. (2014). Long-term assessment of an innovative mangrove rehabilitation project: case study on Carey Island, Malaysia. The Scientific World Journal, 2014.

6. **Motamedi, S.**, Roy, C., Shamshirband, S., Hashim, R., Petković, D., & Song, K.-I. (2015). Prediction of ultrasonic pulse velocity for enhanced peat bricks using adaptive neuro-fuzzy methodology. Ultrasonics, 61(April), 103–113.

7. **Motamedi, S.**, Roslan Hashim, Song, K.I., Rozainah Zakaria. (2014) Mangrove plantation and breakwater systems for shoreline protection: Long-term assessment of the mangrove rehabilitation project at Sungai Haji Dorani, Malaysia. Wetlands, Huesca, Spain.

APPENDIX C : BOREHOLE LOG OF THE STUDY SITE

Borehole log

Field works: The scope of geotechnical investigation for field works was carried out in accordance with **BS 5930: 1999** "*Code of Practice for Soil*". Before commencement of the site investigation activities, for each borehole, a trial pit of up to 2 meters was conducted prior to the drilling. Appendix B contains supplementary information on the quantity of site investigation works in this study.

Drilling: The drilling activities were conducted using a hydraulic feed rotary boring machine. In order to wash the cuttings to the ground level, circulated mud water was pumped through hollow rods into the bottom of the borehole. Also, a cutting tool (a metal crown bit) was attached to the lower end of the drilling rods.

Three boreholes were drilled at three locations, namely BH1, BH2 and BH3. The drilling works were terminated at all the boreholes, where the depth reached three times the SPT N value of 100 blows in three-meter intervals. Each borehole had a diameter of 100 mm in soil and the total drilling depth in soil was 100 m $\pm$ 3 m. The borelogs can be found in Appendix B.

Standard Penetration Test: (SPT) The SPT tests were done in line with **BS 1377: 1999** "*Methods of test for soils for civil engineering purposes. Classification tests: Part 9*". The scope of works for the SPT tests were to a) determine the penetration resistance of split-barrel sampler, and b) identify the soil classification by obtaining the disturbed samples of the soil from various depths of boreholes.The tests were conducted by employing a split-barrel sampler (sb-sampler), which was attached to the lower end of the boring rods.

The sb-sampler was driven into various depths of soil through the weight of standard hammer (63.5 kg) falling freely from a height of 76 cm onto an anvil that was connected to the top of the boring rods. The sb-sampler was driven 45 cm into the soil stratum with the number of blows required for each 15 cm of the penetration recorded. The SPT N-value was then recorded as the number of blows for the last penetration of 30 cm.

No further blows were applied when 100 blows reached the total depth prior to full penetration of 30 cm and the final penetration depth was recorded. Once the test was considered terminated, the sb-sampler was withdrawn and the remaining extracted soil from the sampler were labeled and maintained in a plastic container. The extracted soils were used to classify the soil category in the existing boreholes. In this study, a total number of 34 SPT tests were conducted (see Appendix B).

Undisturbed and disturbed sampling: Undisturbed soil sampling is considered when the in-situ structure and water content of the soil samples are essential for determination of soil properties by mechanical soil tests, such as triaxial compression, shear test, soil physical tests and odometer test. A total of five undisturbed (UD) samples were taken at the depth in which the soil layers changed in the borehole or at the predetermined depth (see Appendix B).

In this study, the undisturbed sampling was conducted using a thin-wall tube sampler with the length of 80 cm and outer diameter of 7.5 cm. In order to remove the remaining soil resulting from the cutting activities, the boreholes were washed out with water prior to undisturbed sampling. Further, the depth pf sample collection at the bottom of the borehole was measured. The sample tube was lowered when it reached to the bottom of the hole and it was pushed into the soil. The sample tube was withdrawn to the surface after the tube was jacked to the required depth. To form a seal on both sides of the undisturbed (UD) tube, molten was applied in thin layers. This was done to prevent changes in the moisture content of the withdrawn soil samples.

In this study, the disturbed samples were obtained using a split-barrel sampler and further were sealed in a plastic container. The samples were collected for the identification of soil type. A total of 19 numbers of disturbed samples were collected from the boreholes (see Appendix B).

Laboratory tests: In this study, four laboratory tests were conducted on the undisturbed samples collected from the boreholes. The main objective of these tests were to evaluate the compressibility characteristics, shear strength and classification of soil samples. The tests were carried out in line with **BS 1377: 1999** "*Methods of test for soils for civil engineering purposes.*". The classification of soil was based on the *Standard Test Method for the Particle-Size Analysis of Soils* (ASTM D 422) and the Unified Soil Classification System (USCS). Table B.1 summarizes the list of laboratory tests and the their standard that were conducted on the UD samples in this study.

Table B.1: List of labratory tests on UD samples that were conducted in this study.

Name of Test	Standard
Moisture Content	BS 1377: 1999 : Part 2 - Test 3
Bulk and Dry Density	BS 1377: 1999 : Test 7:2
Atterberg Limits	BS 1377: 1999 : Test 4.5 and Test 5.3
UU Triaxial	BS 1377: 1999 : Part 7 - Test 9

C.1.0. SUMMARY OF LABORATORY TEST RESULTS

Borehole No.	Sample No.	Depth (m)	Bulk Density (Mg/m^3)	Dry Density (Mg/m^3)	Specific Gravity	Moisture Content (%)	Atterberg Limit: Liquid Limit (%)	Atterberg Limit: Plastic Limit (%)	Atterberg Limit: Plasticity Index (%)	Grain Size Distribution: Gravel (%)	Grain Size Distribution: Sand (%)	Grain Size Distribution: Silt (%)	Grain Size Distribution: Clay (%)	Triaxial Compression UCT: Cohesion (kN/m^2)	Triaxial Compression UU: Cohesion (kN/m^2)	Triaxial Compression UU: Phi Angle (°)	Triaxial Compression CU: Cohesion (kN/m^2)	Triaxial Compression CU: Phi Angle (°)	Triaxial Compression CID: Cohesion (kN/m^2)	Triaxial Compression CID: Phi Angle (°)	Consolidation: Initial Void Ratio	Consolidation: Compression Index	Consolidation: Preconsolidation Pressure (kN/m^2)	Vane: Undisturbed Shear Strength (kN/m^2)	Vane: Remoulded Shear Strength(kN/m^2)	Particle Density (Mg/m^3)	Chemical Soil: Total Sulpahte Content (%)	Chemical Soil: pH Value	Chemical Soil: Chloride Content	Chemical Soil: Sulpahte Content in 2:1 water :soil extract	Chemical Water: Sulpahte Content	Chemical Water: pH Value	Chemical Water: Salinity
1	UD 1	3.00-3.50	2.00	1.57		27	55	29	26						10.3	0																	
	UD 2	6.00-6.50	1.96	1.58		24	37	23	14						10.4	0																	
	UD 3	9.00-9.50	2.02	1.62		25	51	25	26						13.4	0																	
2	UD 1	-	-	-		-	-	-	-						-	-																	
	UD 2	-	-	-		-	-	-	-						-	-																	
	UD 3	-	-	-		-	-	-	-						-	-																	
3	UD 1	6.00-6.50	1.73	1.09		58	37	19	18						13.0	0																	
	UD 2	9.00-9.50	1.89	1.49		27	28	12	16						18.8	0																	

C.2.0. Borelog data

SHEET NO: 1 OF 2

CLIENT : University of Malaya PROJECT : Site Investigation for Carey Island LOCATION :	

PROJECT NO:	BOREHOLE NO: BH 1	WATER LEVEL : 1.5m
DRILLING DATE STARTED: 11/01/2015	BOREHOLE DIA:	REDUCED LEVEL : NORTHING:
DRILLING DATE COMPLETED:	CORE DIA: 75MM	EASTING:
PREPARED BY:	DRILLING METHOD: RCG	

Description	Graphic Log	Depth (m) (Thickness)	Scale	SPT (N-values)		Samples & Tests			Geological Classification	Grain Size Analysis G/SA/S/C	Unified Soil Classification	Shear Strength		Bulk Density (Mg/m)	Water Content (%)	Atternberg Limit (%)	
				0 20 40 60 80 100	Blows/cm	Legend	Type & No.	Depth(m)				C (kN/m^2)	Ψ (°)			LL	PL
Soft, light grey & light yellow, slightly Sandy Silt	- - : :	(6.00) 6.00	1 2 3 4 5 6		4/30 (1/2/2)		UD1 P1 D1	3.00-3.50 3.50-3.95			MS	10.3 (UU)	0	2.00	27	55	29
Very soft, black, Clay with decayed wood pieces.	x x * *	(3.00) 9.00	7 8 9		1/30 (0/0/1)		UD2 P2 D2	6.00-6.50 6.50-6.95			C	10.4 (UU)	0	1.96	24	37	23
Loose, black, Silty Clay,fine to medium Sand	: : * *	(3.00) 12.00	10 11 12		8/30 (2/3/3)		UD3 P3 D3	9.00-9.50 9.50-9.95			SC	13.4 (UU)	0	2.02	25	51	25
	:																

SHEET NO: 2 OF 2

	CLIENT : University of Malaya PROJECT : Site Investigation for Carey Island LOCATION :

PROJECT NO:	BOREHOLE NO: BH 1	WATER LEVEL : 1.5m
DRILLING DATE STARTED: 11/01/2015	BOREHOLE DIA:	REDUCED LEVEL : NORTHING:
DRILLING DATE COMPLETED:	CORE DIA: 100mm	EASTING:
PREPARED BY:	DRILLING METHOD: RCG	

Description	Graphic Log	Depth (m) (Thickness)	Scale	SPT (N-values) 0 20 40 60 80 100	Blows/cm	Samples & Tests: Legend	Type & No.	Depth(m)	Geological Classification	Grain Size Analysis G/SA/S/C	Unified Soil Classification	Shear Strength C (kN/m^2)	Shear Strength Ψ (°)	Bulk Density (Mg/m)	Water Content (%)	Atternberg Limit (%) LL	PL
Firm to very stiff, light grey to greenish grey, spotted white, slightly Sandy Silt	I I X X I I X X I I X X I I X X I I X X I I X X	(4.00) 24.00	21 22 23 24		21/30 (5/8/12)		P7	21.00-21.45			MS						
Medium dense, light yellow, some light grey, slightly Silty Sand with some gravels.	: : X X : : X X : : X X : : X X : : X X : : X X : : X X	(3.00) 9.00	25 26 27 28 29 30		23/30 (5/8/14) 17/30 (7/11/6)		P8 D5 P9	24.00-24.45 27.00-27.45			SM						
Very dense, dark reddish brown, Silty Sand with gravels	X X X X X X X X X X X X X X X X X X X X	(3.00) 12.00	31 32 33		100/11 (58/100)		P10 D6	30.00-33.45			SC						

SHEET NO 1 0F 2	CLIENT : University of Malaya PROJECT : Site Investigation for Carey Island LOCATION :	
PROJECT NO:	BOREHOLE NO: BH 2	WATER LEVEL : 2m
DRILLING DATE STARTED: 12/01/2015	BOREHOLE DIA: 100mm	REDUCED LEVEL : NORTHING:
DRILLING DATE COMPLETED:14/01/2015	CORE DIA: 75mm	EASTING:
PREPARED BY:	DRILLING METHOD: RCG	

Description	Graphic Log	Depth (m) (Thickness)	Scale	SPT (N-values) 0 20 40 60 80 100	Blows/cm	Samples & Tests: Legend	Samples & Tests: Type & No.	Samples & Tests: Depth(m)	Geological Classification	Grain Size Analysis G/SA/S/C	Unified Soil Classification	Shear Strength C (kN/m^2)	Shear Strength Ψ (°)	Bulk Density (Mg/m)	Water Content (%)	Atternberg Limit (%) LL	Atternberg Limit (%) PL
Firm yellowish brown to dark brown, Sandy Clay with stones	= = + + = = + + = = + + = = + + = = + + = = + +	(6.00) 6.00	1 2 3 4 5 6		5/30 (2/2/3)		P1 D1	3.00-3.45			CS						
Soft, dark brown to black, Sandy Clay with decayed wood pieces	- - = = - - = = - - = = - - = = - - = =	(3.00) 9.00	7 8 9		4/30 (1/2/2) 9/30 (3/4/5)		P2 D2 P3 D3	6.00-6.45 9.00-9.45			CS						
Loose to medium dense, grey, Clayey, medium to coarse Sand	= = x x = = x x = = x x = = x x = = x x = = x x	(6.00) 15.00	10 11 12 13 14 15		20/30 (5/6/12)		P4	12.00-12.45			S						

SHEET NO 2 OF 2	CLIENT : University of Malaya PROJECT : Site Investigation for Carey Island LOCATION :	
PROJECT NO:	BOREHOLE NO: BH 2	WATER LEVEL : 2m
DRILLING DATE STARTED: 12/01/2015	BOREHOLE DIA: 100mm	REDUCED LEVEL : NORTHING: EASTING:
DRILLING DATE COMPLETED:14/01/2015	CORE DIA: 75mm	
PREPARED BY:	DRILLING METHOD: RCG	

Description	Graphic Log	Depth (m) (Thickness)	Scale	SPT (N-values)		Samples & Tests			Geological Classification	Grain Size Analysis G/SA/S/C	Unified Soil Classification	Shear Strength		Bulk Density (Mg/m)	Water Content (%)	Atternberg Limit (%)	
				0 20 40 60 80 100	Blows/cm	Legend	Type & No.	Depth(m)				C (kN/m^2)	Ψ (°)			LL	PL
Hard, white to light grey, slightly Sandy Silt	+ + . . + + . . + + . .	(1.00) 21.00	21		50/30 (15/22/ 28)		P7 D5	21.00-21.45			MS						
Hard, light grey to light bluish grey, Sandy Silt with gravels	X X x x X X x x X X x x X X x x X X x x X X x x X X x x X X x x X X x x X X x x	(9.00) 30.0	22 23 24 25 26 27 28 29 30		55/30 (18/25/ 30)		P8 P9	24.00-24.45 27.00-27.45			MS						

SHEET NO : 1 OF 1	CLIENT : University of Malaya PROJECT : Site Investigation for Carey Island LOCATION :	
PROJECT NO:	BOREHOLE NO: BH 3	WATER LEVEL : 2
DRILLING DATE STARTED: 13/01/2015	BOREHOLE DIA: 100mm	REDUCED LEVEL : NORTHING:
DRILLING DATE COMPLETED:15/01/2015	CORE DIA: 75mm	EASTING:
PREPARED BY:	DRILLING METHOD: RCG	

Description	Graphic Log	Depth (m) (Thickness)	Scale	SPT (N-values) 0 20 40 60 80 100	SPT (N-values) Blows/cm	Samples & Tests Legend	Samples & Tests Type & No.	Samples & Tests Depth(m)	Geological Classification	Grain Size Analysis G/SA/S/C	Unified Soil Classification	Shear Strength C (kN/m²)	Shear Strength Ψ (°)	Bulk Density (Mg/m)	Water Content (%)	Atternberg Limit (%) LL	Atternberg Limit (%) PL
Very Soft, dark grey to black, Clay with some wood pieces	. . - - . . - - . . - - . . - - . . - - . . - -	(6.00) 6.00	1 2 3 4 5 6	.	0/30 (0/0/0)		D1 P1	3.50-3.95			C						
Very loose, light greenish grey.Clayey, medium Sand with some gravels	- - + + - - + + - - + +	(3.00) 9.00	7 8 9	.	1/30 (0/0/1)		UD1 P2 D3	6.00-6.50 6.50-6.95			SC	13.0UU	0	1.73	58 7	37	19
Loose, brown, slightly Silty, medium sand	_ _ _ _ _ _ _ _ _ _ _ _	(3.00) 12.00	10 11 12	.	8/30 (2/3/5)		UD2 P3 D3	9.00-9.50 9.50-9.95			SM	18.8UU	0	1.89	27	28	12

C.3.0. Laboratory test results

PROJECT – Site Investigation for Carey Island					Boreholes – 3	
					Sample – UD1	
VISUAL DESCRIPTION – Light Gray Organic CLAY With Decayed Vegetation					Depth (m) – 6.0-6.5	
					Job Number -	
	Liquid Limit(%)				Plastic Limit (%)	
Container Weight (g)	3.73	3.74	3.74	3.77	7.91	7.68
Wet Mass + Container Weight (G)	9.74	11.16	11.32	9.96	10.38	10.27
Dry Mass + Container Weight (g)	8.23	9.19	9.19	8.12	9.98	9.86
Moisture Content (%)	33.6	36.1	39.1	42.3	19.3	18.8
Penetration (mm)	15.10	20.00	22.50	25.00		

C.3.1. Atterberg limits

PROJECT – Site Investigation for Carey Island					Boreholes – 3	
					Sample – UD2	
VISUAL DESCRIPTION – Light Olive Gray Clayey SAND					Depth (m) – 9.0-9.5	
					Job Number -	
	Liquid Limit(%)				Plastic Limit (%)	
Container Weight (g)	3.71	3.74	3.78	3.70	7.98	7.99
Wet Mass + Container Weight (G)	10.11	10.63	12.44	11.37	11.64	11.47
Dry Mass + Container Weight (g)	8.78	9.13	10.48	9.56	11.25	11.10
Moisture Content (%)	26.2	27.8	29.3	30.9	11.9	11.9
Penetration (mm)	16.90	20.00	22.60	24.83		

Liquid Limit (%) – 28, Plastic Limit (%) – 12, Plasticity Index (%) – 16

PROJECT – Site Investigation for Carey Island					Boreholes – 1	
					Sample – UD2	
VISUAL DESCRIPTION – Dark Yellowish Orange Sandy CLAY					Depth (m) – 6.00-6.50	
					Job Number -	
	Liquid Limit(%)				Plastic Limit (%)	
Container Weight (g)	3.76	3.70	3.72	3.82	7.95	7.90
Wet Mass + Container Weight (G)	9.86	10.14	10.62	12.52	10.49	10.41
Dry Mass + Container Weight (g)	8.34	8.44	8.69	10.04	10.01	9.94
Moisture Content (%)	33.2	35.9	38.8	39.9	23.3	23.0
Penetration (mm)	16.60	18.50	21.40	23.60		

Liquid Limit (%) – 37, Plastic Limit (%) – 23, Plasticity Index (%) – 14

PROJECT – Site Investigation for Carey Island					Boreholes – 1	
					Sample – UD3	
VISUAL DESCRIPTION – Light Brown Sandy Clay					Depth (m) – 9.00-9.50	
					Job Number -	
	Liquid Limit(%)				Plastic Limit (%)	
Container Weight (g)	3.77	3.70	3.77	3.72	7.97	7.90
Wet Mass + Container Weight (G)	10.23	9.30	10.89	10.13	11.65	11.64
Dry Mass + Container Weight (g)	8.15	7.42	8.45	7.88	10.91	10.88
Moisture Content (%)	47.5	50.5	52.1	54.1	25.2	25.5
Penetration (mm)	16.15	18.80	21.55	23.85		

Liquid Limit (%) – 51, Plastic Limit (%) – 22, Plasticity Index (%) – 26

PROJECT – Site Investigation for Carey Island					Boreholes – 1	
					Sample – UD1	
VISUAL DESCRIPTION – Dark Yellowish Orange Sandy CLAY					Depth (m) – 3.0-3.5	
					Job Number -	
	Liquid Limit(%)				Plastic Limit (%)	
Container Weight (g)	3.74	3.75	3.77	3.73	8.12	8.15
Wet Mass + Container Weight (G)	9.09	10.15	9.92	10.21	11.03	11.02
Dry Mass + Container Weight (g)	7.25	7.93	7.73	7.85	10.38	10.38
Moisture Content (%)	52.4	53.1	55.3	57.3	28.8	28.7
Penetration (mm)	16.55	17.95	21.30	23.55		

Liquid Limit (%) – 55, Plastic Limit (%) – 29, Plasticity Index (%) – 26

C.3.2. Unconsolidated Undrained triaxial compression

PROJECT – Site Investigation for Carey Island				Boreholes – 3	
				Sample – UD1	
VISUAL DESCRIPTION – Very Soft Light Gray Organic CLAY				Depth (m) – 6.0-6.5	
With Decayed Vegetation				Job Number -	
Stage	Cell Pressure (kN/m^2)	Maximum Deviator Stress (kN/m^2)	Moisture Content (%)	Bulk Density (Mg/m^3)	Dry Density (Mg/m^3)
1	60	26	108	1.39	0.67
2	120	23	36	1.89	1.38
3	240	30	31	1.92	1.46

Sample Type - Undisturbed Shearing Rate (mm/min) - 1.52

PROJECT – Site Investigation for Carey Island				Boreholes – 3	
				Sample – UD2	
VISUAL DESCRIPTION – Very Dense Light Olive Gray Clayey SAND				Depth (m) – 9.0-9.50	
				Job Number -	
Stage	Cell Pressure (kN/m^2)	Maximum Deviator Stress (kN/m^2)	Moisture Content (%)	Bulk Density (Mg/m^3)	Dry Density (Mg/m^3)
1	85	242	33	1.86	1.39
2	170	600	23	1.87	1.52
3	340	888	25	1.94	1.55

Sample Type - Undisturbed Shearing Rate (mm/min) - 1.52

PROJECT – Site Investigation for Carey Island				Boreholes – 1	
				Sample – UD2	
VISUAL DESCRIPTION – Firm To Stiff Dark Yellowish Orange SANDY CLAY				Depth (m) – 6.0-6.50	
				Job Number -	
Stage	Cell Pressure (kN/m^2)	Maximum Deviator Stress (kN/m^2)	Moisture Content (%)	Bulk Density (Mg/m^3)	Dry Density (Mg/m^3)
1	60	163	23	1.95	1.58
2	120	179	26	1.96	1.56
3	240	288	23	1.97	1.60

Sample Type - Undisturbed Shearing Rate (mm/min) - 1.52

PROJECT – Site Investigation for Carey Island				Boreholes – 1	
				Sample – UD3	
VISUAL DESCRIPTION – Stiff Light Brown Sandy CLAY				Depth (m) – 9.0-9.50	
				Job Number -	
Stage	Cell Pressure (kN/m^2)	Maximum Deviator Stress (kN/m^2)	Moisture Content (%)	Bulk Density (Mg/m^3)	Dry Density (Mg/m^3)
1	85	138	28	1.98	1.54
2	170	193	27	2.02	1.59
3	340	476	21	2.05	1.69

Sample Type - Undisturbed Shearing Rate (mm/min) - 1.52

PROJECT – Site Investigation for Carey Island				Boreholes – 1	
				Sample – UD1	
VISUAL DESCRIPTION – Stiff Dark Yellowish Orange Sandy CLAY				Depth (m) – 3.0-3.50	
				Job Number-	
Stage	Cell Pressure (kN/m^2)	Maximum Deviator Stress (kN/m^2)	Moisture Content (%)	Bulk Density (Mg/m^3)	Dry Density (Mg/m^3)
1	50	119	28	1.97	1.55
2	100	217	28	1.99	1.55
3	200	287	26	2.05	1.63

Sample Type: Undisturbed Shearing Rate (mm/min): 1.52

C.3.3. Moisture content and density

PROJECT -				JOB NUMBER -	
Borehole Number	Sample Number	Depth (m)	Moisture Content (%)	Bulk Density (Mg/m^3)	Dry Density (Mg/m^3)
1	UD1	3.0-3.50	27	2.00	1.57
	UD2	6.0-6.50	24	1.96	1.58
	UD3	9.0-9.50	25	2.02	1.62
3	UD1	6.0-6.50	58	1.73	1.09
	UD2	9.0-9.50	27	1.89	1.49

Borehole Number	Sample Number	Depth (m)	Visual Description
1	UD1	3.0-3.50	Dark Yellowish Orange Sandy CLAY
	UD2	6.0-6.50	Dark Yellowish Orange Sandy CLAY
	UD3	9.0-9.50	Light Brown Sandy CLAY
3	UD1	6.0-6.50	Light Gray Organic CLAY With Decayed Vegetation
	UD2	9.0-9.50	Light Olive Gray Clayey SAND

C.3.4. Summary of the soil laboratory results

PROJECT – Site Investigation for Carey Island				JOB NUMBER -		
Borehole Number		1			3	
Sample Number		UD1	UD2	UD3	UD1	UD2
Depth (M)	From	3.0	6.0	9.0	6.0	9.0
	To	3.50	6.50	9.50	6.50	9.50
Moisture Content (%)		27	24	25	58	27
Density (Mg/m^3)	Bulk Density	2.00	1.96	2.02	1.73	1.89
	Dry Density	1.57	1.58	1.62	1.09	1.49
Atterberg Limit (%)	Liquid Limit	55	37	51	37	28
	Plastic Limit	29	23	25	19	12
	Plasticity Index	26	14	26	18	16
Triaxial Compression	Type of test	UU	UU	UU	UU	UU
	Cohesion (kN/m^2)	103	104	134	13	288
	Phi Angle, Phi (degree)	0	0	0	0	0

SAND

Relative Density according to Standard Penetration Test	
N-value (blows/300mm of penetration)	Relative Density
0-4	Very Loose
4-10	Loose
10-30	Medium dense
30-50	Dense
> 50	Very Dense

CLAY AND SILT

Approximate Relation of Consistency to Standard Penetration Test	
N-value (blows/300mm of penetration)	Consistency
< 2	Very soft
2 – 4	Soft
4 - 8	Firm
8 – 15	Stiff
15 – 30	Very Stiff
> 30	Hard

C.3.5. Classification of rock quality in relation to the discontinuities

Quality classification	ROD %	Fracture frequency per metre
Very poor	0 - 25	Over 15
Poor	25 - 50	15 – 18
Fair	50 - 75	8 – 5
Good	75 - 90	5 – 1
Excellent	90 - 100	Less than 1

C.3.6. Rock weathering classification

Term	Description	Grade
Fresh	No visible sign of rock material weathering; perhaps slight discoloration on major discontinuity surfaces	I
Slightly weathered	Discoloration indicates weathering of rock material and discontinuity surfaces. All the rock material may be discoloured by weathering	II
Moderately weathered	Less than half of the rock material is decomposed or disintegrated to a soil. Fresh or discoloured rock is present either as a continous framework or as corestones	III
Highly weathered	More than half of the rock material is decomposed or disintegrated to a soil. Fresh or discoloured rock is present either as a continuous framework or as corestones	IV
Completely weathered	All rock material is decomposed and/or disintegrated to soil. The original mass structure is still largely intact	V
Residual soil	All rock material is converted to soil. The mass structure and material fabric are destroyed. There is a large chance in volume, but the soil has not been significantly transported	VI

APPENDIX D : TEMPORAL AND SPATIAL CHANGES IN TOPOGRAPHY OF CAREY ISLAND SITE

Temporal and spatioal changes in topography of Carey island Site

Topography of the site in September 2014

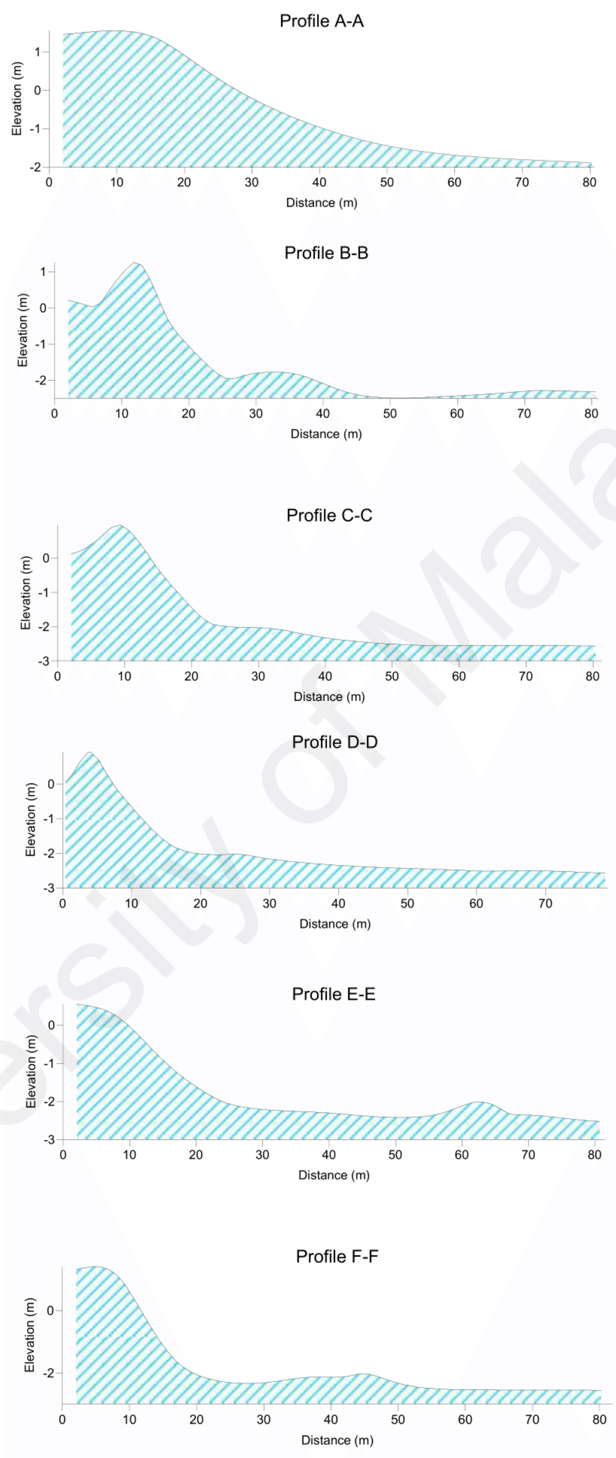

Profile of cross-sections A-A to F-F along Y-direction in September 2014.

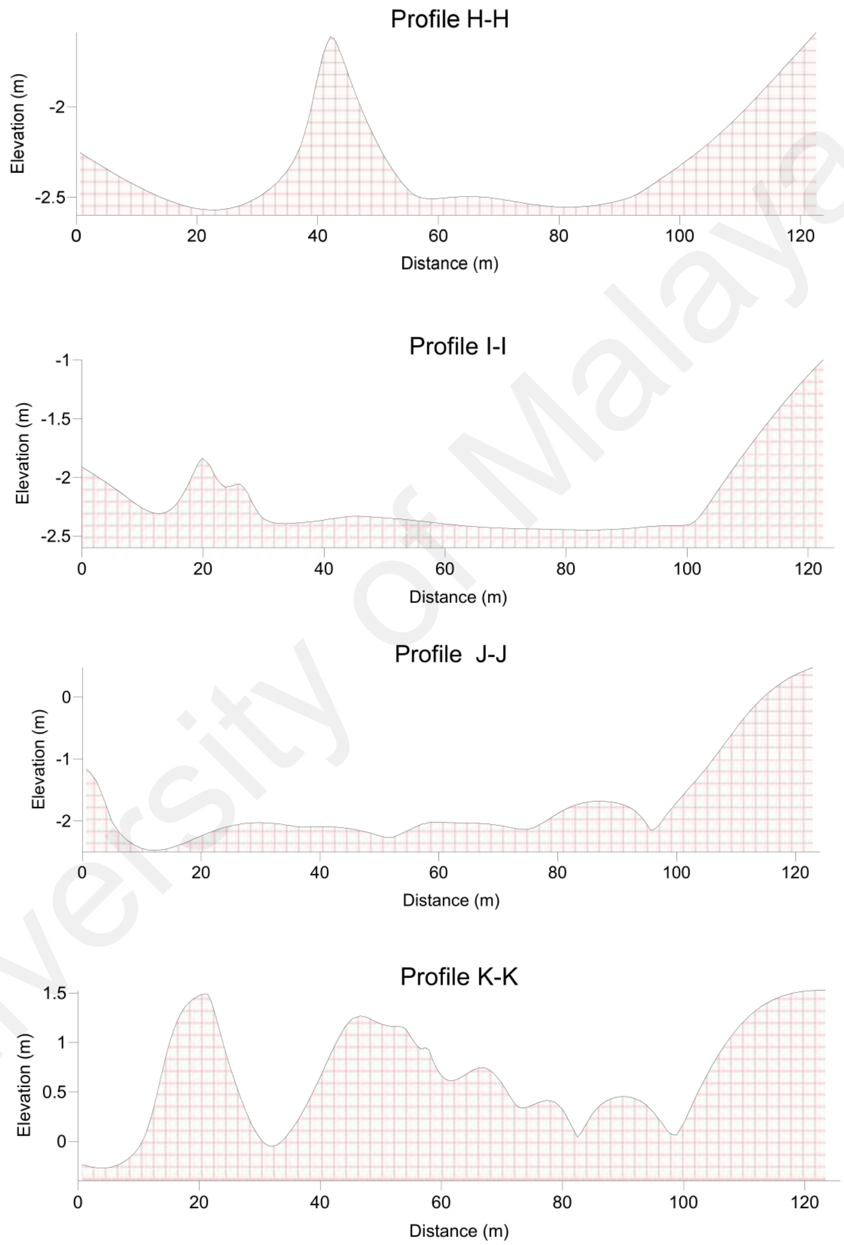

Profile of cross-sections H-H to K-K along X-direction in September 2014.